α-fluoroamides in biotransformations

Banks, John W.

α-FLUOROAMIDES IN BIOTRANSFORMATIONS

John W. Banks

PhD Thesis

Department of Chemistry

University of Durham

2004

COPYRIGHT

DECLARATION

The work contained in this thesis was carried out in the laboratories at Pfizer, Morpeth between January 1996 and January 2003. All the work was carried out by the author, unless otherwise indicated. It has not been previously submitted for a degree at this or any other university.

Durham University
Department of Chemistry

Abstract

α-FLUOROAMIDES IN BIOTRANSFORMATIONS

By John W. Banks

Classically hydrolytic enzymes, such as lipases, are considered to exhibit selectivity at a stereogenic centre, based on the steric nature of the adjacent substituent. In this study we report on the selectivity of hydrolytic enzymes (acylase's and protease's) on compounds containing both hydrogen and fluorine atoms at the stereogenic centre. A selectivity of 96% de is reported for the hydrolysis of an α-fluoroamide using *Aspergillus melleus* acylase. The K_m and V_{max} values are reported for each diastereomer, which demonstrate a ten-fold preference for the (*S*, *S*)-isomer over the (*S*, *R*)-isomer. A similar phenomenon is established for the analogous α-chloroamide and a comparison of reaction rates for non-halogenated amides is made. This effect has been rationalised by; a) the fluorine substituent controlling of the conformation of the amide bond and b) the stabilisation of the enzyme / amide intermediate.

Furthermore a selection of racemic α-fluoroamides were prepared and their solid state conformations determined by X-ray crystallography. The C-F and the amide bonds are found to orientate in a very specific manner with respect to each other, consistent with a very specific stereoelectronic alignment.

Attempts at preparing the elusive dipeptide with a fluorine atom alpha to the amide bond proved unsuccessful, however, one attempt led to the formation of a dimeric compound for which X-ray crystal analysis secured the structure. ^{19}F variable temperature NMR was used to examine the barrier to rotation that existed for this dimeric compound.

ACKNOWLEDGEMENTS

I would like to thank Prof. David O'Hagan for his valued support and guidance throughout the last eight years and for the patience he has shown when my other commitments have interfered with the progress of this research.

I would like to thank Prof. David Parker for stepping in as my supervisor when Prof. David O'Hagan moved to St. Andrews.

I would also like to thank Dr. Anthony P. Ketteringham and my colleagues at Morpeth for their continued support throughout this period of study, without which this project would not have been brought to completion.

Finally I would like to thank my wife Joanne and two children, Christopher and Kieran, for their patience and understanding during the many occasions when I have been unavailable during the last eight years.

Table of Contents

ABBREVIATIONS

5-FDA	5'-Fluoro-5'-deoxyadenosine
Å	Angstrom
Ac	Acetyl
AMA	*Aspergillus melleus* acylase
Ar	Aryl
B	Billion
B. Pt.	Boiling point
BF_4^-	Tetrafluoroborate
BIP	*Bacillus icheniformis* protease
br	Broad
Bz	Benzyl
cal	calorie
CFC	Chlorofluorocarbon
CN^-	Nitrile
CNS	Central nervous system
CoA	Coenzyme A
CSDS	Cambridge structural database system
d	Doublet
D. cymosum	*Dichapetalum cymosum*
D. toxicarium	*Dichapetalum toxicarium*
DCM	Dichloromethane
de	Diasteriomeric excess
DMF	Dimethylformamide
DNA	Deoxyribonucleic acid
ee	Enantiomeric excess

EI	Electron impact
HIV-1	Human immunosuppressive virus-1
HKA	Hog kidney acylase
HMG-CoA	3-Hydroxy-3-methylglutaryl-coenzyme A
h	Hour
Hz	Hertz
IR	Infrared
K_m	Binding affinity
LDA	Lithium diisopropylamide
Lit.	Literature
M	Molar concentration (mol dm^3)
m	Multiplet
M. Pt.	Melting point
Min	Minutes
mm	Millimetres
mM	Millimoles
mol	mole
m/z	Mass to charge ratio
NMR	Nuclear magnetic resonance
PLE	Pig liver esterase
ppm	Parts per million
PTFE	Polytetrafluoroethene
q	quartet
R	Alkyl
[S]	Initial substrate concentration
s	Singlet
S. cattleya	*Streptomyces cattleya*

SAM	(*S*)-adenosylmethionine
SCP	*Streptomyces caespitrum* protease
STM	Scanning tunnelling microscopy
t	Triplet
TLC	Thin layer chromatography
UV	Ultraviolet
v	Reaction velocity
V_{max}	Maximum rate of reaction
w/w	Weight / weight

Chapter 1 - Introduction to fluorine substitution and its application in biomedicinal chemistry

1.1 Historical review

Fluorine[1], mainly as the mineral fluorspar (CaF_2), is the thirteenth most abundant element in the Earth's crust. In 1529, Georigius Agricola reported the use of fluorspar as a flux and later Schwandhard, in 1670, discovered hydrofluoric acid when he found that the vapours produced when fluorspar was treated with acid etched glass.

Elemental fluorine (F_2) was finally isolated in 1886 by Moisson by electrolysis of potassium hydrogen fluoride in the presence of hydrofluoric acid. Commercial applications, using F_2, were rare until the start of the Second World War when the emerging nuclear industry made it necessary to produce large quantities of elemental fluorine for separating uranium isotopes *via.* the hexafluoride. Other commercial applications include chlorofluorocarbon (CFC) solvents for refrigeration, fluorinated high temperature plastics (polytetrafluoroethene, PTFE) and hydrogen fluoride, which is extensively used in glass etching processes.

In recent times a major increase in organofluorine research has been seen in the pharmaceutical industry. Fluorine substitution has become a popular strategy among medicinal chemists in their attempts to improve the efficacy of active pharmaceuticals.

1.2 Fluorine in natural compounds

Natural products containing fluorine are extremely rare, considering the relative abundance of fluorine, with only thirteen metabolites containing fluorine having been identified[2,3]. The first natural compound containing fluorine to be identified was fluoroacetate **1**, which was isolated from the South American plant *Dichapetalum cymosum* and the latest metabolite to be identified was 4-fluorothreonine from the bacterium *Streptomyces cattleya*. The remaining compounds identified so far are ω-fatty acids, fluoroacetone, nucleocidin and 5'-fluoro-5'-deoxyadenosine (5-FDA).

1.2.1 Fluoroacetate

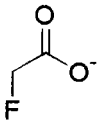

1

Marais first achieved the isolation of fluoroacetate **1** in 1944[4] from the South African plant *D. cymosum*, where potassium monofluoroacetate has been found at levels up to 8000 ppm. Fluoroacetate is highly toxic to most species but certain animals have developed resistance to its effects. For example, the caterpillar *Sindris albimaculatus* can feed on the fruits and leaves of *D. cymosum* and accumulate fluoroacetate as a defence against predators. In addition grazing animals and humans that live where *D. cymosum* grows show higher resistance to the toxin. Fluoroacetate is converted *in vivo* to (2*R*, 3*R*)-fluorocitrate, **3**, as shown in Scheme 1.1, *via*. fluoroacetyl-CoA, **2**.

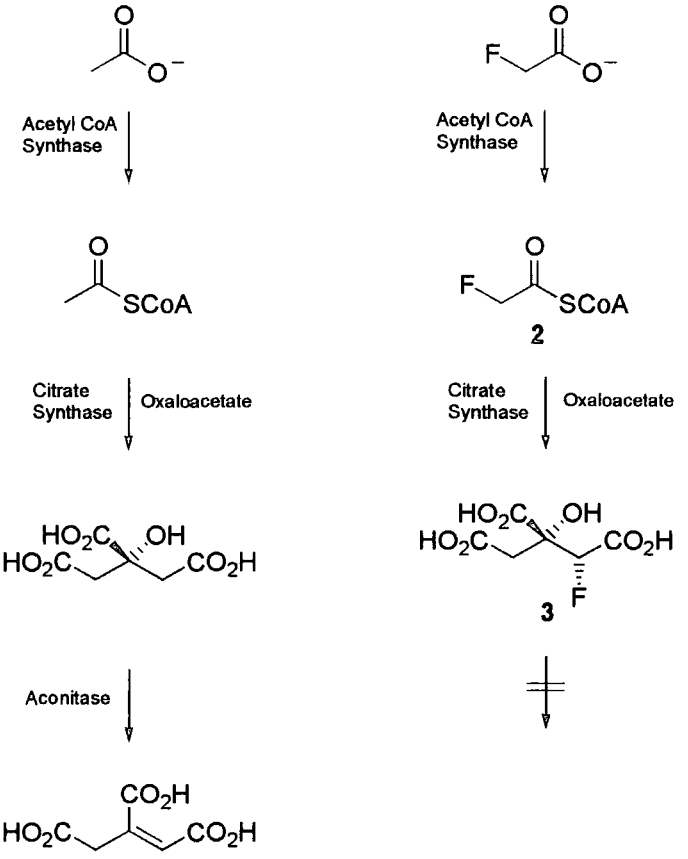

Scheme 1.1: "Lethal synthesis" of fluoroacetate

The conversion of fluoroacetate to fluorocitrate has been termed the lethal synthesis, as (2*R*, 3*R*)-fluorocitrate is an effective inhibitor of the aconitase enzyme, so blocking the normal citrate metabolism, which in turn leads to inhibition of respiration. Interestingly, only the (2*R*, 3*R*)-fluorocitrate stereoisomer is produced by citrate synthase and this is the only stereoisomer that is able to inhibit aconitase.

1.2.2 ω-Fluorofatty Acids

Figure 1.1 shows the naturally occurring ω-fluorofatty acids, which are found in the seeds of *Dichapetalum toxicarium*, a plant that can metabolise fluoroacetate.

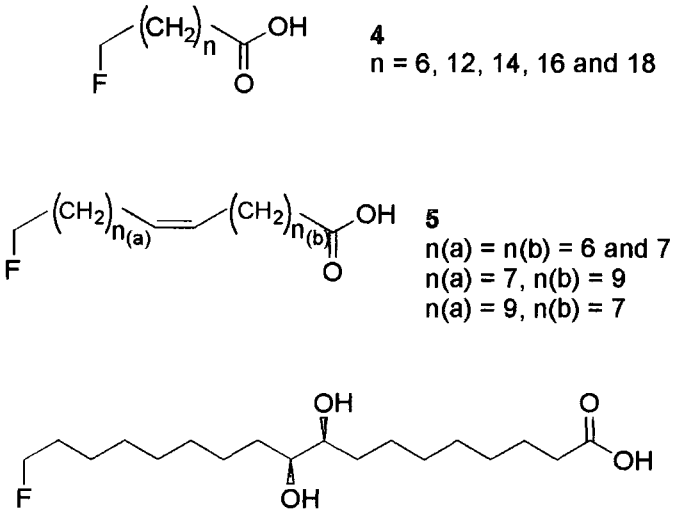

Figure 1.1: Natural ω-fluorofatty acids from *D. toxicarium*

Saturated ω-fluorofatty acids (e. g. ω-fluorocapric acid) have the general structures shown in **4** and to date five different types have been isolated from the seeds of *D. toxicarium*. The most abundant ω-fluorofatty acid is ω-fluorooleic acid, which is a C18 (i. e. n(a) = n(b) = 7) unsaturated acid of the type shown in **5**. For the C_{20} unsaturated acid two isomers are seen with the double bond being at either the 9 or 11 positions. One further type of ω-fluorofatty acid has been identified, 9, 10-dihydroxystearic acid, **6**. It is assumed that this arises from the metabolism of ω-fluorooleic acid *via*. the 9, 10-epoxide. ω-Fluorofatty acids are found in the same chain lengths and unsaturation patterns as their non-fluorinated counterparts and this leads to the conclusion that they are manufactured by the same biosynthetic pathway, which presumably starts from fluoroacetyl-CoA. ω-Fluorofatty acids are extremely

toxic as a consequence of β-oxidation, as they are readily converted to fluoroacetyl-CoA and then to fluorocitrate.

1.2.3 Bacterial metabolites

Two bacteria have been found to elaborate fluorinated metabolites. Nucleocidin, **7**, has been identified as a metabolite of the soil bacteria *Streptomyces calvus*[5] when it is grown in a fluoride ion medium.

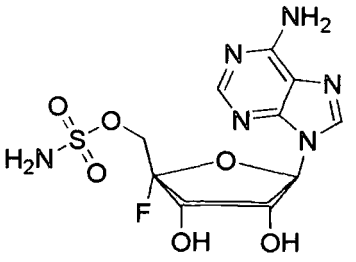

7

The structure of nucleocidin was elucidated in 1969[6]. This metabolite is fundamentally different from those found in plants, as its formation cannot easily be rationalised from fluoroacetate. 4-Fluorothreonine, **8**, is the second fluorine containing metabolite from a bacterium. It has been isolated from *Streptomyces cattleya*.

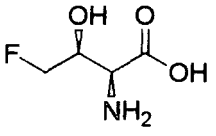

8

S. cattleya co-produces fluoroacetate and 4-fluorothreonine[7]. These metabolites have been the subject of biosynthetic investigations in *S. cattleya*. ^{13}C and ^{2}H labelling studies have revealed that the C-3 and C-4 atoms of fluorothreonine have the same biosynthetic origin and that there is a single fluorination enzyme. Fluoroacetaldehyde, **9**, has also been identified as the precursor to both metabolites as shown in Scheme 1.2.

Initially it was suggested that 4-fluorothreonine was a product of the condensation of fluoroacetaldehyde and glycine but it has now been shown that *L*-threonine is the amino acid that condenses with fluoroacetaldehyde in *S. cattleya*. The pyridinal phosphate dependant transaldolase responsible for the biosynthesis has been isolated

and studies have shown that in the absence of *L*-threonine or fluoroacetaldehyde no fluorothreonine is produced.

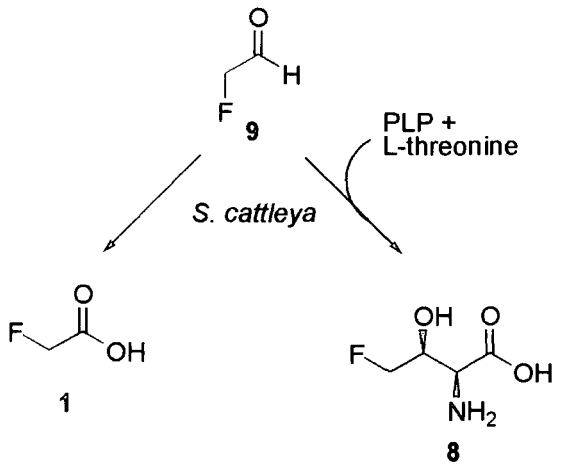

Scheme 1.2: Biosynthesis of fluoroacetate and fluorothreonine

Cell free studies have revealed the nature of biological fluorination in *S. cattleya*[8].

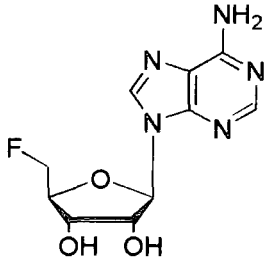

It has been demonstrated that 5'-fluoro-5'-deoxyadenosine **10** (5-FDA), is the product of a fluorinase enzyme, which mediates a reaction between fluoride ion with *S*-adenosylmethionine **11** (SAM), as shown in Scheme 1.3.

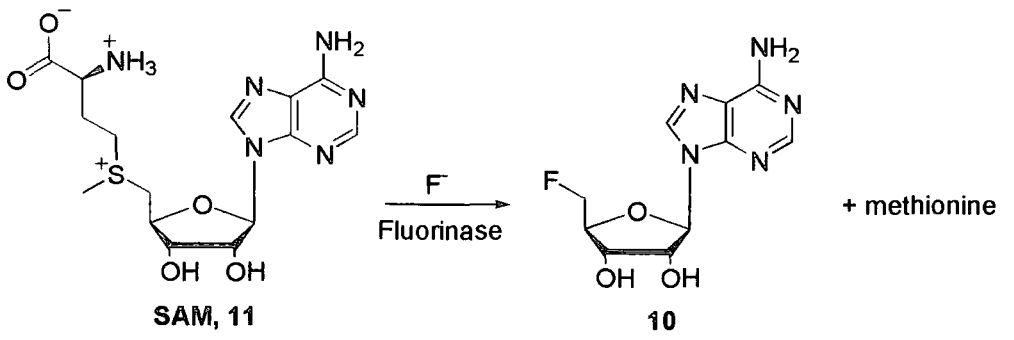

SAM, 11 **10**

Scheme 1.3: The fluorinase reaction in *S. cattleya*

1.3 Fluorine's influence on physico-chemical properties

In spite of nature largely ignoring a role for fluorine, in medicinal chemistry replacement of a hydrogen atom with fluorine is a common tool used to improve the efficacy of a drug target. This approach has been successful due to the changes in the physico-chemical properties of the target molecule caused by the introduction of the fluorine atom.

1.3.1 Steric influence of fluorine

When hydrogen is substituted with fluorine it has long been recognised that the steric impact of this change is very small. The precise size of a fluorine atom in relation to other substituents is a controversial issue and various tables of comparative data exist. For instance, Schlosser and Michel[9] report the following data for comparison between hydrogen, fluorine and other substituents.

Table 1.1: Comparison of Van der Waals radii

X	H	F	O	N
Van der Waals Radii, Å[10]	1.29	1.47	1.52	1.55

Table 1.1 shows that while fluorine is the smallest substituent after hydrogen, its steric influence is expected to be closer to that of oxygen at first glance, as they have very similar Van der Waals radii. However, measurement of Van der Waals radii is not the only factor when considering steric crowding in a molecule as this may also be influenced by interatomic attraction and repulsion.

The steric parameter devised by Charton[11] aims to link the Van der Waals radii to kinetic data obtained from rates of ester hydrolysis.

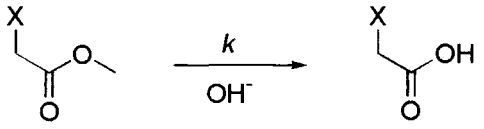

Table 1.2: Comparison of steric parameters

X	H	F	CH_3	CF_3
υ	0.00	0.27	0.52	0.91

Table 1.2 shows that for the groups studied the steric influence of fluorine is again closer to the hydrogen atom than the other substituents.

A generally appreciated method for measuring steric effects of substituents is to measure the energy required for conformational transformations to occur. This has been studied for various substituents on the cyclohexane moiety for the transitions between the equatorial and axial conformers, generally termed "A values".

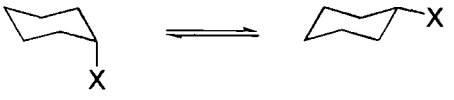

Table 1.3: Comparison of $\Delta G°$ for conformational transformations

X	H	F	OCH_3	CH_3	$CH(CH_3)_2$	CF_3
$\Delta G°_{ax/eq}$ (kcal mol^{-1})	0.00	0.15[12]	0.65[13]	1.7[8]	2.1[8]	2.4[14]

It is clear from Table 1.3 that fluorine and hydrogen have the closest steric match.

Another demonstration of the steric similarity between hydrogen and fluorine has been illustrated using scanning tunnelling microscopy (STM)[15] to investigate the two-dimensional packing of mono-fluorinated stearic acids deposited on graphite. STM analysis indicates that very little packing disorder is observed when fluorine replaces

hydrogen, which confirms that hydrogen and fluorine can be considered closely isosteric.

1.3.2 Electronic effects of fluorine

While the steric requirements of fluorine and hydrogen have been demonstrated to be similar the electronic nature of the two atoms is very different. The higher electronegativity of fluorine over hydrogen renders them very different in this regard and hence the subsequent reactivity of a molecule can change dramatically on replacing hydrogen for fluorine.

1.3.2.1 Anomeric effect

The anomeric effect[16], which has been widely discussed in carbohydrate chemistry, can be rationalised by the donation of electron density arising from oxygen non-bonding electrons into a C-O anti bonding σ* orbital. This stereoelectronic effect preferentially stabilises the axial conformer.

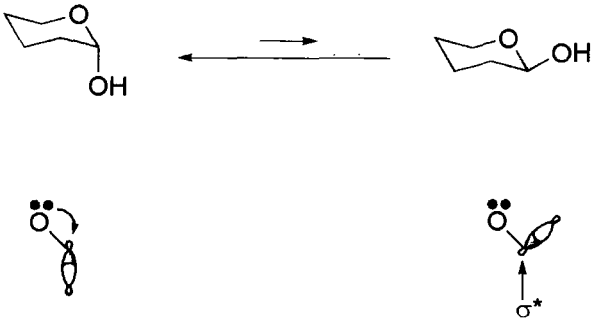

Figure 1.2: Anomeric effect

This effect is also observed for fluorine. For example the preferred conformation of fluoropyran has the C-F bond axial[17] as illustrated in Figure 1.3.

Figure 1.3: Anomeric effect in fluoropyran

In fluoropyran the C-F bond prefers the axial conformation, rather than the perhaps more sterically favoured equatorial conformation. The axial conformation positions the lone pair on the oxygen antiperiplanar to the C-F bond and this allows donation of electron density into the σ* C-F anti bonding orbital.

1.3.2.2 Anh - Eisenstein effect

Anh and Eisenstein[18] originally undertook investigations into the electronic factors involved in nucleophilic attack on carbonyl of an α-chlorocarbonyl compounds. This was extended by Paddon - Row to include the α-fluorine analogues[19]. The latter study investigated the trajectory of nucleophilic attack (CN^-) on the carbonyl of 2-fluoropropanal as shown in Figure 1.4.

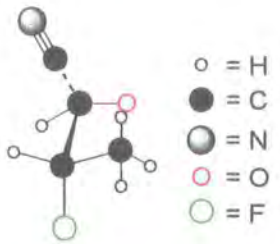

Figure 1.4: Paddon – Row study on nucleophilic attack to a α-fluorocarbonyl

Of the six possible conformations for the intermediate in the above reaction, Paddon – Row found that the orientation depicted in Figure 1.4 was the most stable. They proposed that stabilisation of the transition state during nucleophilic attack involves a number of re-inforcing influences. Two of the most significant influences are stabilisation, *via* donation of electron density from the incoming nucleophile into the C-F σ* orbital, and electrostatic repulsion between the nucleophile and the fluorine atom.

Based on these considerations two diastereomeric transition states can be envisaged for the following reaction where the fluorine and hydrogen atoms are interchanged (Figure 1.5).

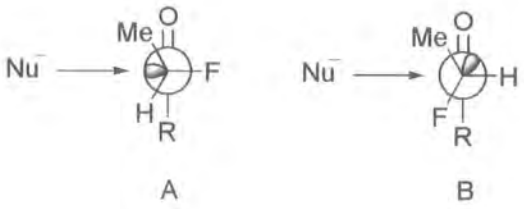

Figure 1.5: C-F σ* in transition states

Transition state A indicates stabilisation by donation of the nucleophile electron density into the C-F σ* orbital. This can only be achieved if the nucleophile approaches *anti* to the fluorine substituent. This trajectory in turn also reduces the electrostatic repulsion between the incoming nucleophile and the fluorine atom. The

transition state arising from conformation A has been calculated to be 7.2 $kJmol^{-1}$ lower in energy than the transition state that arises from conformation B.

1.3.3 Fluorine as a hydrogen bond acceptor

An ongoing discussion in fluorine chemistry is whether organic bound fluorine can take part in hydrogen bonding. In hydrogen bonding, acceptor and donor constituents are required.

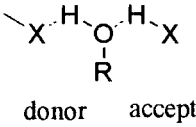

Figure 1.6: Hydrogen bonding interactions showing donors and acceptors

Figure 1.6 shows an alcohol as both an acceptor and a donor. Obviously in the case of fluorine only the acceptor role can be considered, as no acidic hydrogen is available for donation as shown in Figure 1.7.

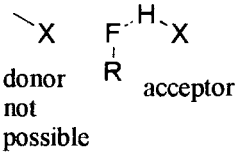

Figure 1.7: Fluorine as a hydrogen bond acceptor

Theoretical calculations[20] have estimated the strength of C-F---H-X interaction to be between 2.0 - 3.2 kcal mol^{-1}, which is about half that of a hydrogen bond to an oxygen atom. This is consistent with the electrostatic influence of fluorine being approximately half that of oxygen[21] and is a reflection of the greater electronegativity and poorer polarisability of fluorine compared to oxygen.

A wide ranging review of X-ray crystal structures in the Cambridge Structural Database System (CSDS) of molecules containing CF, CF_2 and CF_3 groups[22] has revealed F---H interactions up to 3 Å, with mean values being in the range 2.5 to 2.6 Å. This is close to the sum of the van der Waals radii reported in section 1.2.1 and in case where fluorine is argued to be a hydrogen bond acceptor, F---H interactions in the range of 2.00 to 2.30 Å should exist.

A review[23] of the CSDS for F---H contacts of less than 2.35 Å has revealed that short contacts between fluorine and hydrogen do occur but they are infrequent, with only 40 examples being found, and where they do exist they always involve interaction with the hydrogen of hydroxyl or amino compounds. From this information it can be

concluded that organic bound fluorine forms hydrogen bonds to acidic hydrogens but that this interaction is weak and is usually overridden by other intermolecular packing forces in the solid state.

1.4 Pharmaceutical development of fluorinated compounds

Recently there have been many examples of fluorine containing compounds being developed as new chemical entities in the pharmaceutical industry. Reviews[24] have highlighted several important therapeutic areas and modes of action of fluorine containing compounds. Some of the most important compounds are shown in Figure 1.8

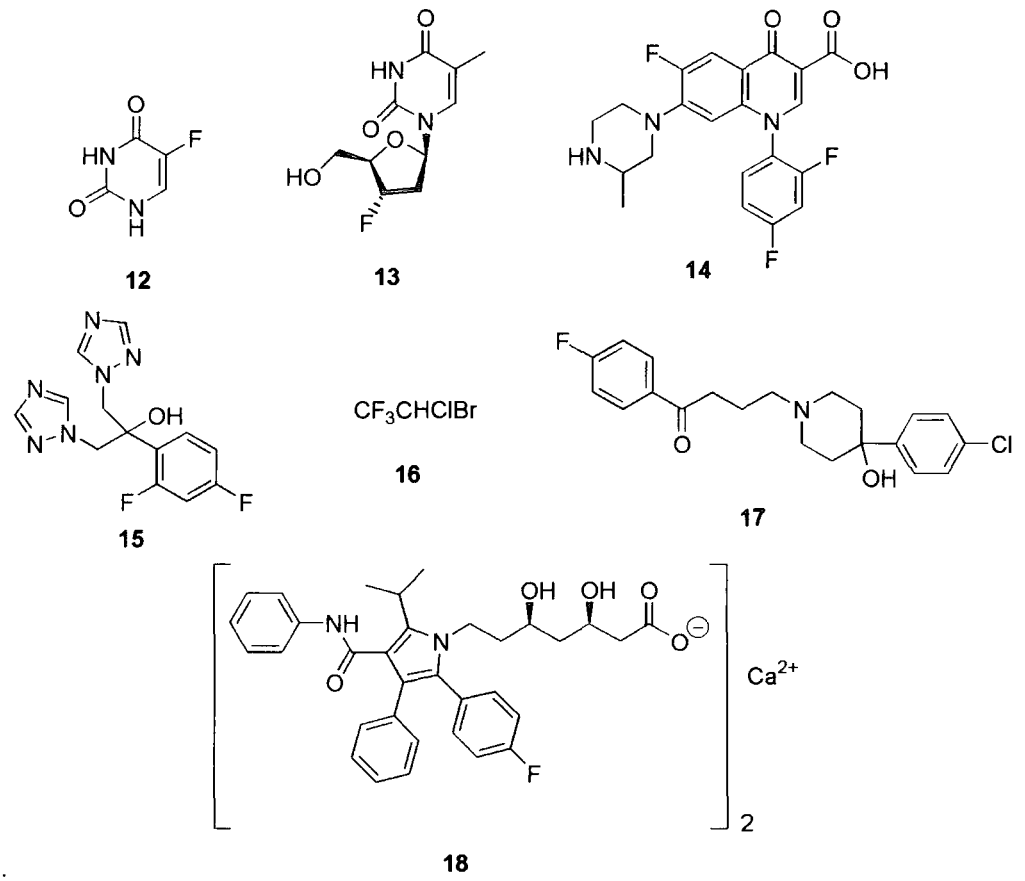

Figure 1.8: Fluorinated pharmaceuticals

Perhaps the best-known fluorine containing pharmaceutical is the anticancer agent 5-fluorouracil, **12**. This molecule is successful as it incorporates a deceptor fluorine. This leads to enzyme inhibition, which blocks thymidylate synthase, the enzyme involved in converting uracil to thiamine in DNA biosynthesis. Thymidylate synthase is extremely active in tumour growth and many variations have been developed to

inhibit this enzyme, leading to molecules with higher efficacy or ones that have been specifically tuned for certain types of tumour.

Fluorine substitution has opened up many opportunities for compounds with antiviral, antibacterial and antifungal properties. Examples are 3-fluorothymidine **13**, which has been studied for its ability to inhibit human immunosuppressive virus-1 (HIV-1) replication. In the field of antibacterials, the fluorinated quinolones have become an important addition to the arsenal of physicians, particularly in light of the recent development of resistant bacteria. Temafloxacin **14**, is a typical example of a fluoroquinolone and many variations of this type of molecule exist. Fluconazole **15**, is a major antifungal agent which is effective in the treatment of a broad range of fungal infections and again other examples of fluoro-substituted azoles exist which exhibit similar properties.

The field of anaesthetics was transformed by the introduction of halothane **13.** It was one of the first anaesthetics developed with minimal side effects and has the key advantage that it is non-flammable.

In the search for drugs that correct central nervous system (CNS) disorders, perhaps one of the best known is haloperidol 17, which is used in the treatment of severely psychotic patients. Without the 4-fluorophenyl group all therapeutic activity is lost. It is postulated that the group increases the lipid solubility, which increases the rate at which the drug is transferred across the blood brain barrier.

The final compound, atorvastatin calcium **18**, is a member of the statin class of drugs, which are used to reduce cholesterol levels. This compound functions by inhibition of the 3-hydroxy-3-methylglutaryl-coenzyme A (HMG-CoA) reductase. This enzyme catalyses the conversion of HMG-CoA to mevalonate, which is an early step in the biosynthesis of cholesterol.

Inspection of the top 100 pharmaceuticals by virtue of number of prescriptions reveals that the most prescribed medicine, atorvastatin calcium, has annual sales in excess of $8B. A further 13 compounds from the top 100 contain at least one fluorine substituent, which supports the fact that fluorine substitution is an important method of improving pharmacological activity of compounds.

1.5 Hydrolytic enzymes

Hydrolytic enzymes are used as catalysts in the hydrolysis of esters and amides to give a carboxylic acid and either the alcohol or amine. The general pathway for the reaction is shown in Scheme 1.4 below.

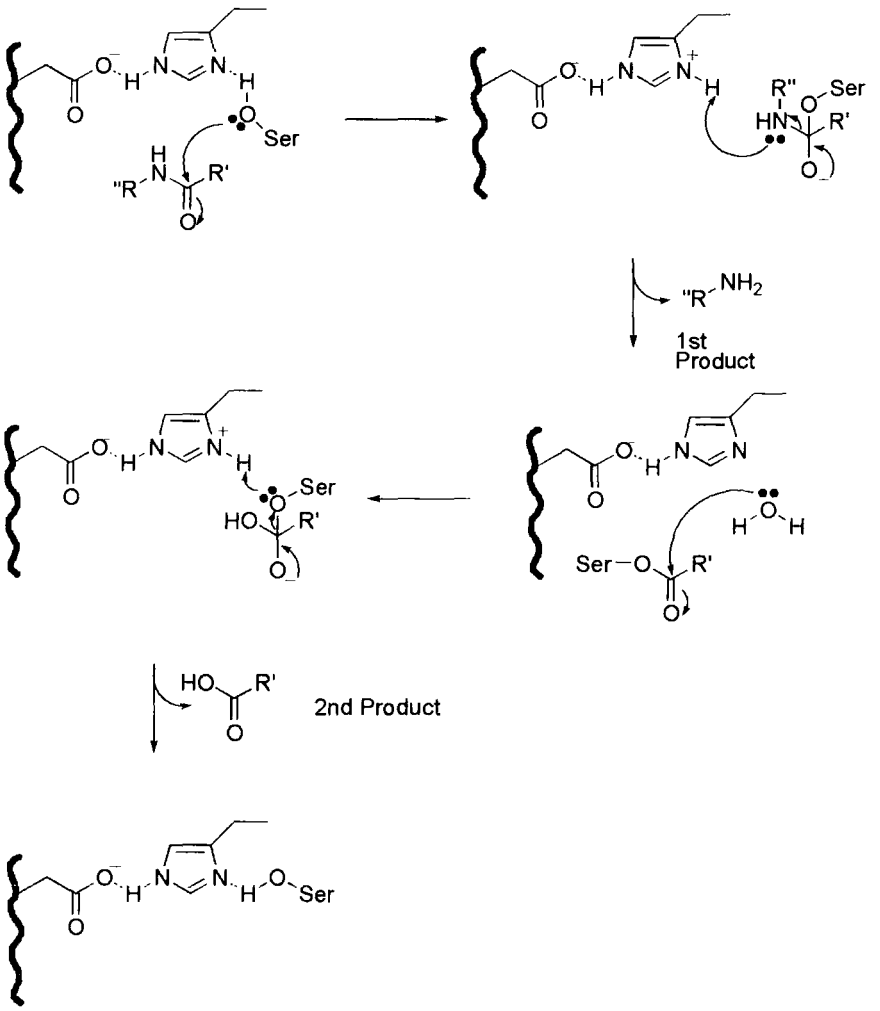

Scheme 1.4: Catalytic hydrolysis of an amide with a hydrolytic enzyme

The first stage in the process is the binding of the substrate to the enzyme. At this time the substrate is forming one or more hydrogen bonds with the enzyme and, depending on the active site, this step can introduce varying degrees of selectivity. The next stage is nucleophilic attack of the serine oxygen on the carbonyl carbon of the substrate. A proton transfer to histidine assists this. The amide bond is then cleaved, again with assisted proton transfer from histidine, to eliminate the first product. Nucleophilic attack on the remaining substrate by water produces the second carboxylate product, while at the same time restoring the enzyme to its initial state.

Enzymes are naturally occurring catalysts, with the most common sources being from animal organs (e.g. pig liver esterase) and bacteria (eg *Aspergillus melleus* and *Pseudomonas fluorescens*). It has long been known that the way the substrate interacts with the enzyme is controlled by the steric arrangement of the molecule. An active site model for Pig Liver Esterase (PLE)[25] has been developed which has helped rationalise the outcome of reactions involving this enzyme. The model shown in

Figure 1.9 displays the four binding regions of the enzyme. Two are hydrophobic and these interact with the aliphatic or aromatic part of the substrate. They are depicted H_L and H_S and can accommodate different sized substituents. The remaining binding regions interact with polar groups present in the substrate and they are denoted as P_F (Front) and P_B (Back).

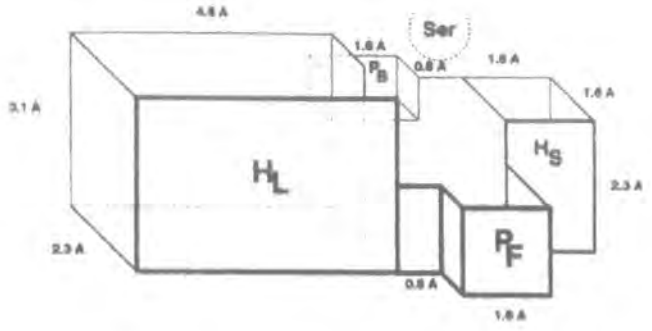

Figure 1.9: PLE active site model

The above model can be used to rationalise the enantiomeric selectivity exhibited in the hydrolysis of esters. The ester carbonyl must locate next to the serine residue while the other substituents will locate based on their size and electronic compatibility. It can clearly be seen that certain orientations of substrates will be favoured over others.

The reaction becomes particularly useful if a chiral or prochiral centre exists in the ester or amide starting material. If this is the case then the reaction may proceed in a stereoselective manner yielding optically pure products. Examples of this approach include the production of α-aryl-α-hydroxyacetates in high enantiomeric excess using pig liver acetone powder (Scheme 1.5), a crude form of pig liver esterase (PLE)[26], and the production of optically pure amino acids from their N-acyl derivatives[27] using acylase I (Scheme 1.6).

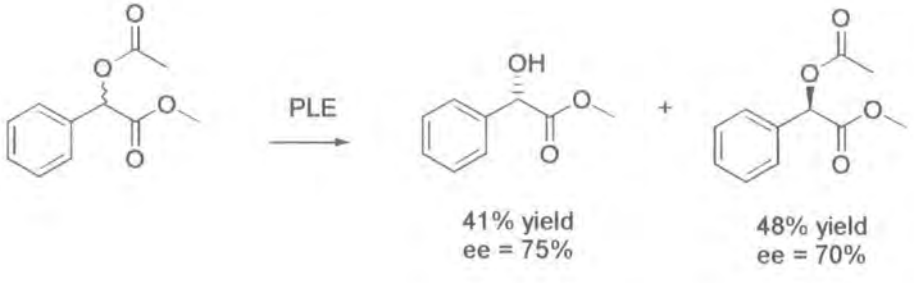

Scheme 1.5: Production of α-aryl-α-hydroxyacetates using PLE

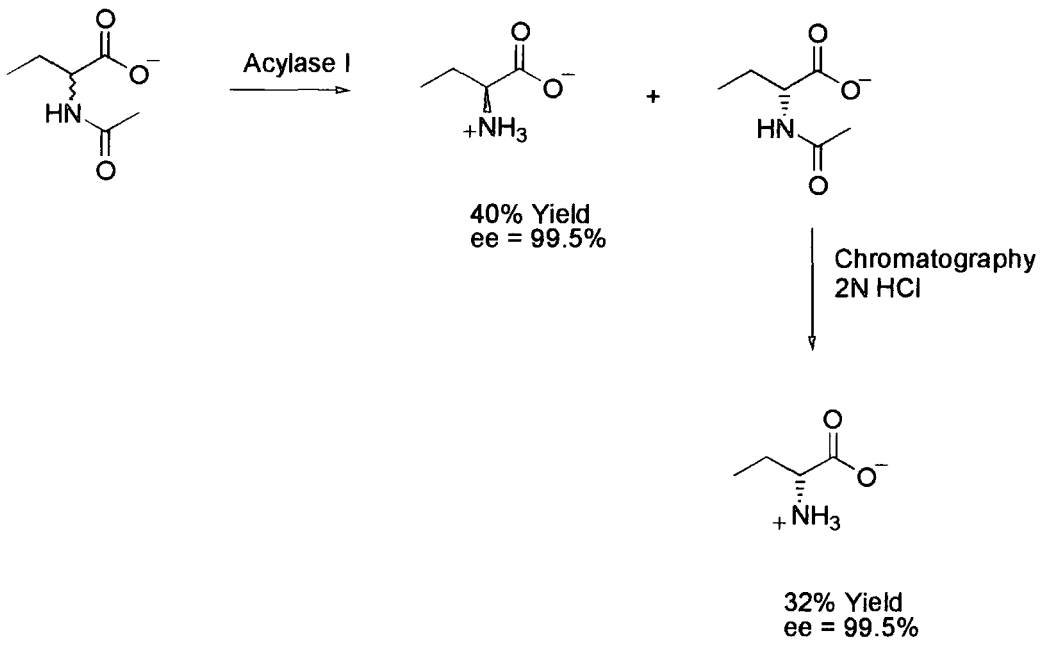

Scheme 1.6: Production of stereochemically pure amino acids using acylase I

There are numerous examples of similar enzymatic resolutions[28]. The experiments described in this thesis were particularly focussed on how the substitution of fluorine would influence the outcome of these hydrolytic reactions.

1.6 Effect of fluorine on enzyme hydrolysis reactions

1.6.1 Electronic effects of fluorine in enzyme hydrolysis reactions

Despite their similar sizes, it has been shown that lipase enzymes can distinguish between fluorine and hydrogen atoms when substituted α to a carboxylate group of an ester. For example, the MY lipase can preferentially hydrolyse one enantiomer of diethyl fluoromalonate[29] at a much greater rate than the other and the resultant product, (*R*)-2-fluoromalonic acid monoethylester, **20**, has been isolated with a 99% ee, as shown in Scheme 1.7.

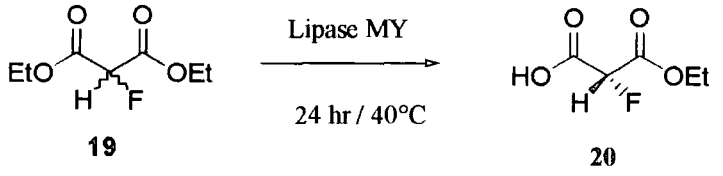

19 **20**

Scheme 1.7: Preferential hydrolysis of one enantiomer of diethyl fluoromalonate

Another example of a similar resolution[30] is the hydrolysis of ethyl (*RS*)-2-fluorohexanoate, **21**, which liberates the residual ester, ethyl (*R*)-2-fluorohexanoate, **22**, with a 99.9 % ee and generates the (*S*)-2-fluorohexanoic acid, **23**, with a 68.5% ee after 60 % conversion as shown in Scheme 1.8.

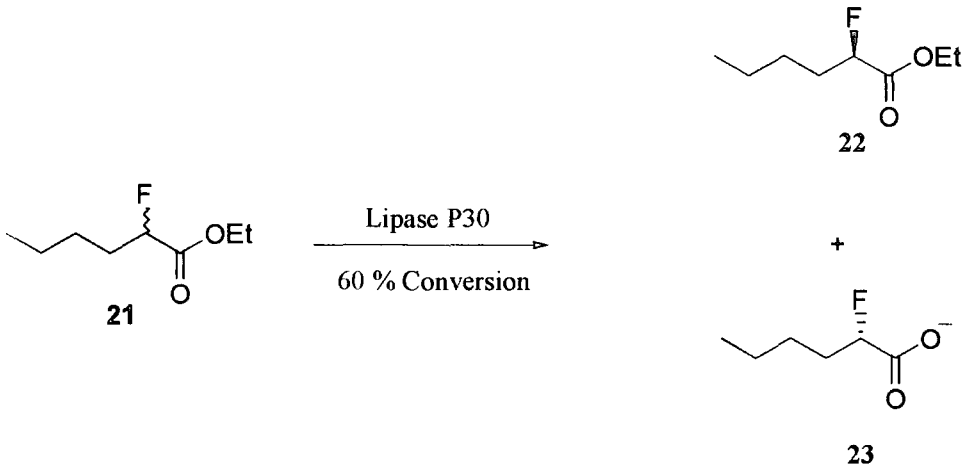

Scheme 1.8: Hydrolysis of ethyl (*RS*)-2-fluorohexanoate

It is difficult to attribute the stereoselectivity observed here to the steric differences between hydrogen and fluorine and the electronic influence of fluorine must be dominating the outcome of the reaction. As discussed in section 1.3 there are two possible transition states. These have the nucleophile approaching either *anti*, A or *gauche*, B to the fluorine atom. The Anh - Eisenstein effect predicts that the nucleophile approaching *anti* to the fluorine will result in the more stable transition state. For the lipase reaction where the fluorine and hydrogen are interchanged the possible transition states for each enantiomer is shown in Figure 1.10

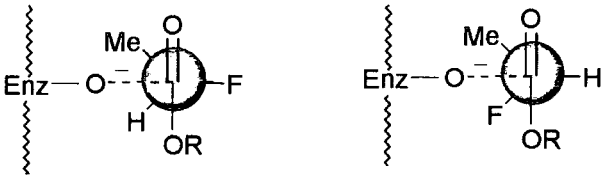

Figure 1.10: Enzyme / α-fluoroester transition states

It can clearly be seen that stabilisation of the intermediate by donation of electron density into the C-F σ* can only be achieved if the nucleophile approaches *anti* to the fluorine substituent, this in turn will also reduce the electrostatic repulsion between the incoming nucleophile and the fluorine atom.

Ab initio calculations [31] confirm that the *anti* transition state of the α-fluoroester / enzyme transition state is more stable than the *gauche* transition state by 2.8 kcal mol^{-1}. This energy difference in transition states is sufficient to account for the enantiomeric excess observed. The effects described above for the α-fluoroester case could clearly apply to the hydrolysis of a α-fluoroamide by an acylase, and this aspect is explored in this thesis.

1.6.2 Molecular modelling of α-fluoroamides

Clearly transition state energies are important in determining the stereochemical outcome (relative rates) of a reaction. Another important factor in enzyme reactions is the initial conformation of the substrate, as this will also influence the binding of the substrate to the enzyme. It has recently been shown by O'Hagan and Rzepa that α-fluoroamides, such as N-methyl-2-(*S*)-fluoropropionamide **24,** adopt a very definite conformation.

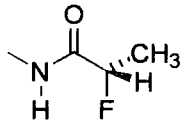

24

This study showed that ~ 5.0 kcal mol^{-1} stabilisation was evident for a single lowest energy conformation[32]. This conformation was found to have the fluorine atom *anti* to the oxygen and *syn* to the hydrogen as shown in Figure 1.13.

It is proposed that the lowest energy conformation is stabilised by stereoelectronic effects in a similar manner to the Anomeric effect discussed for fluoropyran in section 1.3, i.e. donation of electron density from the carbonyl oxygen into the C-F σ* orbital, as shown in Figure 1.11.

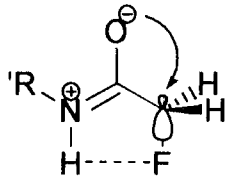

Figure 1.11: Stabilisation of conformation with fluorine *anti* to oxygen

Furthermore it was noticed that the preferred conformation positioned the fluorine and hydrogen in close proximity and this could potentially lead to the formation of a hydrogen bond. Finally, the amide and the C-F dipoles oppose each other and reduce the overall dipole of the amide in this conformation as shown in Figure 1.12.

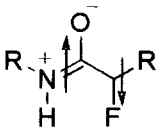

Figure 1.12: Dipoles in α-fluoroamides

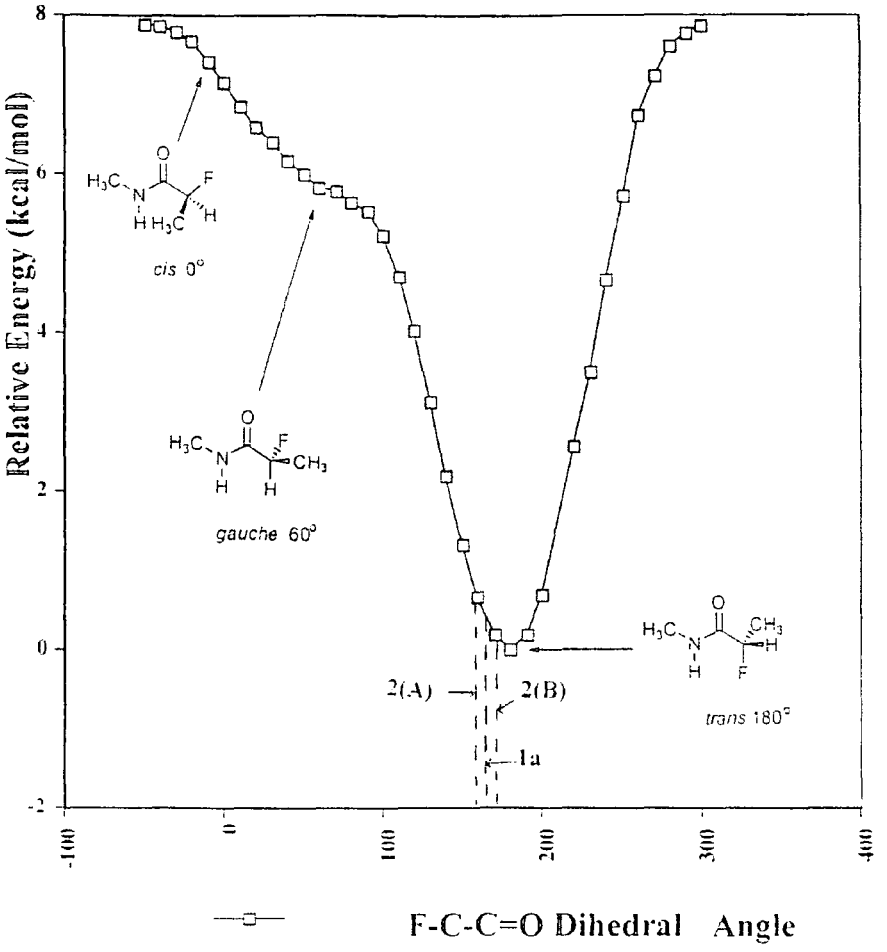

Figure 1.13: Relative conformation energies of **24**

Figure 1.13 indicates that α-fluoroamides fall into a deep energy well with a clear preferred conformation. This energy difference also indicates that **24** will have a very high barrier to rotation and if this substrate were to react with an enzyme it would be this lowest energy conformation that would present itself to the enzyme. The barrier to rotation will have a significant effect on the substrates ability to bind with the acylase as shown in Figure 1.14.

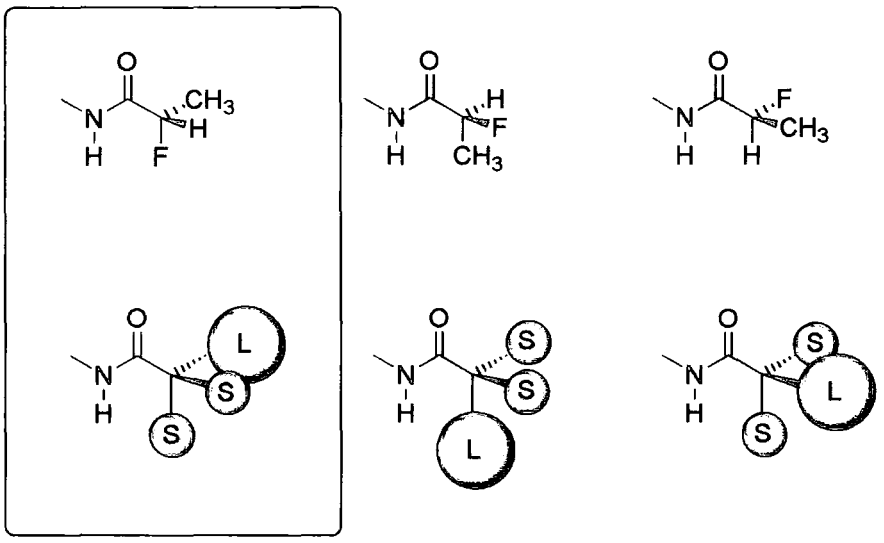

Figure 1.14: Steric requirements for different conformations

Depending on the active site model for the acylase a large, sterically demanding substituent may only be accommodated in one position. If this orientation does not correspond to the lowest energy conformation then the restricted rotation will severely impact on the substrates ability to bind with the acylase.

1.7 Aims and objectives

1.7.1 Effect of fluorine on enzymatic hydrolysis of α-fluoroamides

In this study we were interested in expanding on the lipase hydrolysis of esters to determine if enzymatic hydrolysis of α-fluoroamides could be achieved in an enantioselective manner. This has not been previously explored. It was anticipated that a combination of the Anh - Eisenstein effect (Figure 1.15) and the restricted conformational mobility of α-fluoroamides (Figure 1.16) would contribute to the outcome of the α-fluoroamide hydrolysis reaction and lead to significant kinetic resolutions with acylases.

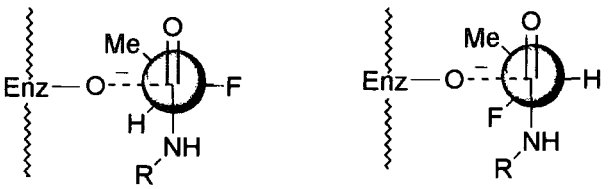

Figure 1.15: Enzyme / α-fluoroamide transition states

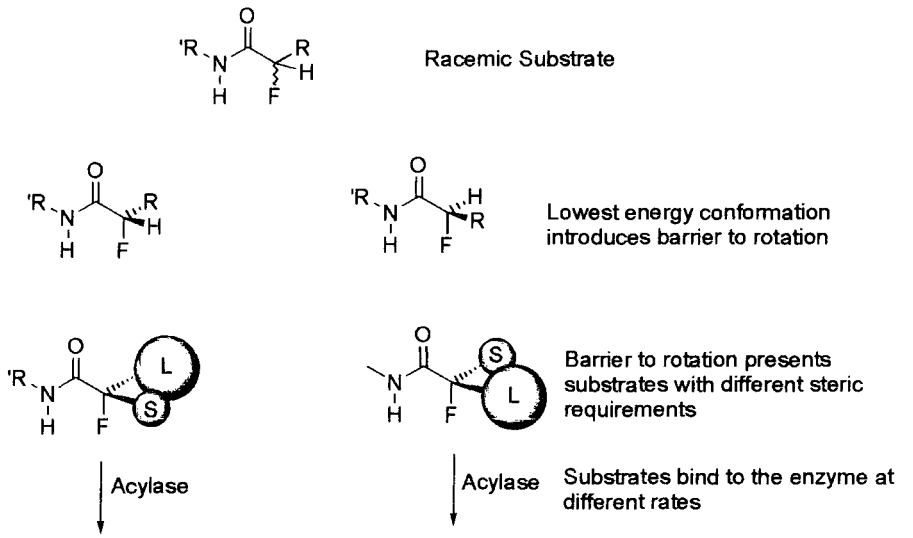

Figure 1.16: Barrier to rotation leading to stereoselectivity

Accordingly the aims and objectives were to:

- Prepare suitable α-fluoroamide substrates.
- Develop an analytical method to monitor enzymatic hydrolysis.
- Screen and identify an enzyme that will mediate a stereoselective hydrolysis.
- Prepare a range of α-fluoroamides and study how the substrate affects the outcome of the hydrolysis.
- Prepare optically pure α-fluoroamides and use these to identify the maximum rate of reaction, V_{max}, and the binding affinity, K_m.

1.7.2 Effect on peptide conformations

Another challenge was to try to prepare an α-fluoropeptide. α-Fluoroamides experience restricted conformational flexibility as discussed above. Thus it was attractive to try to prepare a peptide, such as that shown in Figure 1.17 containing an α-fluoroamino acid residue. Such α-fluoroamino acids or peptides have never been prepared.

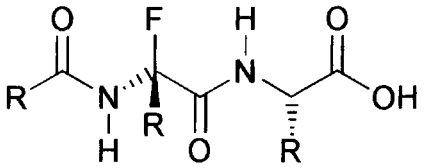

Figure 1.17: α-Fluoropeptide

However, inclusion of a fluorine substituent in a peptide molecule is not trivial as α-fluoroamino acids, such as **25**, are unknown and, for non-fluorinated peptides, amino acids are the standard building blocks.

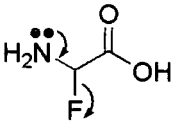

Unstable due to fluoride elimination

25

α-Fluoroamino acids are unstable due to the lone pair on the nitrogen promoting the elimination of F^-. Alternative methods for the preparation of α-fluoropeptides will be investigated, where the nitrogen lone pair is conjugated in such a manner that it is not free to eliminate fluoride in this way. At the outset two synthetic routes were envisaged which seemed to satisfy the above criteria.

The first route involved fluorination of an oxazolone, **26**. Oxazolone **27** holds prospects for further elaboration to α-fluoropeptides.

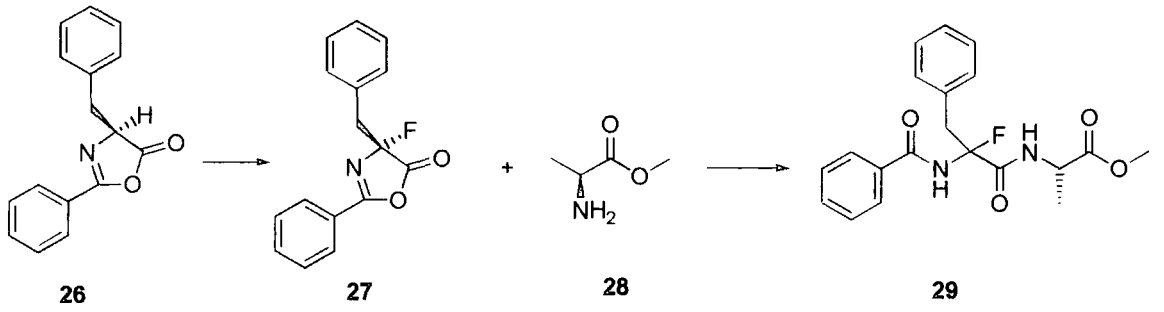

Scheme 1.9: α-Fluoropeptide preparation using oxazolone intermediate

An alternate approach is shown in Scheme 1.10, whereby an α-fluoropeptide is prepared *via*. **32**, following the methodology of Heimgartner.

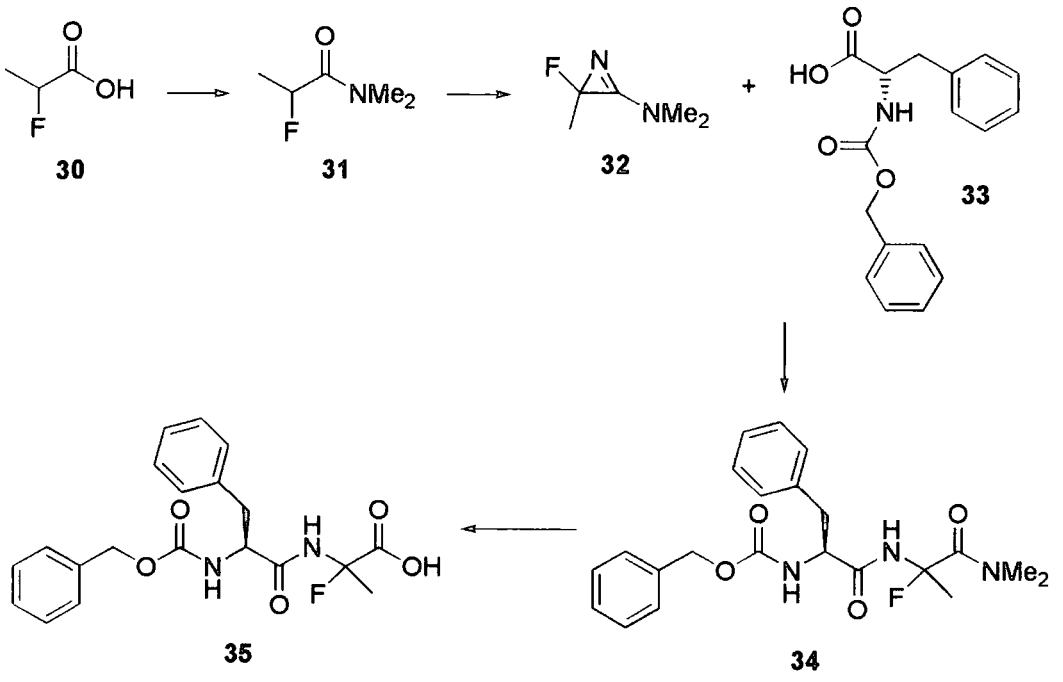

Scheme 1.10: α-Fluoropeptide preparation using aziridine intermediate

These results are discussed in chapter 4.

Chapter 2 - Exploring lipase resolutions of α-fluoroamides

2.1 Rationale for substrate selection

It has been discussed in Chapter 1 that an α-fluoroester can be hydrolysed by a lipase in high enantiomeric purity. In this programme we have extended this to explore the resolution of α-fluoroamides with acylase enzymes.

The initial aim was to identify and synthesise a suitable racemic substrate and a suitable acylase that would stereoselectively catalyse the amide hydrolysis. At the outset N-((*RS*)-2-fluoropropanoyl)-(*S*)-phenylalanine, **36**, was chosen as a candidate substrate for acylase studies.

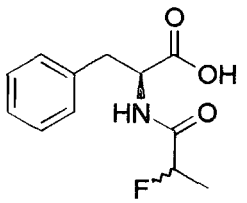

36

The acylated phenylalanine **36** was selected as it provided a challenge to an acylase enzyme to distinguish between diastereoisomers, which differed only by interchanging a hydrogen and a fluorine substituent.

However, it was predicted that the introduction of a fluorine substituent would restrict the rotation of the propionyl moiety, as the lowest energy conformation will have the fluorine *anti* to the carbonyl. Restricting the rotation in this way will then introduce differential binding constants between the diastereoisomers, which may lead to stereoselectivity during hydrolysis.

It was also predicted that having fluorine *anti* to the approaching serine hydroxyl will lead to the most stable transition state and, for reasons explained in the previous chapter, this will be possible for only one of the diastereoisomers due to binding interactions with the enzyme.

N-Acylphenylalanines are expected to be good substrates for a range of acylase enzymes. Also the fluorine atom allows direct observation of the diastereoisomers by ^{19}F NMR, and this provides an excellent analytical basis on which to monitor the diastereoisomer ratio throughout the course of the reaction.

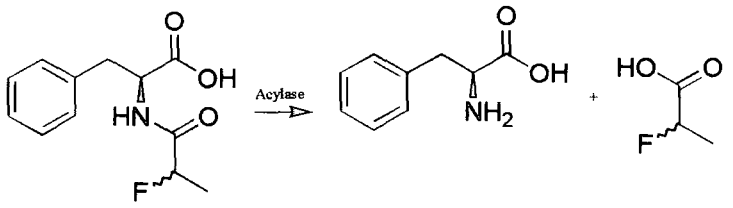

36 **37** **38**

Scheme 2.1: Hydrolysis of **36** with an acylase

Any stereoselectivity exhibited during the hydrolytic reaction will have to be monitored in the residual substrate, as the products of the reaction are phenylalanine **37** and 2-fluoropropionoic acid **38**, both of which only have one stereogenic centre, and so the ability to distinguish stereochemical purity by ^{19}F NMR is lost.

N-((*RS*)-2-Fluoropropionyl)-(*S*)-phenylalanine was also selected as it is derived from the amino acid alanine. This has the advantage of being readily available in either enantiomeric series or in its racemic form. The availability of these stereoisomers provided an excellent basis for establishing the absolute stereochemistry of residual substrates and products as synthetic standards / references could be prepared.

2.2 Synthesis of N-((*R,S*)-2-fluoropropanoyl)-(*S*)-phenylalanine

Various methods for the preparation of **36** were considered but Scheme 2.2, shown below, appeared to offer the most promising route at the outset.[33]

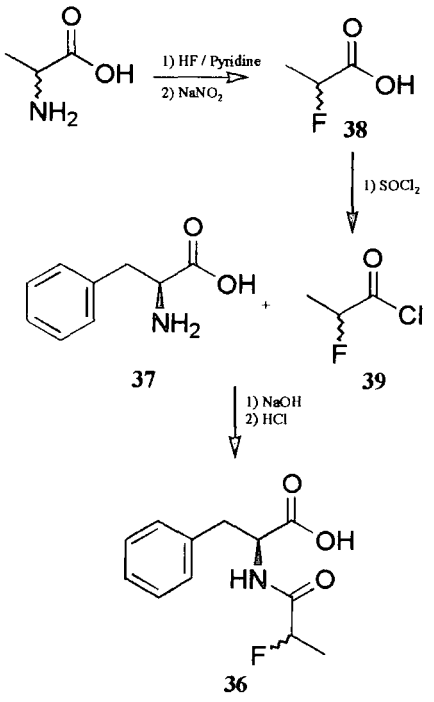

Scheme 2.2: Proposed Synthetic Route to **36**

2.2.1 Diazotisation / fluorination of alanine

The first step in the synthetic sequence involved a diazotisation of the amino acid alanine. Olah[34] has shown that diazotisation reactions of α-amino acids to generate α-hydroxy acids proceed predominantly with retention of stereochemistry, as shown in Scheme 2.3.

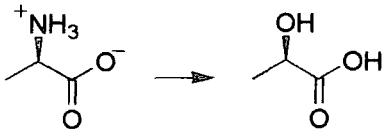

Scheme 2.3: Diazotisation / hydrolysis of α-amino acids

This retention of stereochemistry, which is perhaps counter intuitive, is afforded by the anchiomeric assistance of the carboxylate group as shown in Scheme 2.4. Essentially there are two sequential reactions. The first generates an α-lactone after carboxylate displacement of nitrogen (N_2). The second involves ring opening of the α-lactone by water. Each involves an S_N2 inversion, which leads to overall retention of stereochemistry in this substitution reaction.

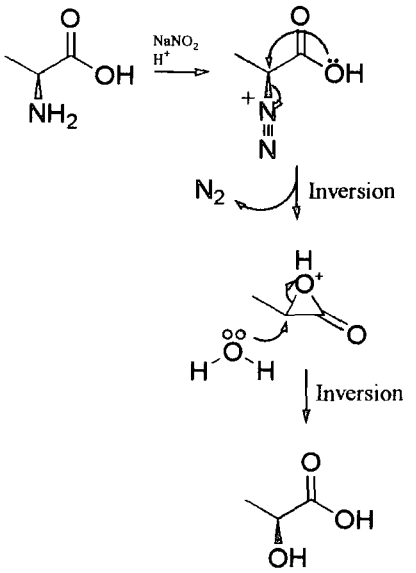

Scheme 2.4: Anchiomeric assistance by carboxylate explains retention of stereochemistry

Although there is a clear dominance of product with retained stereochemistry, Rétey has indicated that there can be a significant level of stereochemical scrambling in these reactions[34]. Diazotisation reactions involve the formation of an R-N_2^+ group, which is an excellent leaving group for any subsequent nucleophilic attack. The reactive species is N_2O_3, which is generated as shown in Scheme 2.5.

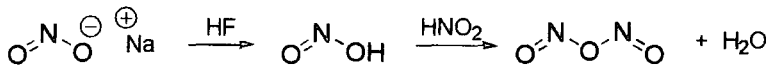

Scheme 2.5: Formation of N_2O_3 from $NaNO_2$ and HF

N_2O_3 then reacts with the amine moiety of the amino acid to generate the diazonium species as shown in Scheme 2.6.

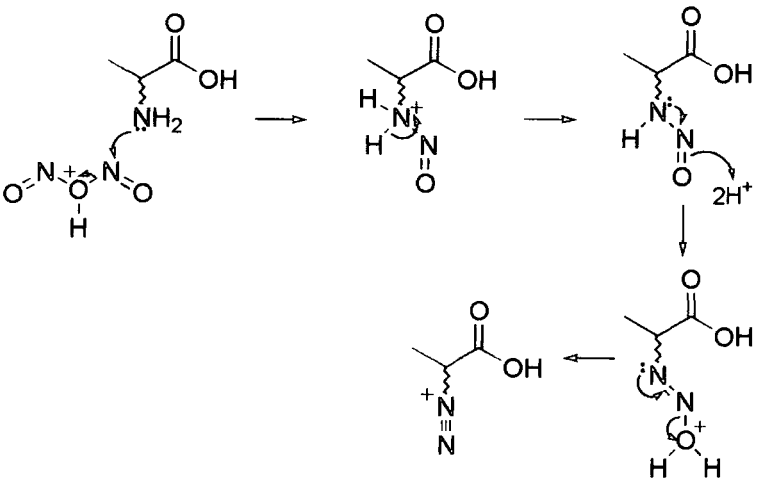

Scheme 2.6: Diazonium salt formation during diazotisation

The final stage of the reaction is a nucleophilic substitution by fluoride ion to generate the desired product, **38**. At this stage there are two possible reaction pathways, one of which leads to an overall inversion of configuration and the second, by means of a double inversion, leading to an overall retention of configuration, as shown in Scheme 2.7.

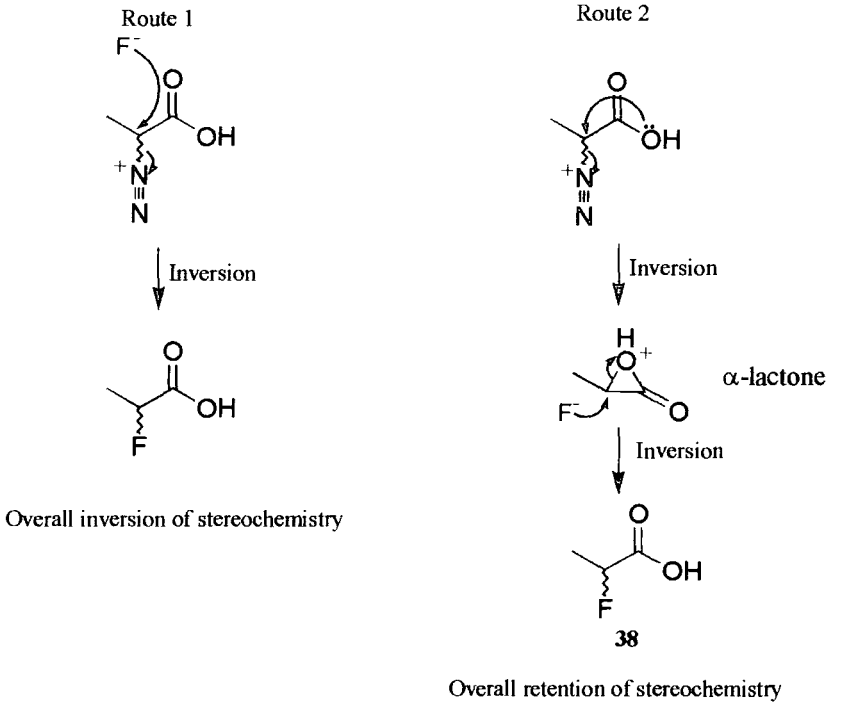

Scheme 2.7: Nucleophilic Substitution by F^-

At this stage little was known about the stereochemical integrity of the fluorination reaction with alanine but this has been explored later in this study using enantiomerically pure starting materials.

2.2.1.1 Other synthetic issues

Initially the conditions suggested by Olah *et al* (1.5 equivalents of sodium nitrite to amino acid, for 4 hours at room temperature)[34a] were used, however the yields were found to be low and variable. Also a side reaction, which generated an α,β-unsaturated product, was evident in the ^{1}H NMR spectrum. This was possibly caused by the elimination of HF from the desired product, giving rise to acrylic acid, **40**.

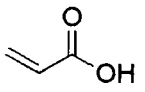

40

After several unsuccessful attempts to reproduce the results achieved by Olah, an alternative method[34b] was tried. This was found to give adequate yields, with no trace of the side reaction. The main difference between the two procedures was the quantities of reagents and the reaction time. Using 3.5 equivalents of sodium nitrite and approximately a 50% reduction in the amount of pyridinium hydrogen fluoride was found to be optimal. Also the reaction time was extended to 16 hours at room temperature.

The anhydride **41** was evident, when monitoring the reaction directly by ^{19}F NMR, as an intermediate in the optimised procedure. Scheme 2.8 shows the likely mechanism for the formation of the anhydride, presumably from activation of the carboxylic acid group by N_2O_3, leading to attack by a second molecule of 2-fluoropropionic acid.

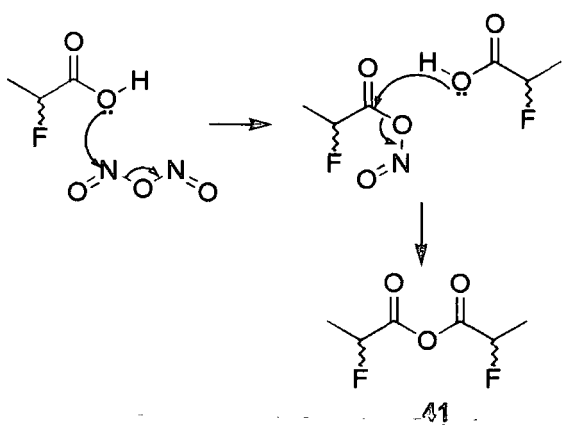

41

Scheme 2.8: Proposed mechanism for anhydride formation

^{19}F NMR clearly shows this anhydride as a pair of diastereoisomers resulting from the *RS* / *SR* and *RR* / *SS* stereoisomers. In optimised experiments the typical ratio of carboxylic acid to anhydride was 8 : 1 as shown in Figure 2.1.

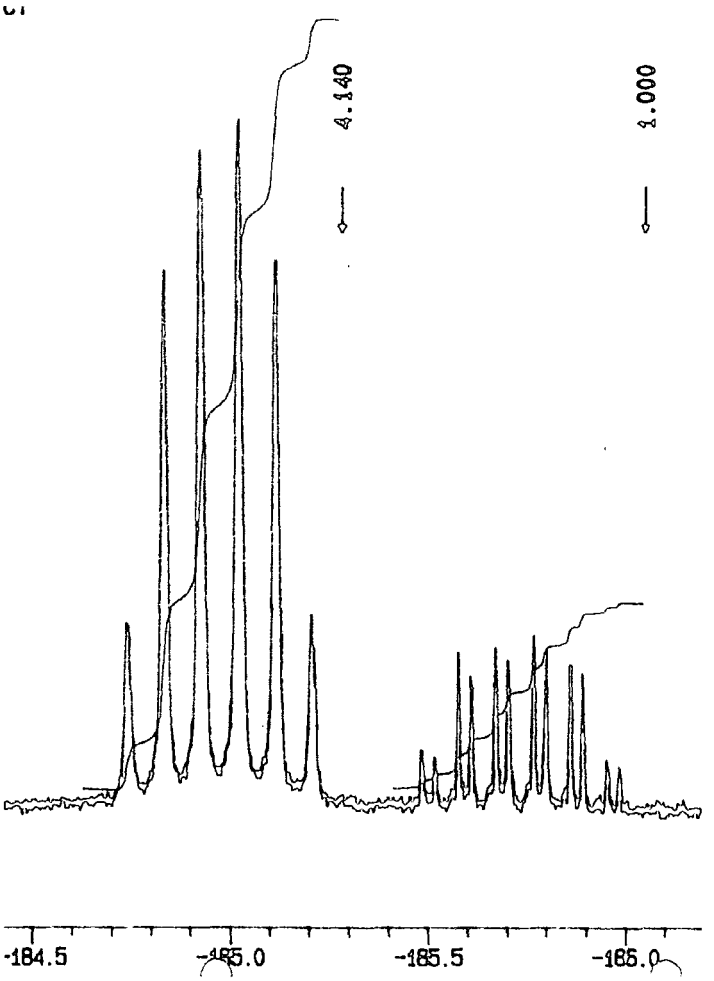

Figure 2.1: ^{19}F NMR of 2-fluoropropionic acid **37** and anhydride **41** in an 8 : 1 ratio

The expected NMR spectrum for 2-fluoropropanoic acid, **37**, is a doublet of quartets but due to overlapping signals only six peaks are seen. The anhydride, **41**, has a more complex ^{19}F NMR spectrum as this is a mixture of diastereoisomers. Each diastereoisomer should exhibit a doublet of quartets and therefore sixteen peaks would be expected, but again due to overlapping signals only twelve peaks are evident.

Impurity **41** was not a cause for concern as the following step was to generate the acid chloride by reaction with thionyl chloride, and the anhydride was anticipated to undergo reaction to the desired acid chloride.

The resultant crude product was purified by vacuum distillation (B. Pt. 66°C @ 13mm Hg), following Olah's method[34a].

2.2.2 Preparation of (*R*, *S*)-2-fluoropropanoyl chloride, 39

Acid chlorides are classically prepared directly from carboxylic acids by their reaction with thionyl chloride,[35] generating sulphur dioxide as a gaseous by-product, so leaving the desired product. Scheme 2.9 shows a possible mechanism for the production of the acid chloride by this method.

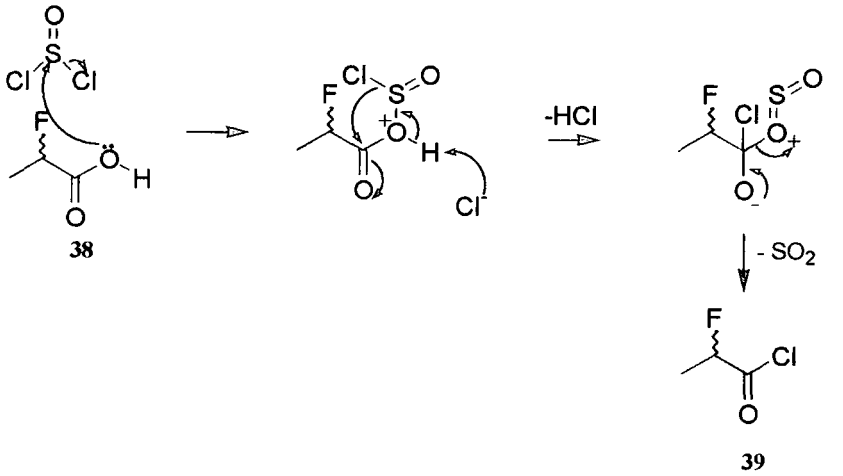

38 39

Scheme 2.9

Initial investigations of this reaction were carried out on a small scale in deuterated chloroform (2 mL). A stoichiometric quantity of thionyl chloride was added to the 2-fluoropropanoic acid, **38**, and the mixture was heated under reflux for 30 minutes and monitored directly by ^{19}F NMR. Further aliquots of thionyl chloride were added until the starting material was no longer evident (i. e. dq at -186 ppm). For this experiment a three-fold excess of thionyl chloride was required to consume all of the acid **38**. At this point a new ^{19}F NMR signal became apparent at -171 ppm (dq), which was subsequently shown to correspond to the desired acid chloride as shown in Figure 2.2.

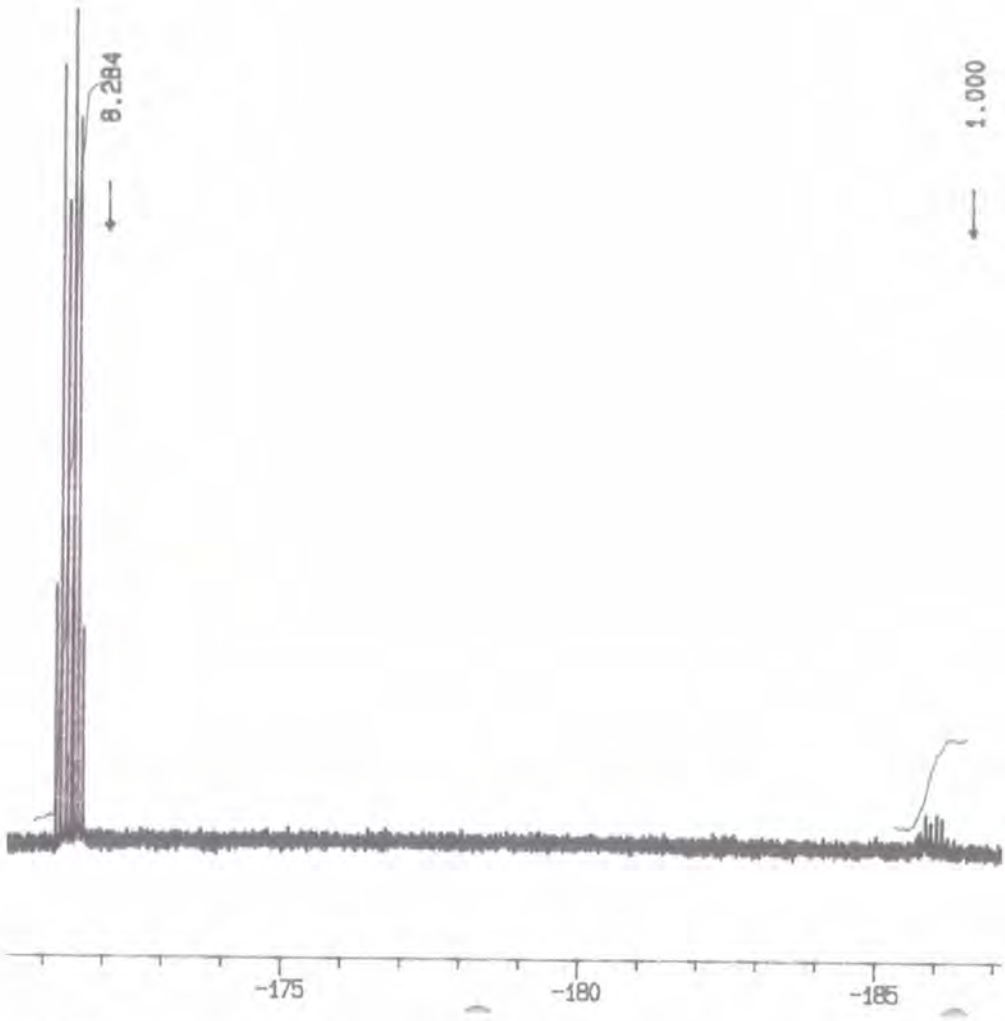

Figure 2.2: The reaction of 2-fluoropropanoic acid, **38** with thionyl chloride

As the level of water present in the acid **38** was variable, different amounts of thionyl chloride was required for each reaction. The method for controlling the addition of thionyl chloride involved dropwise addition at ambient temperature until the vigorous reaction had ceased. Then a stoichiometric amount of thionyl chloride was added and heated to reflux to react with acid **38**. Finally, distillation at atmospheric pressure was carried out to remove any residual acid **38**, to give the desired acid chloride, **39**.

2.2.3 Preparation of N-((*R, S*)-2-fluoropropanoyl)-(*S*)-phenylalanine

Scheme 2.10 shows the preparation of N-((*RS*)-2-fluoropropanoyl)-(*S*)-phenylalanine, **36** from (*S*)-phenylalanine and 2-fluoropropionyl chloride, **39**.

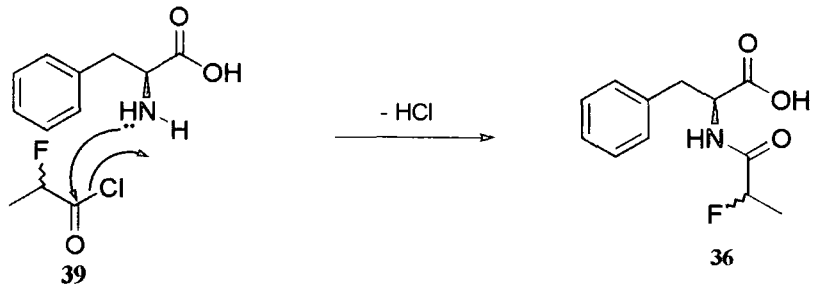

39 36

Scheme 2.10: Preparation of N-((*RS*)-2-fluoropropanoyl)-(*S*)-phenylalanine, **36**

Zabicky and Chenault *et al* have discussed the direct coupling of acid chlorides to phenylalanine.[36] The reaction was initially investigated using propionyl chloride and this proceeded in a straightforward manner producing a colourless oil. When the oil was triturated with hexane it generated the amide as a white crystalline material **42**.

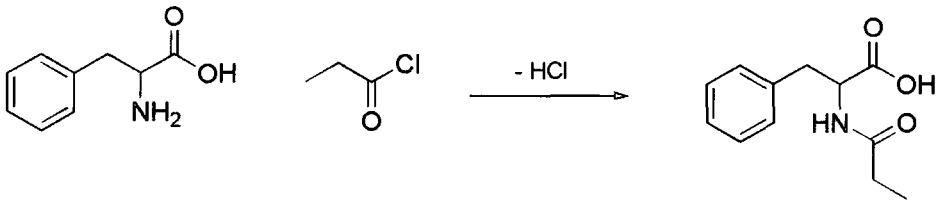

42

Scheme 2.11: Preparation of N-propanoyl-(*S*)-phenylalanine, **42**

When acid chloride **39,** was used the reaction with (*S*)-phenylalanine generated a mixture of products. This included the desired diastereoisomeric mixture N-(*RS*)-2-fluoropropanoyl-(*S*)-phenylalanine **36** but the major product was (*RS*)-2-fluoropropanoic acid **38**. Attempts to reduce the level of **38** involved carrying out the reaction with reduced solvent volumes. This proved successful and suppressed the formation of **38**, yielding the amide, **36** as a colourless oil. This material was essentially pure, as judged by ^{1}H and ^{19}F NMR analysis. A white solid was obtained and recrystallised from ethyl acetate / hexane but unfortunately an X-ray crystal structure of **36** could not be obtained as the product was not sufficiently crystalline.

2.3 Identification of a selective hydrolytic enzyme

As already described in chapter 1 there are many examples of enzymatic hydrolysis of amides. However, to date there have been no examples reported where the amide contains an α-fluorine. The steric impact of substituting fluorine for a hydrogen atom has been demonstrated to be minimal making this a challenging substrate for the

enzyme. It is unknown if an enzyme can distinguish between hydrogen and fluorine in such a system.

2.3.1 Enzymatic hydrolysis protocol

2.3.1.1 Substrate solution preparation

Before any reactions with enzymes could be carried out, the N-acylphenylalanine **36**, had to be converted to a water-soluble form. This was achieved by converting the carboxylic acid to its sodium salt, by taking an aqueous suspension to pH = 7 with dilute NaOH.

2.3.1.2 Enzyme preparation

A number of acylases were selected for this study. These were hog kidney acylase (HKA), *Aspergillus melleus* acylase (AMA), *Bacillus icheniformis* protease (BIP) and the *Streptomyces caespitrum* protease (SCP).

The selected acylases were prepared to varying concentrations in pH 7 phosphate buffer depending on the quoted activities for their reaction rates with N-acetyl-L-methionine, i.e. the higher activity enzymes had the lower concentration solutions. The aim of adjusting the enzyme concentration was to obtain a reaction rate that could be followed readily by ^{19}F NMR analysis. In this regard reaction times of a few hours are more desirable than a few minutes to give sufficient time to run the analysis. It was important that the composition in the NMR tube would not change significantly over the course of the data collection.

The various enzyme solutions were stored under nitrogen at 0°C until they were required. In this form it was found acceptable to store the solutions over several days without significant loss of activity.

An initial experiment to test the feasibility of using ^{19}F NMR to follow these reactions was carried out using HKA and AMA, both supplied by the Sigma Chemical Company.

The results are shown in Table 2.1 and Table 2.2 below.

Table 2.1: Reaction of HKA with amide **36**

Time (h)	Conversion, % *	d.e. %
0	4.6	2
1	34.4	6
2	59.9	28

Table 2.2: Reaction of AMA with amide **36**

Run 1			Run 2		
Time (h)	*Conversion, %	d.e. %	Time (h)	*Conversion, %	d.e. %
0	5.7	4	0	4.2	-2
0.5	21.2	22	0.5	9.1	6
0.75	24.9	28	1	13.3	18
1.75	39.0	64	3	28.4	30
2.25	45.4	72	5	33.6	36
2.75	45.4	84	7	41.6	70
3.25	47.5	76	24	49.4	78
18.33	57.4	96	168	84.7	100

*Conversion as judged by ^{19}F NMR

In the above tables the values of the d.e. % is reported as measured in the residual substrate. The data revealed a low diastereoselectivity in the reaction with HKA, but in the case of AMA there was a very high differentiation by the acylase for each diastereoisomer. The absolute stereochemistry of the preferred diastereoisomer could not be identified at this stage until substrates of a known configuration were prepared. However, it emerged during this study that ^{19}F NMR was a good analytical technique for following these reactions. The only problematical aspect was that at the lower concentrations, peak integrations were not so reliable. Below a concentration of 9 mM, it was difficult to obtain good signal to noise in the time frame required to follow the reaction progress accurately.

Two further protease enzymes, BIP and SCP were investigated for the hydrolysis of **36**. The results from these studies are tabulated below.

Table 2.3: Reaction of BIP and SCP with amide **36**

Time	BIP		SCP	
(h)	Conversion, %	d.e. %	Conversion, %	d.e. %
0	4.7	0	4.1	0
1	3.8	0	5.0	2
3	4.4	2	5.6	0
168	4.2	0	20.0	0

Both BIP and SCP showed very slow rates of hydrolysis and virtually no selectivity in their reaction with the substrate and therefore no further studies were carried out using these enzymes. It emerged form this initial screen that all of the acylases were competent to hydrolyse amide **36**, but only AMA showed a significant level of diastereoselectivity. This emerged as the most interesting enzyme of those screened and accordingly kinetic data using AMA as the catalyst was evaluated. This is discussed in section 2.5.

2.4 Preparation of configurationally defined substrates

As described above the hydrolysis of N-(*RS*)-2-fluoropropanoyl-(*S*)-phenylalanine, **36**, with *Aspergillus melleus* acylase (AMA) displayed a high degree of diastereoselectivity. It was desirable at this stage to prepare a sample of each of the diastereoisomers shown in Figure 2.3, to examine their rates of hydrolysis independently. This was judged necessary to quantify the influence that the different absolute configurations of the fluorine atom were having on the rate of the hydrolysis.

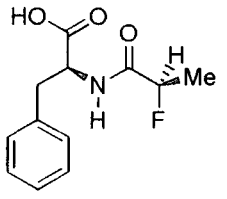

(S, R) **36**

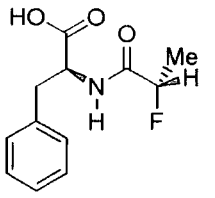

(S, S) **36**

Figure 2.3: The diastereoisomers of **36**

Pure diastereoisomers of **36** were synthesised using the same methodology as previously described for 2-fluoropropionic acid, but this time the stereochemically

pure D-(*R*)-alanine and L-(*S*)-alanine were used as the starting materials for the diazotisation reaction.

Access to the stereochemically pure α-fluoroacids and amides also presented an opportunity to explore the stereoselectivity of the diazotisation / fluorination reaction to prepare the α-fluoroacids. With configurationally pure starting materials the extent of stereochemical scrambling could be assessed.

2.4.1 Stereochemical study of the diazotisation / fluorination reaction

Two approaches were used and these are described in the following sections.

2.4.1.1 Enantiomeric analysis of 2-fluoropropionic acid by a chiral base method

The chiral base used for this study was (*S*)-2-(diphenylmethyl)pyrrolidine, **43**, a base previously developed in the research group for NMR analysis of chiral acids. This pyrrolidine when treated with racemic 2-fluoropropanoic acid **38**, generated two diastereoisomeric salts, **44**, which could be resolved by ^{19}F NMR as shown in Scheme 2.12.

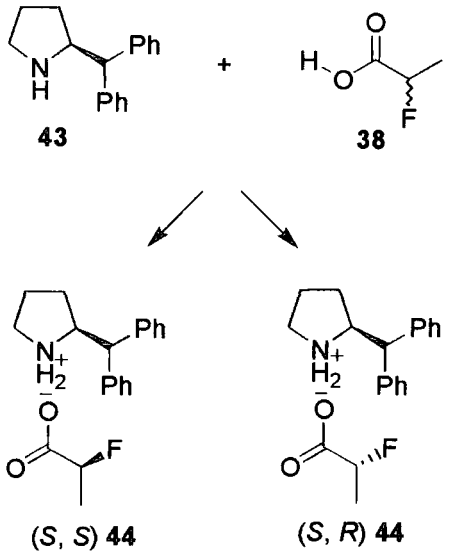

Scheme 2.12: The diastereoisomeric salts of **44** for ^{19}F NMR enantiomeric analysis

The two diastereoisomers were detected as two resolved sets of signals in the ^{19}F NMR spectrum as dq at −173.96 ppm and at -174.16 ppm respectively.

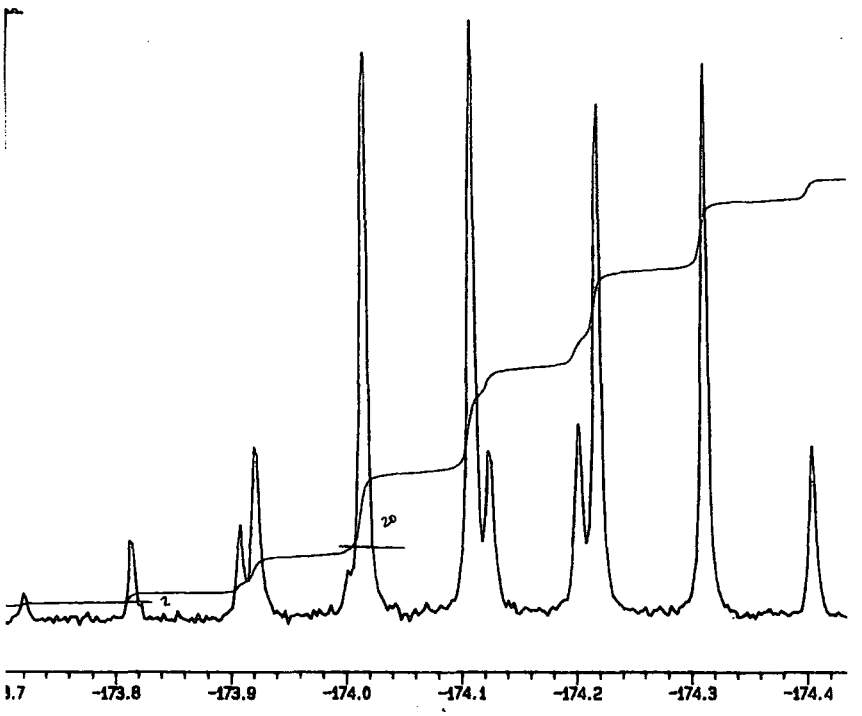

Figure 2.4: ^{19}F NMR analysis of a 10:1 mixture of the diastereoisomeric salts of 44

When 43 was reacted with (*S*)-2-fluoropropionic acid, prepared from L-(*S*)-alanine, the ^{19}F NMR showed a major (dq at -174.16ppm) and a minor signal (dq at -174.06ppm). Integration demonstrated that the ratio of the two was 10 : 1. This result confirmed that the diazotisation reaction was not completely stereospecific. There was a small, but significant (≈ 10%) contribution arising presumably from direct substitution of the diazonium group by fluoride ion, leading to a product resulting from inversion of configuration.

2.4.1.2 Enantiomeric analysis of 2-fluoropropionic acid by preparation of a diastereoisomeric amide

A second method was used to evaluate the stereospecificity of the diazotisation / fluorination reaction. This involved coupling the product of the diazotisation / fluorination reaction of (*S*)-alanine with (*S*)-phenylalanine. The ^{19}F NMR spectrum of the resultant amide (*S, S*) **36** showed two signals, a ddq at -183.35 ppm and a ddq at -183.45 ppm. The peaks were too close to obtain an integration but the ratio was estimated to be in agreement with previous results as shown in Figure 2.5.

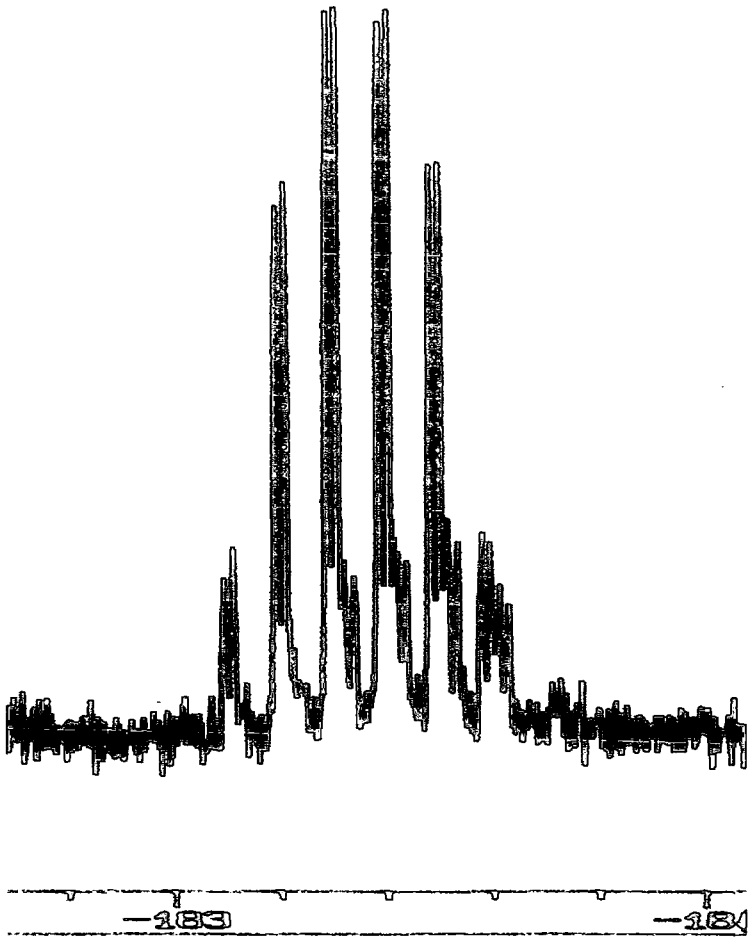

Figure 2.5: ^{19}F NMR of an estimated 10:1 Mixture of (*S*, *S*) **36** and (*S*, *R*) **36**

The complimentary diastereoisomeric amide (*S*, *R*) **36** was also prepared, this time from a sample of the 2-fluoropropionic acid predominant in the (*R*) enantiomer (80% ee). The product again showed two sets of signals in the ^{19}F NMR spectrum at the same chemical shift as discussed above. This time, of course, the ratio was 10 : 1 in favour of the high field signal.

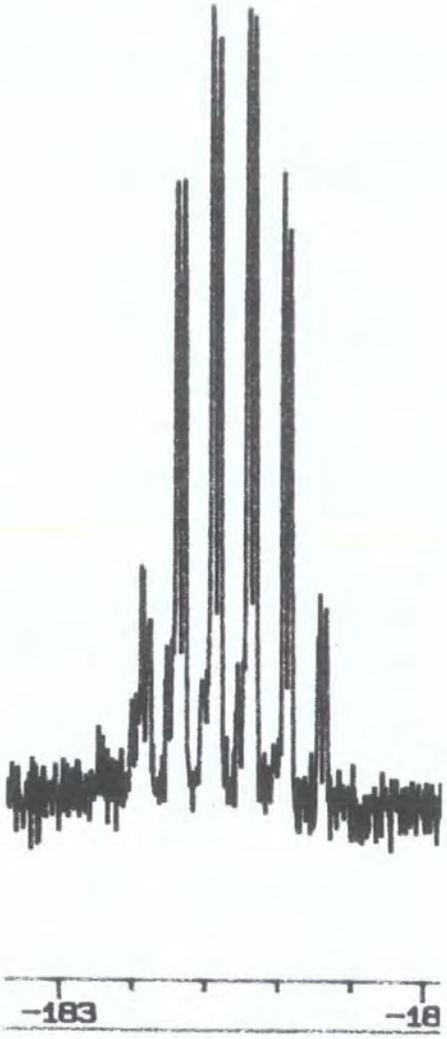

Figure 2.6: ^{19}F NMR of an estimated 10:1 Mixture of (*S*, *R*) **36** and (*S*, *S*) **36**

These results agree well with the results obtained from the enantiomeric analysis using the chiral base, confirming that the diazotisation / fluorination reaction proceeds predominantly with retention of stereochemistry, however, there is a significant (≈ 10%) inversion component.

2.4.2 Purification of the diastereoisomers of 36

As both fluoropropionyl amides, (*S*, *S*) **36** and (*S*, *R*) **36**, were contaminated with the corresponding minor diastereoisomer, purification was desirable prior to exploring these compounds as substrates in acylase reactions. For the slower reacting (*S*, *R*) diastereoisomer **36,** this was achieved in a straightforward manner by using the AMA enzyme to remove the minor (*S*, *S*) diastereoisomer **36**.

However, for the faster reacting diastereoisomer (*S*, *S*) **36,** removal of residual (*S*, *R*) was not readily achievable and it was decided to use this material in the kinetic study

without further purification as the AMA enzyme had already been shown to be almost totally selective in favour of substrate (*S*, *S*) **36** during the hydrolysis of the racemic substrate **36**.

2.5 Kinetic study on stereochemically pure substrates

2.5.1 Enzyme kinetics

In order to compare the two stereoisomers as enzyme substrates it became appropriate to measure their V_{max} and K_m values independently for their hydrolysis with AMA. A discussion of the factors affecting enzyme kinetics by Metzler[37] has been useful in preparing the following summary.

V_{max} is the maximum rate of enzyme turnover, i.e. when the entire enzyme is present as an enzyme / substrate complex and this can only happen when the substrate is present at sufficient concentration to saturate the enzyme. At this substrate concentration

$$V_{max} = \frac{d[P]}{dt}$$

K_m is a measure of binding affinity of the substrate by the enzyme and is the ratio of the sum of the rates of reaction of the enzyme / substrate complex divided by the rate of formation of the enzyme / substrate complex.

This means that for the following reaction:

$$E + S \underset{k_2}{\overset{k_1}{\rightleftharpoons}} ES \xrightarrow{k_3} E + P$$

$$K_m = (k_2 + k_3)/k_1$$

In many cases $k_2 >> k_3$ therefore K_m is related to the binding affinity of a substrate for the enzyme, with higher affinity substrates having the lower values of K_m. Both V_{max} and K_m can be calculated by using the Michaelis - Menten equation which states that:

$$V_0 = \frac{V_{max}}{1 + K_m/[S]} = \frac{V_{max}[S]}{K_m + [S]}$$

The Michaelis - Menten equation can be transformed into several linear forms e.g. Lineweaver - Burk or Eadie - Hoftsee. The Lineweaver - Burk uses the equation:

$$\frac{1}{V_0} = \frac{1}{V_{max}} + \frac{K_m}{V_{max}} \frac{1}{[S]}$$

so a plot of $\frac{1}{V_0}$ against $\frac{1}{[S]}$ would have an intercept of $\frac{1}{V_{max}}$ and a slope of $\frac{K_m}{V_{max}}$.

The Eadie - Hoftsee uses the equation:

$$\frac{V_0}{[S]} = \frac{V_{max}}{K_m} - V_0 \frac{1}{K_m}$$

so a plot of $\frac{V_0}{[S]}$ against V_0 has a slope of $\frac{-1}{K_m}$, a y axis intercept of $\frac{V_{max}}{K_m}$ and an x axis intercept of V_{max}.

From the above two equations it can be appreciated that if we know the initial concentration of the substrate and can monitor the reaction course by following either the decrease in the concentration of substrate or the increase in the concentration of the products we can calculate the V_{max} and K_m values for the AMA enzyme and a given substrate.

2.5.2 Reaction Rate Measurement

Initially, U.V. spectroscopy was explored as a method for following the reaction but, unfortunately, due to absorbance by the AMA enzyme, insufficient intensity of signal could be detected to follow the reaction progress. As ^{19}F NMR had already been successful in monitoring the degree of diastereoselectivity of the AMA enzyme for the mixed substrate, it seemed appropriate to use ^{19}F and ^{1}H NMR to monitor the reaction progress.

The minimum concentration that the reaction substrate could be observed in 64 scans was found to be around 8 mM, but for the slower reacting substrates the NMR acquisition time could be increased and therefore lower concentrations could be measured (4.9 mM was the lowest attempted). This appears to be an appropriate lower limit on which to proceed.

The study was now carried out on both stereochemically pure diastereoisomers (*S*, *S*) **36** and (*S*, *R*) **36**, and the results are tabulated below:

Table 2.4: Reaction of AMA with Substrate (*S*, *R*) **36**

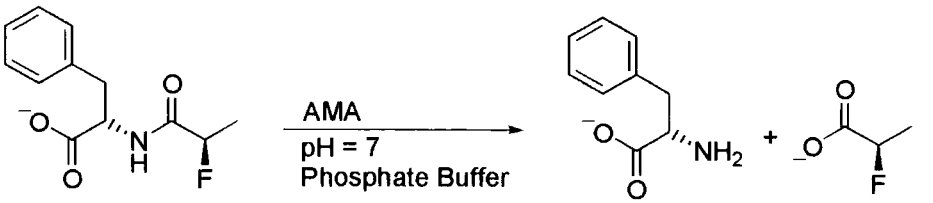

(*S*, *R*) **36**

Run 1		Run 2	
Initial conc. substrate (mM)	Initial velocity ($mMmin^{-1}$)	Initial conc. substrate (mM)	Initial velocity ($mMmin^{-1}$)
10	0.038	4.9	0.022
20	0.066	9.8	0.040
30	0.078	14.6	0.052
40	0.104	19.5	0.061
52.3	0.097	24.4	0.077
		29.3	0.102
		34.2	0.105

Raw data from kinetic study is attached in appendix I.

These results are presented in the following graphs.

(*S*, *R*) **36** + AMA

Run 1 Run 2

Graph 2.1:Reaction velocity vs initial substrate concentration

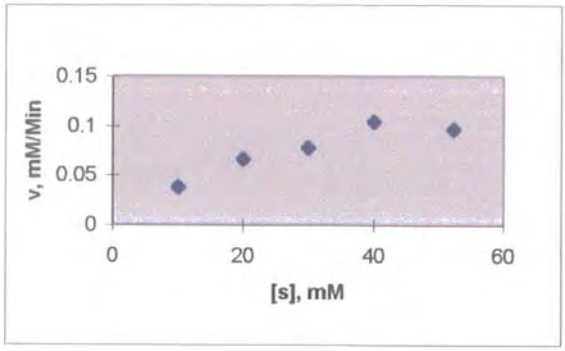

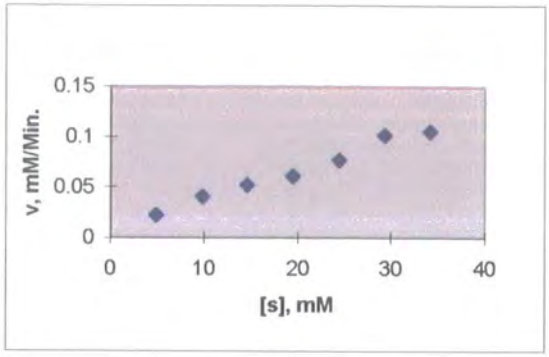

Graph 2.2: Lineweaver-Burk plot

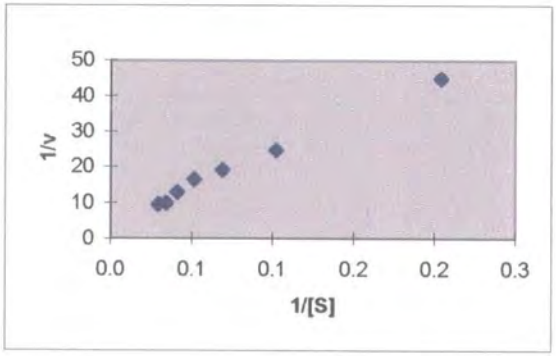

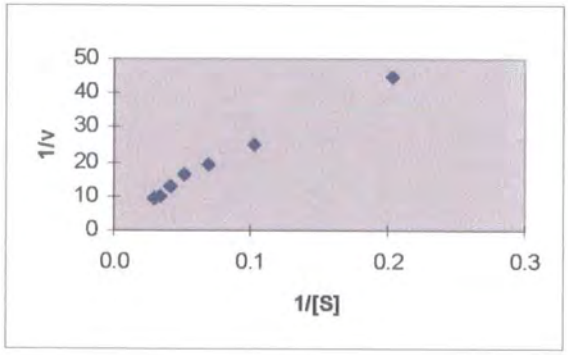

Graph 2.3: Eadie-Hofstee plot

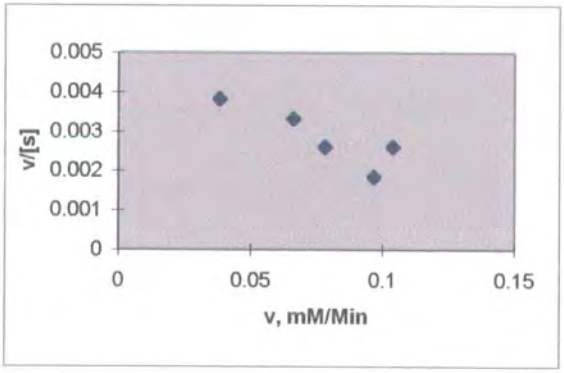

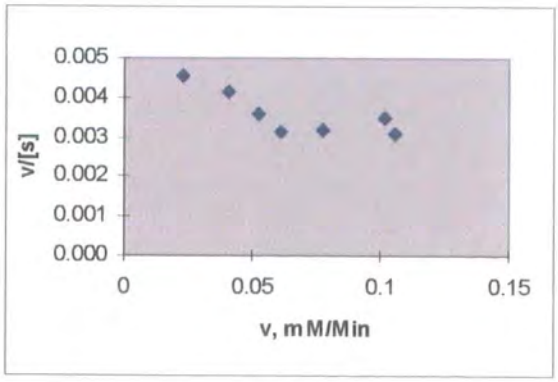

The complimentary diastereoisomer (*S*, *S*) **36** was treated in similar manner to give the following results.

Table 2.5: Reaction of AMA with (*S*, *S*) **36**

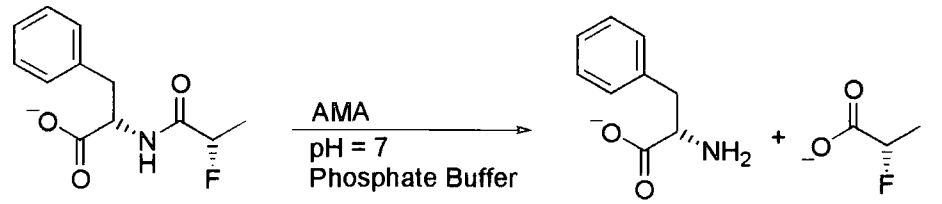

(*S*, *S*) **36**

Run 1		Run 2	
Initial conc. substrate (mM)	Initial velocity ($mMmin^{-1}$)	Initial conc. substrate (mM)	Initial velocity ($mMmin^{-1}$)
8.1	0.359	8.4	0.25
15.3	0.493	16.7	0.40
22.5	0.591	25.1	0.49
30.6	0.704	33.4	0.46
		41.8	0.55
		50.2	0.54
		58.5	0.81
		66.9	0.72

Raw data from kinetic study is attached in appendix I.

These results are presented in the following graphs.

(*S*, *S*) **36** + AMA

Run 1 Run 2

Graph 2.4:Reaction velocity vs initial substrate concentration

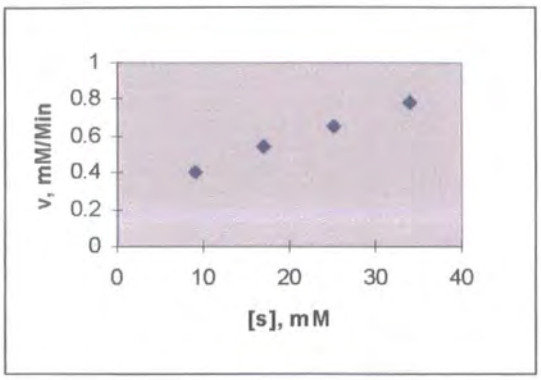

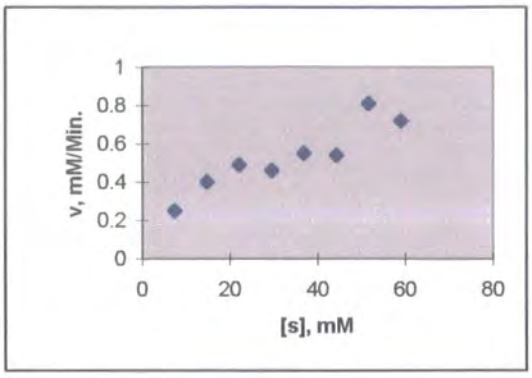

Graph 2.5: Lineweaver-Burk plot

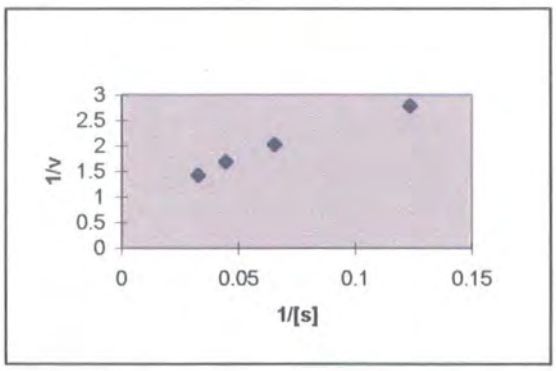

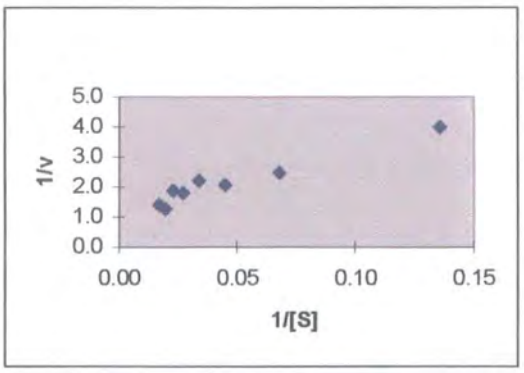

Graph 2.6: Eadie-Hofstee plot

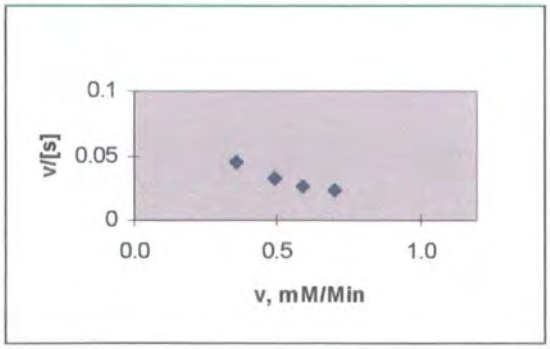

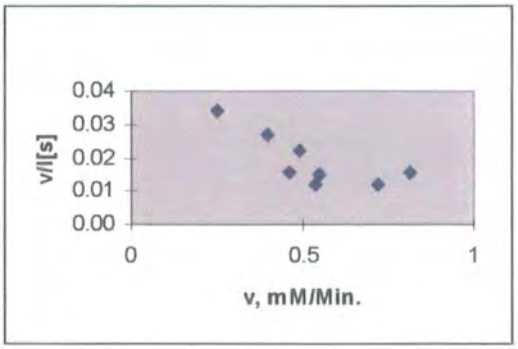

From the above data the K_m and V_{max} values can be calculated for reaction of AMA with substrates (*S*, *S*) **36** and (*S*, *R*) **36** to give the following results.

Table 2.6: *Km* and *Vmax* for the Reaction of AMA with (*S*, *S*) **36** and (*S*, *R*) **36**

Compound		(*S*, *R*) **36**		(*S*, *S*) **36**	
Structure		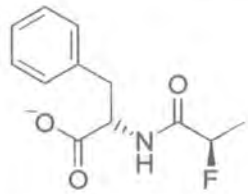		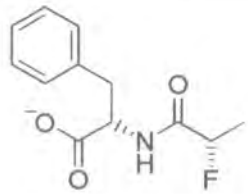	
Run No.		1	2	1	2
Lineweaver - Burk	V_{max}, mmol min^{-1}	0.18	0.22	0.99	0.86
	K_m, M	37.1	43.6	14.4	18.1
Eadie - Hofstee	V_{max}, mmol min^{-1}	0.19	0.22	1.04	0.86
	K_m, M	39.5	48.9	16.1	23.1
V_{max}/K_m		0.0050		0.0566	

As K_m is approximately a measure of the binding affinity of the substrate for the enzyme to form the enzyme / substrate (ES) complex it emerges that both substrates have high K_ms and hence low affinities for the enzyme. The rate of decomposition of the ES complex being many times greater than the rate of formation of the ES complex. However the K_m values do confirm that substrate (*S*, *S*) **36** has a substantially greater affinity for the enzyme than substrate (*S*, *R*) **36**. The increased affinity of (*S*, *S*) **36** is probably due to the restricted rotation of both substrates positioning the fluorine *anti* to the carbonyl in the lowest energy conformation and therefore differentially orientating the bulky methyl group for each diastereoisomer.

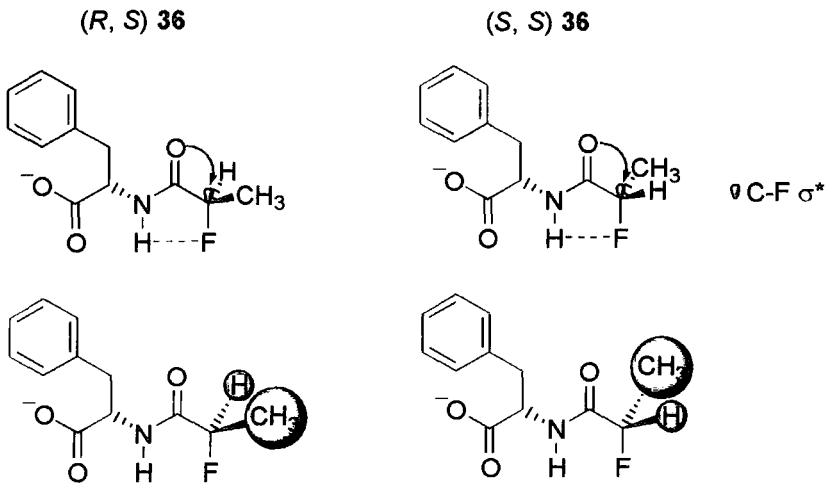

Figure 2.7: Possible reasons for restricted rotation

Figure 2.7 shows the different steric requirements of the two substrates if a barrier to rotation exists and this difference would be sufficient to explain the two-fold difference in the substrates affinity for the enzyme.

V_{max} is the rate at which the product is formed when the entire enzyme is present as ES complex, and from Table 2.6 it can be seen that substrate (*S*, *S*) **36** exhibits a four-fold increase in the rate of de-acylation over substrate (*R*, *S*) **36**. As this four-fold increase in V_{max} cannot be attributed to the restricted rotation of the substrates giving diastereoisomers with differing affinities, then the fluorine substituent must be affecting the rate of hydrolysis also the hypothesis is that an Anh-Eisenstein type stabilisation of the transition state is increasing the hydrolysis rate of (*S*, *S*) **36** over (*R*, *S*) **36** as shown in Figure 2.8.

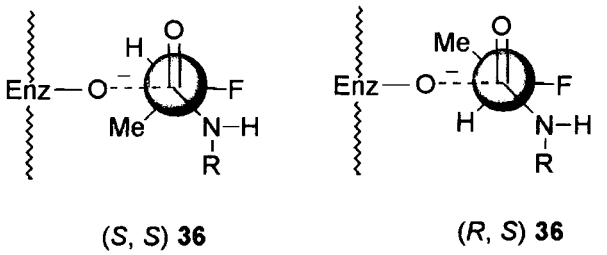

Figure 2.8: Anh-Eisenstein Transition State Stabilisation

Additional stabilisation of the transition state will occur if the nucleophilic serine hydroxyl approaches *anti* to the fluorine as shown in Figure 2.8. For this to happen in both diastereoisomers, it requires the more sterically demanding methyl group to be accommodated in two different positions within the enzyme. From the difference in V_{max} it would appear that the conformation shown for (*S*, *S*) 36 diastereoisomer is

more easily accommodated by the enzyme than that shown for the (*S*, *R*) **36** diastereoisomer.

A useful approximation of the overall enzyme efficiency for each substrate is to compare the V_{max} / K_m values, which shows that the enzyme is an order of magnitude more efficient at de-acylating the (*S*, *S*) **36** diastereoisomer compared to the (*S*, *R*) **36** diastereoisomer. This is consistent with the observed stereochemical outcome of greater than 90% d.e.

At this stage it is not possible to be definitive about what is causing the enzyme to show greater efficiency for one substrate over the other, but it is thought to be a combination of conformational effects on binding and stereoelectronic effects during reaction, which are resulting in this highly stereoselective enzymatic resolution.

2.6 Conclusions

2.6.1 Diazotisation / fluorination reaction

The diazotisation / fluorination of α-amino acids has been shown by two independent methods to proceed predominately with a retention of stereochemistry but there is a significant proportion (≈ 10%) of inversion of stereochemistry under the conditions used as illustrated in Scheme 2.13.

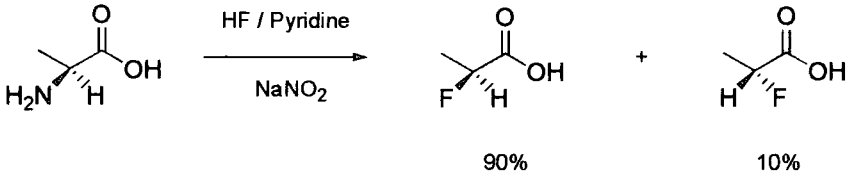

Scheme 2.13: Stereochemistry of fluorination of alanine

The major stereoisomer is formed *via* a double inversion reaction pathway involving anchiomeric assistance from the hydroxyl group on the carboxylic acid. This leads to the overall retention of stereochemistry.

The minor stereoisomer is most probably derived by direct fluoride substitution of the diazonium intermediate leading to an inversion of the stereochemistry.

2.6.2 *Aspergillus melleus* acylase selectivity

Of the four lipase / acylases examined only one showed good stereoselectivity. The *Aspergillus melleus* acylase, AMA selectively hydrolysed[33] one diastereoisomer of N-(*RS*)-2-fluoropropanoyl-(*S*)-phenylalanine, **36**, as shown in Scheme 2.14.

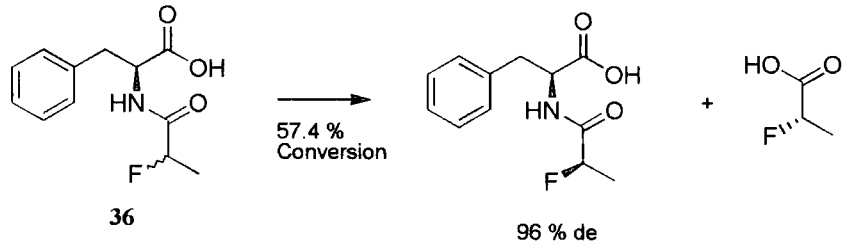

Scheme 2.14: Diastereoselectivity of AMA hydrolysis

By independent synthesis of the stereochemically pure substrates, it has been established that N-(*S*)-2-fluoropropanoyl-(*S*)-phenylalanine **36**, is hydrolysed preferentially over the N-(*R*)-2-fluoropropanoyl-(*S*)-phenylalanine **36**.

2.6.3 Preparation of diastereoisomers, (S, S) 36 and (S, R) 36

The individual diastereoisomers, (*S*, *R*) **36** and (*S*, *S*) **36** were prepared for kinetic studies. Diastereoisomer (*S*, *R*) **36** was prepared as a single stereoisomer, while (*S*, *S*) **36** was prepared to a de of 80%, as determined by ^{19}F NMR.

2.6.4 Enzymatic hydrolysis kinetic data

V_{max} and K_m has been determined for both substrates and this shows that:

- The binding affinity, K_m, of AMA with diastereoisomer (*S*, *S*) **36** is approximately twice that for diastereoisomer (*S*, *R*) **36**.
- The maximum rate of hydrolysis of diastereoisomer (*S*, *S*) **36** is approximately five times the rate of diastereoisomer (*R*, *S*) **36** as demonstrated by their V_{max}.
- The overall enzyme efficiency, which is a function of the two parameters cited above, can be expressed as a V_{max} / K_m value and this demonstrates that the enzyme is an order of magnitude more efficient in the hydrolysis of the diastereoisomer (*S*, *S*) **36** compared to the diastereoisomer (*R*, *S*) **36**.

The difference in binding affinity, K_m, is attributed to conformational effects.

The difference in initial reactivity, V_{max}, is attributed to electronic effects arising from the presence of the fluorine atom. *Ab initio* calculations have predicted that the most stable reaction intermediate will be formed when the nucleophile approaches *anti* to the fluorine. This can happen for both diastereoisomers but it means that the more sterically demanding methyl substituent will occupy a different location within the enzyme. From the results it appears that the location of the methyl group in the (*S*, *S*) **36** case is more easily accommodated by the enzyme.

The above two effects combined are contributing to the overall enzyme efficiency for the (*S*, *S*) **36** case being an order of magnitude greater than the (*S*, *R*) **36** case, resulting in a highly stereoselective biotransformation. Clearly such a reaction could have a synthetic utility in the preparation of homochiral organofluorine compounds.

Chapter 3 - Preparation and resolution of other amides

3.1 Effect of fluorine on the rate of enzymatic hydrolysis

The hydrolysis of N-(*RS*)-2-fluoropropanoyl-(*S*)-phenylalanine with the *Aspergillus melleus* acylase (AMA), and the determination of K_m and V_{max} data for the individual diastereoisomers described in chapter 2 indicates a high degree of diastereoselectivity in the acylase reaction. Further studies were now undertaken to investigate what effects other substituents would have on the outcome of these enzymatic hydrolysis reactions.

Two optically pure substrates, N-propanoyl-(*S*)-phenylalanine **42** and N-fluoroacetyl-(*S*)-phenylalanine **45**, were now used to try to clarify the effect the fluorine atom is having on the rate of the enzyme hydrolysis.

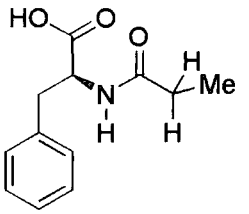

42

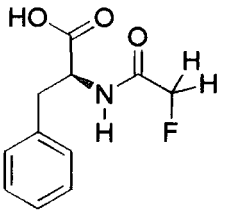

45

It was envisaged that the evaluation of a non-fluorinated amide, **42**, would provide a control for comparison with the fluorinated analogue **36**. α-Fluoroamide **45** will clearly also exhibit the preferred α-fluoroamide conformation similar to **36**, and the rate of hydrolysis for **45** would give a baseline rate for such an amide without any sterically demanding substituents.

3.1.1 Synthesis of Amides 42 and 45

Amide **42** was prepared by combining (*S*)-phenylalanine and propionyl chloride using similar conditions to those developed for the fluoropropionyl analogues described in Chapter 2.

For the fluoroacetyl amide, **45**, the starting material was sodium fluoroacetate, **46**. This was reacted with phthaloyl dichloride, **47**, and fluoroacetyl chloride, **48**, was distilled from the reaction mixture. The fluoroacetyl chloride was then combined with (*S*)-phenylalanine to give the desired α-fluoroamide, **45** as shown in Scheme 3.1 below.

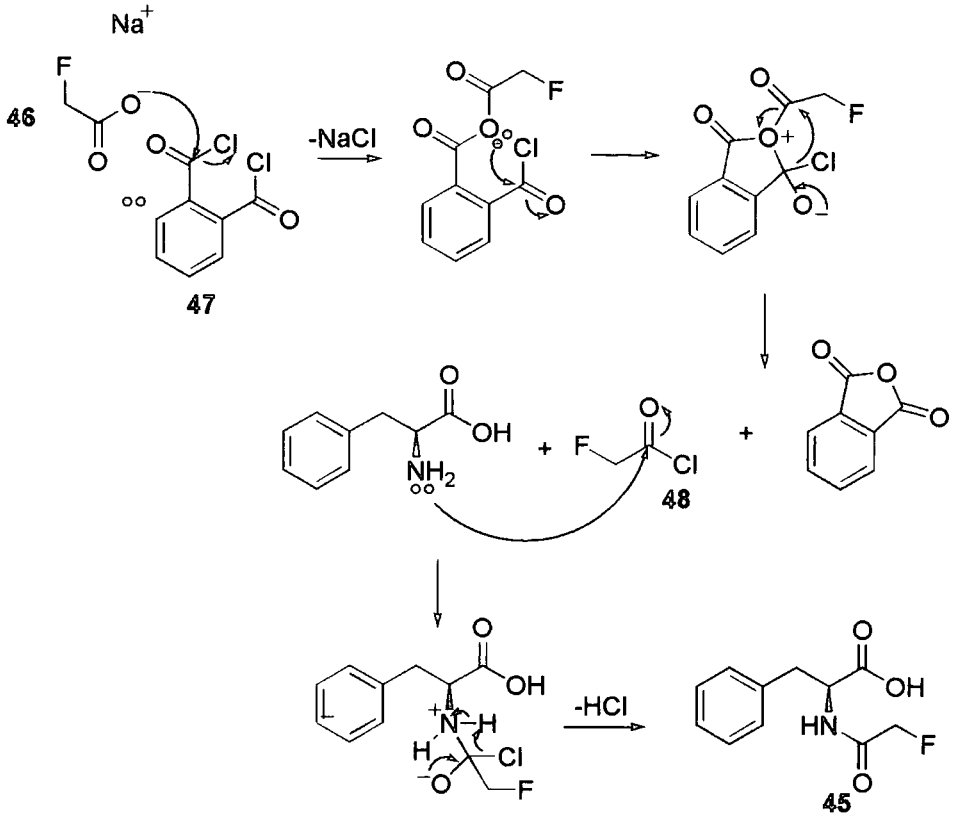

Scheme 3.1: Preparation of N-fluoroacetyl-(*S*)-phenylalanine, 45

3.1.2 Rate of AMA Hydrolysis of Amides 42 and 45

The AMA hydrolyses were carried out as described previously on the sodium salt of the substrates **42** and **45** in a pH = 7 buffered system. The reactions for both substrates were followed once again using NMR spectroscopy. For substrate **45** ^{19}F-NMR was the most convenient. For **42** clearly ^{19}F-NMR was not an option and the reaction was monitored by ^{1}H-NMR.

The results for the comparison of substrates **42** and **45** are included in Table 3.1.

Table 3.1: Initial reaction rates for AMA with **42** and **45**

Substrates			
42		**45**	
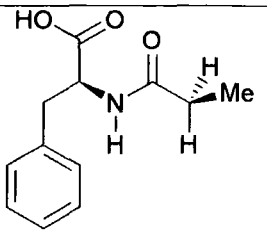		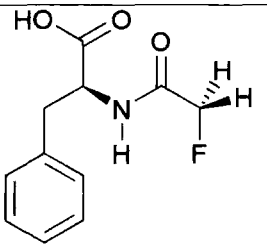	
[S], mM	V_0, mM/min	[S], mM	V_0, mM/min
10	0.42	10	0.16
20	0.68	20	0.19
30	0.94	30	0.23
40	1.08	40	0.27

Raw data from kinetic study is attached in appendix I.

As before, the data was represented in both Lineweaver - Burk and Eadie – Hofstee plots and the K_m and V_{max} values could be calculated.

N-propionyl-(*S*)-phenylalanine, **42**

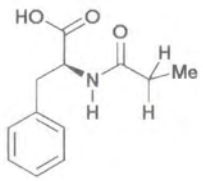

N-fluoroacetyl-(*S*)-phenylalanine, **45**

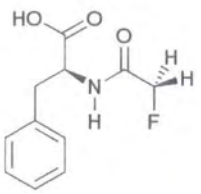

Graph 3.1:Reaction velocity vs initial substrate concentration

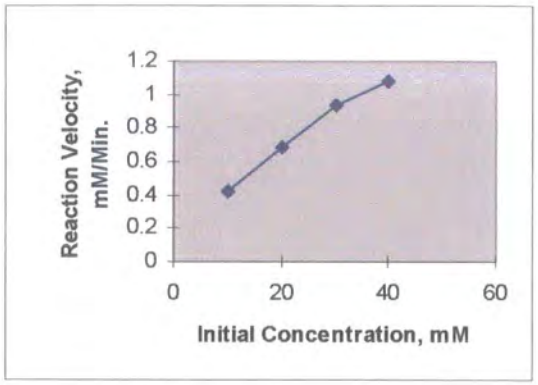

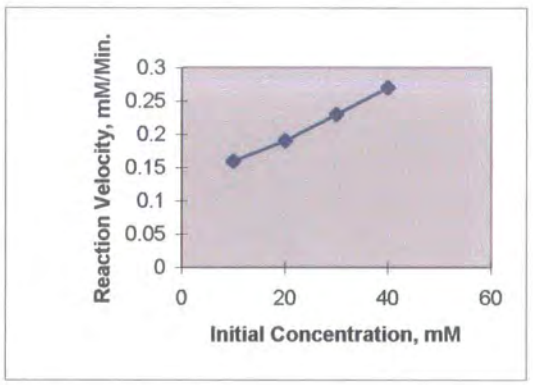

Graph 3.2: Lineweaver-Burk plots

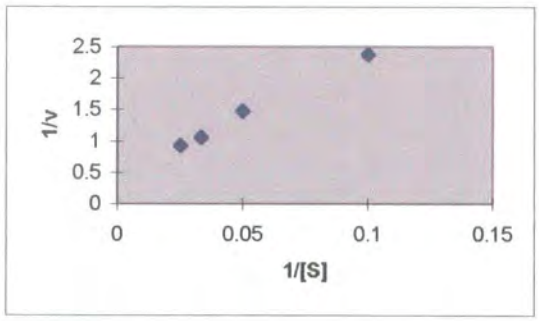

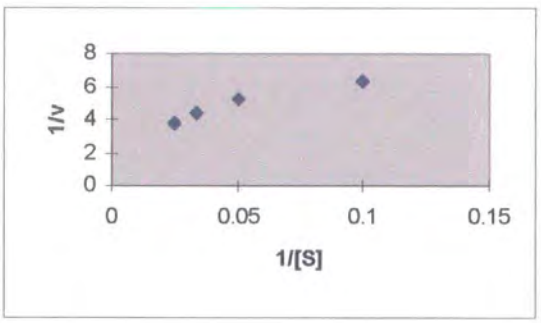

Graph 3.3: Eadie-Hofstee plots

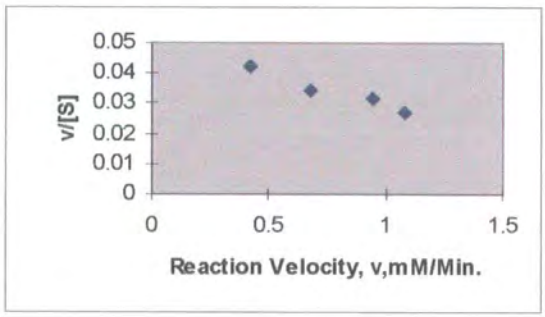

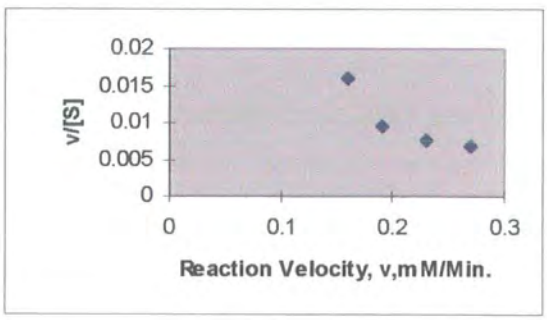

K_m and V_{max} values for substrates **42** and **45** with the AMA enzyme derived from the Lineweaver - Burk treatment of the data are shown in Table 3.2. These results are compared with the data obtained in the previous chapter for the two stereochemically pure diastereoisomers of **36**.

Table 3.2: Comparison of kinetics of acylase hydrolysis of (*R*, *S*) **36**, (*S*, *S*) **36**, **42** and **45**

Substrate	(*R*, *S*) **36**	(*S*, *S*) **36**	**42**	**45**
Structure	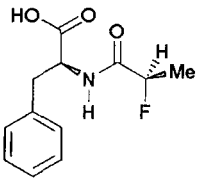	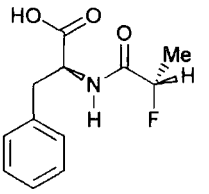	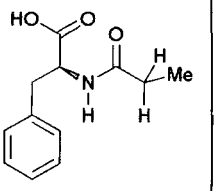	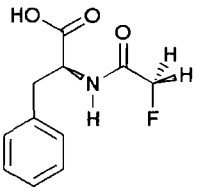
V_{max}, mM/min	0.20	0.93	2.25	0.31
K_m, M	40.3	16.3	43.8	9.7
V_{max} / K_m	0.005	0.057	0.051	0.032

The binding affinity of the substrates for the AMA enzyme demonstrates that the three substrates with a methyl substituent have the higher K_m values, and hence a lower binding affinity to the enzyme. This may be expected on steric grounds but the difference between the K_m values for (*S*, *S*) **36** and **45** is small. It appears that the presence of a methyl substituent can be tolerated if it is in a certain orientation. The binding affinity for **42** is surprisingly poor but this may be due to the non-fluorinated amide having a less restricted rotation and only one of the possible conformations has the methyl substituent in a suitable orientation to bind with the acylase as shown in Figure 3.1.

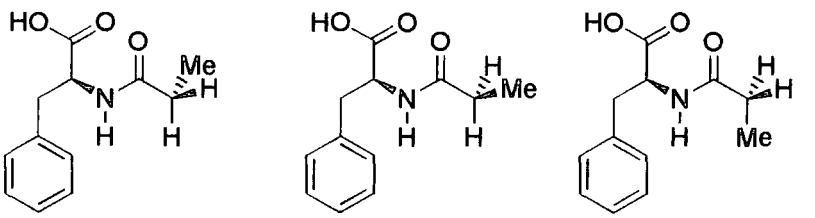

High binding affinity conformation

Low binding affinity conformations

Figure 3.1: Relationship between conformation and binding affinity in **42**

The V_{max} values demonstrate that the fluorinated amides have the slower rates of hydrolysis, but this is only significant if the entire enzyme is present as the enzyme substrate complex. The V_{max} of substrate (*S*, *S*) **36**, while not being as high as **42** is significantly higher than the other α-fluoroamides, which indicates that the methyl substituent in a certain location is beneficial to increasing the maximum rate of hydrolysis. A possible explanation could be that the presence of the methyl substituent in the correct location ensures the substrate is held with the C-F σ* orbital *anti* to the approaching nucleophile. For the cases of the other two fluorinated amides, (*R*, *S*) **36** and **45** either the methyl is in the wrong location to support efficient hydrolysis or there is no methyl present at all and thus the substrate does not bind as efficiently and the C-F σ* orbital is not held *anti* to the approaching nucleophile at all times.

The V_{max} / K_m value is a display of how selective the enzyme would be if it were added to a mixture of the four compounds. The comparative rates of hydrolysis of the four substrates is in the order:

(*S*, *S*) **36** = **42** > **45** >> (*R*, *S*) **36**.

This shows that the acylase would not be able to differentiate between (*S*, *S*) **36** and **42** when binding affinity and the maximum rate of hydrolysis are taken into account. It appears that with (*S*, *S*) **36** forming the greater proportion of enzyme / substrate complex and **42** having the higher maximum rate of hydrolysis, the two effects would cancel each other out. The next most efficient substrate is **45**, which from K_m data is the strongest binding, presumably due to the absence of a methyl substituent. Substrates (*R*, *S*) **36** and **45** have similar maximum rates of hydrolysis but as (*R*, *S*) **36** shows poor binding affinity for the AMA enzyme the overall rate of hydrolysis for (*R*, *S*) **36** is the slowest.

The fact that fluorine does not impact on the binding of the amide to the acylase and yet it has a large effect on the maximum rate of hydrolysis suggests that it suppresses the attainment of the optimal transition state. This perhaps merits a theoretical investigation.

3.1.3 X-Ray crystal structures of substrate 45

After synthesis of the α-fluoroamide **45** it was possible to obtain a suitable crystal for X-ray analysis. The resultant x-ray structure is shown in Figure 3.2.

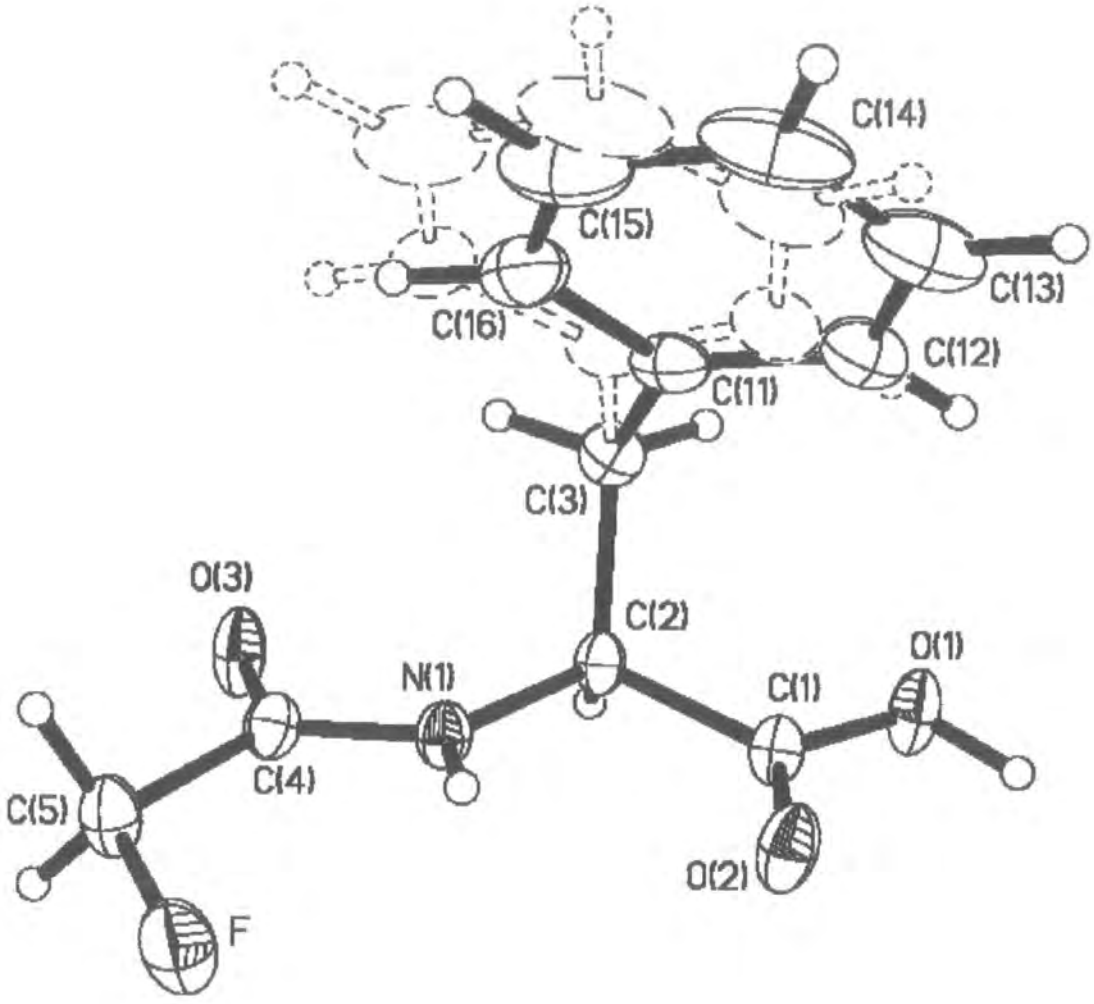

Figure 3.2: X-Ray crystal structure of N-fluoroacetyl-(*S*)-phenylalanine, **45**

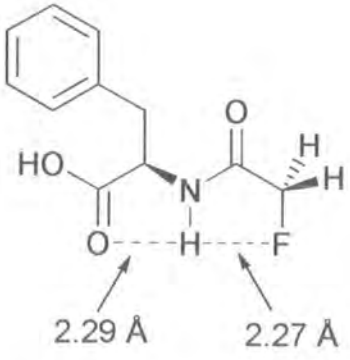

Figure 3.3: Hydrogen Bonding in **45**

Figure 3.3 summarises the main findings from the X-ray crystal structure of **45** and reveals that the C-F bond and the N-H bond are almost co-planar, while at the same time both are *trans* to the amide carbonyl. This finding is consistent with the *ab initio* calculation discussed in chapter 1 for the fluoropropionylamide case.

The X-ray structure also supports the presence of intramolecular hydrogen bonding. Two close contacts were identified. The first, unsurprisingly, between the acid carbonyl group and the N-H group, with a bond length of 2.29 Å. The second, particularly relevant to this investigation, is the close contact between fluorine and hydrogen. The X-ray crystal structure reveals an interatomic distance of 2.27 Å. This separation is much shorter than the sum of the hydrogen and fluorine atomic radii and is in line with the bond lengths reported for other cases where fluorine is thought to be acting as a hydrogen bond acceptor in a stabilising interaction.

The conformation revealed in the X-ray crystal structure of the α-fluoroamide **45** confirms the experimental predictions and supports the theory that rotation is restricted by the donation of electron density into the C-Fσ* antibonding orbital and the presence of this intramolecular hydrogen bonding.

3.2 Comparison of chloro and methyl substituted amides

At this stage the study was extended to a comparison of the effect of chlorine and methyl substitution on substrates for AMA hydrolysis. It was envisaged that the chlorine and methyl groups may be considered to be isosteric, and have similar controlling influences on the initial conformations and the direction of nucleophilic attack. This study therefore required the preparation of a further series of substrates. To this end N-(2-methylpropionyl)-(*S*)-phenylalanine **49**, N-(*S*)-2-chloropropionyl-(*S*)-phenylalanine (*S*, *S*) **50** and N-(*R*)-2-chloropropionyl-(*S*)-phenylalanine (*R*, *S*) **50** were prepared.

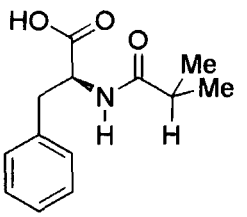

49

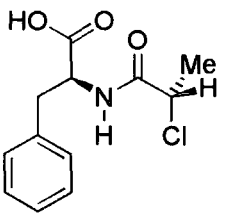

(*S*, *S*) **50**

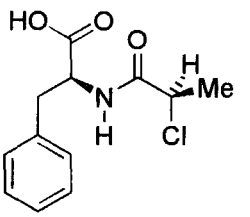

(*R*, *S*) **50**

3.2.1 Synthesis of amides 49 and 50

The acid chlorides required to prepare substrates, **49** and **50**, were all commercially available. These N-acylphenylalanines were therefore prepared in a one step synthesis using similar conditions to those developed for the fluoropropanoyl analogues.

3.2.2 Rate of AMA hydrolysis of amides 49 and 50

Once again ^{1}H NMR was used to follow the rates of hydrolysis of the sodium salts and the results are detailed in Table 3.3.

Table 3.3: Reaction velocities for reaction of AMA with **49**, (*S*, *S*) **50** and (*R*, *S*) **50**

Substrates					
49		(*S*, *S*) **50**		(*R*, *S*) **50**	
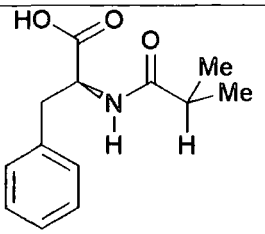		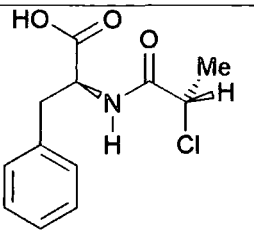		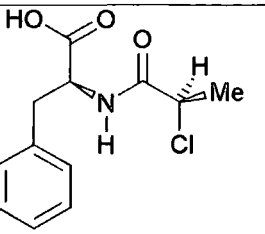	
[S], mM	V_0, mM/min	[S], mM	V_0, mM/min	[S], mM	V_0, mM/min
10	0.134	9.4	2.581	4.7	0.201
20	0.203	18.8	2.978	9.4	0.426
30	0.222	28.2	3.621	14.1	0.346
40	0.257	37.5	4.232	18.8	0.540

Raw data from kinetic study is attached in appendix I.

The Lineweaver – Burke plots were used to determine the K_m and V_{max} values for the above substrates and the results are shown in Table 3.4 below.

Table 3.4: Comparison of kinetics of acylase hydrolysis of **49**, (*S*, *S*) **50** and (*R*, *S*) **50**

Substrate	**49**	(*S*, *S*) **50**	(*R*, *S*) **50**
Structure	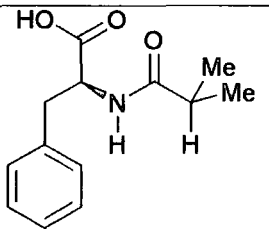	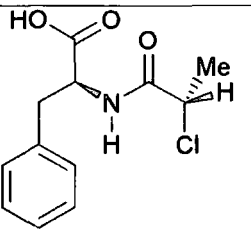	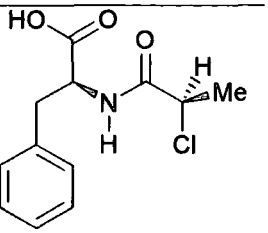
V_{max}, μM/min	0.36	4.71	0.97
K_m, M	17.0	8.2	17.3
V_{max} / K_m	0.021	0.573	0.056

It needs to be emphasised that the reaction velocity data is reported in μM/min as opposed to mM/min for the fluorinated amides reported earlier. Therefore the rates of enzymatic hydrolysis are three orders of magnitude slower than those of the previous substrates. Clearly the extra steric bulk of these substrates is adversely affecting their reactivity with the acylase. Not withstanding this, the trends within this group of substrates follow a similar pattern to that with the α-fluoroamides.

Notably (*S*, *S*) **50** has the highest binding affinity for the enzyme. The higher binding affinity is attributed again to the enzyme being able to accommodate a methyl only if it is held in a certain orientation and it appears that chlorine is satisfying the same role as fluorine with regard to controlling the conformation of this substrate. The ratio for the binding affinity between (*S*, *S*) **50** and (*R*, *S*) **50** is approximately 2, which is similar to the fluorine case. The non-chlorinated amide **49** has a similar binding affinity to (*R*, *S*) **50**, which again mirrors the experience of the fluorine case.

The ratio of the V_{max} values for (*S*, *S*) **50** and (*R*, *S*) **50** are again very close to the α-fluoroamide case, with (*S*, *S*) **50** having the higher value and about 5 times greater than that for (*R*, *S*) **50**. Interestingly the slowest substrate of this group is the non-chlorinated isobutyl substrate. This is probably because **49** contains two methyl substituents, which have to accommodated within the acylase and the second methyl has to be located in a region of the acylase incompatible with this role.

3.2.3 X-Ray crystal structure of amide (*S*, *S*) 50

Two crystal structures were elucidated for (*S*, *S*) **50** depending on the presence of intermolecular hydrogen bonding, which produced conformational changes around the amide bond.

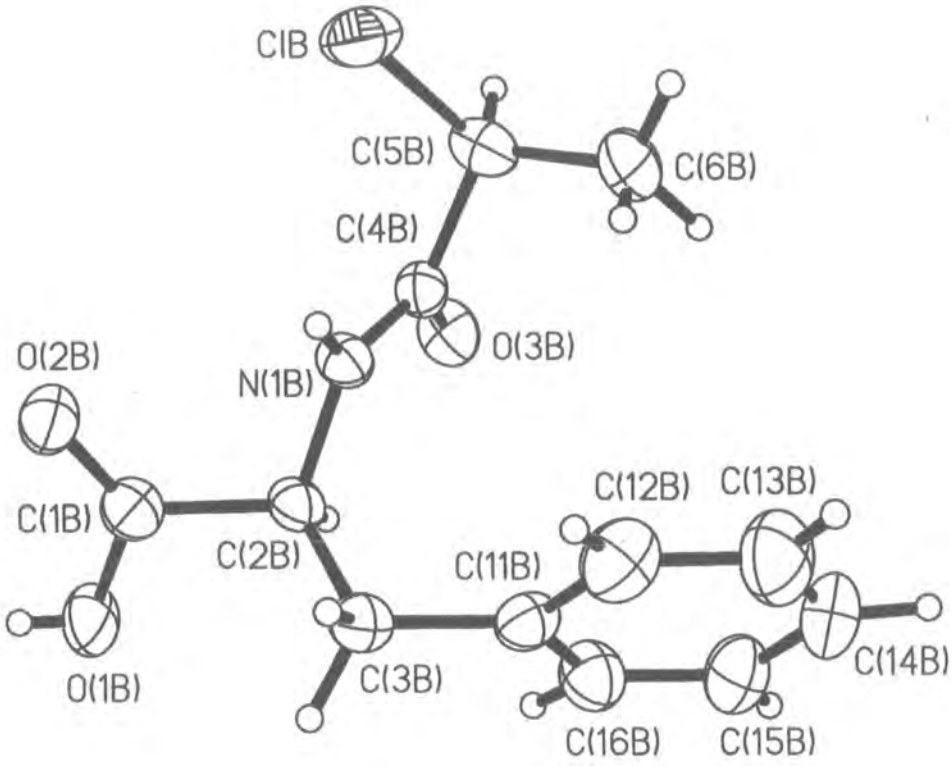

Figure 3.4: X-Ray crystal structure of N-(*S*)-2-chloropropionyl-(*S*)-phenylalanine, (*S*, *S*) **50**

Figure 3.4 shows the crystal structure for (*S*, *S*) **50** where no intermolecular hydrogen bonding is present. This demonstrates an approximately co-planar relationship between the N-H and C-Cl bonds, with both bonds being approximately *trans* to the carbonyl group. Presumably the increased steric influence of chlorine is mitigating against an eclipsing N-H interaction. This is consistent with the findings of the fluoroacetyl amide structures reported in the previous section, and presumably arises for similar reasons.

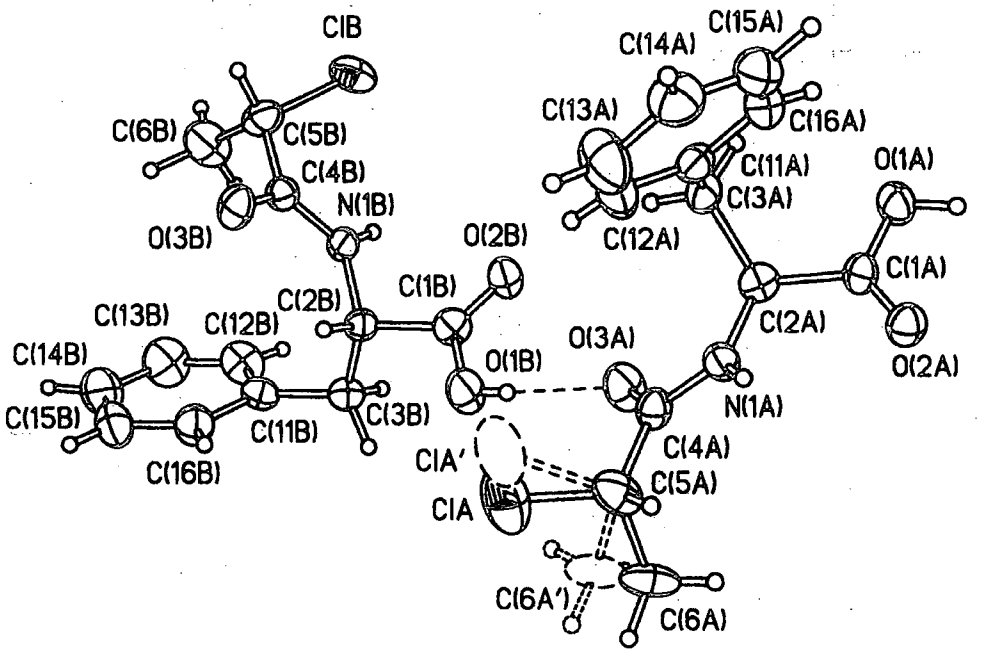

Figure 3.5: X-Ray crystal structure of (*S*, *S*) **50** with intermolecular hydrogen bonding

Where this intermolecular hydrogen bonding is present the co-planar relationship between the N-H and C-Cl bonds is lost as shown in Figure 3.5. This presumably arises because Cl---H bonding is not strong and the larger size of the chlorine mitigates against a co-planar alignment with the N-H bond.

3.2.4 X-Ray crystal structure of amide 49

Again differing X-ray crystal structures of **49** were elucidated depending on the presence of intermolecular hydrogen bonding.

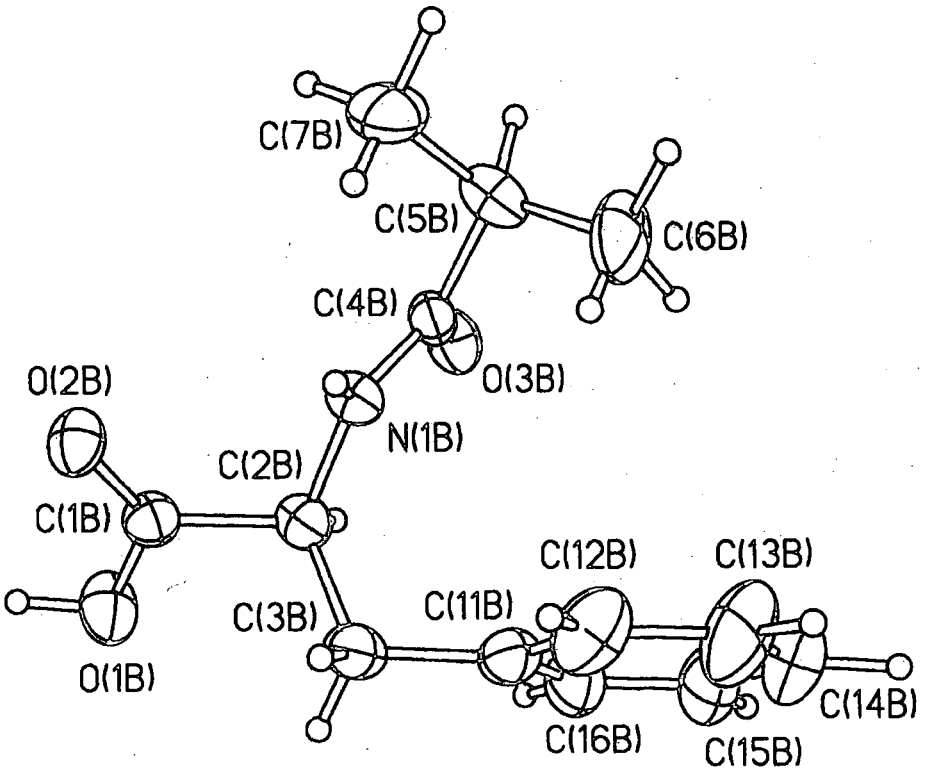

Figure 3.6: X-Ray crystal structure of N-(2)-methylpropionyl-(*S*)-phenylalanine, **49**

Where no intermolecular hydrogen bonding was present the isopropyl group orientated with the N-H bond bisecting the C-C bonds to the methyl substituents and the C-H bond eclipsing and co-planar to the carbonyl. All the evidence suggests that if the C-H bond was replaced by C-F, the isopropyl group would rotate by 180°.

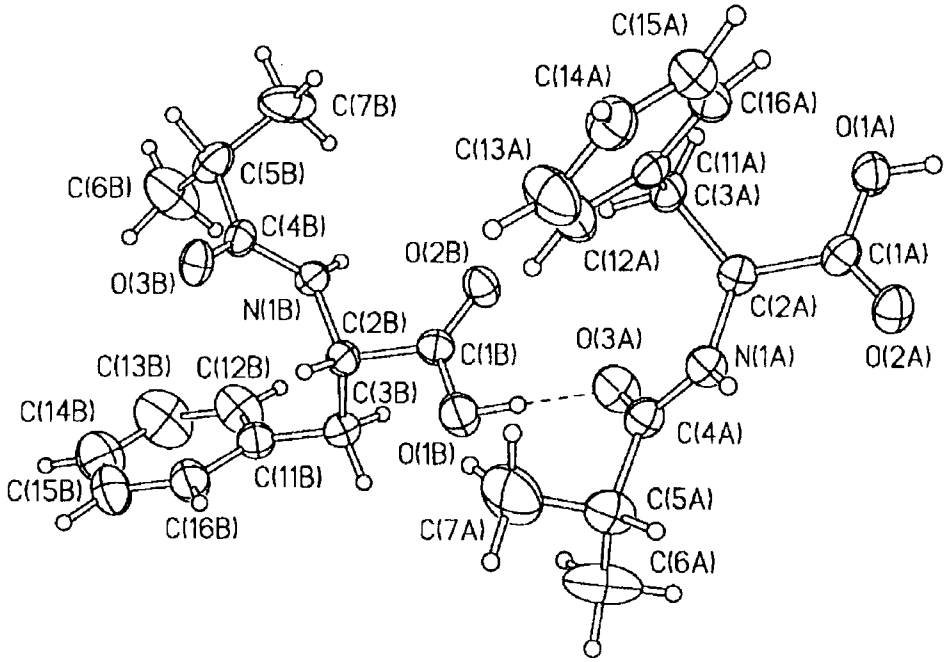

Figure 3.7: X-Ray crystal structure of **49** with intermolecular hydrogen bonding

Where intermolecular hydrogen bonding is present, between the carboxylate hydrogen and the amide carbonyl, the unit cell of substrate **49** revealed two conformers of **49** within the structure. Interestingly the orientation of the isopropyl group was found to have rotated through 180° for one of the conformers.

3.3 Preparation of other α-fluoroamides

The programme was now extended to the preparation of a range of α-fluoroamides. This was carried out to explore a wider range of substrates, to build up a database of their properties, and ultimately to determine if the acylase selectivity already demonstrated for the 2-fluoropropionamide case would extend to other amides. The target α-fluoroamides chosen were N-((*RS*)-2-fluoropropionyl)-aniline **51**, N-((*S*)-2-fluoropropionyl)-aniline (*S*) **51**, N-((*RS*)-2-fluoropropionyl)-benzylamine **52**, N-((*S*)-2-fluoropropionyl)-benzylamine (*S*) **52**, N-((*RS*)-2-fluoro-4-methylpentanoyl)-benzylamine **53** and N-((*RS*)-2-fluoro-2-phenylacetyl)-benzylamine **54** as shown in Figure 3.8.

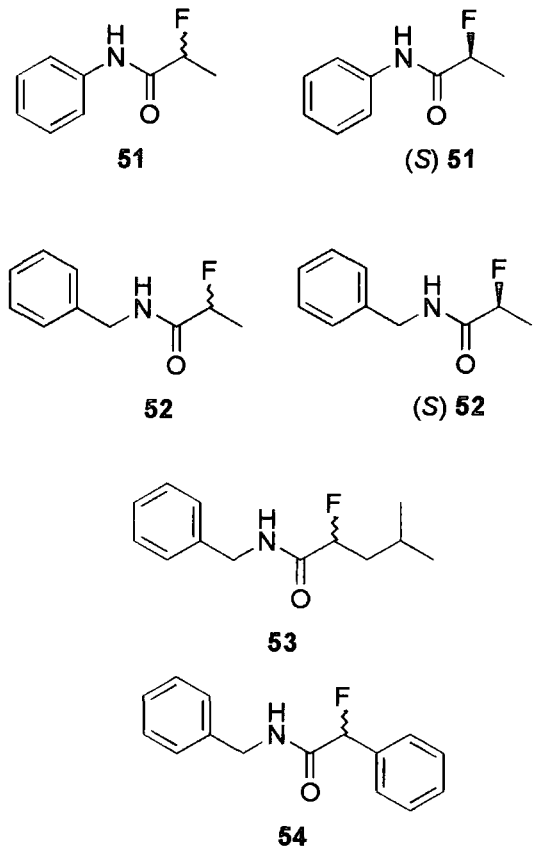

Figure 3.8: α-Fluoroamides screened as AMA substrates of interest

It was desirable to record an X-ray crystal structure for a 2-fluoropropionamide system to again confirm the consistency of the expected C-F / N-H planar conformation. The preparation of (*S*) **51** and (*S*) **52** opened up this possibility. Also with the preparation of racemic α-fluoroamides **51**, **52**, **53** and **54** it may open up the possibility of examining the selectivity of AMA hydrolysis in other substrate systems.

3.3.1 Synthesis of α-fluoroamides

3.3.1.1 N-2-Fluoropropionamides

α-Fluoroamides **51** and **52** were prepared in a similar manner to N-(*R*, *S*)-2-fluoropropionyl-(*S*)-phenylalanine **36** as shown in Scheme 3.2. For the synthesis of (*S*) **51** and (*S*) **52** the optically pure amino acid (*S*)- alanine was used as the starting material in the diazotisation reaction.

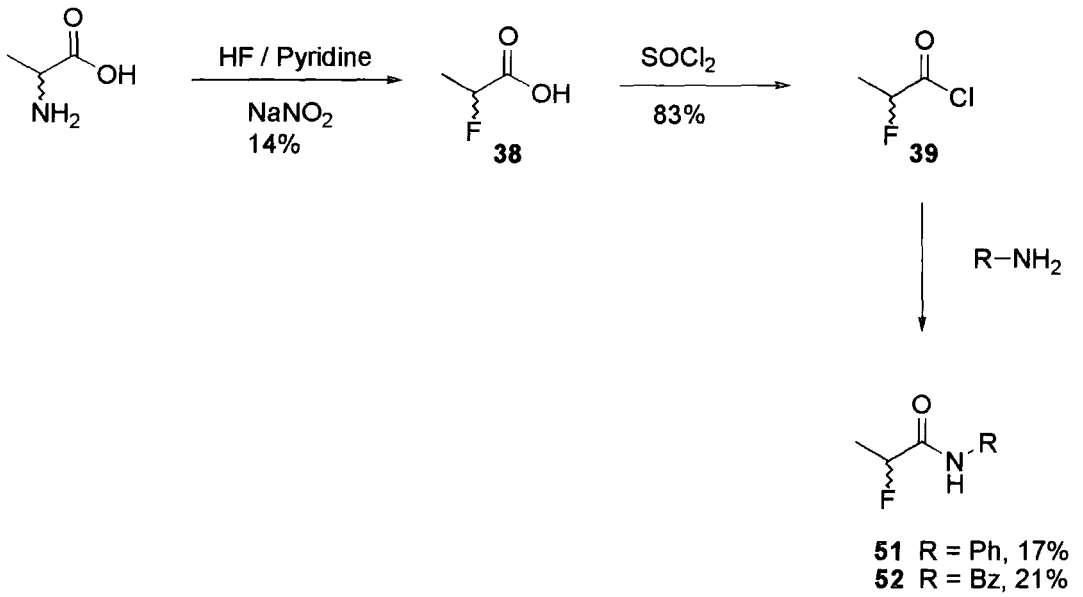

Scheme 3.2: Preparation of 2-fluoropropionamides

3.3.1.2 N-(2-Fluoro-4-methylpentanoyl)-benzylamine

α-Fluoroamide **53** was prepared in a similar manner to that described above, except that the starting material was racemic (*RS*)-leucine as shown in scheme 3.3.

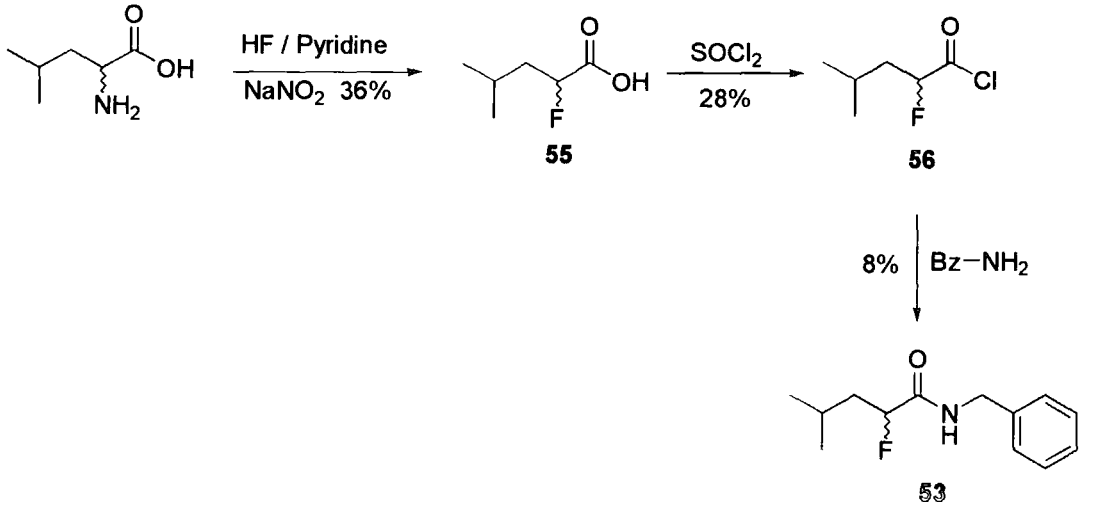

Scheme 3.3: Preparation of N-(2-fluoro-4-methylpentanoyl)benzylamine **53**

3.3.1.3 N-(2-Fluoro-2-phenylacetyl)-benzylamine

α-Fluoroamide **54** was prepared according to Scheme 3.4.

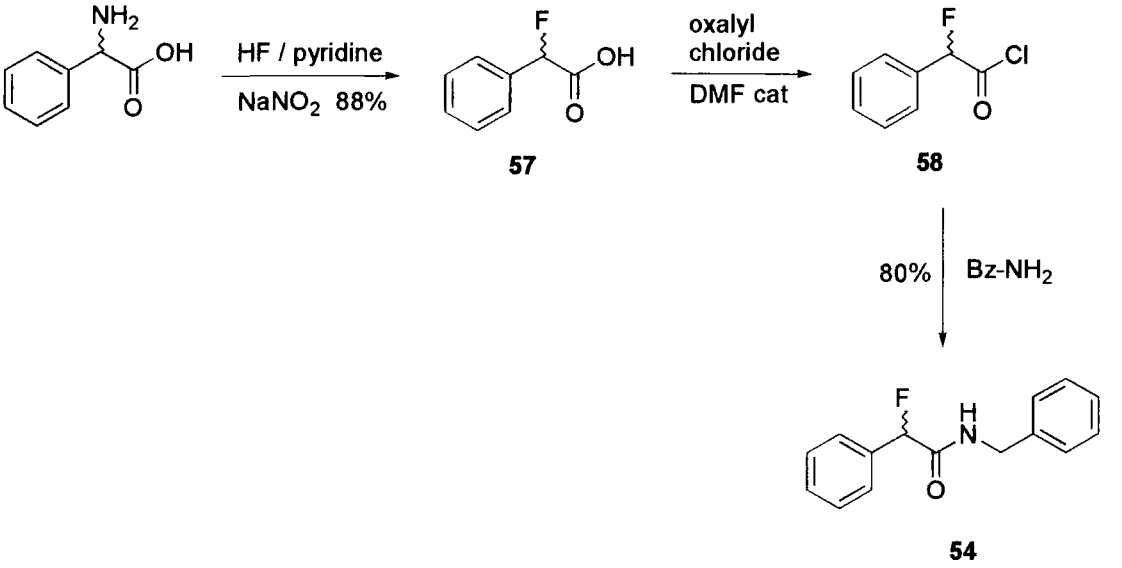

Scheme 3.4: Preparation of N-(2-fluoro-2-phenylacetyl)-benzylamine, **54**

The acid chloride, **58**, could not be prepared by the same synthetic sequence described previously due to difficulties in obtaining the acid chloride from a thionyl chloride reaction. Distillation of the product required a higher temperature due to low volatility, which generated intractable polymerised products. The α-fluorocarboxylic acid **57** was instead reacted with oxalyl chloride in the presence of a catalytic amount of DMF, to liberate the acid chloride, in good yields. The presence of DMF was found to be important as only small conversions were observed *in situ* and the desired product could not be isolated when the reaction was carried out in the absence of DMF.

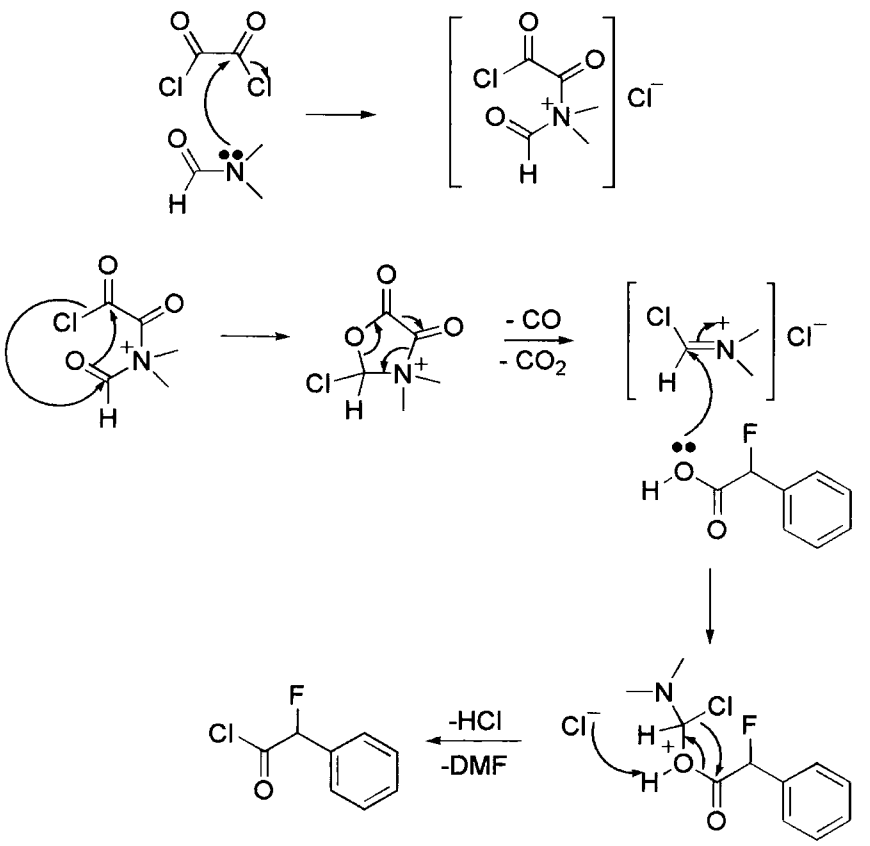

Scheme 3.5: Mechanism for DMF catalysed acid chloride formation

3.3.2 X-Ray crystal structure of amide 51

Obtaining suitable crystals of stereochemically pure α-fluoroamides proved difficult due to inhomogeneity of the crystals. However perseverance resulted in the crystal structure of N-((*S*)-2-fluoropropionyl)-aniline 51 as shown in Figure 3.9.

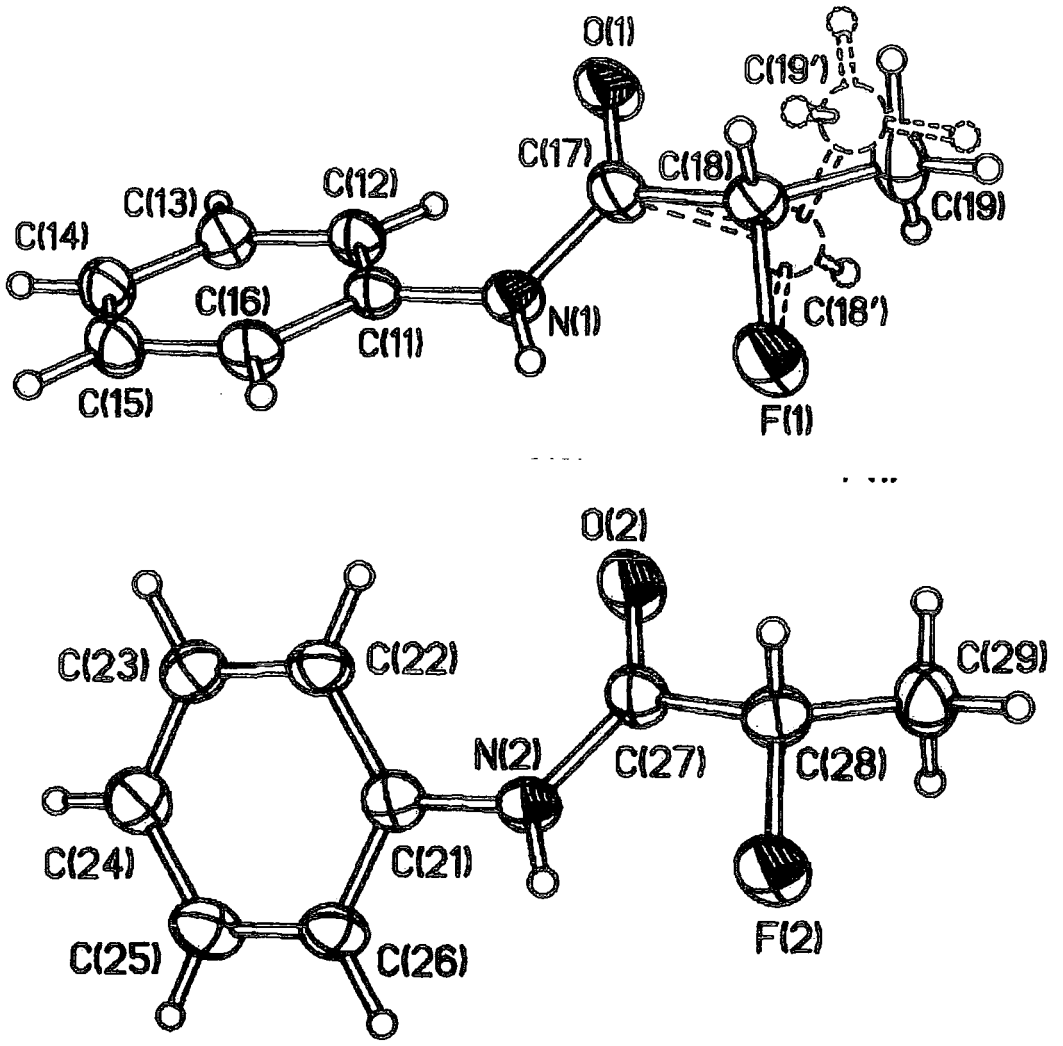

Figure 3.9: X-Ray crystal structures of N-((*S*)-2-fluoropropionyl)-aniline, 51

There are two structures within the unit cell, which differed mainly by rotation of the phenyl ring. Importantly, the conformational arrangement of the amide and the C-F bond was found to be the same for both. Again the C-F bond was found to be co-planar with the N-H bond and both were *trans* to the carbonyl, consistent with previous observations and with the *ab initio* studies reported earlier.

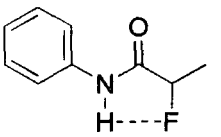

2.17 or 2.22Å

Figure 3.10: Interatomic distance between fluorine and amide hydrogens

The interatomic distances between F and H for the two conformations are shown in Figure 3.10, i.e. 2.17Å between N1(H) and F1 and 2.22Å between N2(H) and F2. The interatomic distances are smaller here than that recorded previously for the fluoroacetyl case (2.27Å). This suggests an even greater barrier to rotation.

3.3.3 Enzymatic resolutions of α-fluoroamides

After completion of the synthesis of the four racemic α-fluoroamides **51**, **52**, **53** and **54** it was now envisaged that they could be used as substrates in AMA hydrolysis. Initially the conditions employed for the previous AMA hydrolyses were used, i.e. reaction in water, buffered to pH =7. The rate of reaction, which is clearly dependent on the solubility of the substrate in water, was so slow that the highest conversion that was estimated by NMR was 0.7% even after an extended reaction period (1 week). This level of conversion was not sufficient to measure any stereoselectivity that may have occurred. Attempts were made to improve the substrate's solubility by the use of 10% ethanol / water mixtures, but while solubility was improved, no improvement in the reaction rate was observed, possibly due to an adverse effect of ethanol on the acylase.

3.4 Conclusions

A selection of amides have been prepared and characterised, of which five were novel α-fluoroamides.

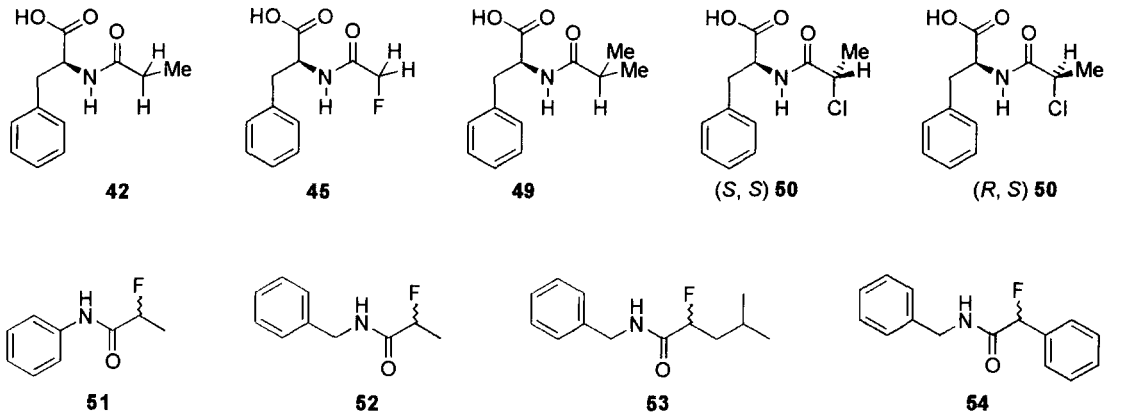

Figure 3.11: Selection of amides

Four of the amides, **45**, **49**, (*S*, *S*) **50** and **51**, have had their X-ray crystal structures determined. In the case of the two α-fluoroamides, **45** and **51**, and the α-chloroamide, (*S*, *S*)**50**, the C-X and N-H bonds have been found to be approximately co-planar and *anti* to the carbonyl.

The solid state structures indicate the presence of intramolecular hydrogen bonding as shown in figure 3.12, with fluorine and chlorine acting as a hydrogen bond acceptor. Hydrogen / fluorine interatomic distances of <2.3Å, which is considerably less than the sum of the Van der Waals radii, have been measured.

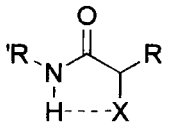

Figure 3.12: Conformation of α-fluoroamides

These observations support the developing hypothesis that restricted rotation is present in all α-fluoroamides due to stereoelectronic effects and intramolecular hydrogen bonding. This conformation is disrupted when intermolecular hydrogen bonding is evident between molecules then the N-H and C-Cl bonds are no longer co-planar.

The rates of hydrolysis of five amides, **42**, **45**, **49**, (*S*, *S*)**50** and (*R*, *S*)**50** have been evaluated in the AMA acylase system and the binding efficiencies, K_m and maximum

rates of hydrolysis, V_{max} have been determined. This has led to the following conclusions.

- As the steric bulk increases α to the carbonyl the ability of the acylase to bind with the substrate decreases as revealed by higher K_m values.
- A methyl substituent can be tolerated and has little impact on K_m only if it is held in one location within the acylase, i.e. that observed in (*S*, *S*) **50** substrate. For all other methyl orientations a marked reduction in binding affinity is seen.

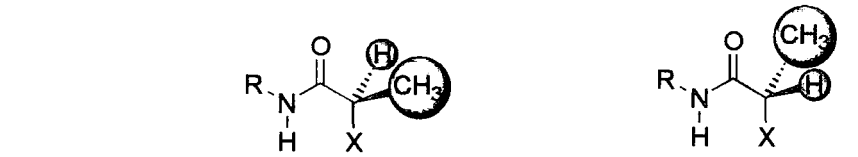

- α-Fluoro and α-chloroamides behave remarkably similar towards the AMA acylase and the same relationship between rates of hydrolysis for (*R*, *S*) and (*S*, *S*) diastereoisomers exists.
- Amides with an α-fluorine do not hydrolyse as fast as the equivalent amides where no fluorine is present. This suggests any stabilisation of the acylase hydrolysis transition state, by Anh Eisenstein effect, is far outweighed by the inherent ground state stability of these α-fluoroamides, relative to their non-fluorinated counterparts.

Chapter 4 - Approaches to the synthesis of α-fluoropeptides

4.1 Introduction

As discussed in previous chapters, α-fluoroamides have been shown to experience restricted conformational flexibility and thus it was attractive to try to prepare an α-fluoro peptide, such as that shown in Figure 4.1.

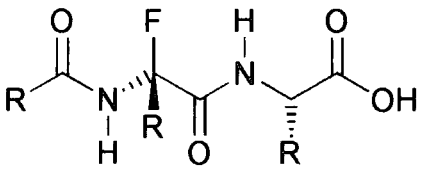

Figure 4.1: α-Fluoropeptide

A peptide which exhibits this restricted conformational flexibility, would be expected to have significantly different biological properties than a non-fluorinated case.

Classically peptides are prepared by N → C=O combinations of amino acids, however any synthetic approach to an α-fluoropeptide could not utilise this route as α-fluoroamino acids, such as, **25**, are unknown.

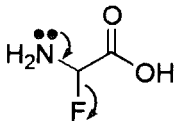

Unstable due to fluoride elimination

25

α-Fluoroamino acids are unstable due to the lone pair on the nitrogen assisting the elimination of fluoride. In this project alternative methods for the preparation of α-fluoropeptides were investigated, where the nitrogen lone pair is not free to eliminate fluoride in this manner. In our target peptide shown above, the α-fluorine is adjacent to an amide nitrogen. For our approach to be successful it was hoped that once the amide bond was in place, any instability due to fluoride being eliminated, would be removed due to conjugation of the nitrogen lone pair with the amide carbonyl.

Other groups[38] have recently tried to synthesise α-fluoropeptides without success, but they have been successful in preparing constrained cyclic pseudo peptides such as **59** shown in Figure 4.2.

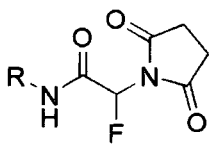

59

Figure 4.2: α-Fluoro pseudo peptide prepared by Bailey[38b]

At the outset two routes seemed to satisfy the above criteria.

4.2 Oxazolone method

Oxazolones have been used to prepare α-substituted amino acids[39]. The general approach has been to carry out the substitution on the oxazolone, which can then liberate the desired amino acid by treatment with acid as shown in Scheme 4.1.

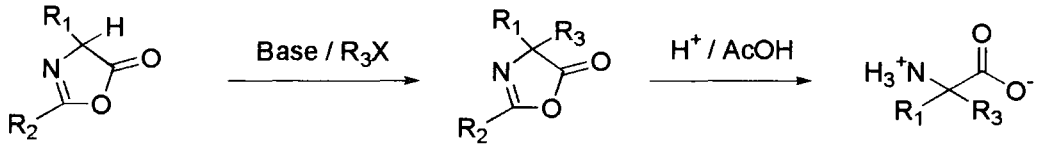

Scheme 4.1: α-Substituted amino acid preparation using oxazolone intermediate

In the case of fluorine substitution, liberation of the amino acid is clearly undesirable as this would certainly lead to elimination of fluoride. However the potential for an oxazolone to provide the backbone of a peptide if the cleavage reaction is carried out in the presence of a protected amino acid offers an opportunity for α-fluoroamide synthesis as shown in Scheme 4.2.

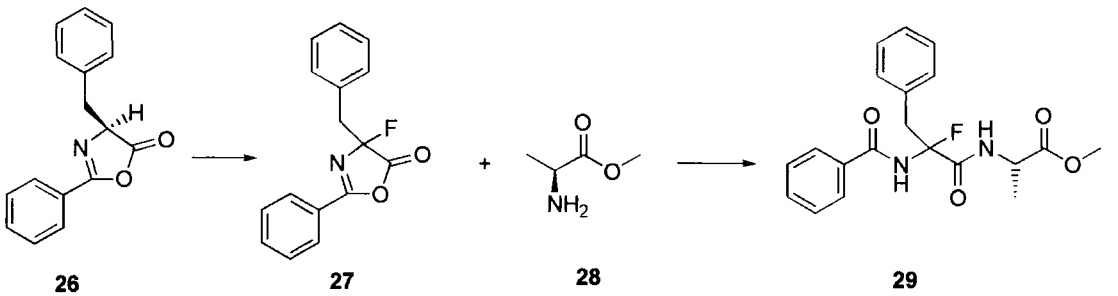

26 27 28 29

Scheme 4.2: α-Fluoropeptide preparation using oxazolone intermediate

4.2.1 Oxazolone synthesis

(*RS*)-4-Benzyl-2-phenyl-5(4*H*)-oxazolone **26** was available in the research group. This compound was prepared by a two-step synthesis, involving formation of the amide bond followed by a dehydration as shown in Scheme 4.3.

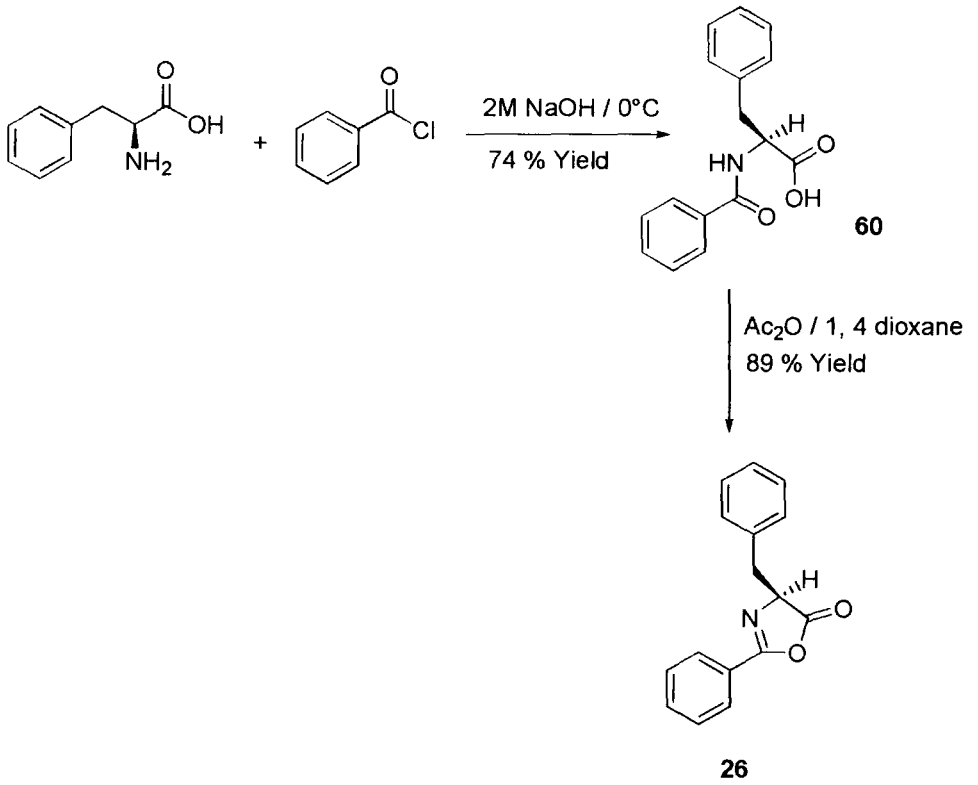

Scheme 4.3: (*RS*)-4-benzyl-2-phenyl-5(4*H*)-oxazolone **26** synthesis

4.2.2 Carbanion formation 61

Treatment of oxazolone **26** with sodium hydride allowed generation of carbanion **61**, as a consequence of deprotonation as shown in Scheme 4.4.

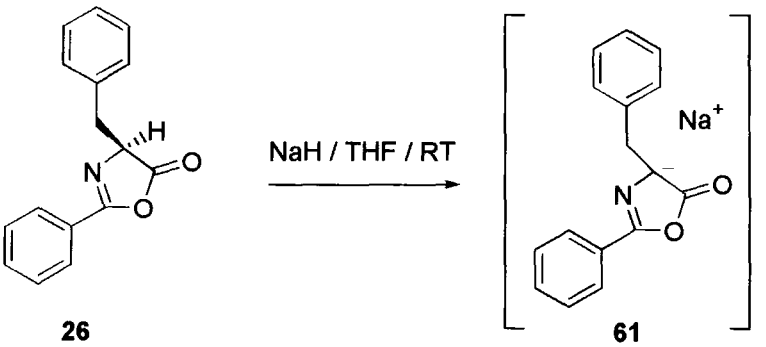

Scheme 4.4: Carbanion synthesis

This reaction was carried out by adding a solution of the oxazolone **26** in THF to a slurry of sodium hydride again in THF at 0°C. After 30 minutes at 0°C the reaction was warmed to ambient temperature for a further 60 minutes. The reaction proceeded smoothly with a gentle evolution of hydrogen gas, which subsided after 30 minutes, leaving a bright yellow solution. Due to the expected reactivity of the carbanion, no attempt was made to isolate this material and fluorination with Selectfluor was performed immediately.

4.2.3 Electrophilic fluorination using Selectfluor

Electrophilic fluorinating agents have been reviewed[40], of which Selectfluor, 1-chloromethyl-4-fluoro-1,4-diazoniabicyclo [2.2.2] octane bis (tetrafluoroborate), **62** is the most widely used example.

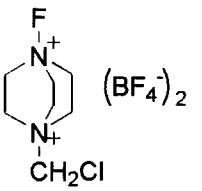

62

Selectfluor is a member of the N-F class of electrophilic fluorinating agents and specific reviews[41] pertaining to its use on a wide range of substrates have been published. Two mechanisms have been proposed for the mode of action of Selectfluor, both of which involve nucleophilic addition to the fluorine in either a one or two step process as shown in Scheme 4.5.

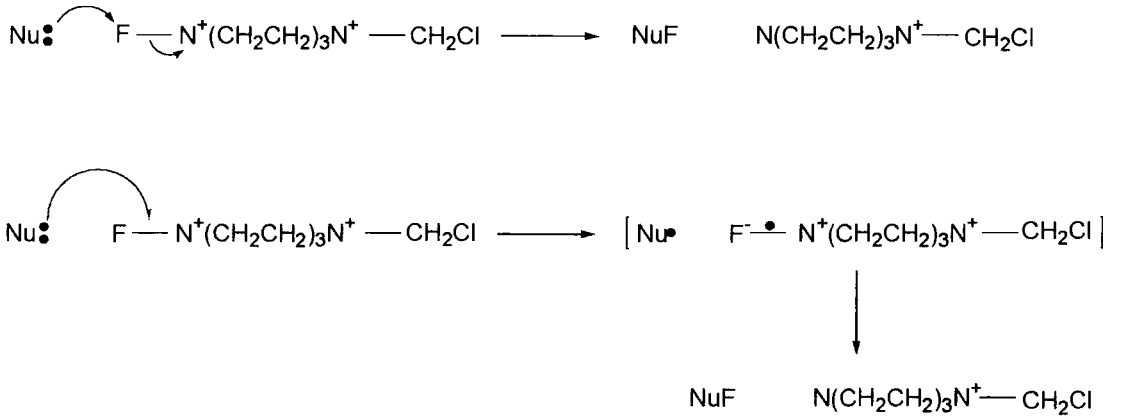

Scheme 4.5: Selectfluor fluorination mechanisms

Fluorination of a carbanion species was of interest in our research to achieve the desired substitution of the oxazolone **61**. Examples[42] of fluorinations of stabilised carbanions include α-sulphonylesters **63** and substituted malonates **64** as shown in Figure 4.3, which have been reported to proceed efficiently and in good yields.

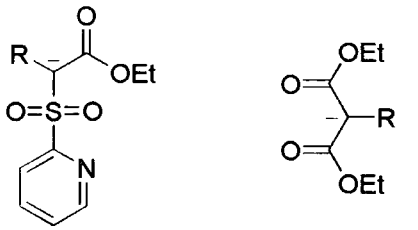

63 64

Figure 4.3: Carbanions suitable for fluorination with Selectfluor

In our case fluorination of carbanion, **61** offered access to **27** as shown in Scheme 4.6.

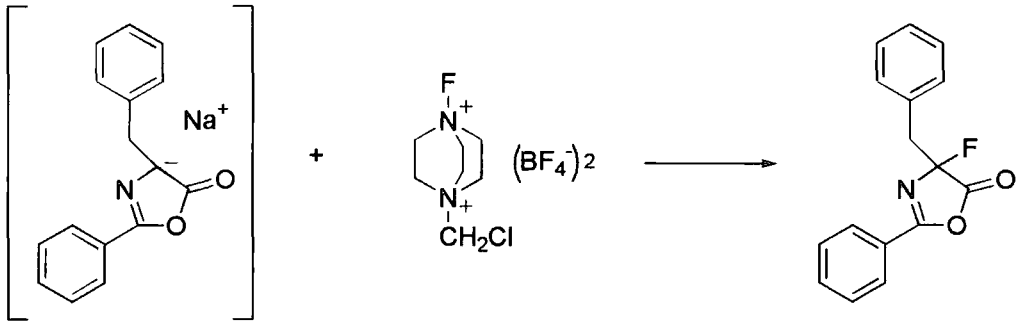

61 62 27

Scheme 4.6: Synthesis of (*RS*)-4-benzyl-4-fluoro-2-phenyl-5-oxazolone, **27**

The reaction was expected to be straightforward and a direct addition of 1 equivalent of Selectfluor to the carbanion solution was initially investigated. At this stage it was noticed that Selectfluor showed poor solubility in the reaction mixture. In an attempt to improve its solubility DMF was added to the reaction mixture prior to the Selectfluor addition. After stirring for 30 minutes a colourless solution remained and ^{19}F NMR analysis on this mixture shows a dd at –127.8 ppm, which is consistent with the formation of the C-F bond. The desired product was extracted into diethyl ether and washed with water until pH > 6. ^{19}F NMR analysis of the recovered product is shown in Figure 4.4 and it corresponds to the desired compound **27**.

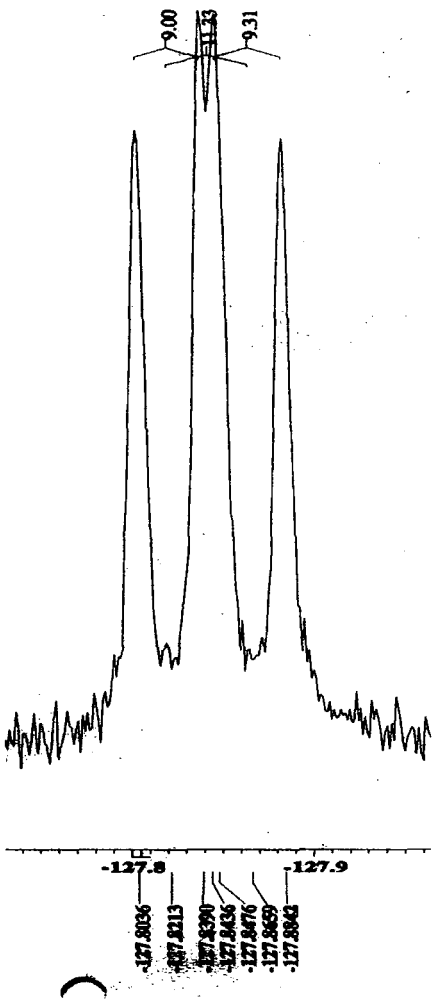

Figure 4.4: ^{19}F NMR of (*RS*)-4-benzyl-4-fluoro-2-phenyl-5-oxazolone, **27**

This would be the expected ^{19}F NMR spectrum from a fluorinated oxazolone, showing coupling (J = 9 Hz and 11 Hz) with the two non-equivalent protons in the adjacent CH_2 group. The reciprocal couplings were also evident in the ^{1}H NMR spectrum.

This material was found to be unstable even when stored in a fridge under nitrogen and for subsequent experiments it was used immediately.

4.2.4 Attempted α-fluoro peptide preparation from 27

At this stage a carboxylate protected amino acid was needed to react with the fluorinated oxazolone to prepare the desired α-fluoro peptide. It was decided that the methyl ester of (*S*)-alanine would be a suitable candidate. This was prepared by the liberation of the free base of (*S*)-alanine methyl ester hydrochloride using triethylamine.

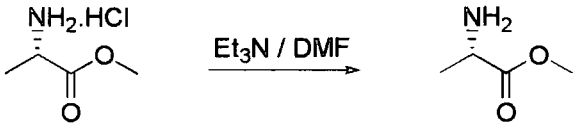

28

Scheme 4.7 Preparation of (*S*)-alanine methylester, **28**

This gave rise to a solution of (*S*)-alanine methylester **28** in DMF and this was used in the attempts to trap the fluorinated oxazolone to generate the α-fluoro peptide as shown in Scheme 4.8.

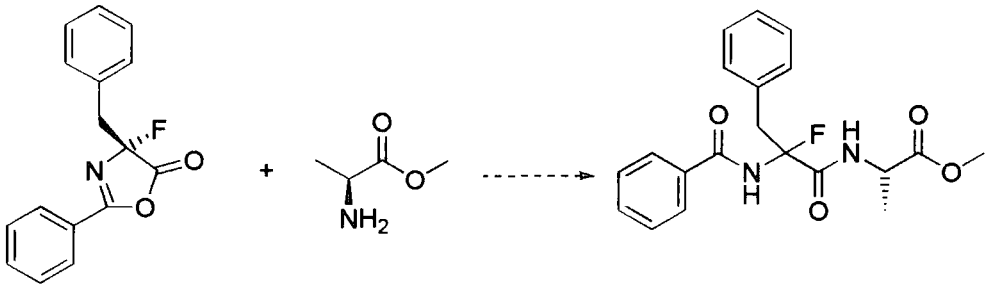

27 **28** **29**

Scheme 4.8: Strategy for α-fluoro peptide synthesis

The fluorinated oxazolone solution was added directly to a solution of 1 equivalent of amino ester **28.** ^{19}F NMR initially showed no change however after a 30-minute reaction time the organic fluorine signals were no longer evident in the NMR spectrum and only a broad peak at –160 ppm, which is consistent with an HF.DMF complex. It was postulated that the peptide was unstable and broke down *via* HF elimination as soon as any α-fluoropeptide was generated.

4.2.5 Alternative oxazolone substituents

Due to the unstable nature of the α-fluoropeptide, a strategy to further reduce the influence of the lone pair on nitrogen was sought. One approach that was investigated was to introduce electron withdrawing groups on the oxazolone as shown in Figure 4.5 to reduce the potential for the lone pair to assist in the elimination of fluoride.

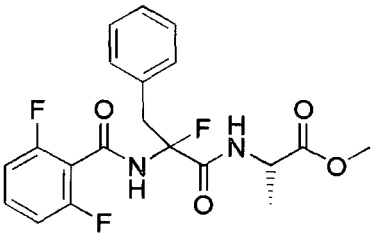

65

Figure 4.5: Proposed structure for a more stable α-fluoropeptide

It was envisaged that α-fluoropeptide, **65** could be prepared by a similar route to that described above for α-fluoropeptide **29**, starting from 2,6-difluorobenzoyl chloride, **66**, as shown in Scheme 4.9 below.

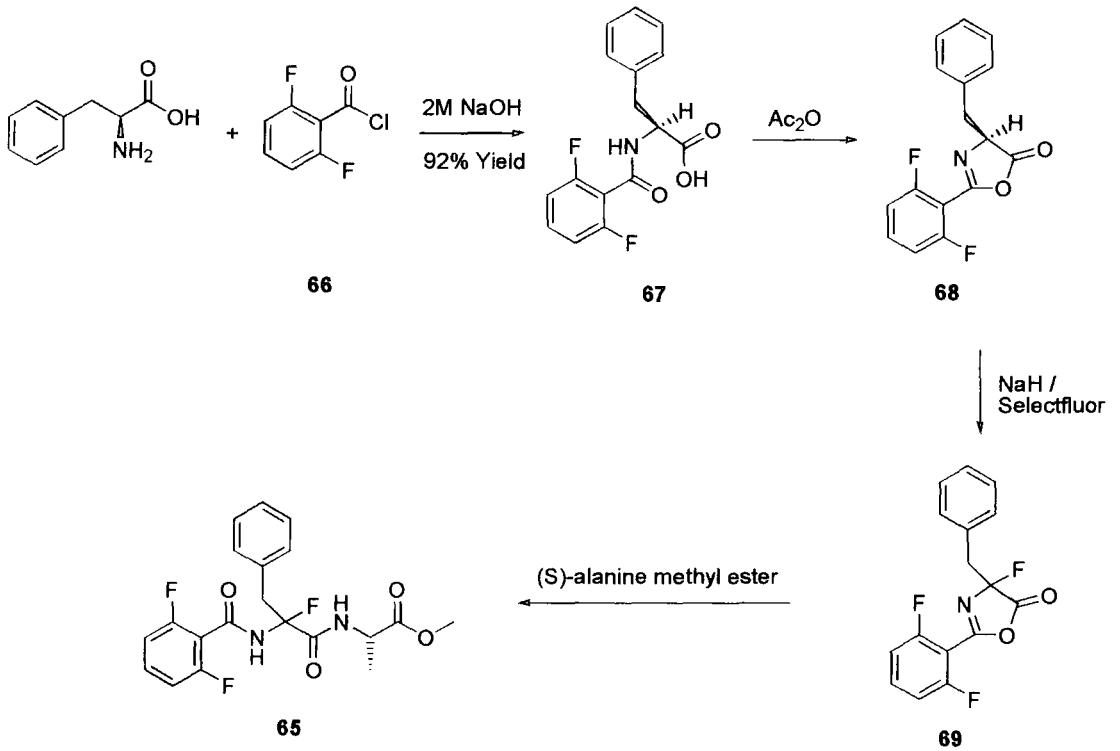

66 **67** **68** **69** **65**

Scheme 4.9: Alternative α-fluoropeptide synthesis

Preparation of the initial amide **67**, proceeded in a straightforward manner and in good yield. Conversion of **67** to oxazolone **68** required more aggressive conditions than those used previously (reflux for 60 minutes compared to ambient) to convert the last traces of the starting material. The resultant product also required chromatographic purification before it was suitable for use in the next stage of the synthesis.

4.2.5.1 Fluorination of oxazolone 61

The next stage in the synthesis was to generate a carbanion to enable fluorination with Selectfluor to be carried out. This again was achieved by reaction with sodium hydride in THF. This reaction produced a bright yellow slurry, which was reacted immediately with 1 equivalent of Selectfluor. The reaction solution was held for 15 minutes at ambient temperature and TLC analysis confirmed that only 1 component was present and that it was different from the starting material. ^{19}F NMR showed the presence of the aromatic CF group but no other organic fluorine substituents could be detected. The reaction was stirred overnight to allow the fluorination to progress, after which time NMR and TLC analysis showed no change. The reaction mixture was worked up in an attempt to identify this new compound by extracting into diethyl ether and washing with water. The solvents were removed and the colourless oil was recrystallised from ethyl acetate / hexane (20:80) to give a white solid.

The white solid was analysed by NMR and MS and initially a tetramer was suggested as a possible structure for the new compound. However after further recrystallisation a crystal was obtained that was suitable for X-ray structure analysis confirming the formation of dimer product. This was 3,5-dibenzyl-1-(2,6-difluorobenzoyl)-3-(2,6-difluorobenzoylamino)pyrrolidine-2,4-dione **70** as shown below in Figure 4.6.

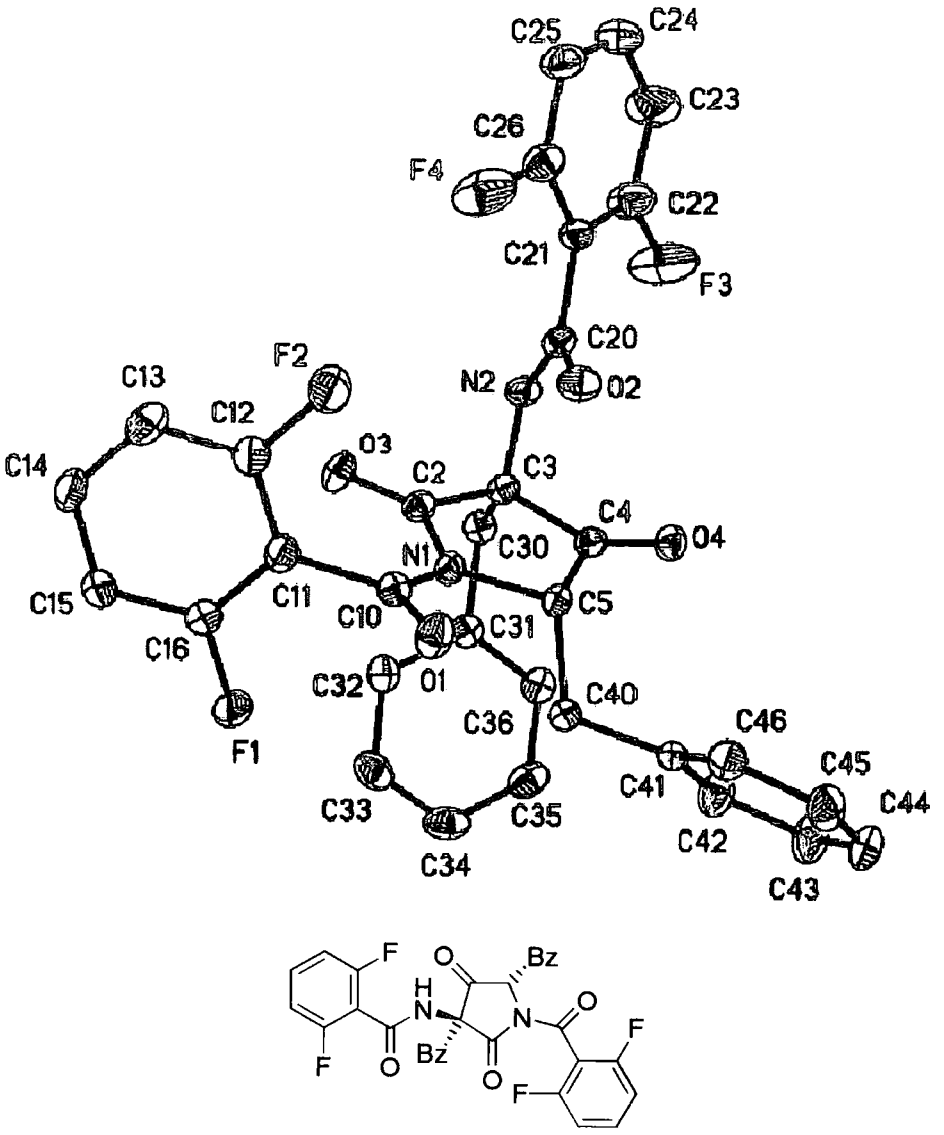

70

Figure 4.6: X-ray structure of 3,5-dibenzyl-1-(2,6-difluorobenzoyl)-3-(2,6-difluorobenzoylamino)pyrrolidine-2,4-dione **70**

The dimerisation of 5-oxazolones has previously been reported[43] when treated with a strong base such as LDA. The dimer arises from the reaction between the carbanion and an unmodified oxazolone as shown in Figure 4.7.

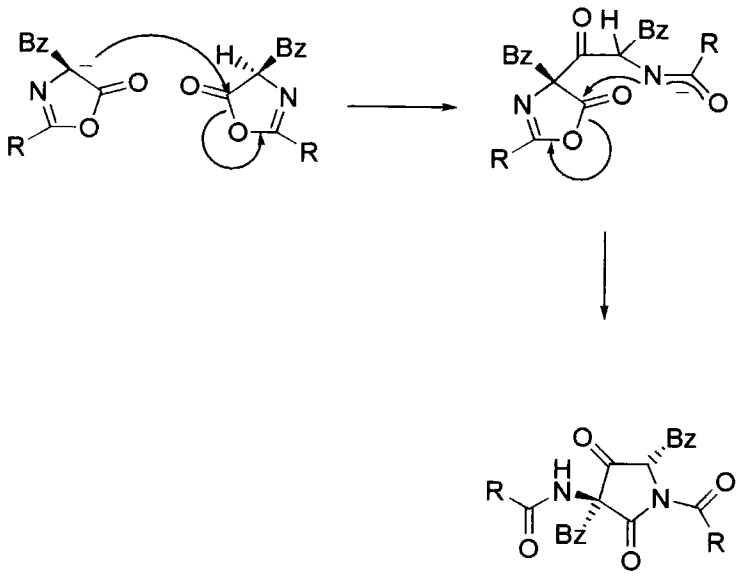

Figure 4.7: Mechanism for dimer formation

4.2.6 Barrier to rotation

An interesting observation from analysis of **70** was how different the two aromatic CF signals were in the ^{19}F NMR spectrum as shown in Figure 4.8.

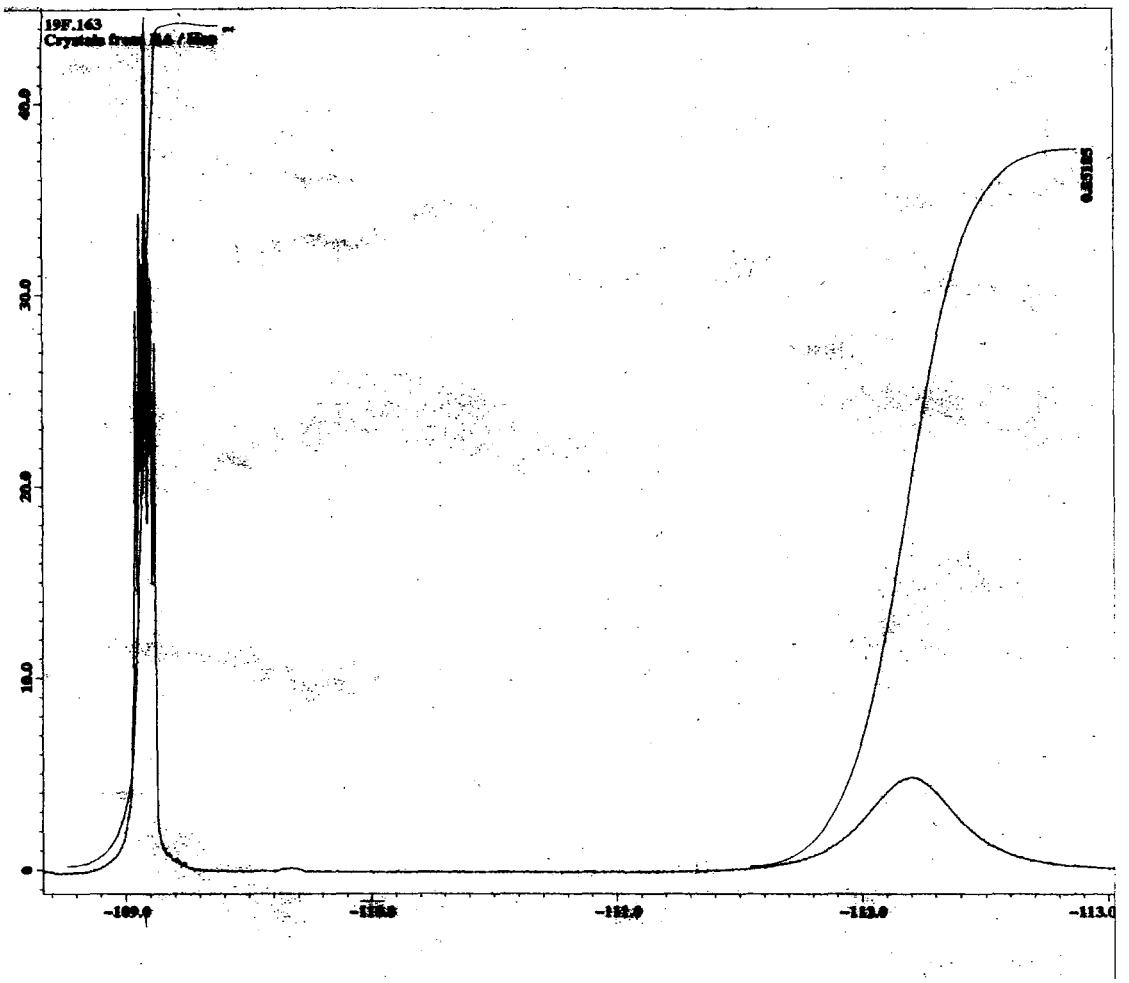

Figure 4.8: ^{19}F NMR spectrum of dimer, **70**

One of the signals was very sharp with the aromatic CH couplings being evident, while the other was a very broad peak with no coupling information visible. It was postulated that one of the difluorophenyl substituents was experiencing restricted rotation as shown in Figure 4.9.

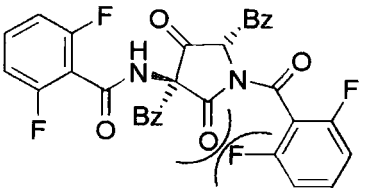

70

Figure 4.9: Restricted rotation of difluorophenyl substituent

Rotation of the 2,6-difluorophenyl substituent at ambient temperature must be at such a rate as to allow the two fluorine nuclei to be detected in different environments by NMR. At higher temperatures the rate of rotation will of course increase and NMR should detect the two fluorine nuclei as one averaged signal. However, at lower than ambient temperatures the rate of rotation of the 2,6-difluorophenyl substituent is reduced so that NMR sees the two fluorine signals with different chemical shifts. In between these extremes will be the coalescence temperature, which has been described as the point where the two signals have neither a maxima or minima between them.

Dynamic NMR can be an excellent tool[44] for determining barriers to rotation if the rates of exchange between two signals are close to the NMR measurement time, which is typically in the millisecond range. In order to determine the energy barrier to rotation, the coalescence point and the chemical shift difference for the two signals needs to be determined. This can be determined by using variable temperature NMR and depending on the type of exchanging system that is present may require either a high or low VT experiment.

With the example shown above in Figure 4.8 the signal of interest is already exchanging at a rate faster than the NMR experiment timescale and therefore a broad signal with a maxima is seen which averages the two individual signals. The temperature therefore needs to be reduced to identify the coalescence point and the chemical shifts of the individual signals. Accordingly ^{19}F NMR spectra were collected in the temperature range –40 to 20°C and the spectra are shown in Figure 4.10.

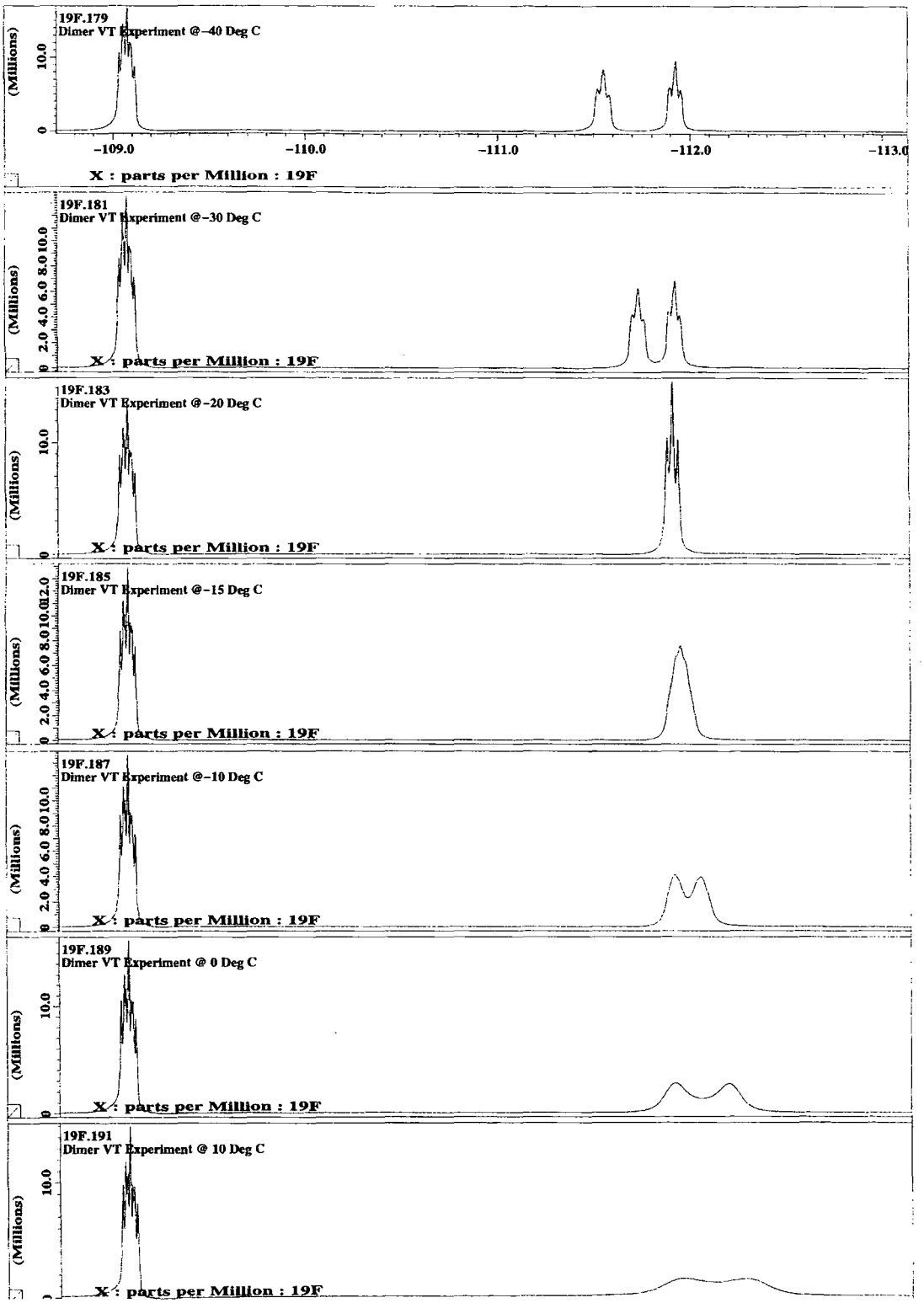

Figure 4.10: ^{19}F VT NMR on dimer

The ^{19}F VT NMR spectra shown above are unusual and do not conform to what was expected from a simple barrier to rotation. As the temperature is reduced the broad signal begins to separate into two signals and the two signals would have expected to sharpen so the individual chemical shifts for the two fluorine signals could be determined. However in the VT NMR analysis of **70** a more complex relationship exists and two effects have been uncovered.

The low field signal at ambient temperature behaves exactly as expected showing a gradual sharpening to reveal coupling with the adjacent aromatic protons. The high field signal at ambient temperature displays a very different response as the temperature is reduced. The chemical shift of this signal is dependant on the temperature at which it is measured, so much so that at temperatures below –30°C this signal has now become the low field signal of the pair. This can be explained by the movement of other substituents (e.g. aryl ring) in the molecule, which would affect the magnetic environment of one of the fluorine atoms.

Secondly a barrier to rotation is evident and a coalescence temperature of approximately 20°C as shown in Figure 4.8 has been determined.

Calculation of the energy barrier to rotation is possible from NMR data if the chemical shift difference and the coalescence temperature of the two signals are known. However in the VT NMR analysis of **70** the chemical shift difference for the two signals could not be determined and therefore the energy barrier to rotation could not be calculated.

4.3 Azirine method

Our second approach to an α-fluoropeptide is shown in **Scheme 4.10** and involves reaction of a protected amino acid with azirine **71**.

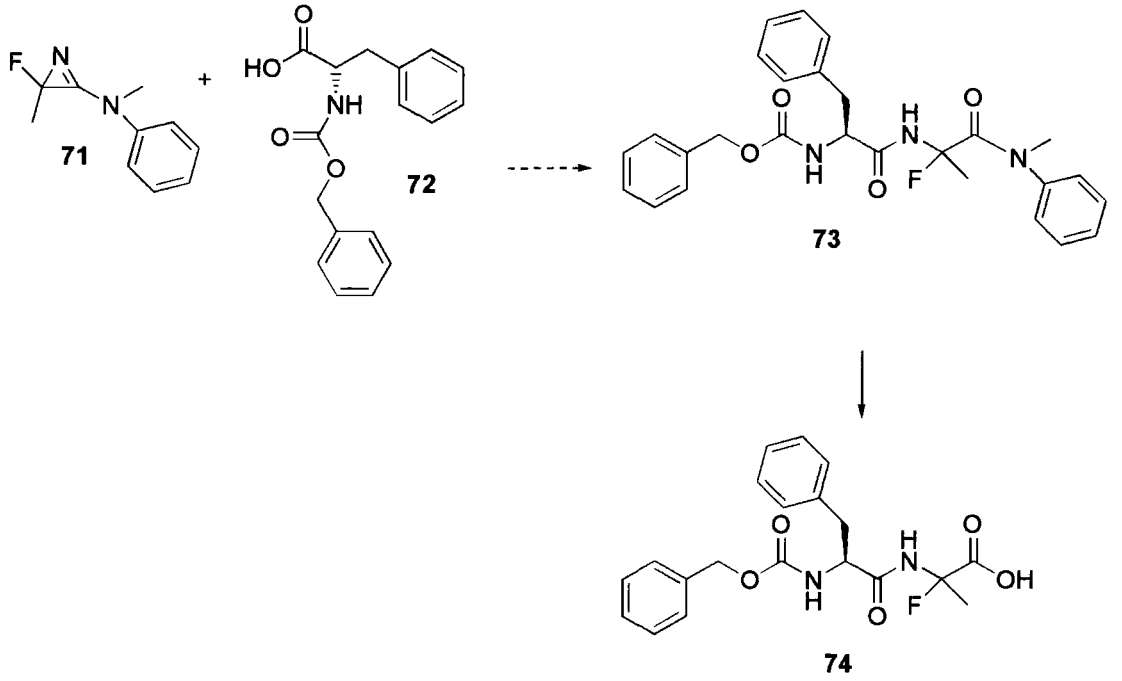

Scheme 4.10: α-Fluoropeptide preparation using azirine intermediate

At the outset this approach appeared desirable as it was already demonstrated for the preparation of non-fluorinated peptides[45]. This approach has been demonstrated to be very successful in preparing a wide variety of α-substituted peptides with the only question being whether an α-fluoropeptide could be prepared in this manner. The major difficulty with this approach at the outset was the preparation of the azirine **71** as no examples of fluorinated azirines have been reported.

4.3.1.1 Attempted fluorinated azirine preparation

Preparation of azirine **71** was attempted as shown below in Scheme 4.11.

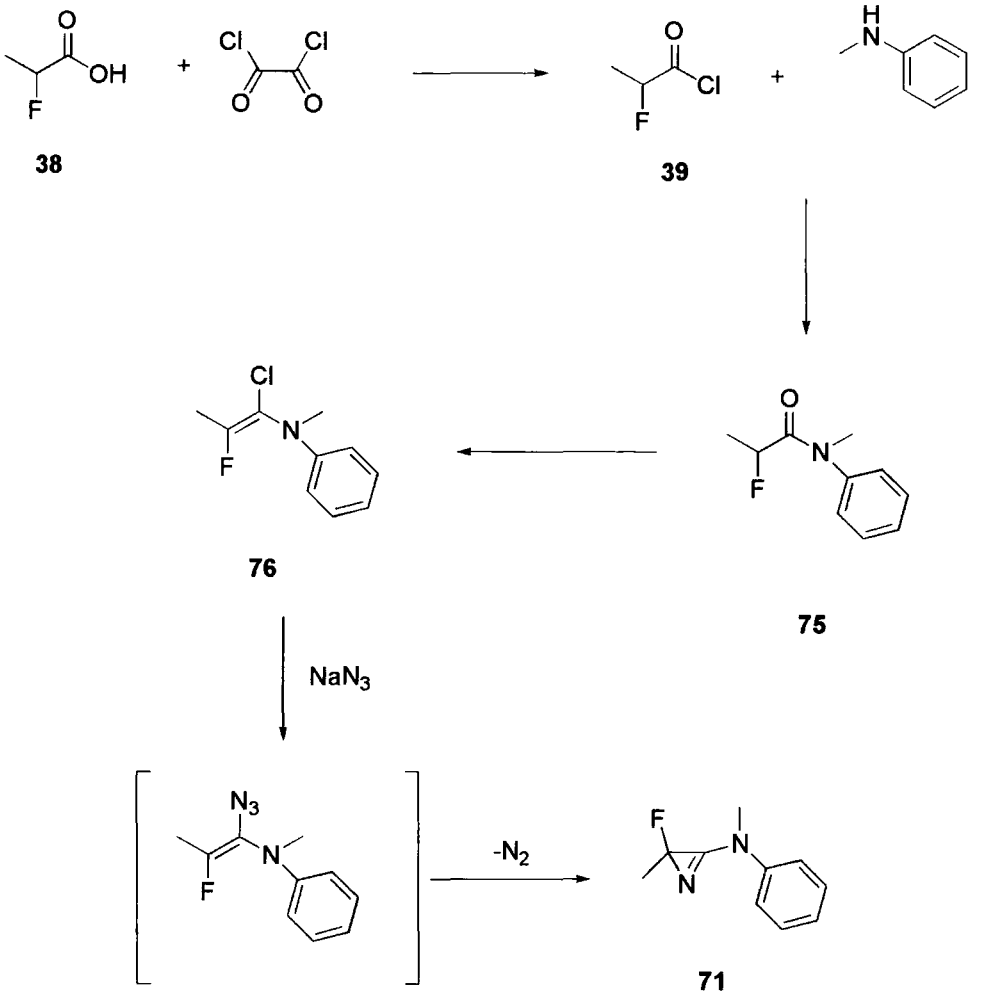

Scheme 4.11: Preparation of azirine **63**

4.3.1.1.1 Synthesis of amide 75

N-(2-fluoropropionyl)-N-methyl aniline **75** was prepared in a straightforward manner using the methodology previously described for preparing the acid chloride **39**, followed by reaction with N-methylaniline. The amide was produced in moderate yields (46%) as a colourless oil. A DCM solution of amide **75** was prepared (1 g / 10 mL) for future use in the azirine synthesis.

4.3.1.1.2 Synthesis of chlorofluoroenamine 76

The initial approach to prepare the chlorofluoroenamine **76** involved the use of phosgene. This has been reported[46] to be successful in the preparation of non-

fluorinated chloroenamines and involves the production of an imminium chloride intermediate as shown in Scheme 4.12.

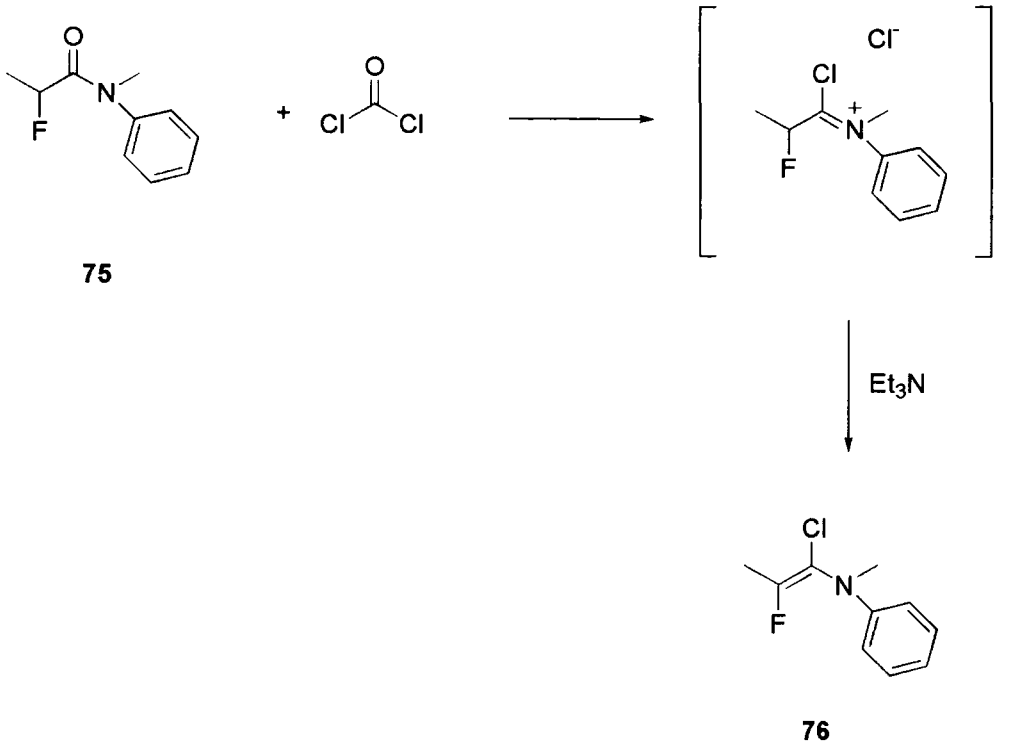

75

76

Scheme 4.12: Preparation of chlorofluoroenamine **76**

Phosgene was generated from triphosgene, which is a white solid and is easy to handle. Triphosgene generates three equivalents of phosgene *in situ* eliminating the need to handle highly toxic phosgene gas. Initially the reaction was attempted in two stages with the phosgene reaction being carried out initially. However ^{19}F NMR and TLC did not indicate that the reaction was taking place. A review[47] on the use of phosgene pointed to increased reactivity if triethylamine was present. At this stage a new component was evident in the ^{19}F NMR spectrum with a chemical shift of -109.6 ppm however it was a minor component alongside the starting material **75**, and no further attempts to improve the phosgene reaction were made.

An alternative approach using oxalyl chloride as the chlorinating agent was tried with the addition of oxalyl chloride being carried out at –70°C. The reaction mixture was warmed to ambient temperature for 60 minutes, cooled to –70°C and the triethylamine was added. Again the reaction mixture was warmed to ambient temperature at which point TLC confirmed that four components were present and that the starting material was the minor component. The reaction was left overnight at ambient temperature but no further change was observed by TLC analysis. The crude product was purified by column chromatography over silica gel to give a red / orange oil. A possible

explanation for the vivid colour in the product could be the charge transfer equilibrium shown below.

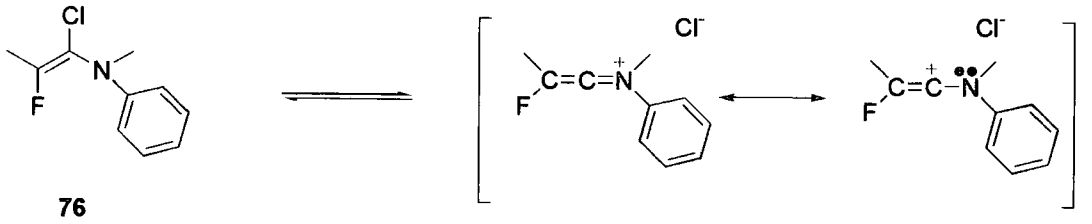

Figure 4.11: Chlorofluoroenamine equilibrium

The ^{19}F NMR spectrum showed a quartet (16 Hz) at −102.1ppm, which is consistent with the desired product.

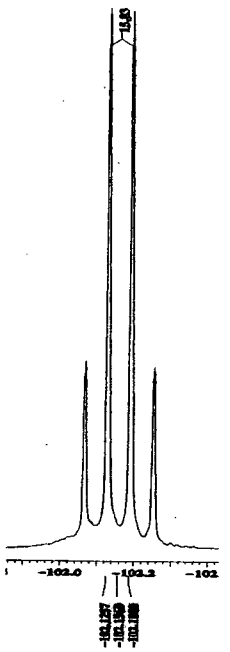

Figure 4.12: ^{19}F NMR of chlorofluoroenamine **76**

4.3.1.1.3 Cyclisation reaction

Cyclisation of non-fluorinated chloroenamines can be achieved *via* a two-stage reaction with a diazonium intermediate[46,48] to give exclusively the 2*H*-azirines as shown in Scheme 4.13.

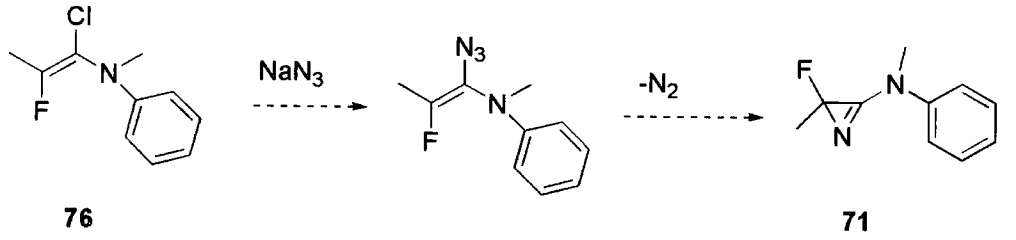

Scheme 4.13: Strategy to azirine formation

For chlorofluoroenamine the reaction was initially carried out in diethyl ether, with 1 equivalent of sodium azide but after 2 days at ambient temperature no conversion could be detected by TLC and NMR analysis. In an attempt to improve the solubility of the sodium azide, DMF was added to the reaction mixture but after a further two days at ambient no reaction could be detected. Finally the reaction was heated under reflux for 8 hours but once again no reaction products could be detected.

4.4 Conclusions

- Of the two routes assessed towards α-fluoropeptide synthesis, the oxazolone method would appear to have the greatest prospects.
- Oxazolone **27** was prepared and although unstable it was possible to attempt an α-fluoropeptide synthesis, by trapping with alanine methyl ester. However this led to a very unstable product and elimination of fluoride as determined by ^{19}F NMR.

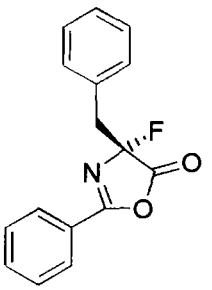

27

- Alternative methods for isolating the α-fluoropeptide, such as increasing the reactivity of the trapping species and deactivating the nitrogen, are worthy of further investigation.
- Attempts to improve the stability of the oxazolone by incorporating electron-withdrawing groups have proved unsuccessful and in our case this has promoted dimerisation to pyrrolidone **70**.

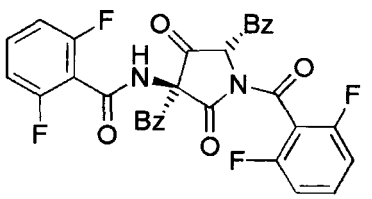

70

- An interesting phenomenon has been investigated for pyrrolidone **70** concerning the barriers to rotation of the difluorophenyl substituents. Variable temperature ^{19}F NMR has been used to monitor the changes to the two fluorine signals as the temperature is reduced. This has shown that this is not a simple barrier to rotation and that interaction with other substituents (e.g. aryl) on the pyrrolidone, are changing the environment and hence the chemical shift of one of the fluorine atoms.
- A method for preparing chlorofluoroenamines **76** has been developed.

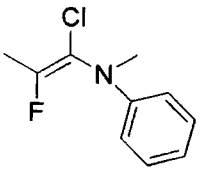

76

- Investigations into the use of azirines to prepare α-fluoropeptides have proved unsuccessful due to the difficulty in preparing fluoroazirines from chlorofluoroenamines.

Chapter 5 - Experimental and References

5.1 General Section

All practical work was carried out in the laboratories of Pfizer, Whalton Road, Morpeth. Unless otherwise stated reactions were carried under a nitrogen atmosphere at room temperature with stirring. All reactions involving the use of hydrofluoric acid were carried out in Teflon equipment due to its incompatibility with glass. All solvents used were high purity grade supplied by Romil Chemical Company. All starting materials and reagents were purchased from Aldrich Chemical Company unless otherwise stated.

TLC analysis for following reaction progress was carried out on Merck, Kieselgel 60 coated glass plates and visualisation by UV, phosphomolybdic acid or sulphuric acid was used.

Melting points were determined using a differential scanning calorimeter, with the melting range being the start and end of the endotherm.

NMR spectra were recorded on a Jeol EX 270 MHz spectrometer on a deuterochloroform solution unless otherwise stated. ^{1}H NMR were ran at 270 MHz, ^{13}C NMR were ran at 67.9 MHz and ^{19}F NMR were ran at 254.2 MHz.

IR spectra were recorded using a Nicolet magna IR, which is fitted with a microscope to enable spectra of an individual crystal to be determined.

MS analysis was performed on a VG TRIO 1000 spectrometer.

X-ray crystal structures were determined at the University of Durham by Dr Andres Goeta.

5.2 Experimental for Chapter 2

5.2.1 (*RS*)-2-Fluoropropionic acid, 38

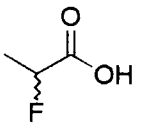

A 250 mL Teflon bottle, containing a magnetic follower, was charged with pyridinium polyhydrogen fluoride (100 mL, 70% w/w) and then (*RS*)-alanine, (8.6 g, 96 mmol) was added. The solution was cooled to 0°C and sodium nitrite (22.6 g, 232mmol) was added in five equal portions over 1 hour. The reaction mixture was stirred at 0°C for 1 hour and then warmed to room temperature and then stirred overnight. The reaction was quenched by addition to ice water (200 mL), extracted into diethyl ether (3 x 200 mL), washed with sodium chloride solution (3 x 200 mL, 5% w/v) and dried over anhydrous sodium sulphate, filtered, evaporated and distilled *in vacuo* (68°C at 20 mbar) to afford a colourless liquid as the pure product.

Yield: 1.4g, 15.2 mmol, 14%.

^{1}H NMR (d_6 Acetone): 5.12(1H, dq, J 48.5, 6.9, CFH), 1.61(3H, dd, J 23.5, 6.9, Me).

^{13}C NMR (d_6 Acetone): 85.1(d, *J* 182.7, CFH), 18.2(d, *J* 22.3, CH_3), No carbonyl signal detected.

^{19}F NMR (d_6 Acetone): -184.76(dq, *J* 48.3, 23.5, CFH).

5.2.2 (*RS*)-2-Fluoropropionyl chloride, 39

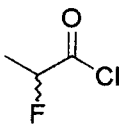

Thionyl chloride was added dropwise to (*RS*)-2-fluoropropionic acid, (1.00 g, 10.9 mmol) at room temperature until effervescence ceased. This signalled the absence of free water in the (*RS*)-2-fluoropropionic acid. A further 1 equivalent of thionyl chloride was added and the reaction was heated to reflux for 60 min. A sample was removed for ^{1}H and ^{19}F NMR analysis to confirm the absence of starting material. The product was distilled from the reaction mixture at atmospheric pressure to give a colourless liquid.

Yield: 1.0 g, 9.1 mmol, 83%.

^{1}H NMR: 5.14(1H, dq, *J* 48.6, 7.0, CFH), 1.66(3H, dd, *J* 22.8, 6.8, Me).

^{13}C NMR: 172.5(d, *J* 27.9, C=O), 90.3(d, *J* 194.5, CFH), 17.6(d, *J* 21.9, CH_3).

^{19}F NMR: -171.4(dq, *J* 49.1, 23.0, CFH).

5.2.3 N- (*R,S*)-2-Fluoropropionyl-(*S*)-phenylalanine, 36

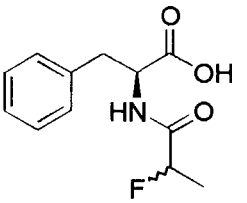

(*S*)-Phenylalanine (2.63g, 16 mmol) was dissolved in 4M NaOH (12 mL, 48 m mol). The reaction was cooled to 0°C and (*RS*)-2-fluoropropionyl chloride (1.6g, 14 m mol) was added dropwise. The reaction was warmed to room temperature and stirred for 30 minutes, acidified to pH = 3 with concentrated HCl and the product extracted into ethyl acetate (100 mL), washed with sodium chloride solution (3 x 100 mL, 5% w/v) and dried over anhydrous sodium sulphate, filtered and evaporated *in vacuo* to afford the crude product as a colourless oil as a mixture of diastereoisomers.

Yield: 0.6g, 2.5 mmol, 16%.

^{1}H NMR: 7.23(5H, m, ArH), 6.92(1H, m, NH), 5.03(1H, dq, *J* 39.1, 6.8, CFH), 4.90(1H, overlapping dd, *J* 6.8, 6.8, CH), 3.19(2H, m, CH_2), 1.48(3H, 2 overlapping dd, *J* 24.5, 6.8, CH_3).

^{13}C NMR: 174.2(C=O), 174.1(C=O), 171.2(d, *J* 19.0, C=O), 171.1(d, *J* 20.0, C=O), 135.3(Ar-C), 135.3(Ar-C), 129.3(Ar-C), 129.2(Ar-C), 128.6(Ar-C), 128.5(Ar-C), 127.2(Ar-C), 127.2(Ar-C), 88.3(d, *J* 183.6, CFH), 88.2(d, *J* 183.5, CFH), 52.6(CH), 52.4(CH), 37.4(CH_2), 37.2(CH_2), 18.2(d, *J* 21.9, CH_3), 18.12(d, *J* 20.9, CH_3).

^{19}F NMR: -182.8(ddq, *J* 49.2, 24.7, 4.2, CFH), -182.9(ddq, *J* 49.8, 25.2, 4.3, CFH).

5.2.4 N- (*R, S*)-2-Fluoropropionyl-(*S*)-phenylalanine sodium salt

N-(*R, S*)-2-Fluoropropionyl-(*S*)-phenylalanine, **36**, (0.60g, 2.5 mmol) was dissolved in the minimum quantity of 4M NaOH (5 mL). The pH of the solution was adjusted to pH = 7 using concentrated HCl and then diluted to a final volume of 10 mL using distilled water to give a 0.25 M solution of **36** sodium salt.

5.2.5 Acylase hydrolysis reaction

Various acylase solutions (hog kidney acylase (HKA), *Aspergillus melleus* acylase (AMA), *Bacillus icheniformis* protease (BIP) and the *Streptomyces caespitrum* protease (SCP)) were prepared at varying concentrations (HKA 11.5 $mgmL^{-1}$, AMA 219 $mgmL^{-1}$, BIP 6.4 $mgmL^{-1}$ and SCP 159.7 $mgmL^{-1}$) in pH = 7 phosphate buffer, depending on their quoted activity for hydrolysing N-acetyl-L-methionine. An NMR

tube was then filled with 0.5 mL of **36** sodium salt and 0.5 mL of the buffered enzyme solution. The NMR tubes were warmed to 37°C and the NMR spectra were recorded to monitor the progress of the hydrolysis.

5.2.6 (*R*)-2-Fluoropropionic Acid, (*R*) 38

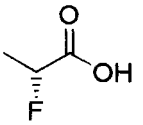

A 250 mL Teflon bottle, containing a magnetic follower, was charged with pyridinium polyhydrogen fluoride (100 mL, 70% w/w) and then (*R*)-alanine, (8.6 g, 96 mmol) was added. The solution was cooled to 0°C and sodium nitrite (22.6 g, 232 mmol) was added in five equal portions over 1 hour. The reaction mixture was stirred at 0°C for 1 hour and then warmed to room temperature and then stirred overnight. The reaction was quenched by addition to ice water (200 mL), extracted into diethyl ether (3 x 200 mL), washed with sodium chloride solution (3 x 200 mL, 5% w/v) and dried over anhydrous sodium sulphate, filtered, evaporated and distilled *in vacuo* at 23 mbar to afford a yellow liquid of mixed acid and anhydride products.

Yield: 1.6g, 17.4 mmol, 18%.

^{1}H NMR (d_6-Acetone): 5.12(1H, dq, J 48.5, 6.9, CFH), 1.61(3H, dd, J 23.5, 6.9, Me).

^{13}C NMR (d_6-Acetone): 85.1(d, *J* 182.7, CFH), 18.2(d, *J* 22.3, CH_3), No carbonyl signal was observed.

^{19}F NMR (d_6-Acetone): -184.8(dq, *J* 48.3, 23.5, CFH).

5.2.7 (*R*)-2-Fluoropropionyl chloride, (*R*) 39

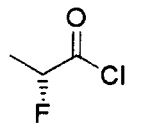

Thionyl chloride, (4.56g, 38.3 mmol) was added dropwise to (*R*)-2-fluoropropionic acid, (1.00 g, 10.9 mmol) at room temperature. The reaction was heated under reflux for 30 min and a sample was removed for ^{1}H and ^{19}F NMR analysis to confirm the absence of starting material. A mixture of the desired product and thionyl chloride was distilled from the reaction mixture at atmospheric pressure to give the product as a yellow liquid.

Yield: 1.26 g, 11.3 mmol, 104% (desired product plus thionyl chloride).

^{1}H NMR: 5.14(1H, dq, *J* 48.6, 7.0, CFH), 1.66(3H, dd, *J* 22.8, 6.8, Me).

^{13}C NMR: 172.5(d, *J* 27.9, C=O), 90.3(d, *J* 194.5, CFH), 17.6(d, *J* 21.9, CH_3).

^{19}F NMR: -171.4(dq, *J* 49.1, 23.0, CFH).

5.2.8 N-(*R*)-2-Fluoropropionyl-(*S*)-phenylalanine, (*R*,*S*)36

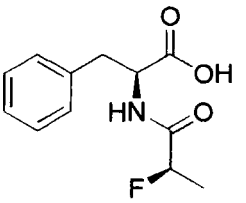

(*S*)-Phenylalanine (1.81g, 11 mmol) was dissolved in 4M NaOH (11 mL, 44 mmol). The reaction was cooled to 0°C and (*R*)-2-fluoropropionyl chloride (1.26g, 11.3 mmol) was added dropwise. The reaction was warmed to room temperature and stirred for 30 minutes, acidified to pH = 3 with concentrated HCl and the product extracted into ethyl acetate (100 mL), washed with sodium chloride solution (3 x 100 mL, 5% w/v) and dried over anhydrous sodium sulphate, filtered and evaporated *in vacuo* to afford the crude product as a colourless oil (0.23 g). NMR showed that the product was a mixture of (*R*, *S*) **36** and (*S*, *S*) **36** in a ratio 9:1. Further purification was afforded by treating the mixture with 4M NaOH (1 mL), acidifying to pH = 7 with HCl and reacting with a buffered solution (pH = 7) of *Aspergillus melleus* acylase until no (*S*, *S*) **36** diastereoisomer remained. The pH of the reaction mixture was then adjusted to 2 using HCl, extracted into ethyl acetate, dried over anhydrous sodium sulphate, filtered and evaporated *in vacuo* to afford the pure product, as judged by ^{19}F NMR, as colourless oil.

Yield: 93.6 mg, 0.8 mmol, 9%.

^{1}H NMR: 7.23(5H, m, ArH), 6.92(1H, m, NH), 5.03(1H, dq, *J* 39.1, 6.8, CFH), 4.90(1H, overlapping dd, *J* 6.8, 6.8, CH), 3.28(1H, dd, *J* 14.0, 7.0, CH_2a), 3.11(1H, dd, *J* 14.0, 7.0, CH_2b), 1.55(3H, dd, *J* 24.5, 6.8, CH_3).

^{13}C NMR: 174.2(C=O), 171.2(d, *J* 19.0, C=O), 135.3(Ar-C), 129.3(Ar-C), 128.6(Ar-C), 127.2(Ar-C), 88.3(d, *J* 183.6, CFH), 52.6(CH), 37.2(CH_2), 18.0(d, *J* 20.9, CH_3).

^{19}F NMR: -182.9(ddq, *J* 49.8, 25.2, 4.3, CFH).

5.2.9 N- (*R*)-2-Fluoropropionyl-(*S*)-phenylalanine sodium salt

N-(*R*)-2-Fluoropropionyl-(*S*)-phenylalanine, (*R*, *S*)**36**, (0.20g, 0.8 mmol) was dissolved in the minimum quantity of 4M NaOH (1 mL). The pH of the solution was adjusted to pH = 7 using concentrated HCl and then diluted to a final volume of 10 mL using distilled water to give a 83.6 mM solution of (*R*, *S*)**36** sodium salt.

5.2.10 (S)-2-Fluoropropionic acid, (S) 38

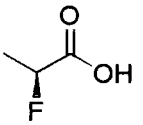

A 125 mL Teflon bottle, containing a magnetic follower, was charged with pyridinium hydrogen fluoride (100 mL, 70% w/w) and then (*R*)-alanine, (8.6 g, 96 mmol) was added. The solution was cooled to 0°C and sodium nitrite (22.6 g, 232 mmol) was added in five equal portions over 1 hour. The reaction mixture was stirred at 0°C for 1 hour and then warmed to room temperature and then stirred overnight. The reaction was quenched by addition to ice water (100 mL), extracted into diethyl ether (3 x 100 mL), washed with sodium chloride solution (3 x 100 mL, 5% w/v) and dried over anhydrous sodium sulphate, filtered, evaporated and distilled *in vacuo* at 23 mbar to afford a yellow liquid of mixed acid and anhydride products.

Yield: 1.31g, 14.2 mmol, 15%.

^{1}H NMR (d_6-Acetone): 5.12(1H, dq, J 48.5, 6.9, CFH), 1.61(3H, dd, J 23.5, 6.9, Me).

^{13}C NMR (d_6-Acetone): 85.1(d, *J* 182.7, CFH), 18.2(d, *J* 22.3, CH_3), no carbonyl signal evident.

^{19}F NMR (d_6-Acetone): -184.76(dq, *J* 48.3, 23.5, CFH).

5.2.11 (S)-2-Fluoropropionyl chloride, (S) 39

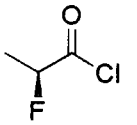

Thionyl chloride, (1.42 g, 11.9 mmol) was added dropwise to (*R*)-2-fluoropropionic acid, (1.00 g, 10.9 mmol) at room temperature. The reaction was heated under reflux for 30 min and a sample was removed for ^{1}H and ^{19}F NMR analysis to confirm the absence of starting material. Further portions (0.2 mL) of thionyl chloride were added until NMR analysis confirmed the disappearance of the starting material. The desired product was distilled from the reaction mixture at atmospheric pressure to give a colourless liquid.

Yield: 0.17 g, 1.5 mmol, 14%.

^{1}H NMR: 5.03(1H, dq, *J* 48.7, 6.9, CFH), 1.61(3H, dd, *J* 23.5, 6.9, Me).

^{13}C NMR: 172.5(d, *J* 27.9), 90.3(d, *J* 194.5), 17.6(d, *J* 21.9).

^{19}F NMR: -184.3(dq, *J* 48.0, 23.7, CFH).

5.2.12 N-(*S*)-2-Fluoropropionyl-(*S*)-phenylalanine, (*S*, *S*)36

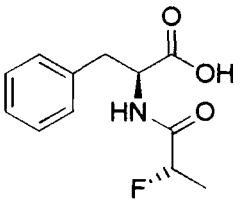

(*S*)-Phenylalanine (0.25g, 1.5 mmol) was dissolved in 4M NaOH (1.2 mL, 4.8 mmol). The reaction was cooled to 0°C and (*S*)-2-fluoropropionyl chloride (0.17g, 1.5 mmol) was added dropwise. The reaction was warmed to room temperature and stirred for 30 minutes, acidified to pH = 3 with concentrated HCl and the product extracted into ethyl acetate (100 mL), washed with sodium chloride solution (3 x 100 mL, 5% w/v) and dried over anhydrous sodium sulphate, filtered and evaporated *in vacuo* to afford the crude product as a colourless oil. Recrystallisation from hexane and chloroform yielded the product as a white crystalline solid, which contained a 9:1 mixture (in favour of *S*, *S* **36**) of the diastereoisomers.

Yield: 0.23 g, 0.8 mmol, 28%.

M. Pt.: 87.0 - 87.5°C.

FTIR Microscopy: 3388(s), 3335(s), 2979(s), 2800(br), 1729(s), 1624(s), 1545(s), 1227(s)

EI (m/z): 239(5), 194(10), 148(100), 131(13), 120(30), 103(22), 91(95), 77(27), 65(27), 47(33).

^{1}H NMR: 7.23(5H, m, ArH), 6.92(1H, m, NH), 5.03(1H, dq, *J* 39.1, 6.8, CFH), 3.28(1H, dd, *J* 14.0, 7.0, CH_2a), 3.11(1H, dd, *J* 14.0, 7.0, CH_2b), 1.55(minor diastereoisomer, dd, *J* 24.5, 6.8, CH_3), 1.43(3H, 2 dd, *J* 24.5, 6.8, CH_3).

^{13}C NMR: 173.8(C=O), 171.2(d, *J* 19.0, C=O), 135.4(Ar-C), 129.3(Ar-C), 128.6(Ar-C), 127.2(Ar-C), 88.3(d, *J* 183.6, CFH), 52.4(CH), 37.4(CH_2), 18.1(d, *J* 21.9, CH_3).

^{19}F NMR: -182.8(ddq, *J* 49.2, 24.7, 4.2, CFH), -182.9(minor diastereoisomer, ddq, *J* 49.8, 25.2, 4.3, CFH).

5.2.13 Acylase kinetic study

The typical procedure for an acylase hydrolysis reaction was to charge to an NMR tube with the required quantity of a sodium salt solution of the substrate. This was adjusted to give final solutions typically in the range 5 to 70 mM. To this a solution of AMA enzyme in phosphate buffer (pH = 7, 0.2 mL), with concentration adjusted for the activity was added. The total volume in the NMR tube was made up to 1 mL with

the addition of more phosphate buffer. The initial rate of hydrolysis was followed by NMR.

5.3 Experimental for Chapter 3

5.3.1 N-Propionyl-(*S*)-phenylalanine, 42

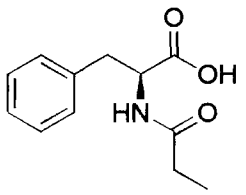

(*S*)-Phenylalanine (5.0 g, 30 mmol) was dissolved in 4M NaOH (23 mL, 90 mmol). The reaction was cooled to 0°C and propionyl chloride (2.8 g, 30 mmol) was added dropwise. The reaction was warmed to room temperature and stirred for 30 minutes, acidified to pH = 3 with concentrated HCl and the product extracted into ethyl acetate (100 mL), washed with water until pH = 6 and dried over anhydrous sodium sulphate, filtered and evaporated *in vacuo* to afford the product as a white solid. The product was recrystallised from ethyl acetate / hexane.

Yield: 2.0g, 9.0 mmol, 30.1%

M. Pt.: 132.5 - 133.5°C (Lit M. Pt. 132°C[49])

FTIR Microscopy: 3342(s), 2979(s), 2800(br), 1709(s), 1617(s), 1545(s).

EI (m/z): 221(8), 203(5), 177(6), 148(100), 131(12), 120(40), 104(23), 91(71), 74(45), 65(22), 57(81)

^{1}H NMR: 7.25(5H, m, ArH), 5.89(1H, d, *J* 7.7, NH), 4.84(1H, dt, *J* 7.4, 5.9, CH), 3.24(1H, dd, *J* 14.0, 5.8, Non equivalent CH_2), 3.12(1H, dd, J 14.1, 6.2, Non equivalent CH_2), 2.21(2H, q, *J* 7.7, CH_2), 1.10(3H, t, *J* 7.7, CH_3)

^{13}C NMR: 174.2(C=O), 174.1(C=O), 135.7(Ar-C), 129.4(Ar-C), 128.8(Ar-C), 127.4(Ar-C) 53.2(CH), 37.2(CH_2), 29.5(CH_2), 9.6(CH_3).

5.3.2 2-Fluoroacetyl chloride, 48

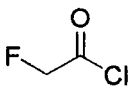

Sodium fluoroacetate (4.4g, 44 mmol) was added to pthaloyl dichloride (6.97 mL, 48 mmol) and heated under reflux for 1 hour. The product was distilled from the mixture

at atmospheric pressure keeping the temperature below 95°C to give a colourless liquid.

Yield: 1.3g, 13.5 mmol, 31%

^{1}H NMR: 5.05(2H, d, CH_2F)

^{13}C NMR: 82.16(CH_2F, d, *J* 198.3), no carbonyl signal evident.

^{19}F NMR: -209.74(t, *J* 46.7, CH_2F)

5.3.3 N-Fluoroacetyl-(S)-phenylalanine, 45

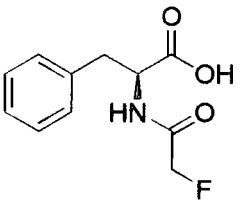

(*S*)-Phenylalanine (2.23g, 13.5 mmol) was dissolved in 4M NaOH (13.5 mL, 53.9 mmol). The reaction was cooled to 0°C and fluoroacetyl chloride (1.3 g, 13.5 mmol) was added dropwise. The reaction was warmed to room temperature and stirred for 30 min, acidified to pH = 3 with concentrated HCl and the product extracted into ethyl acetate (100 mL), washed with water until pH = 6 and dried over anhydrous sodium sulphate, filtered and evaporated *in vacuo* to afford the crude product as a colourless oil. The product was recrystallised from dichloromethane / hexane.

Yield: 0.87g, 3.9 mmol, 28.6%

M. Pt.: 144 - 145°C

Elemental Analysis: Found, % C 58.60, %H 5.37, %N 6.10

Calculated, % C 58.66, %H 5.37, %N 6.22

FTIR Microscopy: 3387(s), 2960(s), 2800(br), 1742(s), 1650(s), 1564(s)

EI (m/z): 148(100), 131(5), 120(20), 103(10), 91(95)65(15).

^{1}H NMR: 7.25(5H, m, ArH), 6.68(1H, d, *J* 7.2, NH), 4.97(1H, ddd, *J* 7.2, 6.6, 5.8, CH), 4.78(2H, d, *J* 47.0, CH_2F), 3.26(1H, dd, *J* 14.0, 5.8, Non equivalent CH_2), 3.15(1H, dd, *J* 14.0, 6.6, Non equivalent CH_2)

^{13}C NMR: 175.0(C=O), 168.1(C=O, d, *J* 18.2), 135.1(Ar C), 129.3(Ar C), 128.9(Ar C), 127.6(Ar C), 80.2(CH_2-F, d, *J* 186), 52.5(CH), 37.5(CH_2).

^{19}F NMR: -225.58(dt, *J* 47.2, 2.5, CFH_2).

X-ray Analysis: See appendix II

5.3.4 N-(2-Methylpropionyl)-(*S*)-phenylalanine, 49

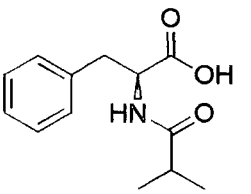

(*S*)-Phenylalanine (5.0 g, 30 mmol) was dissolved in 4M NaOH (23 mL, 90 mmol). The reaction was cooled to 0°C and 2-methylpropionyl chloride (3.23 g, 30 mmol) was added dropwise. The reaction was warmed to room temperature and stirred for 30 min, acidified to pH = 3 with concentrated HCl and the product extracted into ethyl acetate (100 mL), washed with water until pH = 6 and dried over anhydrous sodium sulphate, filtered and evaporated *in vacuo* to afford the crude product as a white solid. The product was recrystallised from ethyl acetate / hexane.

Yield: 2.40 g, 10.2 mmol, 34.0%

M. Pt.: 110.5 – 112.0°C (Lit. M. Pt. 110 – 112°C[50])

Elemental Analysis: Found, % C 65.38, %H 7.25, %N 5.83

Calculated, % C 66.36, %H 7.28, %N 5.95

FTIR Microscopy: 3388(s), 3335(s), 1729(s), 1624(s), 1551(s).

EI (m/z): 235(21), 191(190), 148(100), 120(67), 104(33), 90(65), 85(65), 71(75), 65(38).

^{1}H NMR: 9.37(1H, s, COOH), 7.25(5H, m, ArH), 6.05(1H, d, *J* 7.4, NH), 4.87(1H, dt, *J* 7.4, 5.9, CH), 3.25(1H, dd, *J* 14.0, 5.5, Non equivalent CH_2), 3.12(1H, dd, J 14.1, 5.9, Non equivalent CH_2), 2.36(1H, septet, *J* 6.9, CH), 1.09(3H, d, *J* 6.9, CH_3), 1.07(3H, d, *J* 6.9, CH_3).

^{13}C NMR: 177.7(C=O), 174.7(C=O), 135.7(Ar C), 129.5(Ar C), 128.6(Ar C), 127.3(Ar C), 53.0(CH), 37.3(CH_2), 35.5(CH), 19.5(CH_3), 19.2(CH_3).

X-ray Analysis: See appendix III

5.3.5 N-(*R*)-2-Chloropropanoyl-(*S*)-phenylalanine, (*R*, *S*)50

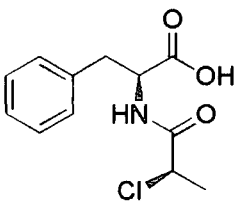

Thionyl chloride, (1.12 g, 9.43 mmol) was added dropwise to (*R*)-2-chloropropanoic acid, (0.93 g, 8.57 mmol) at room temperature. The reaction was heated under reflux for 60 min. ^{1}H NMR showed that some starting material was still present so a further

aliquot (0.10g, 0.84 mmol) was added and the reaction was heated for a further 20 min. After this time ^{1}H NMR confirmed the absence of starting material and the reaction mixture was cooled to ambient temperature.

The reaction mixture was added dropwise to a solution of (*S*)-phenylalanine (1.65g, 10 mmol) in 4M NaOH (7.5 mL) while maintaining the temperature at 0°C. The reaction mixture was stirred at ambient temperature for a further 30 minutes after which time the pH was adjusted to 3 by the addition of concentrated HCl. The product was extracted into ethyl acetate, washed with water, dried over anhydrous sodium sulphate, filtered and evaporated *in vacuo* to afford the crude product as a colourless oil.

Yield: 0.47g, 1.8 mmol, 21.0%

^{1}H NMR: 7.28(5H, m, ArH), 6.92(1H, d, *J* 7.2, NH), 4.85(1H, ddd, *J* 7.9, 6.2, 5.7, CH), 4.38(1H, q, *J* 7.1, CHCl), 3.24(1H, dd, *J* 14.0, 5.5, Non equivalent CH_2), 3.15(1H, dd, *J* 14.0, 6.3, Non equivalent CH_2), 1.70(3H, d, *J* 6.9, CH_3).

^{13}C NMR: 174.87(C=O), 169.76(C=O), 135.17 (Ar C), 129.36 (Ar C), 128.87(Ar C), 127.55 (Ar C), 55.59(CH_2-Cl), 53.37(CH), 37.31(CH_2), 22.62(CH_3).

5.3.6 N-(*S*)-2-Chloropropanoyl-(*S*)-phenylalanine, (*S*, *S*)50

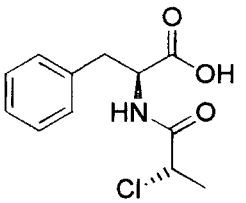

Thionyl chloride, (1.12 g, 9.43 mmol) was added dropwise to (*S*)-2-chloropropanoic acid, (0.93 g, 8.57 mmol) at room temperature. The reaction was heated under reflux for 30 minutes. ^{1}H NMR was used to confirm the absence of starting material and the reaction mixture was cooled to ambient temperature.

The reaction mixture was added dropwise to a solution of (*S*)-phenylalanine (1.65g, 10 mmol) in 4M NaOH (7.5 mL) while maintaining the temperature at 0°C. The reaction mixture was stirred at ambient temperature for a further 30 min after which time the pH was adjusted to 3 by the addition of concentrated HCl. The product was extracted into ethyl acetate, washed with water, dried over anhydrous sodium sulphate, filtered and evaporated *in vacuo* to afford the crude product as colourless oil. A white solid was obtained by trituration with hexane, which was recrystallised from hexane / chloroform to afford a crystalline solid suitable for X-ray analysis.

Yield: 0.55g, 2.1 mmol, 24.6%

M. Pt.: 98 - 99°C (Lit. M. Pt. 88 – 89°C[49])

FTIR Microscopy: 3374(s), 3322(s), 2980(s), 2800(br), 1743(s), 1663(s), 1558(s)

EI (m/z): 255(1), 219(6), 203(5), 176(6), 148(77), 120(28), 91(100), 65(26), 57(34).

^{1}H NMR: 7.28(5H, m, ArH), 6.92(1H, d, *J* 7.4, NH), 4.87(1H, ddd, *J* 7.8, 6.3, 5.7, CH), 4.36(1H, q, *J* 7.2, CHCl), 3.26(1H, dd, *J* 14.0, 5.7, Non equivalent CH_2), 3.13(1H, dd, *J* 14.0, 6.3, Non equivalent CH_2), 1.64(3H, d, *J* 7.2, CH_3).

^{13}C NMR: 174.95(C=O), 169.64(C=O), 135.17 (Ar C), 129.43 (Ar C), 128.80(Ar C), 127.52 (Ar C), 55.41(CH_2-Cl), 53.25(CH), 37.39(CH_2), 22.62(CH_3).

X-ray Analysis: See appendix IV.

5.3.7 N-((*S*)-2-Fluoropropionyl)-aniline, 51

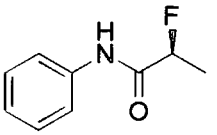

(*S*)-2-Fluoropropionyl chloride, (*S*) **39**, (0.20 g, 1.8 mmol) was added dropwise to a solution of aniline (0.34 g, 3.6 mmol) in diethyl ether (10 mL). The reaction was stirred for 10 minutes, filtered and evaporated *in vacuo* to afford the crude product. The crude product was dissolved in chloroform (10 mL) and filtered to remove the aniline hydrochloride by product and evaporated *in vacuo* to produce an off white solid. This was recrystallised from chloroform / hexane to produce an off white crystalline product suitable for X-ray analysis.

Yield: 0.05g, 0.3 mmol, 17.0%.

M. Pt.: 58.6 – 59.6°C.

Elemental Analysis: Found, % C 64.27, %H 6.04, %N 8.32

Calculated, % C 64.30, %H 5.95, %N 8.33

^{1}H NMR: 7.98(1H, s, NH), 7.1 – 7.6(5H, m, ArH), 5.11(1H, dq, *J* 49.5, 6.9, CHF), 1.67(3H, dd, *J* 25.0, 6.9, CH_3).

^{13}C NMR: 174.95(C=O), 129.20(Ar C), 125.02(Ar C), 120.03(Ar C), 89.00(d, *J* 184.8, CHF), 18.51(d, *J* 21.3, CH_3).

^{19}F NMR: -179.96(1F, ddq, J 49.6, 24.8, 6.7, CFH).

X-ray Analysis: See appendix V.

5.3.8 N-((*S*)-2-Fluoropropionyl)-benzylamine, 52

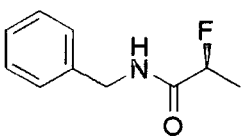

(*S*)-2-Fluoropropionyl chloride, (*S*) **39**, (0.57 g, 5.2 mmol) was added dropwise to a solution of benzylamine (0.50 g, 4.7 mmol) in diethyl ether (10 mL). The reaction was stirred for 10 min and quenched with water (5 mL). The organic layer was separated, dried, filtered and evaporated *in vacuo* to afford the crude product. ^{19}F NMR showed this to be a mixture of the desired product and 2-fluoropropanoic acid. Extraction of a chloroform solution with water removed the free acid. The chloroform solution was dried, filtered and evaporated *in vacuo* to afford a yellow solid. Recrystallisation from hexane gave the product as white needle like crystals.

Yield: 0.18g, 1.0 mmol, 21.1%.

^{1}H NMR: 7.2 – 7.5(5H, m, ArH), 6.60(1H, s, NH), 5.03(1H, dq, *J* 49.5, 6.9, CHF), 4.48(2H, d, *J* 5.9, CH_2), 1.60(3H, dd, *J* 24.7, 6.7, CH_3).

^{13}C NMR: 174.95(C=O), 137.0(Ar C), 128.89(Ar C), 127.87(Ar C), 127.82(Ar C), 88.99(d, *J* 182.7, CHF), 43.09(CH_2), 18.62(d, *J* 21.3, CH_3).

^{19}F NMR: -182.22(1F, ddq, J 49.4, 24.8, 4.5, CFH).

5.3.9 2-Fluoro-4-methylpentanoic acid, 55

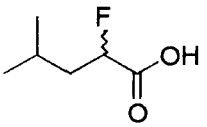

A 125 mL Teflon bottle, containing a magnetic follower, was charged with pyridinium hydrogen fluoride (100 mL, 70% w/w) and (*R, S*)-leucine, (12.65 g, 96 mmol) and the solution was cooled to 0°C. Sodium nitrite (22.60 g, 328 mmol) was added in five equal portions over 1 hour. The reaction mixture was stirred at 0°C for 1 hour and then warmed to room temperature and then stirred overnight. The reaction was quenched by addition to ice water (200 mL), extracted into diethyl ether (3 x 100 mL), washed with sodium chloride solution (3 x 100 mL, 5% w/v) and dried over anhydrous sodium sulphate, filtered, evaporated *in vacuo* to give the crude product. The crude product had high levels of water present and this was removed by azeotropic distillation with toluene under high vacuum to give a mixture of the desired product and anhydride as a yellow liquid. This was further purified by high vacuum distillation (84°C at 3 mbar) to afford the desired product as a colourless liquid.

Yield: 4.64 g, 34.6 mmol, 36%.

^{1}H NMR: 5.00(1H, ddd, *J* 49.6, 9.3, 3.3, CFH), 1.6 – 2.0(3H, m, CH and CH_2), 0.98(6H, d, *J* 6.4, CH_3).

^{13}C NMR: 175.52(d, *J* 23.8, C=O), 87.46(d, *J* 184.0, CHF), 40.92(d, *J* 20.4, CH_2), 24.58(CH), 23.07(CH_3), 21.58(CH_3).

^{19}F NMR: -191.37(ddd, *J* 49.9, 34.8, 18.0 CFH).

5.3.10 2-Fluoro-4-methylpentanoyl chloride, 56

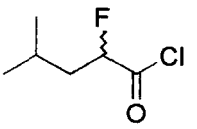

Thionyl chloride (4.12 g, 34.6 mmol) was added to 2-fluoro-4-methylpentanoic acid, **55** and the mixture was heated under reflux. The reaction was continued until the evolution of HCl gas had stopped. Atmospheric distillation produced a colourless liquid, which was found not to contain any desired product. Further distillation of the reaction mixture under reduced pressure (~100 mbar @ 45 – 58°C) produced the desired product as a yellow liquid.

Yield: 1.50 g, 9.8 mmol, 28%.

^{1}H NMR: 5.05(1H, ddd, *J* 49.7, 9.1, 3.5, CFH), 1.6 – 2.0(3H, m, CH and CH_2), 0.98(6H, d, *J* 6.4, CH_3).

^{13}C NMR: 175.52(d, *J* 23.8, C=O), 87.46(d, *J* 184.0, CHF), 40.92(d, *J* 20.4, CH_2), 24.58(CH), 23.07(CH_3), 21.58(CH_3).

^{19}F NMR: -177.23(ddd, *J* 49.8, 34.2, 18.0 CFH).

5.3.11 N-(2-Fluoro-4-methylpentanoyl)benzylamine, 53

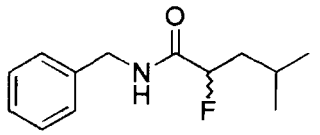

2-Fluoro-4-methylpentanoyl chloride, **56** (1.5 g, 9.8 mmol) was added dropwise to a mixture of ethyl acetate (10 mL), 4M sodium hydroxide (10mL) and benzylamine (1.05 g, 9.8 mmol).The reaction mixture was stirred for 30 minutes after which time the organic and aqueous layers were separated. The ethyl acetate solution was washed with sulphuric acid (5%, 10 mL), water (10 mL), dried, filtered and evaporated *in vacuo* to afford the crude product. Recrystallisation from hexane / diethyl ether (50 : 50) gave the product as a white crystalline solid.

Yield: 0.18 g, 0.8 mmol, 8%.

M. Pt.: 73.5 – 74.5°C.

EI (m/z): 223(15), 167(33), 118(25), 106(12), 91(100).

^{1}H NMR: 7.2 – 7.4(5H, m, ArH), 6.60(1H, s, NH), 4.96(1H, ddd, *J* 50.7, 9.1, 3.7, CFH), 4.48(2H, d, *J* 5.9), 1.6 – 2.0(3H, m, CH and CH_2), 0.96(6H, d, *J* 6.6, CH_3).

^{13}C NMR: 174.95(C=O), 137.67(Ar C), 132.63(Ar C), 128.87(Ar C), 127.79(Ar C), 91.94(d, *J* 185.3, CHF), 43.09(CH_2), 41.32(d, *J* 20.4, CH_2), 24.73(CH), 23.24(CH_3), 21.65(CH_3).

^{19}F NMR: -188.90(m, CFH).

5.3.12 2-Fluoro-2-phenylacetic acid, 57

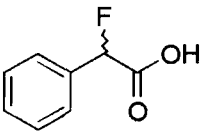

A 125 mL Teflon bottle, containing a magnetic follower, was charged with pyridinium hydrogen fluoride (100 mL, 70% w/w) and (*R, S*)-phenylglycine, (14.52 g, 96 mmol) and the solution was cooled to 0°C. Sodium nitrite (22.60 g, 328 mmol) was added in five equal portions over 1 hour. The reaction mixture was stirred at 0°C for 1 hour and then warmed to room temperature and then stirred overnight. The reaction was quenched by addition to ice water (200 mL), extracted into diethyl ether (3 x 100 mL), washed with sodium chloride solution (3 x 100 mL, 5% w/v) and dried over anhydrous sodium sulphate, filtered, evaporated *in vacuo* to give the crude product. The crude product had high levels of water present and this was removed by azeotropic distillation with toluene under high vacuum to give a yellow solid. The solid was dried under vacuum at room temperature overnight to give the desired product.

Yield: 13.00 g, 84.3 mmol, 88%.

^{1}H NMR: 11.0(1H, s, COOH), 7.3 – 7.7(5H, m, ArH), 5.82(1H, d, *J* 47.5, CFH).

^{13}C NMR: 174.60(d, *J* 28.0, C=O), 133.34(d, 20.2, Ar C), 130.05(Ar C), 129.03(Ar C), 126.77(Ar C), 88.84(d, *J* 186.8, CHF).

^{19}F NMR: -180.91(d, *J* 47.2, CFH).

5.3.13 2-Fluoro-2-phenylacetyl chloride, 58

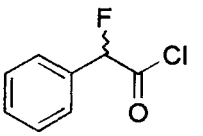

A solution of 2-fluoro-2-phenylacetic acid, **54** (5.00 g, 32.4 mmol) in dichloromethane (50 mL) and dimethylformamide (1 mL) was prepared. To this oxalyl chloride (4.12 g, 32.4 mmol) was added slowly. During the addition vigorous evolution of HCl was seen. The reaction mixture was stirred for a further 60 min after which time HCl evolution had ceased. A further portion of oxalyl chloride (0.73 g, 5.7

mmol) and the reaction was stirred for a further 30 min. ^{19}F NMR confirmed the absence of starting material an the reaction was stopped and the product was held for use in the amide synthesis.

Yield: 7.60 g (mixture of desired product and oxalyl chloride).

^{1}H NMR: 7.3 – 7.7(5H, m, ArH), 5.90(1H, d, *J* 47.7, CFH).

^{13}C NMR: 164.51(C=O), 136.8(Ar C), 130.80(Ar C), 129.31(Ar C), 127.54(Ar C), 94.17(d, *J* 197.8, CHF).

^{19}F NMR: -163.96(d, *J* 47.8, CFH).

5.3.14 N-(2-Fluoro-2-phenylacetyl)benzylamine, 54

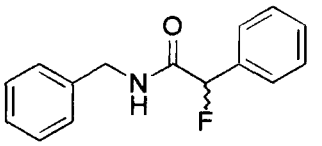

2-Fluoro-2-phenylacetyl chloride, **55** (7.60 g, mixed with excess oxalyl chloride, assume 32.4 mmol) was added dropwise to a mixture of ethyl acetate (50 mL), 4M sodium hydroxide (50mL) and benzylamine (3.47 g, 32.4 mmol).The reaction mixture was stirred for 30 minutes after which time the organic and aqueous layers were separated. The ethyl acetate solution was washed with sulphuric acid (5%, 50 mL), water (50 mL), dried, filtered and evaporated *in vacuo* to afford the crude product. The crude product was recrystallised from hexane / diethyl ether (50 : 50) to obtain a pale yellow crystalline solid.

Yield: 6.66 g, 27.4 mmol, 80%.

M. Pt.: 96.5 – 98.7°C.

EI (m/z): 243(20), 223(33), 118(8), 109(90), 91(100), .

^{1}H NMR: 7.2 – 7.6(10H, m, ArH), 6.80(1H, s, NH), 5.82(1H, d, *J* 48.2, CFH), 4.52(2H, d, *J* 6.2).

^{13}C NMR: 199.00(C=O), 130.50(Ar C), 128.92(Ar C), 128.80(Ar C), 127.95(Ar C), 91.97(d, *J* 187.9, CHF), 43.29(CH_2).

^{19}F NMR: -177.73(dd, *J* 48.3, 3.9, CFH).

5.4 Experimental for Chapter 4

5.4.1 (*RS*)-4-Benzyl-4-fluoro-2-phenyl-5-oxazolone, 27

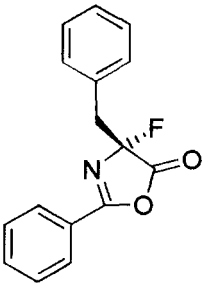

Sodium hydride was washed with heptane, the supernatant decanted and blown dry with nitrogen several times to generated the active sodium hydride powder. A slurry of sodium hydride (0.12 g, 5 mmol) in THF (25 mL) was prepared and cooled to 0°C. To this a solution of (*RS*)-4-benzyl-2-phenyl-5(4*H*)-oxazolone, **26** (1.25 g, 5 mmol) in THF (25 mL) was added dropwise. The reaction mixture was stirred at 0°C for 30 minutes and then at ambient temperature for a further 60 min, after which time a yellow solution was evident. To this solution DMF (10 mL) was added, followed by Selectfluor (1.77 g, 5 mmol). The reaction mixture was stirred for 30 min, after which time ^{19}F NMR indicated the presence of the desired product. The reaction mixture was poured into a mixture of diethyl ether (100 mL) and water (100 mL). The organic layer was washed with a further portion of water (100 mL) and the pH of the aqueous extract was 6.0. The organic layer was dried, filtered and evaporated *in vacuo* to afford the crude product as an unstable yellow oil.

Yield: 1.18 g, 4.4 mmol, 88%.

^{1}H NMR: 7.1 – 8.0(10H, m, ArH), 3.55(1H, dd, J 13.1, 8.9, Non equivalent CH_2), 3.42(1H, dd, *J* 13.2, 11.3, Non equivalent CH_2).

^{19}F NMR: -127.84(dd, *J* 11.3, 9.2, CF).

5.4.2 (*S*)-Alanine methylester, 28

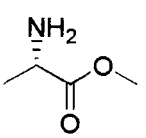

To a solution of (*S*)-alanine methylester hydrochloride (5g, 36 mmol) in DMF (150 mL) add triethylamine (3.64 g, 5 mL, 36 mmol). The reaction mixture was stirred for 10 minutes and a white precipitate was formed. The white solid (triethylammonium

chloride) was removed by filtration to give the desired product as a 0.24 M solution in DMF.

5.4.3 N-2,6-Difluorobenzoyl-(*S*)-phenylalanine, 67

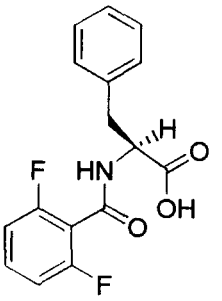

To a solution of (*S*)-phenylalanine (28.1 g, 170 mmol) in 4M NaOH (170 mL) cooled to 0°C 2,6-difluorobenzoyl chloride (31.5 g, 178 mmol) was added dropwise. The reaction mixture was warmed to ambient and stirred for a further 30 minutes. HCl was added to the reaction until a pH of 3.0 had been attained and the product was extracted into ethyl acetate (200 mL) and washed with water (200 mL). The organic layer was dried, filtered and evaporated *in vacuo* to afford the crude product as colourless oil, which was triturated with pentane to produce a white solid. The product was further dried at 40°C under vacuum.

Yield: 48.15 g, 157.7 mmol, 93%.

^{1}H NMR: 6.8 – 7.6(8H, m, ArH), 6.50(1H, d, *J* 7.7, NH), 5.13(1H, ddd, *J* 7.7, 5.7, 5.6, CH), 3.37(1H, dd, *J* 14.0, 5.6, Non equivalent CH_2), 3.24(1H, dd, *J* 14.0, 5.7, Non equivalent CH_2).

^{19}F NMR: -111.40(dd, *J* 5.9, 5.9, CF).

5.4.4 Preparation of (*S*)-4-benzyl-2-(2,6-difluorophenyl)-5(*4H*)-oxazolone, 68

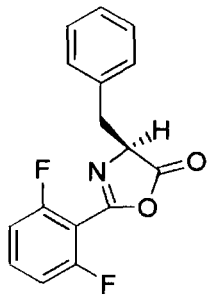

N-2,6-Difluorobenzoyl-(S)-phenylalanine, **67** (10 g, 33 mmol), acetic anhydride (50 mL) and 1,4-dioxan (50 mL) were stirred and the reaction was heated under reflux for 60 min. TLC confirmed the absence of the starting material. The solvents were removed initially by high vacuum distillation and the final traces were removed by

azeotropic high vacuum distillation with toluene to give a pale yellow oil as the crude product. The desired product was obtained by chromatographic purification on silica gel using ethyl acetate (10%) / hexane (90%) as the mobile phase. The fractions containing the desired product were selected by TLC and after combination and removal of solvent *in vacuo* the product was recovered as colourless oil.

Yield: 7.57 g, 26.4 mmol, 80%.

^{1}H NMR: 6.8 – 7.6(8H, m, ArH), 4.72(1H, dd, *J* 6.2, 4.9 CH), 3.41(1H, dd, *J* 14.0, 4.9, Non equivalent CH_2), 3.24(1H, dd, *J* 14.0, 6.2, Non equivalent CH_2).

^{19}F NMR: -107.75(dd, *J* 8.0, 5.9, CF).

5.4.5 3,5-Dibenzyl-1-(2,6-difluorobenzoyl)-3-(2,6-difluorobenzoyl-amino)pyrrolidine-2,4-dione, 70

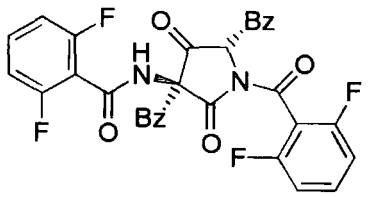

Sodium hydride was washed with heptane and the supernatant decanted and blown dry with nitrogen several times to generated the active sodium hydride powder. A slurry of sodium hydride (0.63 g, 26.4 mmol) in THF (100 mL) was prepared and cooled to 0°C. To this a solution of (*S*)-4-benzyl-2-(2,6-difluorophenyl)-5(4*H*)-oxazolone, **61** (7.57 g, 26.4 mmol) in THF (100 mL) was added dropwise. The reaction mixture was stirred at 0°C for 30 minutes and then at ambient temperature for a further 50 minutes, after which time a yellow slurry was evident. The reaction mixture was poured into diethyl ether (300 mL) and water (300 mL) and separated. The organic layer was washed with water, dried, filtered and evaporated *in vacuo* to afford the crude product as a white solid. The crude product was recrystallised from ethyl acetate / hexane (20:80) to give the product as a white crystalline solid, which was suitable for X-ray structure analysis.

Yield: 1.29 g, 2.2 mmol, 9 %.

M. Pt.: 212.0 – 213.0°C.

EI (m/z): 574(15), 399(23), 301(37), 287(88), 273(66), 256(59), 174(56), 157(100), 105(73).

^{1}H NMR: 6.8 – 7.5(16H, m, ArH), 6.73(1H, t, *J* 3.5, NH), 5.37(1H, dd, *J* 5.7, 3.5, CH), 3.44(1H, dd, *J* 14.2, 5.8, Non equivalent CH_2), 3.29(1H, dd, *J* 14.2, 3.6, Non

equivalent CH_2), 2.28(1H, d, *J* 14.1, Non equivalent CH_2), 2.00(1H, d, *J* 14.1, Non equivalent CH_2).

^{13}C NMR: 202.97(C=O), 170.94(C=O), 161.11(dd, *J* 257.2, 5.3, CF), 160.84(C=O), 160.25(C=O), 159.70(dd, *J* 253.6, 6.8, CF), 135.65(Ar C_{quat}), 133.56(t, *J* 11.4, ArCH), 132.36(t, *J*, 9.9, ArCH), 131.62(Ar C_{quat}), 130.76(ArCH), 130.46(ArCH), 129.11(ArCH), 128.77(ArCH), 128.46(ArCH), 127.69(ArCH), 112.54(dd, *J*, 23.4, 3.1, ArCH), 111.8(m, ArCH) 67.04(CH), 62.22(C_{quat}), 36.06(CH_2), 34.10(CH_2).

^{19}F NMR: -109.07(2F, ddd, J 10.2, 6.0, 3.5, CFH), -112.2(2F, br s, CFH).

X-ray Analysis: See appendix VI.

5.4.6 N-(2-Fluoropropionyl)-N-methyl aniline 75

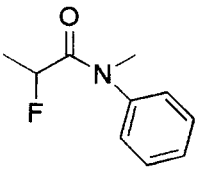

2-Fluoropropionyl chloride (4.00 g, 36.2 mmol) was added dropwise to a solution of N-methyl aniline (4.63 g, 43.2 mmol) in ethyl acetate (20 mL) and 4M NaOH (20 mL). The reaction was stirred for 30 min and the two layers were separated. The organic layer was washed with 5% sulphuric acid, followed by water, dried, filtered and evaporated *in vacuo* to afford the crude product as a yellow oil.

Yield: 3.00 g, 16.6 mmol, 46 %.

^{1}H NMR: 7.2 – 7.5(5H, m, ArH), 4.93(1H, dq, *J* 48.4, 6.4, CFH), 3.31(3H, s, CH_3), 1.39(3H, dd, *J* 24.5, 6.4, CH_3).

^{13}C NMR: 130.04(ArCH), 128.45(ArCH), 127.36(ArCH), 84.50(d, *J* 252, CFH), 18.19(d, *J* 87.4, CH_3), 14.27(CH_3).

^{19}F NMR: -178.80(dq, *J* 48.4, 24.2, CHF).

5.4.7 N-(1-Chloro-2-fluoropropenyl)-N-methyl aniline 76

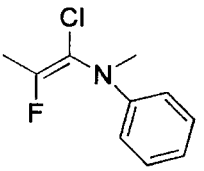

To a solution of N-(2-fluoropropionyl)-N-methyl aniline **75** (1.00 g, 5.52 mmol) in DCM (10 mL) cooled to –70°C was added oxalyl chloride (0.77 g, 6.07 mmol). The reaction was warmed to ambient temperature and stirred for 60 min, after which time it was again cooled to –70°C and triethylamine (0.61 g, 6.07 mmol) was added. The reaction mixture was warmed to ambient temperature over 10 minutes and stirred

overnight. TLC analysis (ethyl acetate / hexane 50:50) determined that the starting material was a minor component and the reaction was stopped. The crude mixture was purified using column chromatography with ethyl acetate / hexane (50:50) as the eluent, which afforded the product as a red / orange oil.

Yield: 0.21 g, 1.1 mmol, 19 %.

^{1}H NMR: 6.8 – 7.4(5H, m, ArH), 3.06(3H, d, *J* 1.0, CH_3), 2.02(3H, d, *J* 15.8 CH_3).

^{19}F NMR: -102.16(q, *J* 15.8, CF).

5.5 References

1. "Handbook of Chemistry and Physics", Eds. D. R. Lide, 78th Edition, **1998**.
2. D. O'Hagan and D. B. Harper, *J. Fluorine Chem.* **1999**, 100, 127
3. M. Meyer and D. O'Hagan, *Chem. in Brit.* **1992**, Sept., 785
4. J. C. S. Marais, *Onderstepoort J. Vet. Sci.Anim. Ind.*, **1944**, 20, 67.
5. S. O. Thomas, *Antibiot. Annun.*, 1956, 716.
6. G. O. Morton, *J. Am. Chem. Soc.*, 1969, **91**, 1535.
7. C. D. Murphy, D. O'Hagan and C. Schaffrath, *Angew. Chem. Int. Ed. Engl.* **2001**, 40, 4479.
8. D. O'Hagan, C. Schaffrath, S. L. Cobb, J. T. G. Hamilton and C. D. Murphy, *Nature* **2002**, 416, 279.
9. M. Schlosser and D. Michel, *Tetrahedron*, **1996**, 52, 99.
10. A. Bondi, *J. Phys. Chem.* **1964**, 68, 441 and **1966**, 70, 3006.
11. M. Charton, *Progr. Phys. Org. Chem.* **1973**, 10, 81.
12. P. Anderson, *Acta Chem. Scand.* **1962**, 16, 2337 and E. L. Eliel and R. J. L. Martin, *J. Am. Chem. Soc.* **1968**, 90, 689.
13. J. A. Hirsch in *Topics Stereochem.* (Ed. N. L. Allinger and E. L. Eliel), 1, 199, Wiley-Interscience, New York, **1967**.
14. E. W. Della, *Tetrahedron. Lett.* **1966**, 7, 3347.
15. A. Stabel, L. Dasaradhi, D. O'Hagan and J. P. Rabe, *Langmuir*, **1995**, 11, 1427.
16. V. G. S. Box, *Heterocycles*, **1990**, 31, 1157.
17. H. Senderowitz, P. Aped and B. Fuchs, *Tetrahedron*, **1993**, 49, 3879.
18. N. T. Anh and O. Eisenstein, *Nouv. J. Chim.*, **1977**, 1, 61.

19a. K. N. Houk, M. N. Paddon-Row, N. G. Rondan, Y. D. Wu, F. K. Brown, D. C. Spellmeyer, J. T. Metz, Y. Li and R. J. Loncharich, *Science*, **1985**, 231, 1108,

b. S. S. Wong and M. N. Paddon-Row, *J. Chem. Soc. Chem. Commun.* **1990**, 456,

c. C. Moberg, H. Adolfsson, K. Warnmark, P. Norrby, K. M. Marstokk and H. Mollendal, *Chem. Eur. J.*, **1996**, 2, 516,

d. L. Dasaradhi and D. O'Hagan, *Bioorg Med. Chem. Lett.*, **1993**, 3, 1655.

20a. B. E. Smart, "Characteristics of C-F Systems" in "Organofluorine Chemistry: Principles and Commercial Applications", Ed. R. E. Banks, Plenium Press, New York, **1994**.

b D. A. Dixon and B. E. Smart, Selective Fluorination in Organic and Bioorganic Chemistry, ACS Symposium Series 456, Ed. Welch J. T., Washington D. C., **1991**.

c Dixon D. A. and Smart B. E., *J. Phys. Chem.*, **1991**, 95, 1602.

21. D. O' Hagan and H. S. Rzepa, , *Chem. Comm.*, **1997**, 645.

22a. Shimoni, L. and Glusker, J. P., *Structural Chem.*, **1994**, 5, 383.

b. Murray-Rust, P., Stalling, W. C., Moniti, C. T., Preston, R. K. and Glusker, J. P., *J. Am. Chem. Soc.*, **1983**, 105, 3206.

23. J. A. K. Howard, V. J. Hoy, D. O'Hagan and G. T. Smith, *Tetrahedron*, **1996**, 52, 12613.

24a. I. Ojima, J. R. McCarthy and J. T. Welch, Biomedical Frontiers of Fluorine Chemistry, Chapter 1, 1 – 24, ACS Symposium Series 639.

b. Aboul-Enein, H. Y., *Tox. Env. Chem.*, **1991**, 29, 235.

c. "Organofluorine Compounds in Medicinal Chemistry and Biomedical Applications", Eds., Filler, R., Kobayashi, Y. and Yagupolskii, L. M., **1993**, Elsevier.

d. B. K. Park and N. R. Kitteringham, *Drug Metabolism Rev.*, **1994**, 26, 605.

e. F. M. D. Ismail, *J. Fluorine Chem.* **2002**, 118, 27.

25. E. J. Toone, M. J. Werth and J. B. Jones, *J. Am. Chem. Soc.*, **1990**, 112, 4946.

26. D. Basavaiah and P. R. Krishna, *Tetrahedron*, **1995**, 51, 2403.

27. H. K. Chenault, J. Dahmer and G. M. Whitesides, *J. Am. Chem. Soc.*, **1989**, 111, 6354.

28a. J. S. Parratt, S. J. Faulconbridge, K. E. Holt, C. L. Rippe, S. P. Savage and S. J. C. Taylor, *Ann. Rep. Prog Chem., Sect. B, Org. Chem.*, **1995**, 92, 253.

b. C. Sambale and M. R. Kula, *Biotech. and App. Biochem.* **1987**, 9, 251.

c. W. J. Hennen, H. M. Sweers, Y. F. Wangand C. H. Wong, *J. Org. Chem.* **1988**, 53, 4939.

d. J. M. Roper and D. P. Bauer, *Synthesis Comm.* **1983**, 1041.

e. I. Chibata, T. Tosa, T. Sato and T. Mori, *Methods in Enzymology*, **1976**, 44, 746.

f. R. Chenevert, M. Letourneau and S. Thioutot, *Can. J. Chem.* **1990**, 68, 960.

g. T. Tosa, T. Mori, N. Fuse and I. Chibata, *Biotech. and Bioeng.* **1967**, 9, 603.

29. T. Kitazume, K. Murata, T. Ikeya, *J. Fluorine Chem.* **1986**, 31, 143.

30. P. Kalaritis, R. W. Regenye, J. J. Partridge and D. L. Coffen, *J. Org. Chem.*, **1990**, 55, 812.

31. C. F. Bridge, D. O'Hagan, K. A. Reynolds and K. K. Wallace, *Chem. Commun.*, **1995**, 2329.

32. J. W. Banks, A. S. Batsanov, J. A. K. Howard, D. O'Hagan, H. S. Rzepa and S. Martin-Santamaria, *J. Chem. Soc. Perkin Trans. 2*, **1999**, 2409.

33. J. W. Banks and D. O'Hagan, *J. Fluorine Chem.*, **2000**, 102, 235.

34a. G. A. Olah, J. T. Welch, Y. D. Vankar, M. Nojima, I. Kerekes and J. A. Olah, *J. Org. Chem.*, **1979**, 44, 3872.

b. R. Keck and J. Retey, *Helv. Chem. Acta, 1980*, 63, 769.

c. F. Faustini, S. De Munari, A. Panzeri, V. Villa and C. A. Gandolfi, *Tetrahedron. Lett.* **1981**, 22, 4533.

d. G. A. Olah, G. K. S. Prakash, and Y. L. Chao, *Helv. Chem. Acta*, **1981**, 64, 2528.

e. J. Barber, R. Keck and J. Retey, *Tetrahedron. Lett.*, **1982**, 23, 1549.

f. J. Mann, *Chem. Soc. Rev.*, **1987**, 16, 381.

35. "Synthetic Reagents", Pizey, Vol. 1, 321.

36. "The Chemistry of Amides", Ed. Challis and Challis, **1970**, pp 759 - 773, Interscience.

37. "Biochemistry", Ed. D. E. Metzler, Int. Ed. **1977**, pp 301, Academic Press, New York.

38a. P. D. Bailey, S. R. Baker, A. N. Boa, J. Clayson and G. M. Rosair, *Tetrahedron. Lett.*, **1998**, 39, 7557.

b. P. D. Bailey, S. R. Baker, A. N. Boa, J. Clayson and G. M. Rosair, *Tetrahedron. Lett.*, **1999**, 40, 7755.

c. Y. Takeuchi, K. Kirihara, K. L. Kirk and N. Shibata, *Chem. Comm.*, **2000**, 785.

39. V. A. Slaviskaya, D. E. Sile, M. Y. Katkevich, E. K. Korchagova and E. Lukevits, *Chem. Het. Comp.*, **1994**, 30, 724.

40a. G. S. Lal, G. P. Pez and R. G. Syvret, *Chem. Rev.*, **1996**, 96, 1737.

b. A. G. Gilicinski, G. P. Pez, R. G. Syvret and G. S. Lal, *J. Fluorine Chem.*, **1992**, 52, 157.

c. J. A. Wilkinson, *Chem. Rev.*, **1992**, 92, 505.

41a. R. E. Banks, *J. Fluorine Chem.*, **1998**, 87, 1.

b. G. S. Lal, *J. Org. Chem.*, **1993**, 58, 2791.

42a. S. F. Wnuk and M. J. Robins, *J. Am. Chem. Soc.*, **1996**, 118, 2519.

b. G. S. Lal, *J. Org. Chem.*, **1993**, 58, 2791.

43a. S. Kobayashi, L. L. Bryant, Y. Tsukamoto and T. Saegusa, *Macromolecules*, **1986**, 19, 1547.

b. R. Mazurkiewicz, A. W. Pierwocha and B. Fryczkowska, *Polish J. Chem.*, **1998**, 72, 113.

44. "NMR Spectrocopy 2nd Ed." Ed. H. Gunther, **1995**, pp 335, Wiley.

45a. H. Heimgartner, *Angew. Chem. Int. Ed.*, **1991**, 30, 238.

b. J. Lehmann, A. Linden and H. Heimgartner, *Helvetica Chemica Acta.*, **1999**, 82, 888.

c. J. Lehmann, A. Linden and H. Heimgartner, *Tetrahedron*, **1999**, 55, 5359.

d. J. Lehmann, A. Linden and H. Heimgartner, *Tetrahedron*, **1998**, 54, 8721.

46. M. Rens and L. Ghosez, *Tetrahedron. Lett.*, **1970**, 43, 3765.

47. L. Cotarca, P. Delogu, A. Nardelli and V. Sunjic, *Synthesis*, **1996**, 553.

48. R. W. Saalfrank, M. Fischer, U. Wirth and H. Zimmermann, *Angew. Chem. Int. Ed.*, **1987**, 26, 1160.

49. S. J. Fu, S. M. Birnbaum and J. P. Greenstein, *J. Am. Chem. Soc.*, **1954**, 76, 6054.

50. D. G. Doherty and E. A. Popenoe, *J. Biol. Chem.*, **1951**, 189, 447.

Appendix I

Raw data from acylase kinetic studies

Reaction of (*S, R*) 36 with AMA (Run 1)

Substrate concentration (mM)	Reaction time (s)	% conversion	Initial rate (mmol min^{-1})	R squared
10	60	7.2	0.038	0.991
	463	10.7		
	807	12.8		
	1383	15.6		
	2087	20.1		
20	60	3.73	0.066	0.968
	518	6.99		
	898	8.35		
30	60	3.18	0.078	0.946
	482	5.89		
	1047	7.47		
40	60	3.16	0.104	0.999
	435	4.73		
	761	6.19		
52.3	60	3.79	0.097	0.999
	443	5.03		
	817	6.12		

Reaction of (*S, R*) 36 with AMA (Run 2)

Substrate concentration (mM)	Reaction time (s)	% conversion	Initial rate (mmol min^{-1})
4.9	2220	16.9	0.022
9.8	1860	12.8	0.040
14.6	1800	10.7	0.052
19.5	2160	11.2	0.061
24.4	2340	12.0	0.077
29.3	1800	10.4	0.102
34.2	2280	11.4	0.105

Reaction of (S, S) 36 with AMA (Run 1)

Substrate concentration (mM)	Reaction time (s)	% conversion	Initial rate (mmol min^{-1})
8.1	109	8.05	0.36
15.3	98	5.26	0.49
22.5	103	4.51	0.59
30.6	108	4.14	0.70

Reaction of (S, S) 36 with AMA (Run 2)

Substrate concentration (mM)	Reaction time (s)	% conversion	Initial rate (mmol min^{-1})
8.36	470	26.5	0.25
16.72	295	13.3	0.40
25.08	298	10.9	0.49
33.44	279	7.3	0.46
41.80	340	8.5	0.55
50.16	304	6.1	0.54
58.52	300	7.8	0.81
66.88	300	6.1	0.82

Reaction of 42 with AMA

Substrate concentration (mM)	Reaction time (s)	% conversion	Initial rate (mmol min^{-1})
10.0	102	7.52	0.42
20.0	138	7.84	0.68
30.0	174	9.06	0.94
40.0	198	8.94	1.08

Reaction of 45 with AMA

Substrate concentration (mM)	Reaction time (s)	% conversion	Initial rate (mmol min^{-1})
10.0	660	17.6	0.16
20.0	1200	18.8	0.19
30.0	1080	13.6	0.23
40.0	1140	12.8	0.27

Reaction of 49 with AMA

Substrate concentration (mM)	Reaction time (min)	% conversion	Initial rate (μmol min^{-1})
10.0	2220	2.96	0.134
20.0	2212	2.24	0.203
30.0	2706	2.01	0.222
40.0	2700	1.73	0.257

Reaction of (*S*, *S*)50 with AMA

Substrate concentration (mM)	Reaction time (min)	% conversion	Initial rate (μmol min^{-1})
9.4	230	6.32	2.58
18.8	252	3.99	2.98
28.2	272	2.69	3.62
37.5	290	3.27	4.23

Reaction of (S, S)50 with AMA

Substrate concentration (mM)	Reaction time (min)	% conversion	Initial rate (μmol min^{-1})
4.7	1390	5.94	0.20
9.4	1322	5.99	0.43
14.1	1350	3.31	0.35
18.8	1378	3.95	0.54

Appendix II

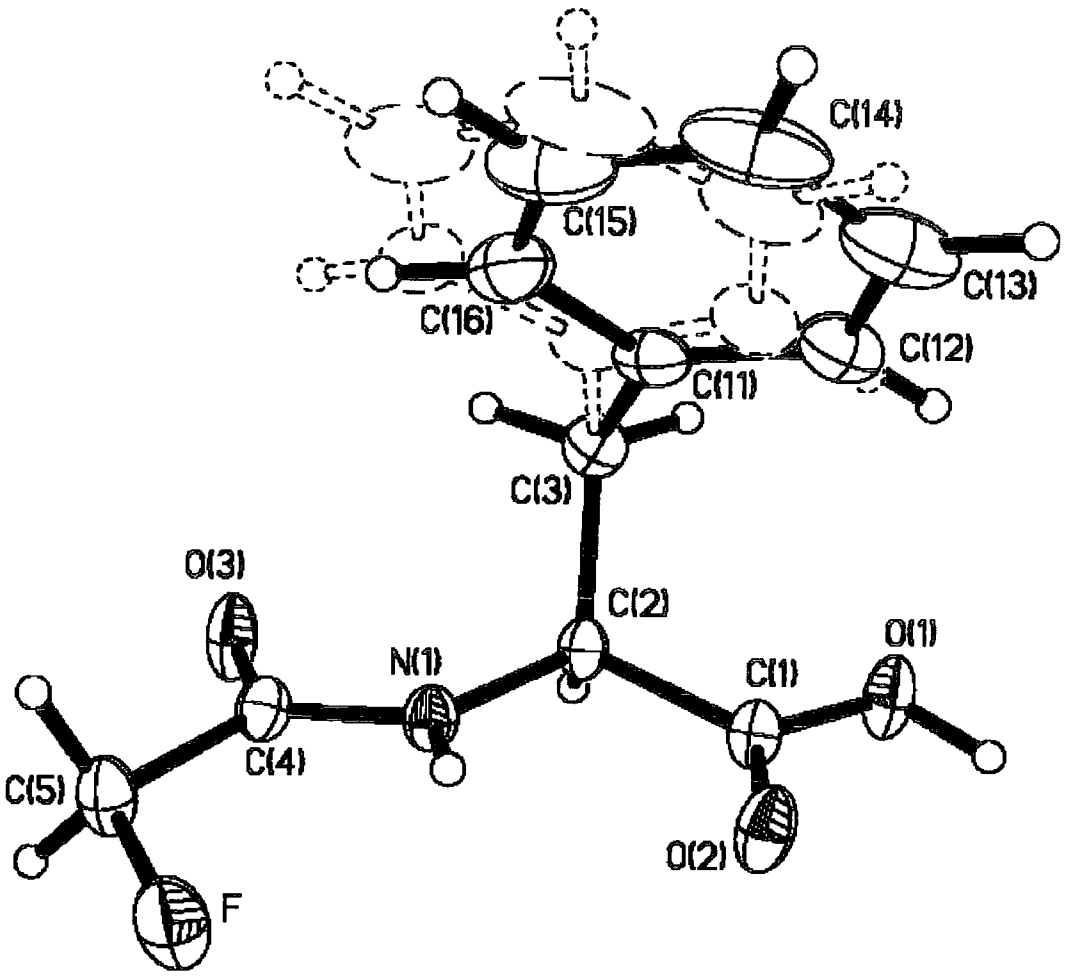

N-Fluoroacetyl-(*S*)-phenylalanine 45

Table 1. Crystal data and structure refinement for N-fluoroacetyl-(S)-phenylalanine **45**.

Identification code		
Empirical formula	C11 H12 F N O3	
Formula weight	225.22	
Temperature	120(2) K	
Wavelength	0.71073 Å	
Crystal system	Orthorhombic	
Space group	$P2_12_12$ (No.)	
Unit cell dimensions	a = 9.3659(6) Å	α= 90°
	b = 16.0026(10) Å	β= 90°
	c = 7.5982(4) Å	γ = 90°
Volume	1138.81(12) Å^3	
Z	4	
Density (calculated)	1.314 g/cm^3	
Absorption coefficient	0.106 mm^{-1}	
F(000)	472	
Crystal size	0.40 × 0.34 × 0.34 mm^3	
θ range for data collection	2.52 to 27.48°.	
Index ranges	$-12 \leq h \leq 12, -18 \leq k \leq 20, -8 \leq l \leq 9$	
Reflections collected	8013	
Independent reflections	2597 [R(int) = 0.0248]	
Reflections with I>2σ(I)	2497	
Absorption correction	None	
Refinement method	Full-matrix least-squares on F^2	
Data / restraints / parameters	2596 / 57 / 192	
Largest final shift/e.s.d. ratio	-0.001	
Goodness-of-fit on F^2	1.097	
Final R indices [I>2σ(I)]	R1 = 0.0317, wR2 = 0.0784	
R indices (all data)	R1 = 0.0335, wR2 = 0.0803	
Absolute structure parameter	0.96(69)	
Largest diff. peak and hole	0.187 and -0.242 e.Å^{-3}	

Table 2. Atomic coordinates ($\times 10^4$) and equivalent isotropic displacement parameters ($Å^2 \times 10^4$) for N-fluoroacetyl-(S)-phenylalanine **45**. U(eq) is defined as one third of the trace of the orthogonalized Uij tensor.

	x	y	z	U(eq)
O(1)	6537(1)	2543(1)	6807(1)	273(2)
O(2)	4471(1)	1904(1)	6118(1)	274(2)
O(3)	6115(1)	2240(1)	167(1)	288(2)
F	3021(1)	1067(1)	1171(1)	384(2)
N(1)	4867(1)	2085(1)	2693(1)	196(2)
C(1)	5547(1)	2276(1)	5699(2)	202(2)
C(2)	5905(1)	2509(1)	3811(2)	176(2)
C(3)	5925(1)	3467(1)	3556(2)	236(3)
C(4)	5063(1)	1969(1)	979(2)	202(2)
C(5)	3911(1)	1494(1)	8(2)	264(3)
C(11A)	4575(4)	3883(4)	4240(5)	249(9)
C(12A)	4304(4)	4057(2)	6017(5)	314(6)
C(13A)	3051(4)	4462(2)	6545(6)	442(7)
C(14A)	2028(4)	4707(2)	5324(7)	504(9)
C(15A)	2268(4)	4527(3)	3542(8)	487(8)
C(16A)	3498(4)	4129(2)	3024(5)	336(6)
C(11B)	4483(4)	3900(4)	3641(5)	249(9)
C(12B)	3939(4)	4103(2)	5244(5)	314(6)
C(13B)	2611(4)	4523(2)	5349(6)	442(7)
C(14B)	1924(4)	4713(2)	3808(8)	504(9)
C(15B)	2469(4)	4524(2)	2194(6)	487(8)
C(16B)	3770(4)	4113(2)	2099(5)	336(6)

Table 3. Bond lengths [Å] and angles [°] for N-fluoroacetyl-(S)-phenylalanine **45**.

O(1)-H(01)	0.91(2)	C(4)-C(5)	1.513(2)
O(1)-C(1)	1.3233(14)	C(11A)-C(12A)	1.402(5)
O(2)-C(1)	1.2127(15)	C(11A)-C(16A)	1.423(4)
O(2)-H(1N)	2.29(2)	C(12A)-C(13A)	1.400(5)
O(3)-C(4)	1.2401(15)	C(13A)-C(14A)	1.390(6)
F-C(5)	1.3934(15)	C(14A)-C(15A)	1.403(8)
F-H(1N)	2.27(2)	C(15A)-C(16A)	1.374(5)
N(1)-H(1N)	0.81(2)	C(11B)-C(12B)	1.359(5)
N(1)-C(4)	1.328(2)	C(11B)-C(16B)	1.391(5)
N(1)-C(2)	1.4584(15)	C(12B)-C(13B)	1.416(5)
C(1)-C(2)	1.520(2)	C(13B)-C(14B)	1.371(8)
C(2)-C(3)	1.545(2)	C(14B)-C(15B)	1.363(7)
C(3)-C(11B)	1.520(2)	C(15B)-C(16B)	1.386(5)
C(3)-C(11A)	1.521(2)		
H(01)-O(1)-C(1)	107.8(14)	C(16A)-C(11A)-C(3)	119.3(3)
C(1)-O(2)-H(1N)	81.4(5)	C(13A)-C(12A)-C(11A)	121.4(3)
C(5)-F-H(1N)	81.4(5)	C(14A)-C(13A)-C(12A)	121.1(4)
H(1N)-N(1)-C(4)	118.3(12)	C(13A)-C(14A)-C(15A)	118.4(4)
H(1N)-N(1)-C(2)	118.8(12)	C(16A)-C(15A)-C(14A)	120.4(4)
C(4)-N(1)-C(2)	122.91(10)	C(15A)-C(16A)-C(11A)	122.5(4)
O(2)-C(1)-O(1)	125.00(11)	C(12B)-C(11B)-C(16B)	121.1(2)
O(2)-C(1)-C(2)	123.46(10)	C(12B)-C(11B)-C(3)	118.7(3)
O(1)-C(1)-C(2)	111.53(10)	C(16B)-C(11B)-C(3)	120.1(3)
N(1)-C(2)-C(1)	106.77(9)	C(11B)-C(12B)-C(13B)	119.5(3)
N(1)-C(2)-C(3)	113.35(10)	C(14B)-C(13B)-C(12B)	118.0(4)
C(1)-C(2)-C(3)	111.36(10)	C(15B)-C(14B)-C(13B)	122.9(3)
C(11B)-C(3)-C(2)	115.9(3)	C(14B)-C(15B)-C(16B)	118.8(4)
C(11A)-C(3)-C(2)	112.4(3)	C(15B)-C(16B)-C(11B)	119.6(4)
O(3)-C(4)-N(1)	123.31(11)		
O(3)-C(4)-C(5)	119.96(11)		
N(1)-C(4)-C(5)	116.72(11)		
F-C(5)-C(4)	111.33(10)		
C(12A)-C(11A)-C(16A)	116.2(2)		
C(12A)-C(11A)-C(3)	124.5(3)		

Table 4. Anisotropic displacement parameters ($Å^2 \times 10^4$) for N-fluoroacetyl-(S)-phenylalanine **45**. The anisotropic displacement factor exponent takes the form: $-2\pi^2[\, h^2 a^{*2} U_{11} + \ldots + 2\, h\, k\, a^*\, b^*\, U_{12}\,]$

	U_{11}	U_{22}	U_{33}	U_{23}	U_{13}	U_{12}
O(1)	224(4)	445(6)	150(4)	16(4)	-23(3)	-75(4)
O(2)	216(4)	430(5)	175(4)	37(4)	8(3)	-68(4)
O(3)	223(4)	488(6)	153(4)	-21(4)	9(3)	-82(4)
F	413(5)	469(5)	271(4)	-39(4)	57(4)	-228(4)
N(1)	180(5)	248(5)	160(5)	-4(4)	14(4)	-23(4)
C(1)	178(5)	272(6)	157(5)	-4(4)	1(4)	6(4)
C(2)	155(5)	232(5)	142(5)	-7(4)	6(4)	-4(4)
C(3)	212(6)	243(6)	253(6)	8(5)	4(5)	-31(5)
C(4)	180(5)	248(5)	177(5)	2(4)	-16(4)	18(4)
C(5)	244(6)	353(7)	193(6)	-31(5)	14(5)	-65(5)
C(11A)	201(7)	177(6)	370(30)	0(20)	-99(14)	-21(6)
C(12A)	320(20)	243(8)	380(20)	-33(14)	69(12)	11(10)
C(13A)	390(20)	261(10)	680(20)	-71(14)	180(14)	16(10)
C(14A)	233(12)	241(11)	1040(20)	-50(20)	100(20)	30(9)
C(15A)	301(13)	307(12)	850(20)	30(20)	-90(20)	34(10)
C(16A)	337(13)	258(8)	410(20)	54(13)	-89(13)	-30(8)
C(11B)	201(7)	177(6)	370(30)	0(20)	-99(14)	-21(6)
C(12B)	320(20)	243(8)	380(20)	-33(14)	69(12)	11(10)
C(13B)	390(20)	261(10)	680(20)	-71(14)	180(14)	16(10)
C(14B)	233(12)	241(11)	1040(20)	-50(20)	100(20)	30(9)
C(15B)	301(13)	307(12)	850(20)	30(20)	-90(20)	34(10)
C(16B)	337(13)	258(8)	410(20)	54(13)	-89(13)	-30(8)

Table 5. Hydrogen coordinates ($\times 10^3$) and isotropic displacement parameters ($Å^2 \times 10^3$) for N-fluoroacetyl-(S)-phenylalanine **45**.

	x	y	z	U(iso)
H(01)	630(2)	236(1)	791(3)	61(6)
H(1N)	415(2)	190(1)	314(2)	29(4)
H(2)	689(2)	230(1)	357(2)	17(3)
H(31)	621(2)	356(1)	231(3)	33(4)
H(32)	664(2)	369(1)	428(2)	29(4)
H(51)	334(2)	192(1)	-65(2)	37(5)
H(52)	437(2)	110(1)	-80(3)	37(4)
H(12A)	498(1)	390(1)	688(1)	38
H(13A)	290(1)	457(1)	776(1)	53
H(14A)	119(1)	499(1)	569(1)	60
H(15A)	158(1)	468(1)	269(1)	58
H(16A)	364(1)	401(1)	181(1)	40
H(12B)	445(1)	396(1)	629(1)	38
H(13B)	221(1)	467(1)	645(1)	53
H(14B)	103(1)	499(1)	387(1)	60
H(15B)	197(1)	467(1)	115(1)	58
H(16B)	417(1)	398(1)	99(1)	40

Table 6. Hydrogen bonds for N-fluoroacetyl-(S)-phenylalanine **45** [Å and °].

D-H...A	d(D-H)	d(H...A)	d(D...A)	<(DHA)
O(1)-H(01)...O(3)#1	0.91(2)	1.74(2)	2.628(1)	165(2)

Symmetry transformations used to generate equivalent atoms: #1 x,y,z+1

Appendix III

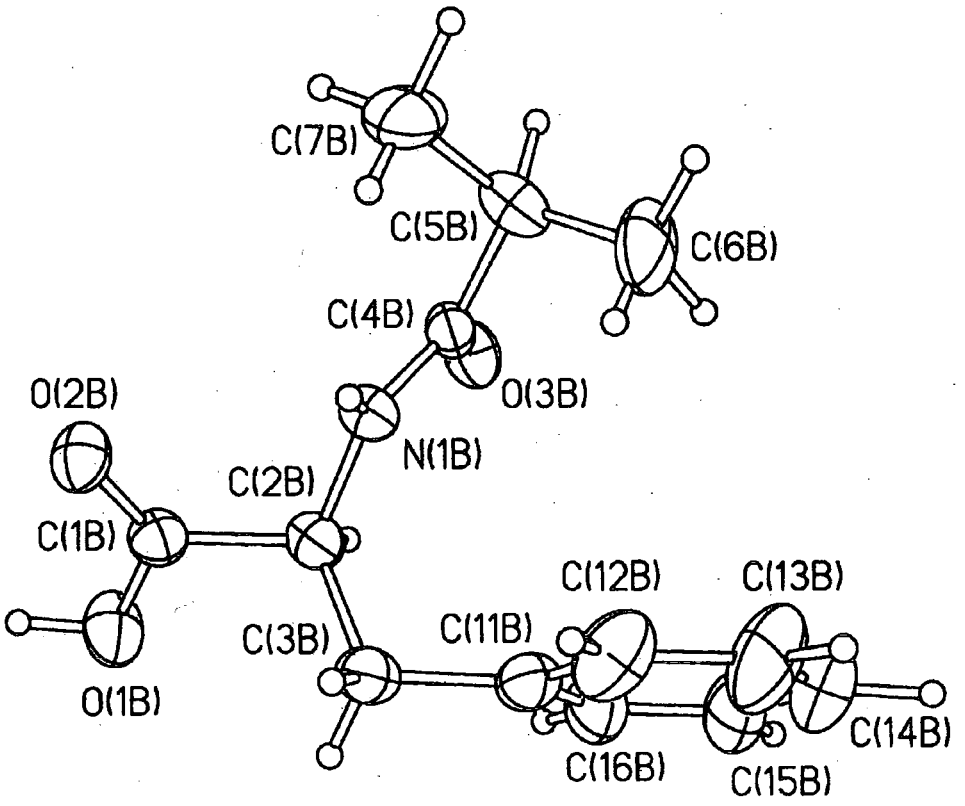

N-(2-Methylpropionyl)-(*S*)-phenylalanine, 49

Table 1. Crystal data and structure refinement for N-(2-methylpropionyl)-(S)-phenylalanine, **49**.

Identification code		
Empirical formula	C13 H17 N O3	
Formula weight	235.28	
Temperature	150(2) K	
Wavelength	1.54178 Å	
Crystal system	Tetragonal	
Space group	$P4_32_12$ (No. 96)	
Unit cell dimensions	a = 12.7734(14) Å	α= 90°
	b = 12.7734(14) Å	β= 90°
	c = 32.356(3) Å	γ = 90°
Volume	5279.2(9) Å^3	
Z	16	
Density (calculated)	1.184 g/cm^3	
Absorption coefficient	0.686 mm^{-1}	
F(000)	2016	
Crystal size	0.40 × 0.36 × 0.12 mm^3	
θ range for data collection	3.72 to 75.0°.	
Index ranges	$-6 \leq h \leq 16$, $-6 \leq k \leq 16$, $-17 \leq l \leq 40$	
Reflections collected	4952	
Independent reflections	4091 [R(int) = 0.0213]	
Reflections with I>2σ(I)	3477	
Absorption correction	None	
Max. and min. transmission	1.0000 and 0.8594	
Refinement method	Full-matrix least-squares on F^2	
Data / restraints / parameters	4090 / 0 / 444	
Largest final shift/e.s.d. ratio	-0.031	
Goodness-of-fit on F^2	1.079	
Final R indices [I>2σ(I)]	R1 = 0.0442, wR2 = 0.1018	
R indices (all data)	R1 = 0.0562, wR2 = 0.1093	
Absolute structure parameter	-0.16(26)	
Extinction coefficient	0.00074(10)	
Largest diff. peak and hole	0.182 and -0.145 e.Å^{-3}	

Table 2. Atomic coordinates ($\times 10^4$) and equivalent isotropic displacement parameters ($Å^2 \times 10^4$) for N-(2-methylpropionyl)-(S)-phenylalanine, **49**. U(eq) is defined as one third of the trace of the orthogonalized Uij tensor.

	x	y	z	U(eq)
O(1A)	3614(2)	5635(2)	712(1)	387(5)
O(2A)	2278(2)	5787(2)	1154(1)	379(5)
O(3A)	3328(2)	2440(2)	1534(1)	435(5)
N(1A)	2252(2)	3705(2)	1316(1)	308(5)
C(1A)	2912(2)	5258(2)	973(1)	303(6)
C(2A)	3023(2)	4089(2)	1023(1)	299(6)
C(3A)	3009(2)	3485(2)	608(1)	332(6)
C(4A)	2457(2)	2873(2)	1549(1)	321(6)
C(5A)	1594(2)	2478(3)	1830(1)	418(7)
C(6A)	2049(4)	2138(5)	2243(1)	757(14)
C(7A)	1021(4)	1582(4)	1610(2)	750(12)
C(11A)	1977(2)	3532(2)	379(1)	316(6)
C(12A)	1215(3)	2776(3)	444(1)	497(8)
C(13A)	267(3)	2816(3)	235(1)	582(10)
C(14A)	80(3)	3583(3)	-49(1)	444(7)
C(15A)	831(3)	4341(3)	-120(1)	441(7)
C(16A)	1769(2)	4315(2)	95(1)	364(6)
O(1B)	3654(2)	459(2)	1623(1)	492(6)
O(2B)	5022(1)	679(1)	1200(1)	375(5)
O(3B)	3913(2)	-2376(2)	773(1)	381(5)
N(1B)	5180(2)	-1433(2)	1078(1)	290(5)
C(1B)	4439(2)	124(2)	1395(1)	324(6)
C(2B)	4527(2)	-1061(2)	1410(1)	317(6)
C(3B)	4963(3)	-1413(2)	1833(1)	420(7)
C(4B)	4846(2)	-2098(2)	791(1)	301(6)
C(5B)	5657(2)	-2504(3)	491(1)	441(7)
C(6B)	6301(4)	-3362(3)	689(2)	771(15)
C(7B)	6323(3)	-1628(3)	321(1)	636(11)
C(11B)	5096(2)	-2585(2)	1860(1)	393(7)
C(12B)	6067(3)	-3059(3)	1834(1)	569(10)
C(13B)	6162(4)	-4138(3)	1850(1)	766(13)

C(14B)	5300(4)	-4758(3)	1890(1)	685(11)
C(15B)	4316(3)	-4305(3)	1917(1)	576(9)
C(16B)	4226(3)	-3230(3)	1897(1)	467(8)

Table 3. Bond lengths [Å] and angles [°] for N-(2-methylpropionyl)-(S)-phenylalanine, **49**.

O(1A)-H(0A)	0.87(4)
O(1A)-C(1A)	1.323(3)
O(2A)-C(1A)	1.206(3)
O(3A)-C(4A)	1.243(3)
N(1A)-H(1A)	0.80(3)
N(1A)-C(4A)	1.330(3)
N(1A)-C(2A)	1.452(3)
C(1A)-C(2A)	1.509(4)
C(2A)-C(3A)	1.549(4)
C(3A)-C(11A)	1.512(4)
C(4A)-C(5A)	1.516(4)
C(5A)-C(6A)	1.518(5)
C(5A)-C(7A)	1.535(6)
C(11A)-C(16A)	1.384(4)
C(11A)-C(12A)	1.387(4)
C(12A)-C(13A)	1.389(5)
C(13A)-C(14A)	1.363(5)
C(14A)-C(15A)	1.383(4)
C(15A)-C(16A)	1.385(4)
O(1B)-H(0B)	0.94(4)
O(1B)-C(1B)	1.317(3)
O(2B)-C(1B)	1.207(3)
O(3B)-C(4B)	1.246(3)
N(1B)-H(1B)	0.89(4)
N(1B)-C(4B)	1.327(3)
N(1B)-C(2B)	1.442(3)
C(1B)-C(2B)	1.518(4)
C(2B)-C(3B)	1.543(4)
C(3B)-C(11B)	1.510(4)
C(4B)-C(5B)	1.512(4)
C(5B)-C(7B)	1.510(5)

C(5B)-C(6B)	1.513(5)
C(11B)-C(12B)	1.382(5)
C(11B)-C(16B)	1.388(4)
C(12B)-C(13B)	1.385(6)
C(13B)-C(14B)	1.362(6)
C(14B)-C(15B)	1.386(6)
C(15B)-C(16B)	1.379(5)

H(0A)-O(1A)-C(1A)	112.9(22)
H(1A)-N(1A)-C(4A)	121.2(22)
H(1A)-N(1A)-C(2A)	118.3(22)
C(4A)-N(1A)-C(2A)	120.5(2)
O(2A)-C(1A)-O(1A)	124.1(3)
O(2A)-C(1A)-C(2A)	124.4(2)
O(1A)-C(1A)-C(2A)	111.4(2)
N(1A)-C(2A)-C(1A)	109.9(2)
N(1A)-C(2A)-C(3A)	112.9(2)
C(1A)-C(2A)-C(3A)	113.5(2)
C(11A)-C(3A)-C(2A)	114.5(2)
O(3A)-C(4A)-N(1A)	120.5(2)
O(3A)-C(4A)-C(5A)	121.8(2)
N(1A)-C(4A)-C(5A)	117.7(2)
C(4A)-C(5A)-C(6A)	110.1(3)
C(4A)-C(5A)-C(7A)	108.4(3)
C(6A)-C(5A)-C(7A)	112.2(4)
C(16A)-C(11A)-C(12A)	117.9(3)
C(16A)-C(11A)-C(3A)	121.4(2)
C(12A)-C(11A)-C(3A)	120.7(3)
C(11A)-C(12A)-C(13A)	120.9(3)
C(14A)-C(13A)-C(12A)	120.5(3)
C(13A)-C(14A)-C(15A)	119.5(3)
C(14A)-C(15A)-C(16A)	120.0(3)
C(15A)-C(16A)-C(11A)	121.1(3)
H(0B)-O(1B)-C(1B)	109.6(24)
H(1B)-N(1B)-C(4B)	121.9(22)
H(1B)-N(1B)-C(2B)	114.7(22)
C(4B)-N(1B)-C(2B)	123.2(2)

O(2B)-C(1B)-O(1B)	124.9(2)
O(2B)-C(1B)-C(2B)	123.9(2)
O(1B)-C(1B)-C(2B)	111.3(2)
N(1B)-C(2B)-C(1B)	110.3(2)
N(1B)-C(2B)-C(3B)	110.9(2)
C(1B)-C(2B)-C(3B)	110.3(2)
C(11B)-C(3B)-C(2B)	112.4(2)
O(3B)-C(4B)-N(1B)	121.5(2)
O(3B)-C(4B)-C(5B)	121.8(2)
N(1B)-C(4B)-C(5B)	116.6(2)
C(7B)-C(5B)-C(4B)	111.5(3)
C(7B)-C(5B)-C(6B)	112.7(3)
C(4B)-C(5B)-C(6B)	110.4(3)
C(12B)-C(11B)-C(16B)	117.6(3)
C(12B)-C(11B)-C(3B)	122.1(3)
C(16B)-C(11B)-C(3B)	120.2(3)
C(11B)-C(12B)-C(13B)	120.8(4)
C(14B)-C(13B)-C(12B)	120.8(4)
C(13B)-C(14B)-C(15B)	119.7(4)
C(16B)-C(15B)-C(14B)	119.2(4)
C(15B)-C(16B)-C(11B)	121.9(4)

Symmetry transformations used to generate equivalent atoms:

Table 4. Anisotropic displacement parameters ($Å^2 \times 10^3$) for N-(2-methylpropionyl)-(S)-phenylalanine, **49**. The anisotropic displacement factor exponent takes the form: $-2\pi^2[\, h^2 a^{*2} U_{11} + \ldots + 2\, h\, k\, a^*\, b^*\, U_{12}\,]$

	U_{11}	U_{22}	U_{33}	U_{23}	U_{13}	U_{12}
O(1A)	41(1)	30(1)	46(1)	-6(1)	11(1)	-6(1)
O(2A)	30(1)	34(1)	51(1)	-6(1)	5(1)	1(1)
O(3A)	30(1)	42(1)	59(1)	9(1)	8(1)	13(1)
N(1A)	23(1)	33(1)	36(1)	2(1)	2(1)	5(1)
C(1A)	25(1)	34(1)	32(1)	-8(1)	-3(1)	-1(1)
C(2A)	22(1)	32(2)	35(1)	-2(1)	1(1)	1(1)
C(3A)	35(2)	27(2)	37(1)	-5(1)	7(1)	3(1)
C(4A)	26(1)	35(2)	35(1)	-4(1)	2(1)	3(1)
C(5A)	31(2)	49(2)	46(2)	9(1)	5(1)	13(2)
C(6A)	56(2)	125(4)	47(2)	30(3)	14(2)	19(3)
C(7A)	51(2)	79(3)	95(3)	4(3)	17(2)	-22(2)
C(11A)	36(2)	30(1)	29(1)	-8(1)	8(1)	-1(1)
C(12A)	60(2)	44(2)	45(2)	10(2)	-11(2)	-17(2)
C(13A)	52(2)	62(2)	61(2)	12(2)	-11(2)	-26(2)
C(14A)	44(2)	45(2)	44(1)	-3(1)	-6(1)	-6(2)
C(15A)	51(2)	40(2)	41(1)	3(1)	1(1)	-2(2)
C(16A)	37(2)	34(2)	38(1)	0(1)	8(1)	-4(1)
O(1B)	45(1)	35(1)	68(1)	-3(1)	29(1)	2(1)
O(2B)	31(1)	32(1)	49(1)	3(1)	7(1)	-2(1)
O(3B)	32(1)	34(1)	49(1)	-9(1)	-7(1)	-5(1)
N(1B)	23(1)	34(1)	30(1)	-5(1)	2(1)	-3(1)
C(1B)	30(1)	34(2)	34(1)	-1(1)	5(1)	-1(1)
C(2B)	28(2)	33(2)	34(1)	-5(1)	5(1)	-8(1)
C(3B)	55(2)	40(2)	31(1)	-4(1)	6(1)	-10(2)
C(4B)	36(2)	24(1)	30(1)	-3(1)	-3(1)	3(1)
C(5B)	43(2)	48(2)	42(1)	-15(1)	6(1)	3(2)
C(6B)	74(3)	45(2)	112(4)	20(2)	49(3)	30(2)
C(7B)	71(3)	69(3)	51(2)	10(2)	30(2)	24(2)
C(11B)	49(2)	39(2)	30(1)	2(1)	-4(1)	-4(2)
C(12B)	43(2)	61(2)	66(2)	17(2)	-13(2)	-3(2)
C(13B)	61(3)	70(3)	98(3)	32(2)	-10(2)	26(2)
C(14B)	89(3)	45(2)	72(2)	18(2)	-3(2)	14(2)

C(15B)	69(3)	37(2)	67(2)	5(2)	2(2)	-4(2)
C(16B)	48(2)	39(2)	53(2)	0(1)	6(2)	-2(2)

Table 5. Hydrogen coordinates ($\times 10^3$) and isotropic displacement parameters ($Å^2 \times 10^3$) for N-(2-methylpropionyl)-(S)-phenylalanine, **49**.

	x	y	z	U(iso)
H(0A)	363(3)	632(3)	71(1)	51(10)
H(1A)	170(3)	400(2)	133(1)	37(9)
H(2A)	367(2)	396(2)	116(1)	25(6)
H(3A1)	359(3)	380(2)	44(1)	45(8)
H(3A2)	319(2)	274(2)	67(1)	38(8)
H(5A)	116(3)	304(3)	186(1)	48(9)
H(6A1)	157(4)	200(4)	246(2)	101(15)
H(6A2)	228(3)	287(4)	236(1)	83(15)
H(6A3)	263(5)	161(4)	222(2)	123(18)
H(7A1)	59(4)	132(4)	183(1)	94(14)
H(7A2)	152(5)	105(5)	154(2)	137(23)
H(7A3)	69(4)	181(4)	128(2)	127(18)
H(12A)	132(2)	222(3)	66(1)	43(8)
H(13A)	-28(4)	228(4)	28(1)	100(15)
H(14A)	-63(3)	365(3)	-18(1)	58(10)
H(15A)	77(3)	488(3)	-33(1)	80(12)
H(16A)	236(3)	483(3)	2(1)	53(9)
H(0B)	359(3)	119(3)	160(1)	74(12)
H(1B)	584(3)	-124(3)	109(1)	57(10)
H(2B)	388(2)	-136(2)	136(1)	19(6)
H(3B1)	571(3)	-109(3)	189(1)	60(10)
H(3B2)	453(2)	-115(2)	205(1)	41(8)
H(5B)	530(2)	-274(2)	19(1)	47(8)
H(6B1)	670(4)	-367(4)	48(1)	99(15)
H(6B2)	584(4)	-387(4)	83(1)	101(16)
H(6B3)	668(4)	-304(4)	95(2)	105(19)
H(7B1)	676(3)	-193(3)	10(1)	81(12)
H(7B2)	671(4)	-133(5)	58(2)	140(21)
H(7B3)	582(5)	-106(5)	17(2)	141(20)

H(12B)	665(4)	-266(4)	183(1)	98(16)
H(13B)	682(4)	-452(4)	186(1)	108(16)
H(14B)	539(3)	-555(4)	191(1)	91(13)
H(15B)	370(3)	-475(3)	196(1)	70(11)
H(16B)	357(3)	-292(3)	191(1)	70(12)

Table 6. Torsion angles [°] for N-(2-methylpropionyl)-(S)-phenylalanine, **49**.

O(2A)-C(1A)-C(2A)-N(1A)	0.6(4)
C(1A)-C(2A)-N(1A)-C(4A)	-149.4(2)
C(2A)-N(1A)-C(4A)-C(5A)	-176.6(2)
N(1A)-C(4A)-C(5A)-C(7A)	96.2(3)
N(1A)-C(2A)-C(3A)-C(11A)	59.9(3)
C(2A)-C(3A)-C(11A)-C(12A)	-90.9(3)
O(2B)-C(1B)-C(2B)-N(1B)	-16.5(4)
C(1B)-C(2B)-N(1B)-C(4B)	-120.7(3)
C(2B)-N(1B)-C(4B)-C(5B)	-173.6(2)
N(1B)-C(4B)-C(5B)-C(7B)	-47.3(4)
N(1B)-C(2B)-C(3B)-C(11B)	-55.8(3)
C(2B)-C(3B)-C(11B)-C(12B)	104.4(3)

Table 7. Hydrogen bonds for N-(2-methylpropionyl)-(S)-phenylalanine, **49** [Å and °].

D-H...A	d(D-H)	d(H...A)	d(D...A)	<(DHA)
O(1A)-H(0A)...O(3B)#1	0.87(4)	1.72(4)	2.576(3)	167(3)
O(1B)-H(0B)...O(3A)	0.94(4)	1.65(4)	2.580(3)	172(4)
N(1A)-H(1A)...O(2B)#2	0.80(3)	2.19(3)	2.956(3)	162(3)
N(1B)-H(1B)...O(2A)#3	0.89(4)	2.09(4)	2.936(3)	160(3)

Symmetry transformations used to generate equivalent atoms:

#1 x,y+1,z #2 x-1/2,-y+1/2,-z+1/4 #3 x+1/2,-y+1/2,-z+1/4

Appendix IV

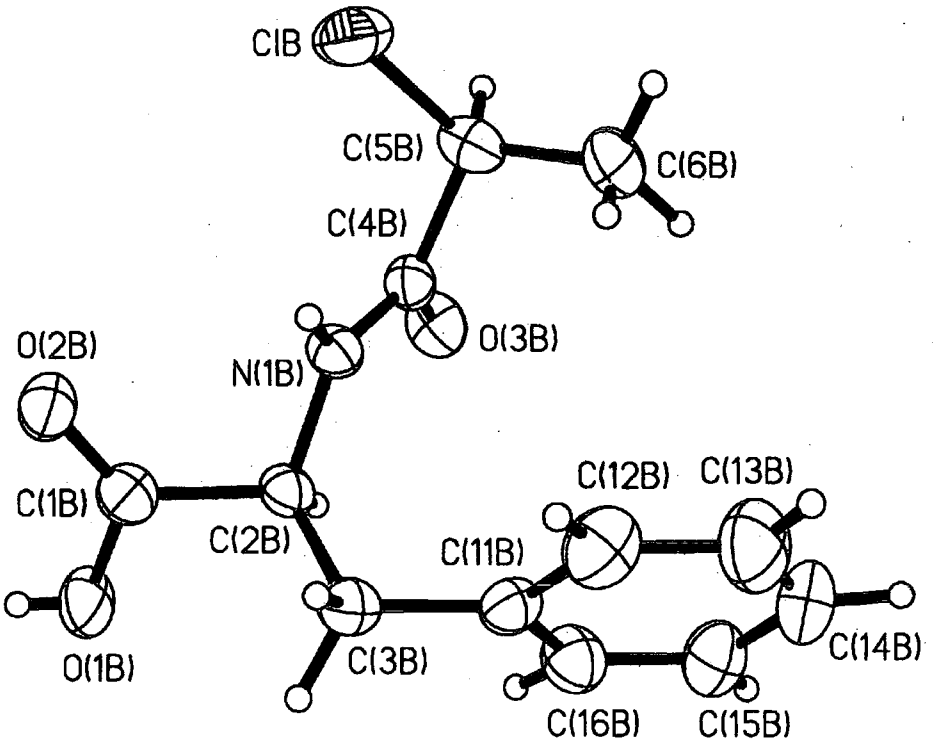

N-(*S*)-2-Chloropropanoyl-(*S*)-phenylalanine, (*S*, *S*)50

Table 1. Crystal data and structure refinement for N-(S)-2-chloropropanoyl-(S)-phenylalanine, (S, S)**50**.

Identification code		
Empirical formula	C12 H14 Cl N O3	
Formula weight	255.69	
Temperature	150(2) K	
Wavelength	1.54178 Å	
Crystal system	Tetragonal	
Space group	$P4_32_12$ (No. 96)	
Unit cell dimensions	a = 12.772(2) Å	α= 90°
	b = 12.772(2) Å	β= 90°
	c = 32.044(2) Å	γ = 90°
Volume	5227.1(12) Å^3	
Z	16	
Density (calculated)	1.300 g/cm^3	
Absorption coefficient	2.575 mm^{-1}	
F(000)	2144	
Crystal size	0.28 × 0.24 × 0.12 mm^3	
θ range for data collection	3.73 to 75.09°.	
Index ranges	$-7 \leq h \leq 16$, $-7 \leq k \leq 16$, $-17 \leq l \leq 40$	
Reflections collected	5349	
Independent reflections	4274 [R(int) = 0.0269]	
Reflections with I>2σ(I)	3465	
Absorption correction	Psi-scans	
Max. and min. transmission	1.0000 and 0.7830	
Refinement method	Full-matrix least-squares on F^2	
Data / restraints / parameters	4274 / 0 / 416	
Largest final shift/e.s.d. ratio	0.102	
Goodness-of-fit on F^2	1.040	
Final R indices [I>2σ(I)]	R1 = 0.0489, wR2 = 0.1176	
R indices (all data)	R1 = 0.0666, wR2 = 0.1298	
Absolute structure parameter	0.00(2)	
Extinction coefficient	0.00057(10)	
Largest diff. peak and hole	0.199 and -0.360 e.Å^{-3}	

Table 2. Atomic coordinates ($\times 10^4$) and equivalent isotropic displacement parameters ($Å^2 \times 10^4$) for N-(S)-2-chloropropanoyl-(S)-phenylalanine, (S, S)**50**. U(eq) is defined as one third of the trace of the orthogonalized Uij tensor.

	x	y	z	U(eq)
O(1A)	3691(2)	5598(2)	720(1)	402(6)
O(2A)	2311(2)	5760(2)	1145(1)	361(6)
O(3A)	3322(2)	2410(2)	1562(1)	462(7)
N(1A)	2278(2)	3683(2)	1319(1)	308(7)
C(1A)	2969(3)	5221(3)	978(1)	302(8)
C(2A)	3074(3)	4056(3)	1029(1)	325(8)
C(3A)	3052(3)	3451(3)	609(1)	362(9)
C(4A)	2464(3)	2868(3)	1564(1)	318(8)
C(5A)	1595(3)	2539(4)	1850(1)	455(10)
C(6A)	2038(14)	2807(14)	2323(5)	470(20)
ClA	1218(5)	1327(5)	1837(2)	734(8)
C(6A')	2001(6)	2182(7)	2279(2)	470(20)
ClA'	1063(2)	1324(2)	1598(1)	734(8)
C(11A)	2013(3)	3490(3)	386(1)	342(8)
C(12A)	1265(4)	2717(4)	442(2)	555(13)
C(13A)	322(5)	2755(4)	236(2)	650(20)
C(14A)	98(4)	3551(4)	-38(1)	517(11)
C(15A)	820(4)	4328(4)	-95(1)	455(10)
C(16A)	1769(4)	4292(3)	114(1)	436(10)
O(1B)	3694(3)	408(3)	1632(1)	480(8)
O(2B)	5055(2)	706(2)	1203(1)	375(6)
O(3B)	3979(2)	-2384(2)	747(1)	400(7)
N(1B)	5237(3)	-1396(2)	1050(1)	287(6)
C(1B)	4487(3)	116(3)	1394(1)	341(8)
C(2B)	4600(3)	-1068(3)	1399(1)	287(8)
C(3B)	5073(3)	-1441(3)	1815(1)	350(8)
C(4B)	4881(3)	-2047(3)	761(1)	294(8)
C(5B)	5673(3)	-2454(3)	443(1)	411(9)
C(6B)	6285(5)	-3395(4)	617(2)	620(20)
ClB	6573(1)	-1459(1)	288(1)	480(3)
C(11B)	5188(3)	-2614(3)	1831(1)	331(8)

C(12B)	6142(4)	-3102(4)	1776(2)	496(11)
C(13B)	6227(5)	-4176(4)	1784(2)	600(14)
C(14B)	5351(5)	-4785(4)	1844(2)	606(14)
C(15B)	4389(4)	-4321(4)	1903(2)	520(12)
C(16B)	4306(4)	-3241(3)	1892(1)	426(10)

Table 3. Bond lengths [Å] and angles [°] for N-(S)-2-chloropropanoyl-(S)-phenylalanine, (S, S)**50**.

O(1A)-H(0A)	0.91(7)	C(15A)-C(16A)	1.386(6)
O(1A)-C(1A)	1.328(4)	O(1B)-H(0B)	0.68(4)
O(2A)-C(1A)	1.212(4)	O(1B)-C(1B)	1.321(5)
O(3A)-C(4A)	1.243(4)	O(2B)-C(1B)	1.212(4)
N(1A)-H(1A)	0.94(5)	O(3B)-C(4B)	1.230(4)
N(1A)-C(4A)	1.325(5)	N(1B)-H(1B)	0.84(5)
N(1A)-C(2A)	1.458(5)	N(1B)-C(4B)	1.325(4)
C(1A)-C(2A)	1.503(5)	N(1B)-C(2B)	1.446(4)
C(2A)-C(3A)	1.551(5)	C(1B)-C(2B)	1.520(5)
C(3A)-C(11A)	1.508(6)	C(2B)-C(3B)	1.538(5)
C(4A)-C(5A)	1.499(5)	C(3B)-C(11B)	1.506(6)
C(5A)-C(6A')	1.539(8)	C(4B)-C(5B)	1.528(5)
C(5A)-ClA	1.622(8)	C(5B)-C(6B)	1.538(7)
C(5A)-C(6A)	1.65(2)	C(5B)-ClB	1.784(4)
C(5A)-ClA'	1.876(5)	C(11B)-C(12B)	1.380(6)
C(11A)-C(16A)	1.379(6)	C(11B)-C(16B)	1.396(6)
C(11A)-C(12A)	1.386(6)	C(12B)-C(13B)	1.376(7)
C(12A)-C(13A)	1.376(7)	C(13B)-C(14B)	1.376(8)
C(13A)-C(14A)	1.374(7)	C(14B)-C(15B)	1.377(7)
C(14A)-C(15A)	1.367(6)	C(15B)-C(16B)	1.385(6)
H(0A)-O(1A)-C(1A)	100.1(44)	N(1A)-C(2A)-C(1A)	109.3(3)
H(1A)-N(1A)-C(4A)	120.1(29)	N(1A)-C(2A)-C(3A)	112.1(3)
H(1A)-N(1A)-C(2A)	119.1(29)	C(1A)-C(2A)-C(3A)	113.4(3)
C(4A)-N(1A)-C(2A)	120.6(3)	C(11A)-C(3A)-C(2A)	114.3(3)
O(2A)-C(1A)-O(1A)	123.4(3)	O(3A)-C(4A)-N(1A)	121.6(3)
O(2A)-C(1A)-C(2A)	125.2(3)	O(3A)-C(4A)-C(5A)	121.6(3)
O(1A)-C(1A)-C(2A)	111.4(3)	N(1A)-C(4A)-C(5A)	116.7(3)

C(4A)-C(5A)-C(6A')	112.3(4)	C(14B)-C(15B)-C(16B)	119.6(5)
C(4A)-C(5A)-ClA	118.2(4)	C(15B)-C(16B)-C(11B)	120.9(4)
C(4A)-C(5A)-C(6A)	104.4(7)		
ClA-C(5A)-C(6A)	108.8(7)		
C(4A)-C(5A)-ClA'	103.7(3)		
C(6A')-C(5A)-ClA'	105.2(4)		
C(16A)-C(11A)-C(12A)	117.1(4)		
C(16A)-C(11A)-C(3A)	121.5(4)		
C(12A)-C(11A)-C(3A)	121.3(4)		
C(13A)-C(12A)-C(11A)	121.1(5)		
C(14A)-C(13A)-C(12A)	121.0(5)		
C(15A)-C(14A)-C(13A)	118.9(5)		
C(14A)-C(15A)-C(16A)	120.1(4)		
C(11A)-C(16A)-C(15A)	121.8(4)		
H(0B)-O(1B)-C(1B)	112.7(39)		
H(1B)-N(1B)-C(4B)	122.8(32)		
H(1B)-N(1B)-C(2B)	115.3(32)		
C(4B)-N(1B)-C(2B)	121.9(3)		
O(2B)-C(1B)-O(1B)	125.1(4)		
O(2B)-C(1B)-C(2B)	124.6(3)		
O(1B)-C(1B)-C(2B)	110.3(3)		
N(1B)-C(2B)-C(1B)	109.5(3)		
N(1B)-C(2B)-C(3B)	111.1(3)		
C(1B)-C(2B)-C(3B)	110.8(3)		
C(11B)-C(3B)-C(2B)	112.0(3)		
O(3B)-C(4B)-N(1B)	124.5(3)		
O(3B)-C(4B)-C(5B)	118.5(3)		
N(1B)-C(4B)-C(5B)	116.9(3)		
C(4B)-C(5B)-C(6B)	111.1(3)		
C(4B)-C(5B)-ClB	111.7(3)		
C(6B)-C(5B)-ClB	109.3(3)		
C(12B)-C(11B)-C(16B)	118.1(4)		
C(12B)-C(11B)-C(3B)	122.1(4)		
C(16B)-C(11B)-C(3B)	119.8(4)		
C(13B)-C(12B)-C(11B)	121.2(5)		
C(14B)-C(13B)-C(12B)	120.1(5)		
C(13B)-C(14B)-C(15B)	120.1(5)		

Table 4. Anisotropic displacement parameters ($Å^2 \times 10^3$) for N-(S)-2-chloropropanoyl-(S)-phenylalanine, (S, S)**50**. The anisotropic displacement factor exponent takes the form: $-2\pi^2[h^2 a^{*2}U_{11} + ... + 2 h k a^* b^* U_{12}]$

	U_{11}	U_{22}	U_{33}	U_{23}	U_{13}	U_{12}
O(1A)	42(2)	33(2)	45(1)	2(1)	10(1)	-6(1)
O(2A)	33(1)	33(1)	42(1)	-2(1)	3(1)	3(1)
O(3A)	39(2)	38(2)	61(2)	9(1)	8(1)	11(1)
N(1A)	31(2)	29(2)	33(1)	3(1)	3(1)	1(2)
C(1A)	28(2)	27(2)	36(2)	-3(1)	-2(1)	-6(2)
C(2A)	27(2)	37(2)	33(2)	-2(2)	-1(2)	2(2)
C(3A)	43(2)	27(2)	39(2)	-3(2)	8(2)	3(2)
C(4A)	28(2)	27(2)	39(2)	-2(2)	2(2)	3(2)
C(5A)	42(2)	49(3)	46(2)	16(2)	7(2)	13(2)
C(6A)	32(3)	79(6)	30(2)	10(4)	11(2)	16(5)
ClA	56(1)	55(1)	110(2)	12(2)	7(2)	-12(1)
C(6A')	32(3)	79(6)	30(2)	10(4)	11(2)	16(5)
ClA'	56(1)	55(1)	110(2)	12(2)	7(2)	-12(1)
C(11A)	39(2)	31(2)	33(2)	-8(2)	5(1)	-3(2)
C(12A)	70(4)	40(3)	56(3)	12(2)	-14(2)	-18(3)
C(13A)	67(4)	58(3)	71(3)	13(3)	-22(3)	-30(3)
C(14A)	50(3)	58(3)	48(2)	-1(2)	-9(2)	-2(3)
C(15A)	50(3)	46(3)	41(2)	2(2)	-2(2)	-3(2)
C(16A)	54(3)	33(2)	44(2)	1(2)	2(2)	-7(2)
O(1B)	48(2)	31(2)	65(2)	4(2)	24(2)	11(2)
O(2B)	34(2)	30(1)	48(1)	4(1)	6(1)	0(1)
O(3B)	32(2)	39(2)	48(2)	-8(1)	-3(1)	-7(1)
N(1B)	25(2)	29(2)	32(1)	-4(1)	5(1)	-4(1)
C(1B)	29(2)	36(2)	37(2)	0(2)	2(2)	4(2)
C(2B)	27(2)	29(2)	31(2)	-3(1)	7(1)	0(2)
C(3B)	37(2)	36(2)	31(2)	-1(2)	5(2)	-1(2)
C(4B)	32(2)	27(2)	29(2)	0(1)	-1(1)	3(2)
C(5B)	42(2)	45(2)	36(2)	-8(2)	7(2)	3(2)
C(6B)	69(4)	44(3)	73(3)	9(3)	33(3)	24(3)
ClB	46(1)	60(1)	39(1)	11(1)	12(1)	4(1)
C(11B)	34(2)	37(2)	28(2)	5(2)	0(1)	2(2)
C(12B)	42(3)	53(3)	54(2)	9(2)	-5(2)	0(2)
C(13B)	53(3)	53(3)	74(3)	7(2)	-2(3)	17(3)
C(14B)	83(4)	36(3)	63(3)	11(2)	3(3)	13(3)

C(15B)	60(3)	37(3)	58(3)	6(2)	4(2)	-5(3)
C(16B)	39(2)	41(3)	48(2)	-3(2)	4(2)	0(2)

Table 5. Hydrogen coordinates ($\times 10^3$) and isotropic displacement parameters ($Å^2 \times 10^3$) for N-(S)-2-chloropropanoyl-(S)-phenylalanine, (S, S)**50**.

	x	y	z	U(iso)
H(0A)	351(6)	628(6)	72(2)	121(25)
H(1A)	161(4)	400(4)	132(1)	62(15)
H(2A)	374(3)	398(3)	114(1)	27(9)
H(3A1)	363(3)	377(3)	43(1)	27(9)
H(3A2)	322(3)	282(3)	67(1)	22(10)
H(5A)	94(3)	301(3)	182(1)	30(10)
H(6A1)	152(1)	262(1)	253(1)	64(12)
H(6A2)	218(1)	354(1)	234(1)	64(12)
H(6A3)	267(1)	242(1)	237(1)	64(12)
H(6A4)	142(1)	198(1)	245(1)	64(12)
H(6A5)	237(1)	275(1)	241(1)	64(12)
H(6A6)	247(1)	160(1)	224(1)	64(12)
H(12A)	139(4)	219(4)	58(1)	49(13)
H(13A)	-16(4)	227(5)	29(2)	87(19)
H(14A)	-59(4)	356(3)	-18(1)	50(12)
H(15A)	68(4)	490(4)	-29(2)	65(14)
H(16A)	219(4)	478(4)	9(2)	59(15)
H(0B)	361(4)	93(3)	163(1)	35(14)
H(1B)	584(4)	-115(4)	104(1)	55(14)
H(2B)	388(3)	-136(3)	135(1)	19(8)
H(3B1)	575(3)	-114(3)	186(1)	35(11)
H(3B2)	467(4)	-109(3)	204(1)	51(12)
H(5B)	534(4)	-263(4)	18(2)	72(15)
H(6B1)	680(5)	-361(5)	47(2)	99(22)
H(6B2)	575(4)	-401(5)	71(2)	81(17)
H(6B3)	673(5)	-320(5)	87(2)	92(21)
H(12B)	665(4)	-269(4)	176(1)	47(14)
H(13B)	686(5)	-442(5)	175(2)	95(21)
H(14B)	537(4)	-551(4)	182(1)	56(14)
H(15B)	381(4)	-472(4)	194(1)	52(14)
H(16B)	363(3)	-291(3)	191(1)	35(10)

Table 6. Torsion angles [°] for N-(S)-2-chloropropanoyl-(S)-phenylalanine, (S, S)**50**.

O(2A)-C(1A)-C(2A)-N(1A)	-1.5(5)
C(1A)-C(2A)-N(1A)-C(4A)	-148.1(3)
C(2A)-N(1A)-C(4A)-C(5A)	-179.6(3)
N(1A)-C(4A)-C(5A)-ClA	126.6(4)
N(1A)-C(4A)-C(5A)-ClA'	104.9(3)
N(1A)-C(2A)-C(3A)-C(11A)	57.4(4)
C(2A)-C(3A)-C(11A)-C(12A)	-93.0(5)
O(2B)-C(1B)-C(2B)-N(1B)	-18.2(5)
C(1B)-C(2B)-N(1B)-C(4B)	-120.6(4)
C(2B)-N(1B)-C(4B)-C(5B)	-171.7(3)
N(1B)-C(4B)-C(5B)-ClB	-39.3(4)
N(1B)-C(2B)-C(3B)-C(11B)	-58.5(4)
C(2B)-C(3B)-C(11B)-C(12B)	103.1(4)

Table 7. Hydrogen bonds for N-(S)-2-chloropropanoyl-(S)-phenylalanine, (S, S)**50** [Å and °].

D-H...A	d(D-H)	d(H...A)	d(D...A)	<(DHA)
O(1A)-H(0A)...O(3B)#1	0.91(7)	1.81(7)	2.606(4)	145(6)
O(1B)-H(0B)...O(3A)	0.68(3)	1.94(4)	2.611(4)	174(5)
N(1A)-H(1A)...O(2B)#2	0.94(5)	2.02(5)	2.945(4)	166(4)
N(1B)-H(1B)...O(2A)#3	0.84(5)	2.18(5)	2.938(4)	150(4)

Symmetry transformations used to generate equivalent atoms:

#1 x,y+1,z #2 x-1/2,-y+1/2,-z+1/4 #3 x+1/2,-y+1/2,-z+1/4

Appendix V

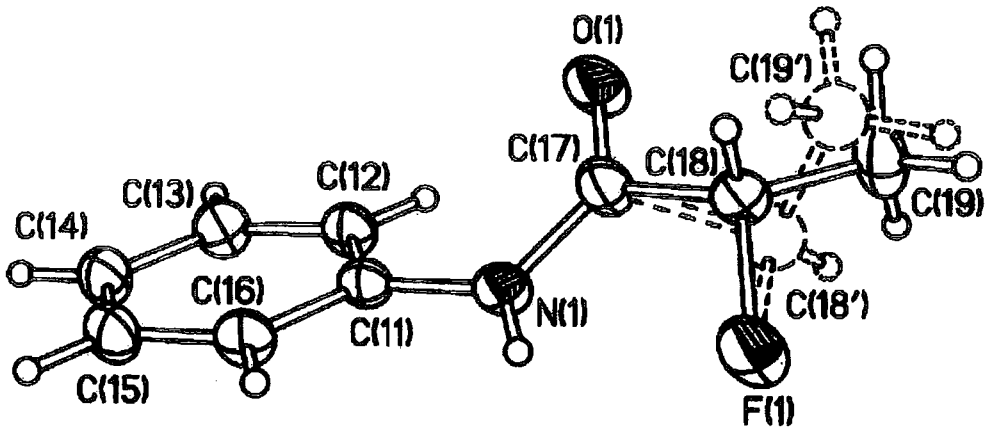

N-((*S*)-2-Fluoropropionyl)-aniline, 51

Table 1. Crystal data and structure refinement for N-((S)-2-fluoropropionyl)-aniline, **51**.

Identification code	99srv205	
Empirical formula	C9 H10 F N O	
Formula weight	167.18	
Temperature	150(2) K	
Wavelength	1.54184 Å	
Crystal system	Triclinic	
Space group	P1	
Unit cell dimensions	a = 5.367(1) Å	α= 106.65(2)°.
	b = 8.821(4) Å	β= 101.84(2)°.
	c = 9.893(3) Å	γ = 105.13(2)°.
Volume	412.8(2) $Å^3$	
Z	2	
Density (calculated)	1.345 Mg/m^3	
Absorption coefficient	0.867 mm^{-1}	
F(000)	176	
Crystal size	0.40 x 0.17 x 0.07 mm^3	
Theta range for data collection	4.90 to 74.96°.	
Index ranges	-6<=h<=6, 0<=k<=11, -11<=l<=11	
Reflections collected	1593	
Independent reflections	1592 [R(int) = 0.0155]	
Absorption correction	None	
Refinement method	Full-matrix least-squares on F^2	
Data / restraints / parameters	1582 / 3 / 236	
Goodness-of-fit on F^2	1.092	
Final R indices [I>2sigma(I)]	R1 = 0.0431, wR2 = 0.1122	
R indices (all data)	R1 = 0.0492, wR2 = 0.1536	
Absolute structure parameter	0.0(2)	
Largest diff. peak and hole	0.217 and -0.290 $e.Å^{-3}$	

Table 2. Atomic coordinates (x 10^4) and equivalent isotropic displacement parameters ($Å^2$x 10^3) for N-((S)-2-fluoropropionyl)-aniline, **51**. U(eq) is defined as one third of the trace of the orthogonalized U^{ij} tensor.

	x	y	z	U(eq)
F(1)	5391(4)	6587(3)	7242(2)	53(1)
N(1)	2309(5)	4023(3)	4863(3)	26(1)
O(1)	-1529(5)	4391(3)	5333(3)	40(1)
C(11)	1118(6)	2612(3)	3513(3)	25(1)
C(12)	-1265(7)	2391(4)	2488(3)	28(1)
C(13)	-2323(7)	982(4)	1193(3)	31(1)
C(14)	-1046(7)	-203(4)	912(4)	33(1)
C(15)	1351(7)	40(4)	1942(4)	35(1)
C(16)	2443(6)	1453(4)	3232(4)	30(1)
C(17)	928(6)	4738(4)	5691(3)	33(1)
C(18)	2658(8)	5968(5)	7264(4)	28(1)
C(19)	1829(9)	7454(6)	7781(5)	42(2)
C(18')	2519(39)	6656(24)	6813(21)	37(5)
C(19')	1997(38)	6580(22)	8203(19)	36(5)
F(2)	9911(4)	7956(3)	4431(2)	39(1)
N(2)	6869(6)	5729(3)	1864(3)	28(1)
O(2)	3041(5)	6178(3)	2268(3)	43(1)
C(21)	5717(6)	4475(4)	426(3)	28(1)
C(22)	3156(6)	3259(4)	11(4)	31(1)
C(23)	2154(7)	2015(4)	-1382(4)	35(1)
C(24)	3662(7)	1959(5)	-2373(4)	37(1)
C(25)	6194(7)	3155(5)	-1955(4)	36(1)
C(26)	7236(6)	4408(4)	-551(3)	31(1)
C(27)	5475(6)	6458(4)	2681(3)	30(1)
C(28)	7116(7)	7654(4)	4254(3)	32(1)
C(29)	6647(8)	9301(4)	4606(4)	42(1)

Table 3. Bond lengths [Å] and angles [°] for N-((S)-2-fluoropropionyl)-aniline, **51**.

F(1)-C(18)	1.433(4)
F(1)-C(18')	1.54(2)
N(1)-H(1)	0.84(4)
N(1)-C(17)	1.348(4)
N(1)-C(11)	1.422(4)
O(1)-C(17)	1.222(4)
C(11)-C(16)	1.387(4)
C(11)-C(12)	1.388(5)
C(12)-C(13)	1.389(4)
C(13)-C(14)	1.388(5)
C(14)-C(15)	1.390(5)
C(15)-C(16)	1.388(4)
C(17)-C(18)	1.541(5)
C(17)-C(18')	1.61(2)
C(18)-C(19)	1.480(6)
C(18')-C(19')	1.47(3)
F(2)-C(28)	1.418(4)
N(2)-H(2)	0.78(4)
N(2)-C(27)	1.352(4)
N(2)-C(21)	1.418(4)
O(2)-C(27)	1.220(4)
C(21)-C(26)	1.385(4)
C(21)-C(22)	1.398(5)
C(22)-C(23)	1.383(4)
C(23)-C(24)	1.392(5)
C(24)-C(25)	1.379(5)
C(25)-C(26)	1.394(4)
C(27)-C(28)	1.524(4)
C(28)-C(29)	1.494(5)
H(1)-N(1)-C(17)	114.7(26)
H(1)-N(1)-C(11)	118.7(26)
C(17)-N(1)-C(11)	125.1(3)
C(16)-C(11)-C(12)	120.3(3)
C(16)-C(11)-N(1)	117.7(3)
C(12)-C(11)-N(1)	122.0(3)
C(11)-C(12)-C(13)	119.1(3)
C(14)-C(13)-C(12)	121.2(3)

C(13)-C(14)-C(15)	119.1(3)
C(16)-C(15)-C(14)	120.2(3)
C(11)-C(16)-C(15)	120.1(3)
O(1)-C(17)-N(1)	125.5(3)
O(1)-C(17)-C(18)	119.4(3)
N(1)-C(17)-C(18)	114.8(3)
O(1)-C(17)-C(18')	112.5(7)
N(1)-C(17)-C(18')	116.1(7)
F(1)-C(18)-C(19)	106.9(3)
F(1)-C(18)-C(17)	107.7(3)
C(19)-C(18)-C(17)	113.6(4)
C(19')-C(18')-F(1)	95.0(14)
C(19')-C(18')-C(17)	101.9(13)
F(1)-C(18')-C(17)	99.4(11)
H(2)-N(2)-C(27)	119.9(30)
H(2)-N(2)-C(21)	114.6(30)
C(27)-N(2)-C(21)	125.3(3)
C(26)-C(21)-C(22)	119.7(3)
C(26)-C(21)-N(2)	118.8(3)
C(22)-C(21)-N(2)	121.3(3)
C(23)-C(22)-C(21)	119.5(3)
C(22)-C(23)-C(24)	120.9(3)
C(25)-C(24)-C(23)	119.5(3)
C(24)-C(25)-C(26)	120.3(3)
C(21)-C(26)-C(25)	120.2(3)
O(2)-C(27)-N(2)	125.0(3)
O(2)-C(27)-C(28)	119.1(3)
N(2)-C(27)-C(28)	115.8(3)
F(2)-C(28)-C(29)	108.7(3)
F(2)-C(28)-C(27)	109.4(2)
C(29)-C(28)-C(27)	112.0(3)

Symmetry transformations used to generate equivalent atoms:

Table 4. Anisotropic displacement parameters ($Å^2 x\ 10^3$) for N-((S)-2-fluoropropionyl)-aniline, **51**. The anisotropic displacement factor exponent takes the form: $-2\pi^2[\ h^2\ a^{*2}U^{11} + \ldots + 2\ h\ k\ a^*\ b^*\ U^{12}\ ]$

	U^{11}	U^{22}	U^{33}	U^{23}	U^{13}	U^{12}
F(1)	16(1)	65(2)	48(1)	-15(1)	4(1)	6(1)
N(1)	15(2)	33(1)	26(1)	6(1)	3(1)	8(1)
O(1)	19(1)	50(1)	38(1)	0(1)	8(1)	9(1)

C(11)	18(2)	27(1)	28(1)	8(1)	7(1)	9(1)
C(12)	23(2)	30(1)	30(1)	10(1)	7(1)	12(1)
C(13)	25(2)	34(2)	29(2)	7(1)	3(1)	10(1)
C(14)	27(2)	31(1)	32(1)	0(1)	6(1)	7(1)
C(15)	25(2)	33(2)	44(2)	6(1)	11(2)	14(1)
C(16)	16(2)	34(1)	35(2)	8(1)	3(1)	11(1)
C(17)	21(2)	37(2)	29(2)	-1(1)	6(1)	7(1)
C(18)	13(2)	35(2)	25(2)	2(2)	1(1)	5(2)
C(19)	23(3)	39(2)	46(3)	-8(2)	3(2)	15(2)
F(2)	20(1)	49(1)	38(1)	3(1)	1(1)	15(1)
N(2)	14(2)	32(1)	32(1)	7(1)	3(1)	10(1)
O(2)	21(1)	46(1)	47(1)	-2(1)	3(1)	14(1)
C(21)	23(2)	31(1)	28(1)	11(1)	4(1)	12(1)
C(22)	22(2)	35(2)	35(2)	12(1)	9(1)	9(1)
C(23)	25(2)	36(2)	35(2)	9(1)	5(1)	6(1)
C(24)	31(2)	41(2)	30(2)	5(1)	4(1)	12(1)
C(25)	28(2)	49(2)	32(2)	12(1)	10(1)	15(1)
C(26)	22(2)	39(2)	33(2)	12(1)	7(1)	11(1)
C(27)	22(2)	33(2)	33(2)	7(1)	6(1)	13(1)
C(28)	21(2)	34(2)	36(2)	8(1)	6(1)	9(1)
C(29)	30(2)	36(2)	47(2)	0(2)	7(2)	13(1)

Table 5. Hydrogen coordinates (x 10^4) and isotropic displacement parameters ($Å^2$x 10^3) for N-((S)-2-fluoropropionyl)-aniline, **51**.

	x	y	z	U(eq)
H(1)	3982(87)	4317(48)	5293(42)	24(9)
H(12)	-2160(7)	3193(4)	2656(3)	33
H(13)	-3954(7)	824(4)	487(3)	37
H(14)	-1807(7)	-1170(4)	28(4)	40
H(15)	2258(7)	-755(4)	1765(4)	42
H(16)	4103(6)	1638(4)	3928(4)	35
H(18)	2595(8)	5349(5)	7966(4)	36
H(191)	-54(9)	7069(6)	7786(5)	33(7)
H(192)	1989(9)	8121(6)	7144(5)	33(7)
H(193)	3004(9)	8148(6)	8791(5)	33(7)
H(18')	2246(39)	7590(24)	6486(21)	48
H(194)	2880(38)	7695(22)	8984(19)	53
H(195)	2723(38)	5771(22)	8493(19)	53
H(196)	41(38)	6223(22)	8055(19)	53
H(2)	8445(90)	6052(50)	2148(43)	27(10)
H(22)	2125(6)	3284(4)	686(4)	37
H(23)	407(7)	1197(4)	-1664(4)	42
H(24)	2951(7)	1100(5)	-3327(4)	44
H(25)	7229(7)	3132(5)	-2628(4)	44
H(26)	9003(6)	5210(4)	-256(3)	38
H(28)	6576(7)	7120(4)	4963(3)	42
H(291)	7648(8)	10005(4)	5642(4)	43(6)
H(292)	4712(8)	9121(4)	4442(4)	43(6)
H(293)	7299(8)	9865(4)	3960(4)	43(6)

Table 6. Torsion angles [°] for N-((S)-2-fluoropropionyl)-aniline, **51**.

C(16)-C(11)-N(1)-C(17)	-143.3(3)
C(11)-N(1)-C(17)-C(18)	166.3(3)
N(1)-C(17)-C(18)-F(1)	24.5(5)
C(26)-C(21)-N(2)-C(27)	149.0(3)
C(21)-N(2)-C(27)-C(28)	174.4(3)
N(2)-C(27)-C(28)-F(2)	9.9(4)

Symmetry transformations used to generate equivalent atoms:

Appendix VI

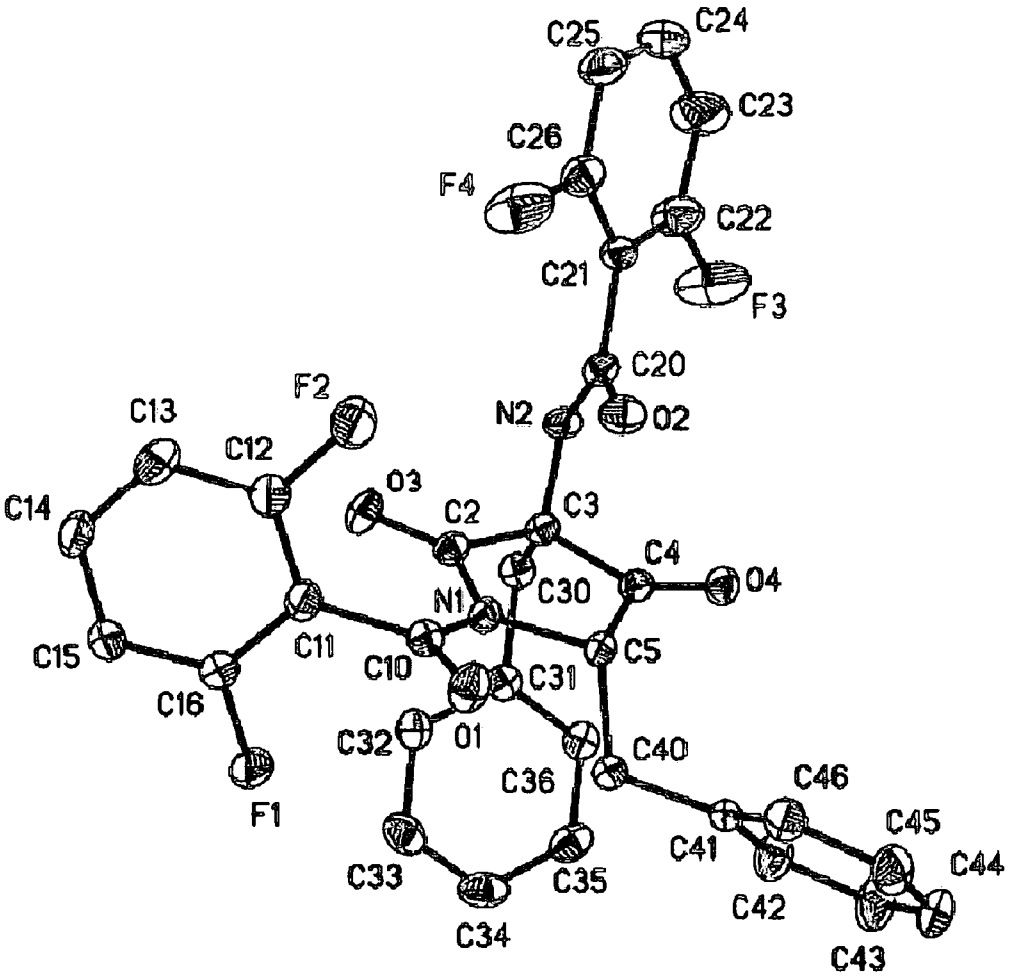

3,5-Dibenzyl-1-(2,6-difluorobenzoyl)-3-(2,6-difluorobenzoylamino)pyrrolidine-2,4-dione, 70

Table 1. Crystal data and structure refinement for 3,5-dibenzyl-1-(2,6-difluorobenzoyl)-3-(2,6-difluorobenzoylamino)pyrrolidine-2,4-dione, **70**.

Identification code	00srv264	
Empirical formula	C64 H44 F8 N4 O8	
Formula weight	1149.03	
Temperature	100(2) K	
Wavelength	0.71073 Å	
Crystal system	Monoclinic	
Space group	C2/c	
No. of reflections for cell determination	5176	
Theta range for cell determination	2.72° - 28.22°	
Unit cell dimensions	a = 19.713(1) Å	α= 90°.
	b = 14.119(1) Å	β= 93.807(1)°.
	c = 19.154(1) Å	γ = 90°.
Volume	5319.3(6) $Å^3$	
Z	4	
Density (calculated)	1.435 Mg/m^3	
Absorption coefficient	0.114 mm^{-1}	
F(000)	2368	
Crystal size	0.26 x 0.26 x 0.08 mm^3	
Crystal shape	rectangular plate	
Crystal colour	colourless	
Diffractometer	Bruker SMART-CCD	
Data collection method	ω scans	
Theta range for data collection	1.78 to 28.28°.	
Index ranges	-26<=h<=26, -18<=k<=18, -25<=l<=25	
Reflections collected	29740	
Independent reflections	6595 [R(int) = 0.0470]	
Completeness to theta = 28.28°	99.8 %	
Absorption correction	None	
Refinement method	Full-matrix least-squares on F^2	
Data / restraints / parameters	6595 / 0 / 467	
Goodness-of-fit on F^2	1.064	
Final R indices [I>2sigma(I)]	R1 = 0.0543, wR2 = 0.1236	
R indices (all data)	R1 = 0.0762, wR2 = 0.1345	
Largest diff. peak and hole	0.387 and -0.402 $e.Å^{-3}$	

Table 2. Atomic coordinates (x 10^4) and equivalent isotropic displacement parameters ($Å^2$x 10^3) for 3,5-dibenzyl-1-(2,6-difluorobenzoyl)-3-(2,6-difluorobenzoylamino)pyrrolidine-2,4-dione, **70**. U(eq) is defined as one third of the trace of the orthogonalized U^{ij} tensor.

	x	y	z	U(eq)
O(1)	6176(1)	1399(1)	-653(1)	28(1)
O(2)	4206(1)	2430(1)	-150(1)	26(1)
O(3)	5583(1)	4150(1)	-299(1)	25(1)
O(4)	4717(1)	2162(1)	1411(1)	25(1)
N(1)	5738(1)	2566(1)	-5(1)	19(1)
N(2)	4343(1)	3785(1)	457(1)	21(1)
F(1)	7310(1)	3179(1)	-475(1)	69(1)
F(2)	5211(1)	2855(1)	-1715(1)	42(1)
F(3)	2958(1)	3818(2)	902(1)	63(1)
F(4)	3526(1)	3217(1)	-1390(1)	52(1)
C(2)	5479(1)	3474(1)	68(1)	18(1)
C(3)	5029(1)	3499(1)	690(1)	19(1)
C(4)	5032(1)	2456(1)	942(1)	19(1)
C(5)	5525(1)	1884(1)	528(1)	19(1)
C(10)	6065(1)	2234(1)	-583(1)	21(1)
C(11)	6272(1)	2961(1)	-1105(1)	22(1)
C(12)	5845(1)	3230(1)	-1669(1)	24(1)
C(13)	6027(1)	3868(2)	-2166(1)	29(1)
C(14)	6667(1)	4269(2)	-2092(1)	30(1)
C(15)	7112(1)	4041(2)	-1527(1)	40(1)
C(16)	6900(1)	3394(2)	-1047(1)	36(1)
C(20)	3976(1)	3197(1)	20(1)	20(1)
C(21)	3277(1)	3516(1)	-233(1)	22(1)
C(22)	2785(1)	3787(2)	209(1)	38(1)
C(23)	2125(1)	4001(2)	-22(2)	55(1)
C(24)	1949(1)	3960(2)	-726(2)	46(1)
C(25)	2415(1)	3698(2)	-1194(1)	36(1)
C(26)	3065(1)	3469(1)	-937(1)	28(1)
C(30)	5313(1)	4193(1)	1259(1)	21(1)
C(31)	6004(1)	3915(1)	1590(1)	20(1)
C(32)	6600(1)	4097(1)	1256(1)	24(1)
C(33)	7230(1)	3817(2)	1565(1)	31(1)
C(34)	7270(1)	3366(2)	2209(1)	33(1)
C(35)	6681(1)	3190(2)	2546(1)	29(1)

C(36)	6052(1)	3456(1)	2238(1)	23(1)
C(40)	6142(1)	1514(1)	982(1)	21(1)
C(41)	5982(1)	667(1)	1429(1)	19(1)
C(42)	6030(1)	722(2)	2153(1)	30(1)
C(43)	5934(1)	-83(2)	2558(1)	39(1)
C(44)	5796(1)	-944(2)	2241(1)	34(1)
C(45)	5734(1)	-1003(2)	1517(1)	32(1)
C(46)	5822(1)	-202(1)	1118(1)	25(1)

Table 3. Bond lengths [Å] and angles [°] for 3,5-dibenzyl-1-(2,6-difluorobenzoyl)-3-(2,6-difluorobenzoylamino)pyrrolidine-2,4-dione, **70**.

O(1)-C(10)	1.208(2)	C(15)-C(16)	1.380(3)
O(2)-C(20)	1.226(2)	C(15)-H(15)	0.92(3)
O(3)-C(2)	1.210(2)	C(20)-C(21)	1.499(3)
O(4)-C(4)	1.199(2)	C(21)-C(22)	1.383(3)
N(1)-C(2)	1.391(2)	C(21)-C(26)	1.387(3)
N(1)-C(10)	1.399(2)	C(22)-C(23)	1.379(3)
N(1)-C(5)	1.483(2)	C(23)-C(24)	1.371(4)
N(2)-C(20)	1.353(2)	C(23)-H(23)	0.96(4)
N(2)-C(3)	1.452(2)	C(24)-C(25)	1.374(4)
N(2)-H(2N)	0.84(2)	C(24)-H(24)	0.97(3)
F(1)-C(16)	1.353(3)	C(25)-C(26)	1.380(3)
F(2)-C(12)	1.355(2)	C(25)-H(25)	0.95(3)
F(3)-C(22)	1.349(3)	C(30)-C(31)	1.517(3)
F(4)-C(26)	1.346(3)	C(30)-H(302)	0.99(2)
C(2)-C(3)	1.533(3)	C(30)-H(301)	0.98(2)
C(3)-C(30)	1.542(3)	C(31)-C(32)	1.397(3)
C(3)-C(4)	1.550(2)	C(31)-C(36)	1.398(3)
C(4)-C(5)	1.525(3)	C(32)-C(33)	1.396(3)
C(5)-C(40)	1.538(3)	C(32)-H(32)	0.96(2)
C(5)-H(5)	0.98(2)	C(33)-C(34)	1.386(3)
C(10)-C(11)	1.508(3)	C(33)-H(33)	0.96(3)
C(11)-C(12)	1.378(3)	C(34)-C(35)	1.387(3)
C(11)-C(16)	1.380(3)	C(34)-H(34)	0.93(3)
C(12)-C(13)	1.375(3)	C(35)-C(36)	1.390(3)
C(13)-C(14)	1.381(3)	C(35)-H(35)	0.95(3)
C(13)-H(13)	0.92(3)	C(36)-H(36)	0.92(2)
C(14)-C(15)	1.385(3)	C(40)-C(41)	1.516(3)
C(14)-H(14)	0.95(3)	C(40)-H(402)	0.97(2)

C(40)-H(401)	0.96(2)	C(43)-H(43)	0.98(3)
C(41)-C(42)	1.387(3)	C(44)-C(45)	1.387(3)
C(41)-C(46)	1.391(3)	C(44)-H(44)	0.93(3)
C(42)-C(43)	1.395(3)	C(45)-C(46)	1.383(3)
C(42)-H(42)	0.97(3)	C(45)-H(45)	0.89(3)
C(43)-C(44)	1.378(3)	C(46)-H(46)	0.99(2)

C(2)-N(1)-C(10)	125.39(15)	C(12)-C(13)-C(14)	118.4(2)
C(2)-N(1)-C(5)	114.05(15)	C(12)-C(13)-H(13)	118.5(17)
C(10)-N(1)-C(5)	119.58(15)	C(14)-C(13)-H(13)	123.0(17)
C(20)-N(2)-C(3)	117.93(16)	C(13)-C(14)-C(15)	120.7(2)
C(20)-N(2)-H(2N)	120.6(15)	C(13)-C(14)-H(14)	122.2(15)
C(3)-N(2)-H(2N)	119.8(15)	C(15)-C(14)-H(14)	117.1(15)
O(3)-C(2)-N(1)	126.28(17)	C(16)-C(15)-C(14)	118.1(2)
O(3)-C(2)-C(3)	124.20(16)	C(16)-C(15)-H(15)	120.1(18)
N(1)-C(2)-C(3)	109.52(15)	C(14)-C(15)-H(15)	121.7(18)
N(2)-C(3)-C(2)	110.02(15)	F(1)-C(16)-C(11)	116.82(18)
N(2)-C(3)-C(30)	109.17(15)	F(1)-C(16)-C(15)	119.9(2)
C(2)-C(3)-C(30)	111.21(15)	C(11)-C(16)-C(15)	123.3(2)
N(2)-C(3)-C(4)	110.19(15)	O(2)-C(20)-N(2)	120.92(17)
C(2)-C(3)-C(4)	103.25(14)	O(2)-C(20)-C(21)	121.82(17)
C(30)-C(3)-C(4)	112.88(15)	N(2)-C(20)-C(21)	117.26(16)
O(4)-C(4)-C(5)	125.87(16)	C(22)-C(21)-C(26)	115.45(18)
O(4)-C(4)-C(3)	124.74(17)	C(22)-C(21)-C(20)	123.57(18)
C(5)-C(4)-C(3)	109.33(15)	C(26)-C(21)-C(20)	120.72(18)
N(1)-C(5)-C(4)	103.49(14)	F(3)-C(22)-C(23)	118.7(2)
N(1)-C(5)-C(40)	111.08(15)	F(3)-C(22)-C(21)	117.93(19)
C(4)-C(5)-C(40)	113.10(16)	C(23)-C(22)-C(21)	123.3(2)
N(1)-C(5)-H(5)	111.2(13)	C(24)-C(23)-C(22)	118.5(3)
C(4)-C(5)-H(5)	108.1(13)	C(24)-C(23)-H(23)	125(2)
C(40)-C(5)-H(5)	109.7(13)	C(22)-C(23)-H(23)	116(2)
O(1)-C(10)-N(1)	120.79(17)	C(23)-C(24)-C(25)	121.0(2)
O(1)-C(10)-C(11)	122.03(17)	C(23)-C(24)-H(24)	117.3(17)
N(1)-C(10)-C(11)	117.18(16)	C(25)-C(24)-H(24)	121.6(17)
C(12)-C(11)-C(16)	116.06(18)	C(24)-C(25)-C(26)	118.4(2)
C(12)-C(11)-C(10)	122.04(18)	C(24)-C(25)-H(25)	122.3(15)
C(16)-C(11)-C(10)	121.90(18)	C(26)-C(25)-H(25)	119.2(15)
F(2)-C(12)-C(13)	119.56(18)	F(4)-C(26)-C(25)	118.9(2)
F(2)-C(12)-C(11)	117.08(17)	F(4)-C(26)-C(21)	117.89(18)
C(13)-C(12)-C(11)	123.34(19)	C(25)-C(26)-C(21)	123.2(2)

C(31)-C(30)-C(3)	113.96(15)	C(41)-C(40)-C(5)	113.68(15)
C(31)-C(30)-H(302)	111.8(12)	C(41)-C(40)-H(402)	109.6(12)
C(3)-C(30)-H(302)	104.7(12)	C(5)-C(40)-H(402)	108.9(12)
C(31)-C(30)-H(301)	109.5(12)	C(41)-C(40)-H(401)	107.6(14)
C(3)-C(30)-H(301)	108.3(13)	C(5)-C(40)-H(401)	107.6(13)
H(302)-C(30)-H(301)	108.3(18)	H(402)-C(40)-H(401)	109.3(18)
C(32)-C(31)-C(36)	118.90(18)	C(42)-C(41)-C(46)	118.51(17)
C(32)-C(31)-C(30)	121.30(17)	C(42)-C(41)-C(40)	121.23(17)
C(36)-C(31)-C(30)	119.79(17)	C(46)-C(41)-C(40)	120.16(17)
C(33)-C(32)-C(31)	120.27(19)	C(41)-C(42)-C(43)	120.4(2)
C(33)-C(32)-H(32)	118.1(15)	C(41)-C(42)-H(42)	119.9(16)
C(31)-C(32)-H(32)	121.6(15)	C(43)-C(42)-H(42)	119.7(16)
C(34)-C(33)-C(32)	120.3(2)	C(44)-C(43)-C(42)	120.3(2)
C(34)-C(33)-H(33)	120.5(15)	C(44)-C(43)-H(43)	119.5(17)
C(32)-C(33)-H(33)	119.2(15)	C(42)-C(43)-H(43)	120.2(17)
C(33)-C(34)-C(35)	119.8(2)	C(43)-C(44)-C(45)	119.7(2)
C(33)-C(34)-H(34)	121.7(18)	C(43)-C(44)-H(44)	119.9(17)
C(35)-C(34)-H(34)	118.5(18)	C(45)-C(44)-H(44)	120.3(16)
C(34)-C(35)-C(36)	120.3(2)	C(46)-C(45)-C(44)	119.8(2)
C(34)-C(35)-H(35)	121.4(15)	C(46)-C(45)-H(45)	119.8(17)
C(36)-C(35)-H(35)	118.3(15)	C(44)-C(45)-H(45)	120.4(17)
C(35)-C(36)-C(31)	120.48(19)	C(45)-C(46)-C(41)	121.17(19)
C(35)-C(36)-H(36)	119.1(14)	C(45)-C(46)-H(46)	119.2(14)
C(31)-C(36)-H(36)	120.3(14)	C(41)-C(46)-H(46)	119.6(14)

Table 4. Anisotropic displacement parameters ($Å^2 x\ 10^3$) for 3,5-dibenzyl-1-(2,6-difluorobenzoyl)-3-(2,6-difluorobenzoylamino)pyrrolidine-2,4-dione, **70**. The anisotropic displacement factor exponent takes the form: $-2\pi^2[\ h^2\ a^{*2}U^{11} + ... + 2\ h\ k\ a^*\ b^*\ U^{12}\ ]$

	U^{11}	U^{22}	U^{33}	U^{23}	U^{13}	U^{12}
O(1)	36(1)	20(1)	30(1)	2(1)	11(1)	5(1)
O(2)	26(1)	24(1)	29(1)	-4(1)	-1(1)	5(1)
O(3)	37(1)	17(1)	22(1)	4(1)	5(1)	2(1)
O(4)	24(1)	26(1)	24(1)	5(1)	7(1)	1(1)
N(1)	19(1)	16(1)	21(1)	3(1)	3(1)	2(1)
N(2)	20(1)	18(1)	25(1)	0(1)	-1(1)	5(1)
F(1)	25(1)	102(1)	77(1)	67(1)	-18(1)	-15(1)
F(2)	41(1)	48(1)	34(1)	12(1)	-13(1)	-22(1)
F(3)	53(1)	110(2)	26(1)	-2(1)	6(1)	44(1)
F(4)	58(1)	76(1)	21(1)	-2(1)	2(1)	24(1)
C(2)	20(1)	18(1)	17(1)	0(1)	-2(1)	0(1)
C(3)	19(1)	18(1)	18(1)	1(1)	0(1)	3(1)
C(4)	19(1)	19(1)	19(1)	2(1)	-1(1)	1(1)
C(5)	19(1)	17(1)	20(1)	4(1)	3(1)	0(1)
C(10)	19(1)	21(1)	21(1)	3(1)	3(1)	1(1)
C(11)	24(1)	20(1)	22(1)	2(1)	8(1)	5(1)
C(12)	28(1)	24(1)	21(1)	-2(1)	2(1)	-5(1)
C(13)	38(1)	29(1)	20(1)	3(1)	-2(1)	0(1)
C(14)	33(1)	29(1)	30(1)	13(1)	11(1)	4(1)
C(15)	21(1)	45(1)	54(2)	26(1)	4(1)	-1(1)
C(16)	22(1)	43(1)	43(1)	23(1)	1(1)	2(1)
C(20)	22(1)	21(1)	17(1)	2(1)	2(1)	3(1)
C(21)	20(1)	21(1)	25(1)	2(1)	-1(1)	2(1)
C(22)	31(1)	56(2)	27(1)	5(1)	4(1)	14(1)
C(23)	30(1)	82(2)	53(2)	15(2)	10(1)	25(1)
C(24)	25(1)	53(2)	59(2)	20(1)	-7(1)	5(1)
C(25)	37(1)	34(1)	35(1)	7(1)	-16(1)	-5(1)
C(26)	32(1)	24(1)	27(1)	0(1)	-1(1)	2(1)
C(30)	23(1)	20(1)	21(1)	-3(1)	3(1)	2(1)
C(31)	24(1)	16(1)	21(1)	-4(1)	0(1)	-1(1)
C(32)	28(1)	19(1)	25(1)	-3(1)	4(1)	-3(1)
C(33)	24(1)	26(1)	41(1)	-6(1)	3(1)	-3(1)
C(34)	28(1)	27(1)	42(1)	-7(1)	-12(1)	3(1)
C(35)	37(1)	23(1)	26(1)	-1(1)	-8(1)	1(1)

C(36)	28(1)	20(1)	21(1)	-4(1)	1(1)	-2(1)
C(40)	18(1)	19(1)	25(1)	4(1)	1(1)	1(1)
C(41)	15(1)	17(1)	25(1)	5(1)	3(1)	1(1)
C(42)	40(1)	25(1)	26(1)	1(1)	-4(1)	-9(1)
C(43)	51(1)	40(1)	24(1)	9(1)	-4(1)	-14(1)
C(44)	37(1)	25(1)	41(1)	14(1)	5(1)	-3(1)
C(45)	34(1)	18(1)	43(1)	-1(1)	10(1)	-1(1)
C(46)	27(1)	23(1)	26(1)	-1(1)	8(1)	4(1)

Table 5. Hydrogen coordinates (x 10^4) and isotropic displacement parameters ($Å^2$x 10^3) for 3,5-dibenzyl-1-(2,6-difluorobenzoyl)-3-(2,6-difluorobenzoylamino)pyrrolidine-2,4-dione, **70**.

	x	y	z	U(eq)
H(2N)	4220(12)	4349(18)	509(12)	26(6)
H(5)	5274(11)	1348(16)	308(11)	24(6)
H(13)	5714(13)	4014(19)	-2530(14)	42(7)
H(14)	6819(12)	4714(18)	-2416(13)	35(6)
H(15)	7524(16)	4330(20)	-1453(15)	55(8)
H(23)	1820(19)	4160(30)	333(19)	86(12)
H(24)	1488(15)	4150(20)	-882(15)	55(8)
H(25)	2309(13)	3693(17)	-1686(14)	36(7)
H(302)	5327(11)	4811(16)	1019(11)	22(5)
H(301)	4987(11)	4236(15)	1620(11)	22(5)
H(32)	6592(12)	4427(17)	816(13)	34(6)
H(33)	7635(13)	3947(17)	1327(13)	36(7)
H(34)	7684(15)	3170(20)	2423(15)	50(8)
H(35)	6694(12)	2872(18)	2986(13)	36(7)
H(36)	5664(12)	3296(16)	2455(12)	27(6)
H(402)	6322(11)	2023(15)	1278(11)	18(5)
H(401)	6480(12)	1319(16)	671(12)	27(6)
H(42)	6126(14)	1320(20)	2381(14)	48(8)
H(43)	5963(15)	-40(20)	3071(15)	52(8)
H(44)	5732(13)	-1477(19)	2512(14)	43(7)
H(45)	5630(13)	-1554(19)	1307(14)	40(7)
H(46)	5793(12)	-257(16)	600(12)	30(6)

Table 6. Torsion angles [°] for 3,5-dibenzyl-1-(2,6-difluorobenzoyl)-3-(2,6-difluorobenzoylamino)pyrrolidine-2,4-dione, **70**.

C(10)-N(1)-C(2)-O(3)	-11.9(3)	C(16)-C(11)-C(12)-C(13)	2.0(3)
C(5)-N(1)-C(2)-O(3)	179.56(17)	C(10)-C(11)-C(12)-C(13)	-177.88(19)
C(10)-N(1)-C(2)-C(3)	167.84(16)	F(2)-C(12)-C(13)-C(14)	177.40(19)
C(5)-N(1)-C(2)-C(3)	-0.7(2)	C(11)-C(12)-C(13)-C(14)	-0.9(3)
C(20)-N(2)-C(3)-C(2)	65.7(2)	C(12)-C(13)-C(14)-C(15)	-0.6(3)
C(20)-N(2)-C(3)-C(30)	-171.99(16)	C(13)-C(14)-C(15)-C(16)	0.8(4)
C(20)-N(2)-C(3)-C(4)	-47.5(2)	C(12)-C(11)-C(16)-F(1)	176.3(2)
O(3)-C(2)-C(3)-N(2)	59.1(2)	C(10)-C(11)-C(16)-F(1)	-3.8(3)
N(1)-C(2)-C(3)-N(2)	-120.64(16)	C(12)-C(11)-C(16)-C(15)	-1.7(4)
O(3)-C(2)-C(3)-C(30)	-62.0(2)	C(10)-C(11)-C(16)-C(15)	178.1(2)
N(1)-C(2)-C(3)-C(30)	118.28(16)	C(14)-C(15)-C(16)-F(1)	-177.6(2)
O(3)-C(2)-C(3)-C(4)	176.66(17)	C(14)-C(15)-C(16)-C(11)	0.4(4)
N(1)-C(2)-C(3)-C(4)	-3.05(18)	C(3)-N(2)-C(20)-O(2)	2.9(3)
N(2)-C(3)-C(4)-O(4)	-59.7(2)	C(3)-N(2)-C(20)-C(21)	-178.23(16)
C(2)-C(3)-C(4)-O(4)	-177.16(17)	O(2)-C(20)-C(21)-C(22)	124.6(2)
C(30)-C(3)-C(4)-O(4)	62.7(2)	N(2)-C(20)-C(21)-C(22)	-54.2(3)
N(2)-C(3)-C(4)-C(5)	123.12(16)	O(2)-C(20)-C(21)-C(26)	-49.3(3)
C(2)-C(3)-C(4)-C(5)	5.65(18)	N(2)-C(20)-C(21)-C(26)	131.8(2)
C(30)-C(3)-C(4)-C(5)	-114.54(17)	C(26)-C(21)-C(22)-F(3)	178.2(2)
C(2)-N(1)-C(5)-C(4)	4.2(2)	C(20)-C(21)-C(22)-F(3)	4.0(4)
C(10)-N(1)-C(5)-C(4)	-165.06(15)	C(26)-C(21)-C(22)-C(23)	-0.1(4)
C(2)-N(1)-C(5)-C(40)	-117.41(17)	C(20)-C(21)-C(22)-C(23)	-174.3(3)
C(10)-N(1)-C(5)-C(40)	73.3(2)	F(3)-C(22)-C(23)-C(24)	-179.4(3)
O(4)-C(4)-C(5)-N(1)	176.82(18)	C(21)-C(22)-C(23)-C(24)	-1.1(5)
C(3)-C(4)-C(5)-N(1)	-6.03(18)	C(22)-C(23)-C(24)-C(25)	0.9(5)
O(4)-C(4)-C(5)-C(40)	-62.9(2)	C(23)-C(24)-C(25)-C(26)	0.5(4)
C(3)-C(4)-C(5)-C(40)	114.26(16)	C(24)-C(25)-C(26)-F(4)	-179.7(2)
C(2)-N(1)-C(10)-O(1)	-167.99(18)	C(24)-C(25)-C(26)-C(21)	-1.8(3)
C(5)-N(1)-C(10)-O(1)	0.0(3)	C(22)-C(21)-C(26)-F(4)	179.4(2)
C(2)-N(1)-C(10)-C(11)	12.2(3)	C(20)-C(21)-C(26)-F(4)	-6.2(3)
C(5)-N(1)-C(10)-C(11)	-179.81(16)	C(22)-C(21)-C(26)-C(25)	1.6(3)
O(1)-C(10)-C(11)-C(12)	90.5(2)	C(20)-C(21)-C(26)-C(25)	175.9(2)
N(1)-C(10)-C(11)-C(12)	-89.7(2)	N(2)-C(3)-C(30)-C(31)	174.76(16)
O(1)-C(10)-C(11)-C(16)	-89.4(3)	C(2)-C(3)-C(30)-C(31)	-63.7(2)
N(1)-C(10)-C(11)-C(16)	90.4(2)	C(4)-C(3)-C(30)-C(31)	51.9(2)
C(16)-C(11)-C(12)-F(2)	-176.32(19)	C(3)-C(30)-C(31)-C(32)	79.6(2)
C(10)-C(11)-C(12)-F(2)	3.8(3)	C(3)-C(30)-C(31)-C(36)	-99.5(2)

C(36)-C(31)-C(32)-C(33)	0.4(3)
C(30)-C(31)-C(32)-C(33)	-178.68(18)
C(31)-C(32)-C(33)-C(34)	-0.7(3)
C(32)-C(33)-C(34)-C(35)	0.2(3)
C(33)-C(34)-C(35)-C(36)	0.6(3)
C(34)-C(35)-C(36)-C(31)	-1.0(3)
C(32)-C(31)-C(36)-C(35)	0.4(3)
C(30)-C(31)-C(36)-C(35)	179.53(18)
N(1)-C(5)-C(40)-C(41)	-167.68(15)
C(4)-C(5)-C(40)-C(41)	76.5(2)
C(5)-C(40)-C(41)-C(42)	-115.4(2)
C(5)-C(40)-C(41)-C(46)	68.3(2)
C(46)-C(41)-C(42)-C(43)	1.5(3)
C(40)-C(41)-C(42)-C(43)	-174.9(2)
C(41)-C(42)-C(43)-C(44)	0.5(4)
C(42)-C(43)-C(44)-C(45)	-1.8(4)
C(43)-C(44)-C(45)-C(46)	1.0(3)
C(44)-C(45)-C(46)-C(41)	1.0(3)
C(42)-C(41)-C(46)-C(45)	-2.3(3)
C(40)-C(41)-C(46)-C(45)	174.18(18)

Appendix VII

Published papers

The preferred conformation of α-fluoroamides

John W. Banks,[a] Andrei S. Batsanov,[b] Judith A. K. Howard,[b] David O'Hagan,*[b] Henry S. Rzepa[c] and Sonsoles Martin-Santamaria[c]

[a] *Chemical Technology Department, Searle, Division of Monsanto, Whalton Rd., Morpeth, UK NE61 3YA*
[b] *Department of Chemistry, University of Durham, Science Laboratories, South Road, Durham, UK DH1 3LE. E-mail: David.O'Hagan@durham.ac.uk*
[c] *Department of Chemistry, Imperial College of Science, Technology and Medicine, London, UK SW7 2AY*

Received (in Cambridge, UK) 14th September 1999, Accepted 24th September 1999

X-Ray structures of two α-fluoroamide derivatives show the O=C–C–F moiety tending towards a *trans* planar conformation, for which *ab initio* calculations suggest a deep (up to 8 kcal mol^{-1}) potential minimum.

Fluorine substituents can have profound stereoelectronic and polar effects[1] on the conformation of organic molecules, *e.g.* the *gauche* effect in 1,2-difluoroethane[2] or the fluorine anomeric effect in α-fluoroethers.[3] With *one* fluorine substituent in the α-position to a carbonyl group, as in α-fluoroaldehydes,[4] α-fluoroketones[5] and α-fluoroesters,[6] the preferred conformation of the O=C–C–F moiety is *trans*-planar, but the energy difference between *cis* and *trans*-conformations is rather small (0.8–2.0 kcal mol^{-1}). For fluoroacetamide FCH_2CONH_2, MO calculations[7] suggest a much bigger difference, 7.5 kcal mol^{-1} in favour of the *trans*-disposition of the F and O atoms, which was actually found by X-ray[8] and neutron[7] diffraction studies (it is noteworthy that the parent acetamide adopts an entirely different conformation[9]). It could be expected therefore that introduction of an α-fluorine substituent into a substituted amide will stabilise the N–C(O)–C–F moiety in the conformation with the F atoms *trans* to the carbonyl and *cis* to the NH group. To verify this, we undertook the synthesis and X-ray structural and theoretical studies of mono-fluorinated compounds **1a** and **2**, and of non-fluorinated **1b** for comparison.†

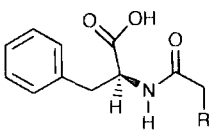

1a R = F

1b R = Me

N-Fluoroacetyl-(*S*)-phenylalanine **1a**, the first *N*-fluoroacylated amino acid derivative, was prepared by coupling (*S*)-phenylalanine with the acid chloride of monofluoroacetic acid FCH_2COCl, and **1b** respectively with C_2H_5COCl. The X-ray structure of **1a** (Fig. 1) shows the C–F bond oriented nearly *cis* to the N–H and *trans* to the C=O bond, with the N(1)C(4)C(5)F torsion angle of −16.0(2)°. The entire HO_2C–C–NH–C(=O)–C–F moiety is roughly planar, with the torsion angles O(2)-C(1)C(2)N(1) −9.2(2)° and C(1)C(2)N(1)C(4) −162.2(1)°, compared to 151.6(2)° and −58.9(3)°, respectively, in **1b**. Thus, while in **1b** both the carboxy and the amide protons participate in *inter*molecular hydrogen bonds (Fig. 2), in **1a** only the former does, while H(1N) forms a bifurcated intramolecular hydrogen bond with F and O(2), at distances H ··· F 2.27(2) and H ··· O 2.29(2) Å.

α-Fluoropropionamide **2** was then studied, to establish whether the *trans* conformation is affected when a substituent is

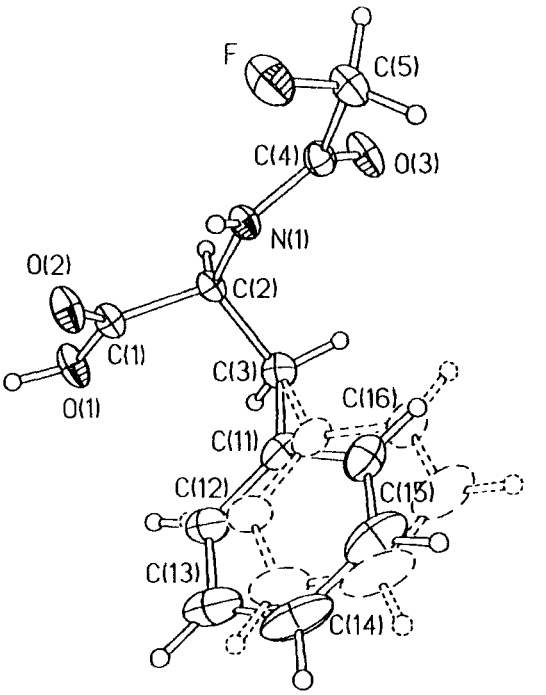

Fig. 1 Molecular structure of **1a** (50% thermal ellipsoids) showing disorder in the phenyl group.

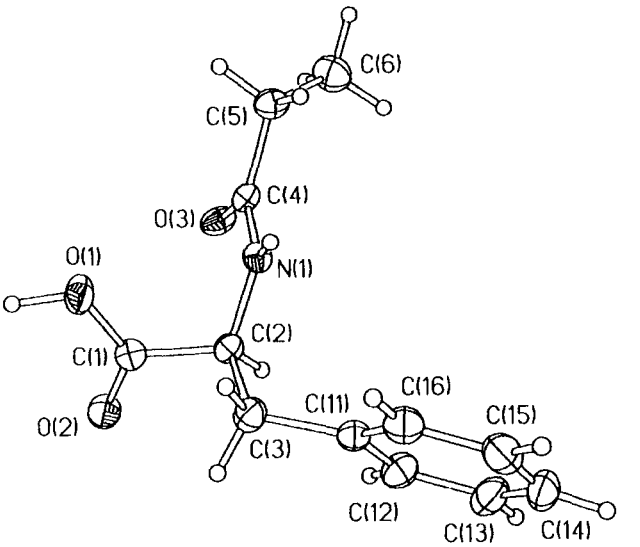

Fig. 2 Molecular structure of **1b**.

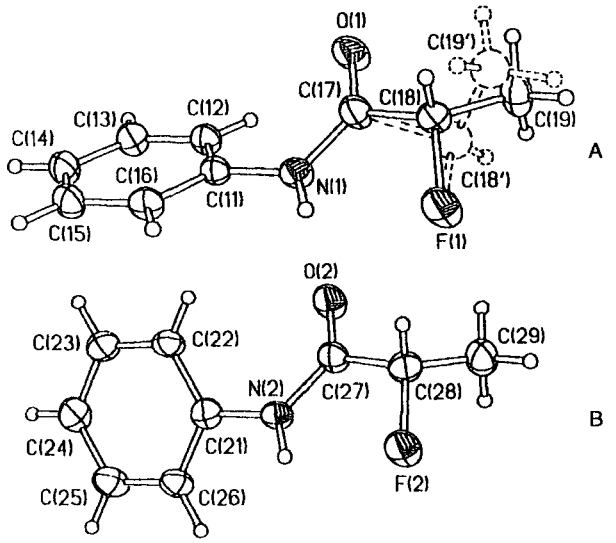

Fig. 3 An asymmetric unit in the structure of **2**, containing *S* (solid) and *R* (dashed) isomers.

attached to the fluoromethyl group. This amide **2** was prepared from (*S*)-alanine by a diazotisation reaction in the presence of hydrogen fluoride–pyridine[10,11] (see Scheme 1), whereby the

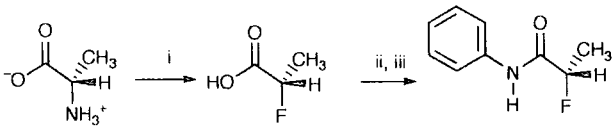

Scheme 1 i, $NaNO_2$, HF·pyridine (83%); ii, $SOCl_2$ (61%); iii, aniline (17%).

amino group is substituted by fluorine with predominant retention of the absolute configuration. The resultant α-fluoropropionic acid **3** comprised 90% of the (*S*) and 10% of the (*R*) enantiomer, as was assessed according to a previously described technique,[12] by ^{19}F NMR of its complex with a chiral base. By treating **3** with thionyl chloride, it was converted to its acid chloride, which was then coupled to aniline to generate **2**, which was characterised by its X-ray crystal structure.

The asymmetric unit of **2** (Fig. 3) contains two molecular sites, one of which (A) is occupied by 79(1)% of (*S*)-**2** and 21(1)% of (*R*)-**2** and the other (B) by the (*S*)-isomer only. Thus the overall (*S*/*R*) enantiomeric composition is *ca.* 9:1, in accordance with the NMR data. Molecule B retains the *anti* planar orientation of the C–F and C=O bonds, with the N–C(O)–C–F torsion angle of 9.9(4)°. At site A, this angle is increased to 24.5(5)° for the major (*S*) component and −35(1)° for the minor (*R*) one. This conformational distortion may be due to the peculiar crystal packing, required to accommodate both enantiomers at the same crystal site. Each molecule is linked with its own translational (along the *x* direction) equivalents by N–H···O hydrogen bonds of equal strength.

An *ab initio* analysis of *N*-methyl-2-(*S*)-fluoropropionamide **4** was carried out at the B3LYP/6-31G*(d) level using the

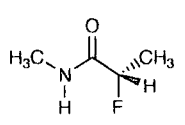

4

GAUSSIAN98 program,[13] in order to quantify the dependence of the conformation on the F–C–C=O torsion angle (τ). The calculated energy profile (Fig. 4) shows a single distinct minimum at τ = 180° (C–F and N–H bonds eclipsed), the maximum at τ = 300° and a plateau at about τ = 60°. The maximum is due

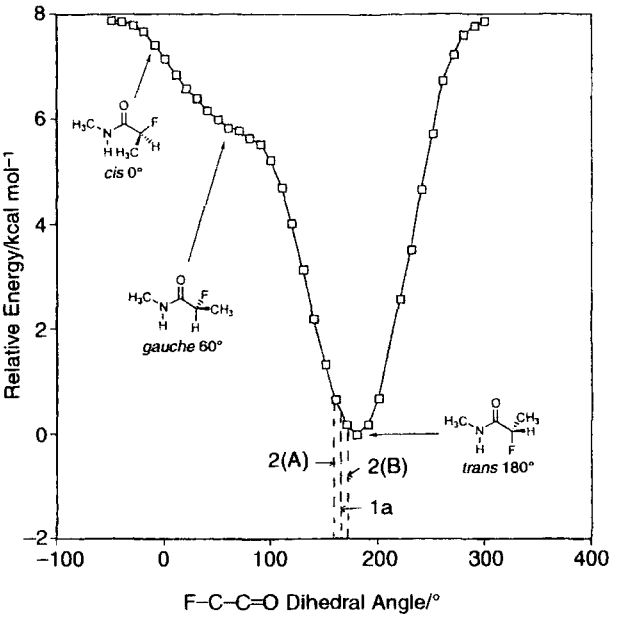

Fig. 4 Rotational energy profile of *N*-methyl-2-fluoropropionamide **4** monitoring rotation around the C–C(O) bond. *Ab initio* calculations were carried out at the B3LYP/6-31G*(d) level. Energies of conformations **1a** and **2** are indicated in the profile.

to H···H steric repulsions when the methyl group approaches N–H, the preferred methyl group location being in the hemisphere proximate to the carbonyl group. The plateau indicates some stabilisation of the *gauche* conformation, in which the C–H bond eclipses N–H. It is noteworthy that fluoroacetamide[7] shows a distinct potential minimum for this conformation, second deepest after that at τ = 180°. The energy difference of *ca.* 7 kcal mol^{-1} between the *cis* (τ = 0) and *trans* (τ = 180°) conformers of **4** is similar to that in fluoroacetamide (7.5 kcal mol^{-1}) and at least four times greater in the other α-fluorocarbonyl systems studied earlier.[4–6] The stabilisation of the *trans* conformer is due mainly to the interaction between fluorine lone pairs and the N–H σ* orbital, which contributes 3.1 kcal mol^{-1}, according to NBO analysis[14] of the interaction energies. The rest of the energy difference is due to minor effects, *viz.* a greater interaction in the *trans* conformation between the C–F σ orbital and both the antiperiplanar C=O σ* orbital (1 kcal mol^{-1}) and the antiperiplanar methyl C–H σ* orbital (1 kcal mol^{-1}). The *trans* conformer also has the smaller dipole moment (2.1 D) since the C=O and C–F bond dipoles are opposed, compared to 4.8 D in the *cis* conformer where they re-inforce the charge separation.

It is important that the fluorine effect can *not* be explained simply by formation of an intramolecular hydrogen bond N–H···F, although the H(1N)···F distance observed in **1a** is typical for such bonds.[15,16] A survey of structural data[15,16] shows that a F atom bonded to carbon (in contrast with 'inorganic' fluorine) forms weak hydrogen bonds, *e.g.* 2.4 kcal mol^{-1} for $H_3CF\cdots HOH$ *vs.* 5 to 10 kcal mol^{-1} for H···O bonds.[15]

In general it has proven very difficult to prepare peptides containing α-fluorinated substituents within the amino acid residues, although there have been some limited successes[17,18] but clearly if synthetic methods were developed the current observations suggest that the substitution of the C–F bond into peptides could perhaps offer a valuable tool for controlling peptide conformation.

Notes and references

† X-Ray diffraction experiments on a Rigaku AFC6S 4-circle diffractometer (Cu-Kα radiation) for **1b** and **2**, SMART 1K CCD area detector diffractometer (Mo-Kα radiation) for **1a**; structure solution (direct methods) and least squares refinement (against F^2 of all data) with

SHELXTL software (G. M. Sheldrick, Bruker Analytical X-ray Systems, Madison, Wisconsin, USA, 1997). CCDC reference number 188/188.

1a: $C_{11}H_{12}FNO_3$, $M = 225.22$, $T = 120$ K, orthorhombic, space group $P2_12_12$ (No. 18), $a = 9.366(1)$, $b = 16.003(2)$, $c = 7.598(1)$ Å, $U = 1138.8(1)$ Å^3, $Z = 4$, $D_x = 1.314$ g cm^{-3}, $\bar{\lambda} = 0.71073$ Å, $\mu = 0.11$ mm^{-1}, 8013 reflections (2596 unique) with $2\theta \leq 55°$, 192 variables refined to $R = 0.032$ [2497 data, $I \geq 2\sigma(I)$], $wR(F^2) = 0.080$, $\Delta\rho_{max,min} = 0.19$, -0.24 e Å^{-3}. The phenyl ring disorder was rationalised as two positions (differing by an 18° libration) with 50% occupancies, which were refined with restraints to regular hexagonal ring and equal anisotropic ADP for two positions of each atom.

1b: $C_{12}H_{15}NO_3$, $M = 221.25$, $T = 150$ K, orthorhombic, space group $P2_12_12_1$ (No. 19), $a = 5.754(2)$, $b = 8.139(2)$, $c = 24.873(2)$ Å, $U = 1164.9(4)$ Å^3, $Z = 4$, $D_x = 1.262$ g cm^{-3}, $\bar{\lambda} = 1.54184$ Å, $\mu = 0.75$ mm^{-1}, 1899 reflections (1597 unique) with $2\theta \leq 150°$, 172 variables refined to $R = 0.036$ [1417 data, $I \geq 2\sigma(I)$], $wR(F^2) = 0.084$, $\Delta\rho_{max,min} = 0.15$, -0.15 e Å^{-3}. The absolute configuration was confirmed by anomalous scattering: Flack parameter $-0.16(33)$.

2: $C_9H_{10}FNO$, $M = 167.18$, $T = 150$ K, triclinic, space group $P1$ (No. 1), $a = 5.367(1)$, $b = 8.821(4)$, $c = 9.893(3)$ Å, $\alpha = 106.65(2)$, $\beta = 101.84(2)$, $\gamma = 105.13(2)°$, $U = 412.8(2)$ Å^3, $Z = 2$, $D_x = 1.345$ g cm^{-3}, $\bar{\lambda} = 1.54184$ Å, $\mu = 0.87$ mm^{-1}, 1582 unique reflections with $2\theta \leq 150°$, 236 variables refined to $R = 0.043$ [1482 data, $I \geq 2\sigma(I)$], $wR(F^2) = 0.154$, $\Delta\rho_{max,min} = 0.22$, -0.29 e Å^{-3}. The absolute configuration was confirmed by anomalous scattering: Flack parameter 0.0(2).

1 D. O'Hagan and H. S. Rzepa, *Chem. Commun.*, 1997, 645.
2 N. C. Craig, A. Chen, K. H. Suh, S. Klee, G. C. Mellau, B. P. Winnewisser and M. Winnewisser, *J. Am. Chem. Soc.*, 1997, **119**, 4789.
3 H. Senderowitz, P. Aped and B. Fuchs, *Tetrahedron*, 1993, **49**, 3879.
4 H. V. Phan and J. R. Durig, *J. Mol. Struct. (THEOCHEM)*, 1990, **209**, 333.
5 R. J. Abraham, A. D. Jones, M. A. Warne, R. Rittner and C. T. Tormena, *J. Chem. Soc., Perkin Trans. 2*, 1966, 533.
6 B. J. van der Veken, S. Truyen, W. A. Herrebout and G. Watkins, *J. Mol. Struct.*, 1993, **293**, 55.
7 D. O. Hughes and R. W. H. Small, *Acta Crystallogr.*, 1962, **15**, 933.
8 G. A. Jeffrey, J. R. Ruble, R. K. McMullan, D. J. DeFrees and J. A. Pople, *Acta Crystallogr., Sect. B*, 1981, **37**, 1885.
9 G. A. Jeffrey, J. R. Ruble, R. K. McMullan, D. J. DeFrees, J. S. Binkley and J. A. Pople, *Acta Crystallogr., Sect. B*, 1980, **36**, 2292.
10 G. A. Olah, G. K. S. Prakash and Y. L. Chao, *Helv. Chim. Acta.*, 1981, **64**, 2528.
11 J. Barber, R. Keck and J. Retey, *Tetrahedron Lett.*, 1982, **23**, 1549.
12 D. J. Bailey, D. OHagan and M. Tavasli, *Tetrahedron: Asymmetry*, 1997, **8**, 149.
13 GAUSSIAN98; M. J. Frisch, G. W. Trucks, H. B. Schlegel, G. E. Scuseria, M. A. Robb, J. R. Cheeseman, V. G. Zakrzewski, J. A. Montgomery, R. E. Stratmann, J. C. Burant, S. Dapprich, J. M. Millam, A. D. Daniels, K. N. Kudin, M. C. Strain, O. Farkas, J. Tomasi, V. Barone, M. Cossi, R. Cammi, B. Mennucci, C. Pomelli, C. Adamo, S. Clifford, J. Ochterski, G. A. Petersson, P. Y. Ayala, Q. Cui, K. Morokuma, D. K. Malick, A. D. Rabuck, K. Raghavachari, J. B. Foresman, J. Cioslowski, J. V. Ortiz, B. B. Stefanov, G. Liu, A. Liashenko, P. Piskorz, I. Komaromi, R. Gomperts, R. L. Martin, D. J. Fox, T. Keith, M. A. Al-Laham, C. Y. Peng, A. Nanayakkara, C. Gonzalez, M. Challacombe, P. M. W. Gill, B. G. Johnson, W. Chen, M. W. Wong, J. L. Andres, M. Head-Gordon, E. S. Replogle and J. A. Pople, Gaussian, Inc., Pittsburgh, PA, 1998.
14 A. E. Reed, L. A. Curtis and F. Weinhold, *Chem. Rev.*, 1988, **88**, 899.
15 J. A. K. Howard, V. J. Hoy, D. O'Hagan and G. T. Smith, *Tetrahedron*, 1996, **52**, 12613.
16 J. D. Dunitz and R. Taylor, *Chem. Eur. J.*, 1997, **3**, 89.
17 Y. Takeuchi, M. Nabetani, K. Takagi, T. Hagi and T. Koizumi, *J. Chem. Soc., Perkin Trans. 1*, 1991, 49.
18 P. D. Bailey, A. N. Boa, G. A. Crofts, M. van Diepen, M. Halliwell, R. E. Gammon and M. J. Harrison, *Tetrahedron Lett.*, 1989, **30**, 7457.

Communication 9/07452J

ELSEVIER

Journal of Fluorine Chemistry 102 (2000) 235–238

JOURNAL OF FLUORINE CHEMISTRY

www.elsevier.com/locate/jfluchem

The enzymatic resolution of an α-fluoroamide by an acylase

John W. Banks[a], David O'Hagan[b,*]

[a]*Chemical Technology Department, Searle, Division of Monsanto, Whalton Rd., Morpeth, NE61 3YA, UK*
[b]*Department of Chemistry, Science Laboratories, University of Durham, South Road, Durham, DH1 3LE, UK*

Received 30 June 1999; received in revised form 19 July 1999; accepted 3 August 1999

Dedicated to Professor Paul Tarrant on the ocassion of his 85th birthday

Abstract

The acylase from *Aspergillus melleus* was able to hydrolyse the amide bond of (*S*)-phenylalanine-*N*-2-(*R,S*)-fluoropropionamide and discriminate the diastereoisomers such that the (*S,S*)-diastereoisomer was hydrolysed by an order of magnitude faster than the (*S,R*)-diasteroisomer. The origin of the kinetic discrimination is attributed to both binding and kinetic effects.

Keywords: ^{19}F-NMR; Acylase; Aspergillus melleus, α-fluoroamide; Enzyme resolution

It is part of the culture of bio-organic chemistry that the fluorine atom is considered to have a steric influence just slightly greater than that of a hydrogen atom [1]. However, electronically fluorine and hydrogen are clearly very different. It is also part of the culture of bio-organic chemistry that lipase and acylase enzymes distinguish substrates through binding interactions which are largely steric in nature. Steric models for the common hydrolytic enzymes have been developed where 'small', 'medium' and 'large' pockets have been identified which define the chirality of the preferred enantiomer of a given substrate enantiomer [2,3]. In general, these models have served well as predictive tools. On the other hand, if an α-fluoroester or α-fluoroamide is presented as a substrate to a hydrolytic enzyme, then the compound is chiral by virtue of the substitution of a hydrogen by a fluorine. It is now not so obvious, on the basis of established steric models, to predict the outcome of such a kinetic resolution, as the fluorine and hydrogen are both 'small' and a distinction based on steric considerations cannot be made, which predicts how these groups will best fit the enzyme surface.

Examples of successful kinetic resolutions with α-fluoroesters are rare [4,5], however, the following one [4] serves to illustrate that certain enzymes can distinguish fluorine and hydrogen at the stereogenic centre.

Lipase P30 was able to selectively hydrolyse the (*S*)-enantiomer of ethyl 2-fluorohexanoate over the (*R*)-enantiomer and on work up the (*R*)-ester was isolated in 99% ee after 60% conversion, as illustrated in Fig. 1. Such a discrimination cannot easily be accounted for on the basis of a steric difference between hydrogen and fluorine, and we have previously suggested that a stereo-electronic effect is responsible for this discrimination [1,6]. The enzyme attacks the ester, via a serine alkoxide nucleophile and becomes acylated. The preferred transition state has the serine alkoxide attacking the carbonyl *anti* to the vicinal fluorine atom. The overlap of the C–F σ* orbital with the carbonyl LUMO stabilises this molecular orbital in transition state A relative to transition state B, and the electron density of the serine nucleophile can donate into the C–F σ* orbital only in transition state A, lowering the energy of *anti* approach to the fluorine atom. Also, the electrostatic repulsion between F and O^- is minimised in transition state A. Calculations suggest up to a 2.5 kcal mol^{-1} difference in the energy of these transition states, and there is a sufficient energy difference to account for the observed kinetic resolution.

In this paper, we report the first study on the enzymatic resolution of an α-fluoroamide with an acylase. We were led to this investigation after a recent evaluation of the preferred conformation of *N*-alkyl α-fluoropropionamides [7]. A number of years ago, both electron [8] and neutron diffraction [9] analyses have demonstrated that the major conformer of monofluoroacetamide ($FCH_2C(O)NH_2$) has the C–F bond *anti* to the C=O bond and *syn* to the N–H bond of the amide in the solid state as illustrated in Fig. 2. The energy difference between this and the next favoured *syn* conformation was calculated to be 7.5 kcal mol^{-1}. In our recent

* Corresponding author. Tel.: +44-191-374-2000.
E-mail address: david.o'hagan@durham.ac.uk (D. O'Hagan).

0022-1139/00/$ – see front matter
PII: S0022-1139(99)00284-5

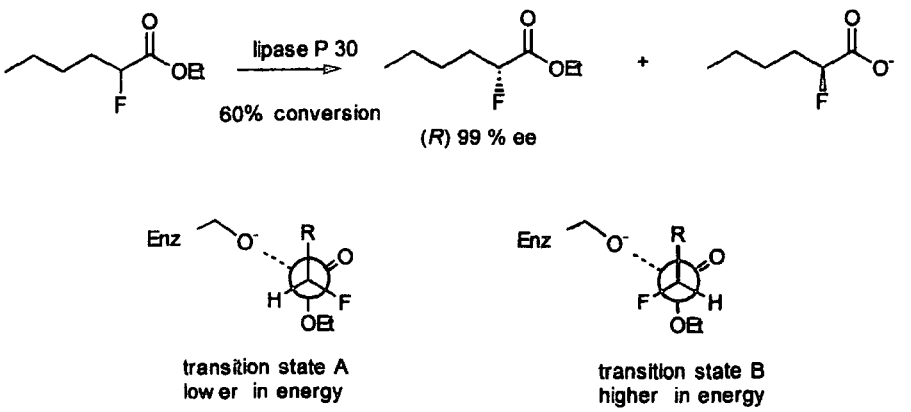

Fig. 1. Rationale for the stereoselectivity observed during the lipase mediated hydrolysis of a racemic α-fluoroester.

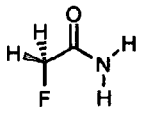

preferred conformation has
C-F and C=O *anti* planar

Fig. 2. Conformation of fluoroacetamide.

study [7], we have investigated the preferred conformation of *N*-alkyl α-fluoropropionamides by both X-ray crystallography and *ab initio* calculations. It is found that the *trans* conformation is again favoured in the solid state for these amides where the C–F bond lies *anti* to the C=O bond as shown in Fig. 3. Calculations revealed that this was the only minimum on the rotational energy profile (around the FC–C(O) bond) and that the barrier to rotation was large at 8.0 kcal mol^{-1}. The fluorine atom and not the methyl group dictates the conformation of these amides.

It follows that with such a conformational preference, where the C–F and N–H bonds are *syn* and co-planar, enantiomers of α-fluoropropionamides will necessarily have to locate their methyl groups in opposite spacial locations around the stereogenic centre (Fig. 3). This is anticipated to impose significantly different diastereomeric interactions during the binding of such enantiomers to an enzyme. With this in mind, we have synthesised (*S*)-phenylalanine *N*-(*R*,*S*)-2-fluoropropionamide as a substrate for acylase hydrolysis as shown in Scheme 1.

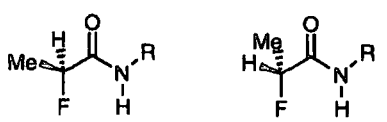

enantiomers of α -fluoropropionamides have preferred conformations with C-F and C=O *anti* planar which dictates the location of the Me

Fig. 3. Conformation of α-fluoropropionamides.

This substrate was chosen as the diastereoisomers are distinguised only by the fluorine atom at the stereogenic centre. Incubation of this substrate with the acylase from *Aspergillus melleus* resulted in a slow hydrolysis. The relative rates of hydrolysis of the two diastereoisomers could be followed analytically, in a very straightforward manner by ^{19}F-NMR, as each diastereoisomer had a unique and resolvable ^{19}F-NMR resonance ((*S*,*S*) −182.1 ppm and (*S*,*R*) −181.67 ppm). The enzymatic reaction was monitored through time in an NMR tube, and the rate slowed down considerably as the reaction approached 50% conversion. The reaction was stopped at 57% conversion where the ratio of isomers was 98 : 2, representing a diastereomeric excess of the residual substrate of 96% de. The major diastereoisomer was (*S*,*R*), the diastereoisomer which is hydrolysed more slowly by the enzyme (Scheme 2).

In order to gain some insight into the origin of the observed selectively, Km and V_{max} data for each diastereoisomer were obtained in separate experiments. This required the preparation of each diastereomer in an enantiomerically enriched form. This was achieved by preparing (*S*)- and (*R*)-2-fluoropropionic acids directly from (*S*)- and (*R*)-alanines by diazotisation and *in situ* treatment with HF-pyridine [10]. The diazotisation reaction is reported to proceed with predominant retention of configuration [11,12]. In the event, it emerged that the product 2-fluoropropionic acids were generated in an enantiomeric excess of 80% ee from the enantiomerically pure alanines. This enantioselectivity was established by recording ^{19}F-NMR of (*S*)-2-(diphenylmethyl)pyrrolidine salts of the resultant

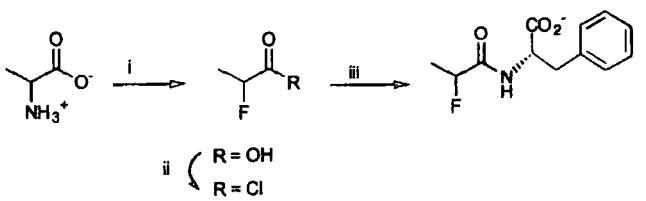

Scheme 1. (i) $NaNO_2$, HF pyridine, 14%; (ii) $SOCl_2$, 83%; (iii) Aq. NaOH, 16%.

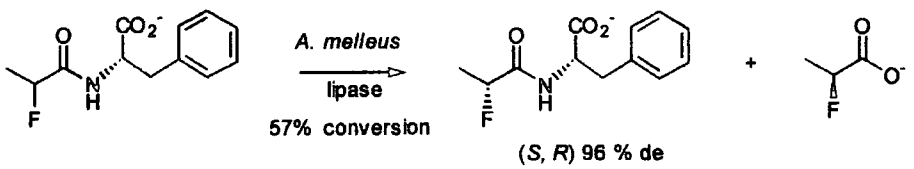

Scheme 2

2-fluoropropionic acids in $CDCl_3$ [13]. The enantiomerically enriched 2-fluoropropionic acids were converted to their acid chlorides after treatment with thionyl chloride and were then coupled directly to (*S*)-phenylalanine. This generated diastereomerically enriched compounds of 80% de, a value which was readily determined by integration of the two fluorine signals in the ^{19}F-NMR spectrum, associated with each diastereoisomer. In the case of the (*S,R*) stereoisomer, the material was stereochemically purified by an initial short bio-transformation with the *A. melleus* acylase, to hydrolyse the 10% (*S,S*) isomer and the diastereomerically pure (*S,R*) substrate was recovered as its sodium salt. The (*S,R*) stereoisomer was enantiomerically pure within the limits of ^{19}F-NMR detection. For the (*S,R*) stereoisomer, improvement of the 80% de was not so readily achievable and this material was used directly for the kinetic study (Table 1).

Initial reaction rates (v) at different substrate concentrations [S] were determined by ^{19}F-NMR analysis, and then plotted as Lineweaver–Burke plots ($1/v$ versus $1/[S]$) to determine V_{max} and Km for each substrate [14]. It emerged that the (*S,S*) substrate has a Km of 16.26 mM and a V_{max} of 0.92 mM min^{-1}, whereas the (*S,R*) substrate had a Km of 40.34 mM and a V_{max} of 0.20 mM min^{-1}. Km is a measure of substrate binding and V_{max} a measure of the rate of product formation (enzyme-substrate complex breakdown). The overall efficiency of the enzyme for each substrate can be estimated by comparing V/K values for each substrate. These values emerge as $V/K = 0.0566$ for the (*S,S*) substrate, and $V/K = 0.005$ for the (*S,R*) substrate. The study predicts one order of magnitude difference in the rates of hydrolysis in favour of the (*S,S*) substrate and the experimental value of 96% de for the residual (*S,R*) diastereoisomer in the previous study is consistent with this analysis. The Km values reveal that there is a differential binding affinity of the substrates by the *A. melleus* lipase. Also the V_{max} values indicate a differential rate of product formation, which is perhaps related to the relative rates of enzyme acylation/deacylation.

Table 1
Kinetic parameters for the hydrolysis of (*S*)-phenylalanine-*N*-2-fluoropropionamides with *Aspergillus melleus*. The data are an average of two separate studies in each case

Substrate diastereomer	Km (mM)	V_{max} (mM min^{-1})	V/K
(*S,S*)[a]	16.26 ± 1.84	0.92 ± 0.07	0.0566
(*S,R*)	40.34 ± 3.21	0.20 ± 0.02	0.0050

[a] 80% de.

In summary, the *A. melleus* lipase can mediate an efficient kinetic resolution between diastereoisomers of (*S*)-phenylalanine-*N*-(*R,S*)-2-fluoropropionamide. Although, acylases have hardly been explored in such reactions, this initial study suggests that they offer an excellent method for preparing enantiomerically enriched 2-fluorocarboxylic acids and amides. The preferred conformation of such amides, where the C–F and C=O bonds orientate *anti* to each other, predicts a discernable binding difference between the enzyme and each diastereomeric substrate. Although, the data reveal that both substrates have Km values in the high mM range, and are poor binders, a two fold difference in binding affinity emerges. Perhaps less obviously, the V_{max} data revealed a four fold difference between the diastereoisomers, and reflects the difference in the rate of product formation (or enzyme-substrate breakdown). Perhaps this latter difference lies in off-loading the 2-fluoroacyl ester-enzyme complex by nucleophilic attack by water, a process which should be susceptible to the stereoelectronic effect discussed above for the lipase hydrolysis of α-fluoroesters [1,6].

The overall kinetic profile of such enzyme resolutions are complex and difficult to deconstruct as there are various factors operating at different stages along the enzyme reaction course, however, it emerges from this study that conformational and stereoelectronic effects can combine to result in highly stereoselective enzymatic resolutions with mono-fluorinated ester and amide substrates.

1. Experimental

FTIR spectra were recorded on a Nicolet Magna IR 550 Spectrometer. NMR spectra were obtained on a Jeol EX 270 MHz spectrometer in $CDCl_3$ or D_2O. Chemical shifts are quoted relative to TMS for ^{1}H- and ^{13}C-NMR spectra and ^{19}F-NMR chemical shifts are quoted as negative relative to fluorotrichloromethane. Solvents were dried and distilled prior to use. Reactions requiring anhydrous conditions were carried out under an atmosphere of nitrogen.

1.1. Preparation of (R,S)-2-fluoropropanoic acid

(*R,S*)-Alanine, (8.6 g, 96 mmol) was added to a stirred solution of pyridinium hydrogen fluoride (100 ml, 70% w/w) in a Teflon bottle. The solution was cooled to 0°C and

sodium nitrite (22.6 g, 232 mmol) was added in five equal portions over 1 h. The reaction mixture was stirred at 0°C for 1 h and was then warmed to room temperature and then stirred overnight. The reaction was quenched by addition to ice water (100 ml). The aqueous solution was extracted into diethylether (3 × 100 ml), washed with sodium chloride solution (3 × 100 ml, 5% w/v) and dried over anhydrous sodium sulphate. The organics were filtered and the solvent was evaporated. The residue was distilled (50°C, 23 mbar) to afford the product (1.4 g, 14%) as a colourless oil. δ_H(270 MHz, $CDCl_3$) 5.12 (1H, dq, *J* 48.5, 6.9, CFH), 1.61 (3H, dd, *J* 23.5, 6.9, Me); δ_C(67.9 MHz, $CDCl_3$) 85.1 (d, *J* 182.7), 18.2 (d, *J* 22.3); δ_F(254.2 MHz, $CDCl_3$) −184.76 (dq, *J* 48.3, 23.5, CFH).

1.2. Preparation of (R,S)-2-fluoropropanoyl chloride

Thionyl chloride, (2.8 g, 23.5 mmol) was added dropwise to heat (*R,S*)-2-fluoropropanoic acid, (1.00 g, 10.9 mmol) at room temperature. The reaction was heated to reflux for 60 min and a sample removed for ^{1}H- and ^{19}F-NMR analysis to confirm the absence of starting material. The product was distilled (bp. 56°C) directly from the reaction mixture at atmospheric pressure to give the product as a colourless oil (1.0 g, 83%). δ_H(270 MHz, $CDCl_3$) 5.14 (1H, dq, *J* 48.6, 7.0, CFH), 1.66 (3H, dd, *J* 22.8, 6.8, Me); δ_C(67.9 MHz, $CDCl_3$) 172.5 (d, *J* 27.9), 90.3 (d, *J* 194.5), 17.6 (d, *J* 21.9); δ_F(254.2 MHz, $CDCl_3$) −171.4 (dq, *J* 49.1, 23.0, CFH).

1.3. Preparation of (S)-phenylalanine-N-2-(R,S)-fluoropropionamide

(*S*)-Phenylalanine (2.63 g, 16 mmol) was dissolved in 4 M NaOH (12 ml, 48 mmol). The reaction was cooled to 0°C and (*R,S*)-2-fluoropropanoyl chloride (1.6 g, 14 mmol) was added dropwise. The reaction was warmed to room temperature and stirred for 30 min, acidified to pH = 3 with a HCl solution and the product was extracted into ethyl acetate (100 ml), washed with brine (3 × 100 ml, 5% w/v) and dried over anhydrous sodium sulphate, filtered and evaporated in vacuo to afford the product as an amorphous white solid (0.6 g, 2.5 mmol, 16%). M.p. 87.0–87.5°C; FTIR 3388 (s), 3335 (s), 2979 (s), 2800 (br), 1729 (s), 1624 (s), 1545 (s), 1227 (s); EI (m/z) 239 (5), 194 (10), 148 (100), 131 (13), 120 (30), 103 (22), 91 (95), 77 (27), 65 (27), 47 (33); δ_H(270 MHz, $CDCl_3$), 7.23 (5H, m, ArH), 6.92 (1H, m, NH), 5.03 (1H, dq, *J* 39.1, 6.8, CFH), 4.90 (1H, overlapping dd, *J* 6.8, 6.8, CH), 3.19 (2H, m, CH_2), 1.48 (3H, 2 overlapping dd, *J* 24.5, 6.8, CH_3); δ_C(67.9 MHz, $CDCl_3$) 174.2, 174.1, 171.2 (d, *J* 19.0), 171.1 (d, *J* 20.0), 135.3, 135.3, 129.3, 129.2, 128.6, 128.5, 127.2, 127.2, 88.3 (d, *J* 183.6, CFH), 88.3 (d, *J* 183.5, CFH), 52.6, 52.4, 37.4, 37.24, 18.3 (d, *J* 21.9), 18.1 (d, *J* 20.9); δ_F(254.2 MHz, $CDCl_3$) −182.79 (ddq, *J* 49.2, 24.7, 4.2, CFH), −182.92 (ddq, *J* 49.8, 25.2, 4.3, CFH).

1.4. Acylase enzyme reaction

(*S*)-Phenylalanine-*N*-2-(*R,S*)-fluoropropionamide was dissolved in 4 M NaOH (three equivalents) and the solution adjusted to pH = 7 with aq. HCl and then diluted to a known volume of phosphate buffer (pH = 7), to give a 50 mM concentration of substrate in solution. Each diastereoisomer was readily observable by ^{19}F-NMR. δ_F(254.2 MHz, $CDCl_3$) −181.67 (dq, *J* 48.7, 25.2, CFH) (*S,S*)-diastereoisomer, −182.10 (dq, *J* 48.5, 25.2, CFH), (*S,R*)-diastereoisomer. The above solution of sodium (*S*)-phenylalanine-*N*-2-(*R,S*)-fluoropropionamide (0.2 ml) (for a 10 mM reaction) and phosphate buffer, (pH = 7, 0.6 ml) was placed in a 5 mm NMR tube. A solution (0.2 ml of a 25 mg/ml, 0.5 units/mg) of the *A. melleus* acylase (Sigma Chem.) in phosphate buffer (pH = 7) was added to initiate the reaction and the reaction maintained at 25°C and monitored by ^{19}F-NMR.

For the kinetic analysis of the individual diastereoisomers, the same conditions were used. For the faster reacting (*S,S*)-diastereoisomer the initial reaction rate could be calculated after 5–10 min by monitoring the integration of the fluorine signals by ^{19}F-NMR. For the slower reacting (*S,R*)-diastereoisomer this required several hours.

References

[1] D. O'Hagan, H.S. Rzepa, Chem. Commun., (1997) 645.
[2] E.J. Toone, M.J. Werth, B.J. Jones, J. Am. Chem. Soc. 112 (1990) 4946.
[3] K. Hult, T. Norin, Pure Appl. Chem. 64 (1992) 1129.
[4] P. Kalaritis, R.W. Regenye, J.J. Partridge, D.L. Coffin, J. Org. Chem. 55 (1990) 812.
[5] T. Kitazume, K. Murata, T. Ikeya, J. Fluorine Chem. 31 (1986) 143.
[6] D. O'Hagan, H.S. Rzepa, J. Chem. Soc., Perkin Trans., Perlin 1 (1994) 3.
[7] J. Banks, A.S. Batsanov, J.A.K. Howard, D. O'Hagan, H. S Rzepa, S. Martin-Santamaria, Perlin 2 (1999) 2409.
[8] D.O. Hughes, R.W.H. Small, Acta Cryst. 15 (1962) 933.
[9] G.A. Jeffrey, J.R. Ruble, R.K. McMullan, D.J. DeFrees, J.A. Pople, Acta Cryst. B37 (1981) 1885.
[10] G.A. Olah, J.T. Welch, Y.D. Vankar, M. Nojima, I. Kerekes, J.A. Olah, J. Org. Chem. 44 (1979) 3872.
[11] J. Barber, R. Keck, J. Retey, Tetrahedron Letts. 23 (1982) 1549.
[12] R. Keck, J. Retey, Helv. Chem. Acta 63 (1980) 769.
[13] D.J. Bailey, D. O'Hagan, M. Tavasli, Tetrahedron Asymm. 8 (1997) 149.
[14] G. Zubay, Biochemistry, 2nd Edition, Maxwell-Macmillan, 1989.